1-1-2013

Modulation of Chloride Secretion by Bile Acids in Airway Epithelial Cells.

Siobhan M. Hendrick
Royal College of Surgeons in Ireland

RCSI

Modulation of Chloride Secretion by Bile Acids in Airway Epithelial Cells

A thesis presented to the National University of Ireland
for the degree of Doctor of Philosophy
by

Siobhán M. Hendrick, B.Sc (Hons)

December 2013

Department of Molecular Medicine
Education and Research Centre, Smurfit building
Royal College of Surgeons in Ireland
Dublin 9

Supervisors:
Prof. Brian J. Harvey
Dr. Catherine M. Greene

I declare that this thesis, which I submit to RCSI for examination in consideration of the award of the higher degree of Doctor of Philosophy, is my own personal effort. Where any of the content presented is the result of input or data from a related collaborative research programme this is duly acknowledged in the text such that it is possible to ascertain how much of the work is my own. Table 2.9 not already obtained a degree in RCSI or elsewhere on the basis of this work. Furthermore, I took reasonable care to ensure that the work is original, and, to the best of my knowledge, does not breach copyright law, and has not been taken from other sources except where such work has been cited and acknowledged within the text.

Signed Siobhán Hendrick

Student Number 10109536

Date 19-12-13

Acknowledgements

Firstly I would like to thank my supervisor Prof. Brian Harvey for providing me with the opportunity to work with his fantastic research team and for all of his leadership during my PhD.

I would also like to thank my co-supervisor Dr. Catherine Greene for her help and advice over the past three years. In addition, I would also like to thank Dr. Stephen Keely for his guidance in helping me to develop this project.

Thank you to the Molecular Medicine team, past and present, for all of their patience and help over the last three years. Your support and advice kept me going during the tough times and ensured that I stayed on track for success throughout my PhD.

I would also like to express my sincere gratitude to Olive and Lorraine who work tirelessly to keep the lab running so smoothly on a day to day basis. They are the glue that holds Mol Med together, and make it such a great lab to work in.

Thanks also to the Higher Education Authority (HEA) (PRTLI Cycle 4) and the National Biophotonics Imaging Platform (NBIP) Ireland for funding this research.

On a personal note, I would like to thank my amazing friends and family for all of their love and support over past three years. Thank you for being there to confide in on bad days and making me realize that it would all be worth it in the end.

Finally, I want to express my deepest gratitude to wonderful Tim, the 'eternal optimist'. Thank you for being my best friend and my number one supporter. I could not have made it through the past three years without your unconditional love and positive spirit, for which I am truly grateful.

List of Abbreviations

ABC transporter- ATP binding cassette transporter

ALI- air-liquid interface

Amphot B- Amphotericin B

ANOVA- analysis of the variance

ASL- airway surface liquid

ATP- adenosine triphosphate

A.U- arbitrary units

BAAT- bile acid CoA amino acid N-acetyltransferase

BAL- bronchoalveolar lavage

BEGM- bronchial epithelial growth medium

Bis I - bisindolylmaleimide I (Bis I)

BOS- bronchiolitis obliterans symdrome.

BSA- bovine serum albumin

CA- cholic acid

cAMP- 3'-5'-cyclic adenosine monophosphate

CBF- ciliary beat frequency

CCh- carbachol

CCN2- connective tissue growth factor 2

CDCA- chenodeoxycholic acid

cDNA- complementary deoxyribonucleic acid

CF- cystic fibrosis

CFTR- cystic fibrosis transmembrane conductance regulator

cGMP- cyclic guanosine monophosphate

CMC- critical micellar concentration

COPD- chronic obstructive pulmonary disease

DAG- diacyl glycerol

DCA-deoxycholic acid

DMEM- Dulbecco's modified eagle medium

DMSO- dimethylsulphoxide

DTT- dithiothreitol

EGF- epidermal growth factor

EGFR- epidermal growth factor receptor

EGTA- ethyleneglycol-bis-β-aminoetyllether N,N,N',N',-tetraacetic acid

ENaC- epithelial sodium channel

Epac- exchange protein directly activated by cAMP

ERK- extracellular signal-regulated kinase

Fsk- forskolin

FGF19- fibroblast growth factor

Fura 2 AM- Fura 2 acetoxy methylester

FXR- farnesoid x receptor

f508del- deletion of phenylalanine at position 508 in CFTR

GAPDH- glyceraldehyde 3-phosphate dehydrogenase

GER- gastroesophageal reflux

GPCR- g-protein coupled receptor

GW4064- 3- [2- [2- chloro- 4- [[3- (2, 6- dichlorophenyl)- 5- (1- methylethyl)- 4- isoxazolyl]methoxy]phenyl]ethenyl]benzoic acid

HBE- human bronchial epithelium

HEPES- N-2-hydroxyethylpiperazine-N-2-ethane sulphonic acid

H89- N-[2-(p-Bromocinnamylamino)ethyl]-5-isoquinolinesulfonamide

ICP- intrahepatic cholestasis of pregnancy

IL- interleukin

INT777- 6α-ethyl-23(*S*)-methyl-3 α,7 α,12 α -trihydroxy-5 β-cholan-24-oic acid

IP3- inositol 1,4,5-trisphosphate

I_{sc}- short circuit current

LCA- lithocholic acid

MAPK- mitogen activated protein kinase

MCC- mucociliary clearance

MMP- matrix metalloproteinase

NKCC1- Na^+K^+ $2Cl^-$ cotransporter

OA- oleanolic acid

PBS- phosphate buffered saline

PCL- periciliary layer

PCR- polymerase chain reaction

PEI- polyethyleneimine

PEI-PEG- poly(ethyleneimine)-poly(ethylene) glycol

PKA- protein kinase A

PKC- protein kinase C

PLC- periciliary layer

PLM- phospholemman

PXR- pregnane x receptor

RDS- respiratory distress syndrome

ROCE- receptor operated Ca^{2+} entry channel

RT-PCR- reverse transcriptase PCR

SDS- sodium dodecylsulphate

SDS-PAGE- SDS- polyacrylamide gel electrophoresis

SEM- standard error of the mean

SERCA- sarco/endoplasmic reticulum Ca^{2+} ATPase

SGK- serum and glucocorticoid induced protein kinase

siRNA- short interfering ribonucleic acid

SMG- submucosal gland

SOCE- store-operated calcium entry

sPLA2- secretory phospholipase 2

TBS- tris buffered saline

TBS-T– tris buffered saline plus tween

TCA- taurocholic acid

TCDCA- taurochenodeoxycholic acid

TDCA- taurodeoxycholic acid

TEER- transepithelial electrical resistance

TGF β- transforming growth factor β

TJ- tight junction

TMEM16A- transmembrane protein 16A

TNFα- tumour necrosis factor α

TUDCA- taurooxycholic acid

UDCA- ursodeoxycholic acid

VAP- ventilator associated pneumonia

Table of Contents

Summary

Bile acids are often present in the lower airways of people with cystic fibrosis and other respiratory distress diseases, probably resulting from the aspiration of gastroesophageal refluxate. The effects of bile acids on airway epithelium ion transport function have not yet been investigated. The effects of the unconjugated secondary bile acids, DCA and UDCA, plus the taurine conjugate of DCA, TDCA, on basal ion transport and carbachol (CCh)- or forskolin (Fsk)- induced Cl^- secretion was investigated in Calu-3 airway epithelial cells grown in an air-liquid interface and mounted in Ussing chambers. Electrogenic transepithelial ion transport was measured as short-circuit current (I_{sc}). These results show that acute (5 min) apical treatment with DCA had no effect on basal I_{sc} but decreased CCh- stimulated I_{sc} by 43%. UDCA had no acute effect on I_{sc} in Calu-3 cells. In contrast, 24 hr apical treatment with DCA or UDCA increased CCh- stimulated I_{sc} by 36% and 65% respectively and 24 hr UDCA treatment also attenuated subsequent Fsk responses by 17%. Furthermore, basolateral TDCA treatment of Calu-3 cells stimulated basal I_{sc} by 39% but had no effect on the I_{sc} responses induced by CCh or Fsk treatment. The I_{sc} responses to TDCA were abolished in Cl^--free Krebs solution indicating that TDCA modulates Cl^- secretion. TDCA had no chronic effect on I_{sc} in Calu-3 cells.

Acute treatment with TDCA produced a 32% increase in CFTR I_{sc} that was abolished by pre-treatment with $CFTR_{inh172}$. It was also found that TDCA increases Cl^- secretion through calcium-activated chloride (CaCC) channels by 18%. In addition, when Na^+/K^+ ATPase generated currents were measured in Ussing chambers, acute treatment with TDCA increased Na^+/K^+ pump activity by 13%, while pre-treatment with ouabain eliminated this effect. Acute treatment with TDCA resulted in a rapid 88% increase in intracellular calcium mobilization, which was abolished in Ca^{2+} -free buffer indicating that TDCA induced Ca^{2+} influx into the cell. In addition, TDCA increased basal cAMP levels and PKA activation. Preliminary data from TGR5 knockdown studies suggest that TGR5 is the membrane receptor involved in TDCA induced Cl^- secretion. In summary, this thesis shows for the first time that low concentrations of bile acids can modulate Cl^- secretion in airway epithelial cells and this effect is dependent upon both the duration and sidedness of exposure to the bile acid.

Preface

Bile acids are acidic steroids synthesized from cholesterol by hepatocytes. The primary function of bile acids is to facilitate lipid transport as mixed micelles in the intestinal tract. However, in recent years accumulating data have shown that bile acids also function as cell signalling molecules, which may activate several signalling pathways to regulate biological processes. In particular, bile acids have been increasingly reported to be involved in modulation of epithelial ion transport in many different tissues, such as the colon and gallbladder (Ao *et al.*, 2013, Devor *et al.*, 1993, Keating and Keely, 2009a, Keely *et al.*, 2007, Keitel *et al.*, 2009, Kelly *et al.*, 2013, Mroz *et al.*, 2013, Ward *et al.*, 2013). Over the past twenty years, there has been a rise in the number reports indicating that bile acids are present in the airways of patients with many pulmonary disorders, such as bronchiolitis obliterans syndrome (BOS), ventilator associated pneumonia (VAP), respiratory distress syndrome (RDS), idiopathic pulmonary fibrosis (IPF) and cystic fibrosis (CF) (Zecca *et al.*, 2004, D'Ovidio *et al.*, 2005, Pauwels *et al.*, 2012, Savarino *et al.*, 2013, Zecca *et al.*, 2008). Furthermore, although the presence of bile acids in the airways has often been associated with a poor prognosis in these patients, no direct correlation between the two has yet been elucidated.

To date the majority of studies investigating bile acid effects on airway pathophysiology have focused on bile acid-induced inflammation (Wu *et al.*, 2009, Vos *et al.*, 2008, Perng *et al.*, 2008), however bile acid modulation of airway epithelial ion transport has not yet been examined. Bile acids are now well established modulators of epithelial ion transport in the colon and gallbladder. The main hypothesis for this study was that bile acids may also regulate ion transport in the lung epithelium. The primary aim of this thesis was therefore to determine whether bile acids were capable of modulating airway epithelial ion transport and to elucidate the ion transport proteins and signalling pathways involved in this process. By doing so, it is hoped that this thesis will provide novel data to explain how bile acid modulation of epithelial ion transport may participate in lung disease.

Chapter 1

General introduction

1-1. The Respiratory System

The respiratory system comprises of the nose, mouth, throat, larynx, trachea, bronchi and lungs. Its main function is to facilitate CO_2/O_2 exchange and transport oxygen via the blood to the tissues where it is required for metabolism. The lungs are a spongy structure where exchange of gases takes place. Each lung is surrounded by a pair of pleural membranes, encasing pleural fluid that helps to reduce friction during breathing. The trachea is branched into bronchi leading on to approximately one million bronchioles which terminally branch off into small hollow air sacs termed alveoli. There are over 700 million alveoli in the human lung which greatly increases the surface area for gas exchange. Each alveolus is surrounded by capillaries facilitating the transport of CO_2/O_2 into the blood.

The mature mammalian airway can be divided by structure and function into three regions: 1) the cartilaginous proximal airway, comprising the trachea, bronchi and submucosal glands, 2) the non-cartilaginous distal bronchioles, comprising the bronchioles, terminal bronchioles, transitional bronchioles and respiratory bronchioles, and 3) the gas exchange region, comprising the alveolar ducts and alveolar sacs (Proud, 2008). For the purpose of this study, we will be focusing on the proximal airway only.

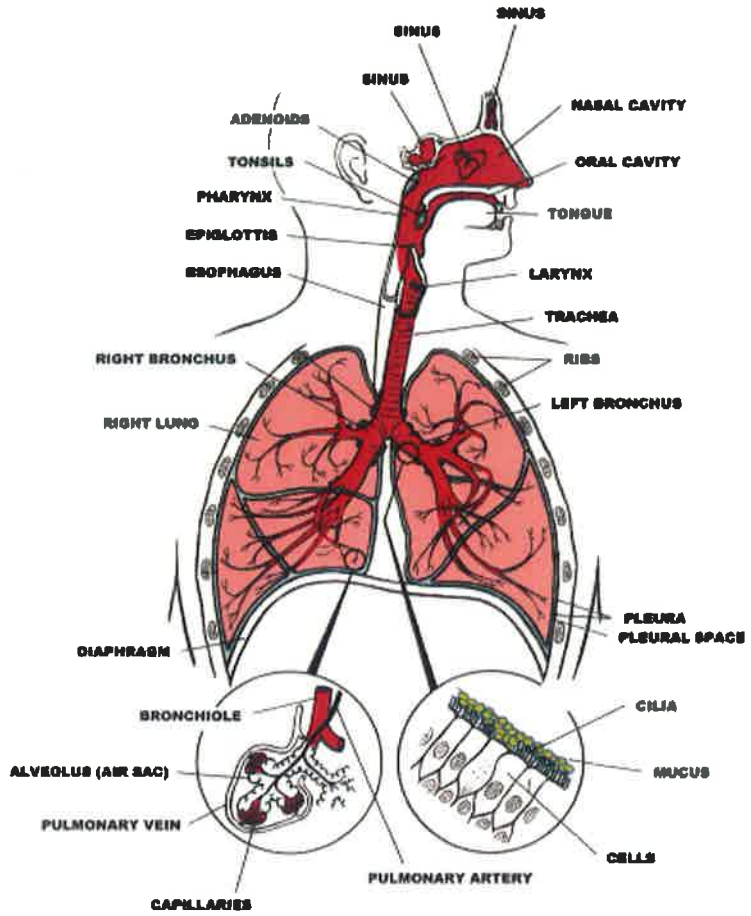

Fig 1.1 Summary Figure of the Respiratory System. Inspired air enters through the nose and mouth, passes down through the respiratory tract where it is filtered and moistened before terminating in the alveoli at the end of the bronchioles, where gas exchange takes place. The region of interest for this study is the surface of the proximal airway, as indicated inset, which is comprised mainly of ciliated cells and submucosal glands that regulate airway surface liquid and mucociliary clearance.
http://serendipity86.wordpress.com/2008/03/16/respiratory-system-protection-against-disease-particulate-matter/

The respiratory tract is the path of air from the nose to the lungs and is lined with a continuous layer of epithelial cells. The large surface of the lung is continuously exposed to a burden of airborne pathogens, resulting in frequent immune responses, and so the airway epithelium plays an important role in airway defence. It forms a barrier between the external and internal environments, prepares the air for optimal gas exchange at the alveoli, and purifies the air by removing particles and bacteria (Zabner *et al.*, 2003).

1-1.1 Airway epithelium – Structure and Function

The airway epithelium is a true example of a dynamic tissue in that it not only forms a physical barrier to inhaled insults but also participates in a number of other crucial airway functions such as mucociliary clearance, airway repair and remodelling, inflammatory response, ion transport and secretion of surfactant proteins, mucins and antimicrobial peptides for airway surface protection. Changes in the cellular composition and architecture of airway epithelial cells are key features in the pathogenesis of many human lung diseases such as, asthma, chronic obstructive pulmonary disease (COPD), cystic fibrosis (CF) and bronchogenic carcinoma.

The surface epithelium lining the proximal human airways is pseudo-stratified; all cells extend to the basement membrane but not all cells extend to the luminal surface (Zabner *et al.*, 2003). The major cell types are ciliated, columnar, undifferentiated, secretory and basal cells (Crystal *et al.*, 2008). Submucosal glands are unique to the proximal airways and are characterized by a variable proportion of ciliated cells, mucus cells and serous cells (De Poitiers *et al.*, 1980). Although the airway epithelium contains many different resident cells, only ciliated columnar and secretory cells of the submucosal gland seem to contribute directly to regulation of airway surface liquid and mucociliary clearance (Wanner *et al.*, 1996). Therefore our investigation of the airway epithelium mainly focuses on the physiological properties of these ciliated and submucosal gland cells.

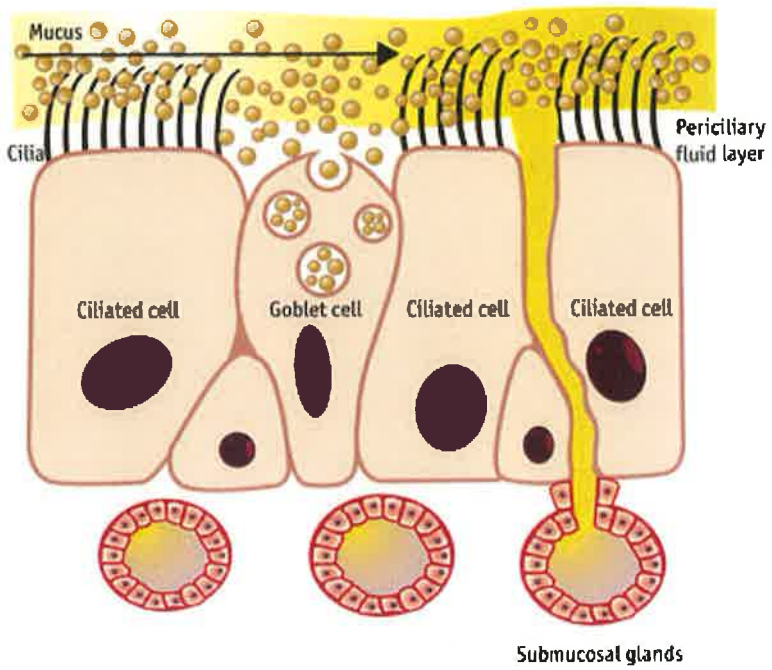

Fig 1.2 Pseudo-stratification of the airway epithelial layer. As shown here, all cells extend to the basement membrane but not all cells extend to the luminal surface. The major cell types in the proximal airway are ciliated, columnar, undifferentiated, secretory and basal cells. Submucosal glands (SMG) contain a variable proportion of ciliated cells, mucus cells and serous cells, required for the transport of newly synthesized mucins out of the SMG. Both the goblet cells and submucosal glands secrete mucins into the ASL, forming an overlying mucus layer that traps inhaled particles and pathogens. The mucus is then removed from the airway by mucociliary clearance, in the presence of adequate levels of periciliary liquid (PCL) which facilitates cilia beating. **Image from:**
http://www.ersnet.org/learning_resources_player/breathe/6_4/8/10.-Review-pathophysiology-web-images/figure-3.jpg

One key feature of the airway epithelium is its ability to transport Na^+ and Cl^- ions in response to increasing or decreasing volumes of apical fluid, thus driving fluid secretion or absorption and regulating airway surface liquid (ASL) volume. This is very important for innate lung defence as it facilitates mucociliary clearance (MCC), the process whereby inhaled pathogens or particulates become trapped in the mucus layer lining the airway epithelium and are transported out of the airways.

It is also important to note that the human airway epithelium plays an important role in response to injury, infection, or toxins by producing various

cytokines and other pro- and anti-inflammatory agents that modulate innate immunity mediators (Zabner *et al.*, 2003, Wu *et al.*, 2009). In their exposed position, airway epithelial cells express many pattern recognition receptors (PRR) to rapidly recognise and respond to pathogen-associated molecular patterns found in microbes or to damage-associated molecular patterns released upon tissue damage, cell death or cellular stress (Lambrecht and Hammad, 2012). The activation of PRR leads to the release of cytokines, chemokines and other antimicrobial peptides that attract and activate adaptive and innate immune cells. However, for the purpose of this study we will focus on the role of ion transport in regulating airway defence via adequate surface hydration, thus facilitating MCC.

Recent studies by Pezzulo *et al* have highlighted the importance of *in vitro* model selection for the study of airway epithelial physiology in both healthy and diseased states (Pezzulo *et al.*, 2011). They demonstrated that the use of well-differentiated primary human airway epithelial cells grown at air-liquid interface in culture most closely resembled that of *in vivo* airway epithelium suggesting that the use of primary cultures and of an air-liquid interface are important to recapitulate airway epithelia biology. Therefore this was the method that we favoured throughout this study.

1-1.2 Ciliated cells

The surface epithelial cells that interface directly with the external environment are mostly ciliated cells. Their function is pathogen detection, fluid and electrolyte transport and mucociliary clearance (Fischer *et al.*, 2009). Therefore these cells play a very important role in both the regulation of homeostasis in the lung microenvironment and also in maintenance of sterility in the airways. Ciliated cells occur with the greatest frequency in the proximal airway epithelium; they have a height of 15-20 μm and are approximately 15 μm in width (Busuttil *et al.*, 1977). They are roughly columnar in shape and contain approximately 200-300 cilia on the apical surface of each cell, with each cilium approximately 6 μm in length and 0.3 μm wide (Proud, 2008, Busuttil *et al.*, 1977). Ciliated cells are attached to the basal lamina via

desmosomes and extend to the apical surface, where they are interconnected via tight junctions (Proud, 2008). The cilia are closely packed towards the central portion of the cell and are more disperse toward the edge of the cell, where microvili are abundant.

1-1.3 Submucosal gland cells

The main function of the sub-mucosal glands (SMG) is to secrete antimicrobial molecules and most of the liquid and mucins that line the airway surface (Fischer *et al.*, 2009). SMG and surface ciliated epithelial cells are thought to be derived from the same precursor cells, with glands arising from invagination of the epithelium during foetal development (Liu *et al.*, 2004). However, Fischer *et al* (Fischer *et al.*, 2009) have shown that the transcriptional profiles of SMG and ciliated airway epithelial cells are divergent and reflect their unique functions.

Each SMG consists of multiple tubules that feed into a collecting duct, which narrows into a ciliated duct that is continuous with the airway surface (Meyrick *et al.*, 1969). The tubules may be interconnecting and are lined with mucus cells in their proximal region and serous cells in their distal acini, fig 1.3. Serous cells are the predominant sites of cystic fibrosis transmembrane conductance regulator (CFTR) expression in the human bronchus and they play a pivotal role in the regulation of ASL (Engelhardt *et al.*, 1992). This suggests mechanisms whereby defects in CFTR expression could lead to defects in mucus production by the human lung.

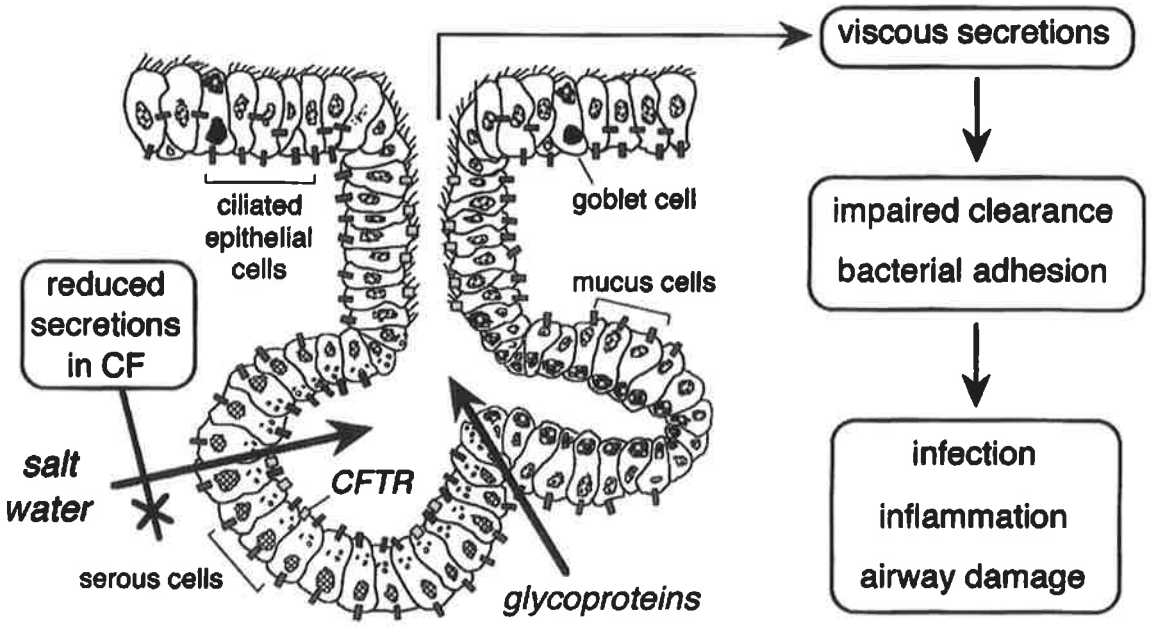

Fig 1.3 Structure of the airway submucosal gland (SMG). This figure illustrates the basic structure of the SMG, with an interconnecting tubule lined with mucus cells in its proximal region and CFTR expressing serous cells in its distal collecting duct. The serous cells secrete fluid which, along with the ciliated cells, creates a mucociliary escalator facilitating the transport of mucins produced by the mucus cells out of the SMG. In CF, secretion by the serous cells is impaired resulting in thick mucus secretions and mucus plugging. **Image from** ***http://www.fasebj.org/content/19/3/431/F3.large.jpg***

Serous gland cells are pyramidal in shape, with electron-dense secretory granules in the apical region and a basally located nucleus (Finkbeiner *et al.*, 2010). Serous cells are located distally from the mucus cells and they secrete fluid that is essential for the transport of macromolecular gland secretions away from the gland duct, maintaining ASL volume and facilitating mucociliary clearance (Ballard and Inglis, 2004). The mucus cells of the submucosal gland are columnar in shape, with a basally-located nucleus (Finkbeiner *et al.*, 2010).The main function of the mucus cells is to secret mucins in the form of the mucus glycoprotein MUC5B, while MUC5AC is produced by the surface goblet cells (Kim, 2012, Crystal *et al.*, 2008, Hattrup and Gendler, 2008).

1-1.4 Tight junctions

In order to maintain the integrity of the epithelial barrier, the paracellular transport of molecules must be tightly regulated. In 1963, using electron microscopy, Farquhar and Palade (Farquhar and Palade, 1963) studied the

epithelia of a number of glands and cavitary organs of the rat and guinea pig and found that in all tissues a characteristic tripartite junction complex could be found between adjacent cells. The three components of this complex, based on distinct morphologies and locations were named the *zonula occludens* or "closing belt", now referred to as the tight junction (TJ), the *zonula adherens* or "adhering belt", now known as adherens junction (AJ) or intermediate junction, and the *macula adherens* or "adhering spot" know known as the desmosome (Farquhar and Palade, 1963).

The TJ is the most apical member of the junctional complex. It is characterized by fusion of the adjacent cell membranes resulting in obliteration of the intercellular space over variable distances. In the airway, TJs are responsible for determining the permeability of the airway surfaces as they regulate access to the paracellular spaces between columnar cells (Wan *et al.*, 2000). The intermediate (gap) junction is characterized by the presence of an intercellular space occupied by homogeneous material of low density that holds epithelial cells together by tight Ca^{2+} -dependent links, connecting the cytoplasm of neighbouring cells to facilitate movement of molecules between cell (Farquhar and Palade, 1963). The desmosome is also characterized by the presence of an intercellular space that contains a central disc of dense material that is specialized for cell-cell adhesion (Green and Jones, 1996).It is believed that the desmosome plays an important role in cell-cell communication and regulation of protein interactions between cells.

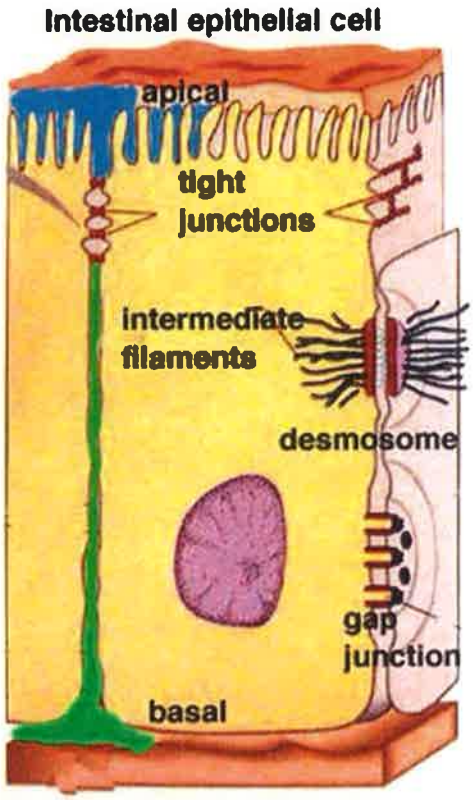

Fig 1.4 Epithelial Cell-Cell and Substratum Adhesion Structures. Tight junctions, desmosomes, gap junctions, and adherens junctions (not shown here) are present in all epithelial cells along the lateral surface. Tight junction regulation determines the permeability of the airway surface by controlling access to the paracellular spaces.
Image from: *http://scienceblogs.com/clock/2006/11/23/cellcell-interactions/php*

Studies by Coyne *et al* found that the tight junctions of airway epithelia exposed to chronic inflammation may exhibit parallel changes in the barrier function to ions and solutes (Coyne *et al.*, 2002). For example, both house dust mite allergens and purified protease allergens from house dust mites penetrate the epithelial barrier by cleavage of the tight junction- associated proteins claudin-1, zona occludens-1 (ZO-1), and occludin (Proud and Leigh, 2011). These studies indicate that disruption of tight junctions may play an important role in the epithelial remodelling that is a key feature of many airway diseases such as asthma, COPD and CF, where chronic inflammation of the airways occurs.

1-2. Airway Surface Liquid

Fluid is very important in the airways not alone as a solvent for gas exchange but also as an integral part of airway defence (Knowles and Boucher, 2002). The airways are covered by a thin film of liquid which humidifies inspired air and enables ciliary beating to clear mucus, pathogens, and other inhaled substances from the lungs. The airway surface liquid (ASL) is an extremely thin layer of aqueous fluid, normally 5μm-10μm deep, that coats the airway mucosal surface protecting it from inhaled dust, bacteria and other harmful substances (Jayaraman *et al.*, 2001, Smith *et al.*, 2008, Chambers *et al.*, 2007). Most airway surface liquid (ASL) is produced by submucosal glands, which secrete a complex mixture of ions, fluid, mucins, and antimicrobial factors when stimulated by agonists that mobilize intracellular Ca^{2+} and /or cAMP (Wine and Joo, 2004).

The ASL consists of at least two layers: the upper layer consists of highly viscous and non-Newtonian mucus, ie the rate of change of mucus deformation over time is not proportional to the viscous stresses that arrive from mucus flow, and a lower periciliary liquid layer. The mucus layer is mainly composed of water (approximately 98%), salt (1%), and glycosylated mucin proteins (1%), secreted by specialised cells (Davis and Dickey, 2008). Electrolyte transport by airway epithelial cells and submucosal glands tightly controls the quantity and composition of airway surface liquid (Itani *et al.*, 2011). Numerous agents are secreted from the epithelium into the ASL including immunoglobulins and anti-microbial factors; these form part of the defensive shield that protects the airways and lungs from bacterial infection (Zabner *et al.*, 2003).

Under conditions where airway surfaces are bathed with large volumes of liquid, normal airway epithelia have the capacity to remove (absorb) this excess liquid (Chambers *et al.*, 2007). Since water cannot be transported directly by biological systems, cells transport ions, which in turn create osmotic gradients providing the driving force for water flow. Net salt transport in the airway epithelium is reflective of a balance between two main ionic

conductances in the apical membrane: a Cl^- conductance dominated by the cystic fibrosis transmembrane regulator (CFTR), and a Na^+ conductance mediated by the epithelial sodium channel (ENaC).

Shear stress can also regulate ASL height in both normal and CF airways though extracellular ATP- and adenosine- (ADO) mediated pathways that modulate ion transport and ASL volume homeostasis (Tarran *et al.*, 2006). Tight regulation of ASL volume by ion transport is essential to the maintenance of the airway microenvironment as illustrated by multiple airway diseases, such as cystic fibrosis (CF), where decreased Cl^- secretion and increased Na^+ absorption cause airway surface dehydration and thereby mucociliary dysfunction.

1-2.1 Mucus layer

Mucus is a gel formed by water (80%), ions and proteins (10%) that contributes to the homeostasis of ASL and to the clearance of pathogens in coordination with the ciliary system (Puchelle *et al.*, 1987). Mucus exhibits complex rheological properties such as shear-thinning, viscoelasticity, and adhesiveness, due to its content of glycosylated mucin polymers (Puchelle *et al.*, 1987). It is normally produced from the goblet cells of the surface epithelium, which consist of a network of secretory tubules and associated ducts but can also be produced by the submucosal glands of the proximal airway epithelium (Meyrick *et al.*, 1969). The best described functions of the airway mucus layer are; hydration, lubrication, protection from proteases and defence against pathogens by trapping airborne microbes and particles (Hattrup and Gendler, 2008).

Mucins (MUC) are a family of heavily glycosylated proteins present in mucus that can be either secreted or membrane tethered (Garcia-Verdugo *et al.*, 2010). They are characterised by a variable number of tandem repeats, usually rich in serine and threonine, termed the mucin domain (Kim, 2012, Hattrup and Gendler, 2008). The majority of mucins produced in the airway belong to the gel-forming sub-family of mucins, especially MUC5AC and

MUC5B, which are highly expressed by the airway epithelium and are major components of most human airway secretions. MUC5AC is localized to goblet cells and MUC5B is localized to mucus cells of the submucosal glands in the healthy airway (Crystal *et al.*, 2008). MUC1, MUC4 and MUC16 are membrane tethered mucins that have been shown to be produced and released by airway surface epithelial cells and serve as a major protective barrier against pathogens (Kim, 2012). Cell surface mucins may contribute to airway pathology through; anchoring obstructive mucus, modulating adhesion, influencing the manner and extent of inflammation and regulating cellular signalling (Hattrup and Gendler, 2008).

1-2.2 Periciliary layer

The lower layer of ASL is a watery fluid consisting principally of salt and water, known as the periciliary liquid layer (PCL), that lubricates the cell surface and mucus layer (Pruliere-Escabasse *et al.*, 2010). In healthy individuals the PCL extends from the cell surface to a depth equal to the length of outstretched cilia (~7 μm) and provides a fluid in which the cilia can beat (Tarran, 2004). If the PCL is not maintained to the correct volume, the cilia would become trapped in the mucus and not be able to beat (Tarran *et al.*, 2001). Conversely, if the volume of PCL is too high the cilia may not be able to make contact with the mucus and apply the necessary force required for mucociliary clearance. It has also been suggested that the role of the PCL is to prevent the adherence of epithelial mucins with the overlying mucus layer (Knowles and Boucher, 2002).

Recently the question has been raised as to why the major molecules of the mucus layer - MUC5AC and MUC5B, do not penetrate into the interciliary space to form one layer. Button *et al* (Button *et al.*, 2012) have attempted to answer this question by proposing a "gel on brush" model of the mucus clearance system. In this model the PCL is occupied by membrane spanning mucins and large mucopolysaccharides that are tethered to cilia, microvilli and epithelial surface. These form an extracellular brush with a sufficiently high concentration to establish a mesh that prevents penetration of the PCL. It is

predicted that this high concentration of macromolecules produces intermolecular repulsion within the layer and so helps to stabilize the PCL and prevent against compression by an osmotically active mucus layer.

Stabilization of the PCL is essential for the formation of the distinct mucus layer and effective mucus clearance and dehydration-induced destabilization of the PCL has been found to result in defective mucus clearance. Matsui *et al* (Matsui *et al.*, 1998) report that CF airways epithelium exhibited abnormally high rates of sodium absorption which leads to depletion of the PCL and abolished MCC, likely initiating CF airway infection. They therefore suggest that therapy for CF should be directed at restoring the volume of PCL on the airway surfaces, rather than modulation of ionic composition.

1-2.3 Mucociliary clearance

Mucus clearance is a major component of the lung innate defence mechanism and the efficiency of mucus clearance is partly dependent on the volume of airway surface liquid (ASL) on airway surfaces (Pruliere-Escabasse *et al.*, 2010). Mucociliary clearance (MCC) is critical to pathogen removal and this is evident in conditions such as CF, COPD or ciliary dyskinesia, where patients experience repeat and chronic respiratory infections.

In order to remove harmful material trapped by the mucus, the mucus layer is transported along the airways and out of the lungs by the activity of a dense mat of microscopic cilia, whereupon it is then swallowed or expectorated (Smith *et al.*, 2008). The superficial human airway epithelium that mediates mucociliary clearance is composed mainly of ciliated cells with a small component of mucin-secreting submucosal gland cells. Each mature ciliated cell may have up to 200 cilia, at a density of 6-8 μm^{-2} (Sleigh *et al.*, 1988). Cilia perform an 'effective stroke' in which they beat forward, engage with the mucus layer and propel it forward. They then perform a 'recovery stroke' in which they return to their initial position but do not drag as much fluid backwards, so that an overall positive flow is produced (Smith *et al.*, 2008). The beat pattern is asymmetric in time – the recovery stroke and subsequent

pause take several times longer than the effective stroke (Sanderson and Sleigh, 1981).

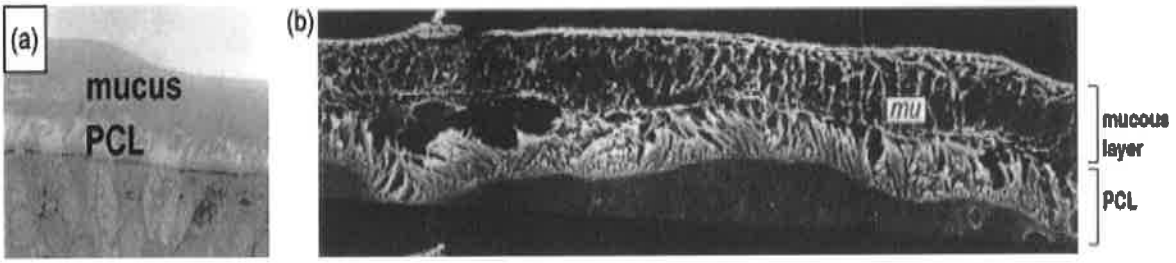

Fig 1.5 Model of Mucociliary clearance in airway epithelium (a) Light imaging depicting the epithelial cells, PCL and mucous layers from human tissue culture (Knowles and Boucher, 2002). (b) SEM data of the ASL of rabbit trachea. The cilia can be seen to move asymmetrically to propel the overlying mucus layer forward. The mucus layer rests on top of the PCL, which is approximately the same height as outstretched cilia (Sanderson and Sleigh, 1981).

Various studies conducted across a number of different species have indicated that increasing intracellular levels of cAMP stimulates ciliary beat frequency (CBF) through protein kinase A (PKA) activation and the subsequent phosphorylation of possibly several ciliary targets, while activation of protein kinase C (PKC) has been shown to decrease CBF in sheep and rabbit trachea explants (Wanner *et al.*, 1996). Intracellular free calcium ($[Ca^{2+}]_i$) has also been shown to be vitally important in regulating both the speed and direction of cilia beating and therefore MCC (Naito and Kaneko, 1972, Li *et al.*, 2012, Zhang and Sanderson, 2003). In mammalian cilia it appears that elevation of $[Ca^{2+}]_i$ increases CBF while decreased $[Ca^{2+}]_i$ results in slowed CBF.

1-3. Airway Epithelial Ion Transport involved in ASL Regulation

The airway epithelium has evolved to be both absorptive and secretory in response to its external environment. One key feature of epithelial cells involved in ion transport is that they are polarized, meaning that they have functionally and morphologically distinct membrane domains in their apical and basolateral regions (Apodaca *et al.*, 2012). Polarized cells have established electrochemical gradients across the epithelium, from apical to

basolateral compartments, thus generating the driving force for movement of ions into and out of the cell, without the requirement for active transport (Schwartz *et al.*, 1985). Changes in the extracellular ion concentration will therefore result in altered transepithelial ion transport. The continuous movement of ions across the cell results in the formation of a potential (voltage Vt) difference (PD) between the two membranes. Due to the active absorption of cations and /or the active secretion of anions by the epithelium, the Vt is generally apically negative with respect to the basolateral side under normal conditions.

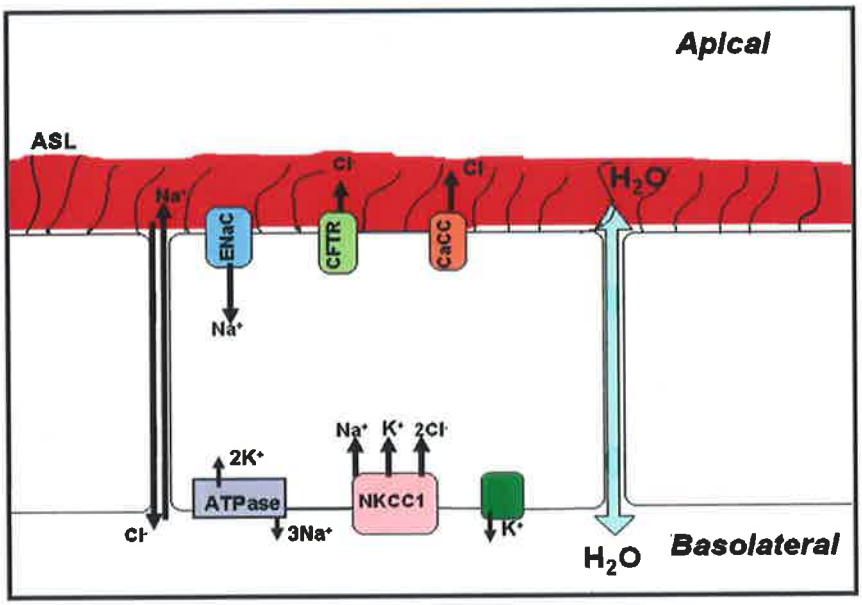

Fig 1.6. Na^+ absorption and Cl^- secretion in airway epithelial cells. ASL height is regulated by the establishment of osmotic gradients across airway epithelium providing the driving force for water flow. For absorption to occur, Na^+ enters the cell from the ASL through the epithelial sodium channel (ENaC) and exits the cell via the basolateral Na^+/K^+ ATPase (transcellular pathway), while Cl^- and water follow passively through the intercellular space (paracellular pathway). In order for secretion to occur, Cl^- enters the cell from the basolateral space principally via the $Na^+/K^+/2Cl^-$ (NKCC1) cotransporter, and may be secreted from the cell by the apical Cl^- channels, the Cystic Fibrosis Transmembrane conductance Regulator (CFTR) and the Ca^{2+} activated Cl^- channel (CaCC), while Na^+ and water follow passively through the paracellular pathway

As shown in fig 1.6, the absorptive pathway of epithelial cells reflects the capacity to actively absorb Na^+ ions, while the secretory pathway reflects how

Cl^- may be secreted from the cell. This sets up an osmotic gradient which provides the driving force for water absorption from the ASL or water secretion into the ASL, depending on the rate of Na^+ absorption or Cl^- secretion. Although many cells in the epithelium contain aquaporins which allow the transport of water molecules directly through the cells, the most common route for fluid transport is via the paracellular pathway. Regulation between absorption and secretion determines the net transport of ions across the epithelium, and is therefore a crucial factor in the maintenance of osmotic balance. Adequate epithelial ion transport is very important for ASL regulation and hence mucociliary clearance and defects in ion transport can lead to severe disease, most notably in the airways, cystic fibrosis.

1-3.1 Sodium absorption

The absorption of sodium depends on the operation of three essential components: 1.apical sodium channels (sodium entry), 2.basolateral Na^+/K^+ pumps (sodium exit) 3.K^+ channels (provide the driving force for sodium transport) (Harvey, 1995). The intracellular concentration of Na^+ is usually kept quite low in comparison to the external environment. This facilitates Na^+ entry through apical ENaC and allows Na^+ to pass through the cell down its electrochemical gradient. However, active transport is required for Na^+ exit at the basolateral membrane as Na^+ is pumped out of the cell by the Na^+/K^+ ATPase, against its electrochemical gradient. By this process, the Na^+/K^+ ATPase is an important regulator of Na^+ absorption and plays a crucial role in the maintenance of the transcellular Na^+ gradient. As the Na^+/K^+ ATPase pumps out Na^+, it also takes in K^+ and therefore K^+ recycling by the basolateral K^+ channels also plays an important role in facilitating Na^+ absorption.

Numerous reports have suggested that sodium hyperabsorption is a contributing factor to ASL depletion in CF disease. Some reports show that even in the presence of functioning CFTR, induced Na^+ hyperabsorption produces a CF-like lung disease in mice (Mall *et al.*, 2004, Zhou *et al.*, 2011). However, other groups have dismissed this theory and show that human CF airways have reduced Cl^- conductance but not increased Na^+ conductance

(Itani *et al.*, 2011), and so this is an area open to much debate. One major difference between these studies was the model selected for investigation. Mall *et al* and Zhou *et al* used a mouse model for their study of the role played by ENaC in CF disease, while Itani *et al* used differentiated primary cultures of tracheal/bronchial epithelia from CF and non-CF patients, and this may account for the differences in results obtained. The murine lung displays large morphological differences between human airways, such as a dominance of clara cells in the tracheobronchial region, and may not be a suitable model for investigation of airway epithelial ion transport in humans. There is, however, no doubt that Na^+ absorption through ENaC plays a vital role in the regulation of fluid on airway surfaces and studies involving ENaC dysfunction have highlighted this importance (Kerem *et al.*, 1999).

1-3.2 Chloride secretion

The apical Cl^- conductance pathway plays a key role in determining the rate at which fluid and electrolyte secretion occurs. The concentration of Cl^- within the cell is maintained at a higher level than that of the extracellular environment. Therefore Cl^- travels along its concentration gradient where it exits mostly through the CFTR or CaCC channels. Cl^- secreton is further enhanced by the activation of basolateral K^+ channels. K^+ exit at the basolateral membrane "hyperpolarizes" the membrane, converting the resting PD from positive to negative and therefore provides an electrochemical driving force for Cl^- exit through the apical membrane. The activity of the Na^+/K^+ ATPase generates an inwardly directed electrochemical gradient for Na^+, providing the driving force for the intracellular accumulation of Cl^- by the electroneutral luminal symporter, NKCC1 (Eisenhut and Wallace, 2011, Ando *et al.*, 1975). This is crucial for sustaining Cl^- secretion since an electrically uncompensated Cl^- efflux would depolarize the cell membrane potential and so inhibit further Cl^- efflux. Agonists that induce intracellular increases in two second messenger systems, cAMP and $[Ca^{2+}]_i$ are generally associated with Cl^- secretion (Begenisich and Melvin, 1998, Welsh and McCann, 1985). Numerous laboratories have now established that the cystic fibrosis transmembrane conductance regulator (CFTR) is the main path for Cl^- conductance across the cell membrane in the airways and is regulated by

PKA in a cyclic Adenosine MonoPhosphate (cAMP)-dependent fashion (Rowe *et al.*, 2005).

In addition to basolateral Cl^- entry through NKCC1 in airway epithelium, the anion exchanger type 2 (AE2 or SLC4A2) has been identified as a major pathway for basolateral Cl^- entry into submucosal gland cells (Huang *et al.*, 2012b). It has been suggested that AE2 plays an important role in basolateral Cl^- loading in Calu-3 cells during cAMP stimulation of Cl^- secretion, accounting for the large bumetanide-insensitive component of fluid secretion reported previously in airway submucosal gland cells, as Cl^- enters the cell through AE2 rather than NKCC1 (Lee *et al.*, 1998, Devor *et al.*, 1999). This highlights how Cl^- secretion in the airway can be coupled to HCO_3^- transport, as export of HCO_3^- is required for Cl^- uptake through AE2. Furthermore, Cl^- exit through CFTR and recycling through apical pendrin has been implicated in the pathway for HCO_3^- secretion in the airways, providing an explanation for the impaired HCO_3^- secretion and acidification of the airways observed in cystic fibrosis (CF) (Garnett *et al.*, 2013). Therefore, not alone will the effects of bile acids on airway secretion be investigated in this thesis, but also the specific ion transporters involved in this process will be identified.

1-4. Ion Transport Proteins

Ion transport proteins are located in the membranes of airway epithelial cells and have structures that allow flow of specific anions or cations into or out of the cell. Therefore these proteins play important roles in the regulation of ASL volume and pH. There are many different types of transport proteins, such as channels, pumps, co-transporters or exchangers, found in epithelial cells depending on the tissues in which they are located. It has been shown in many epithelial cells that ion exchangers, such as Na^+/H^+ or Cl^-/HCO_3^- exchangers, play an important role in the homeostasis of epithelial absorption or secretion (Harvey and Ehrenfeld, 1988, Singh *et al.*, 1997, Devor *et al.*, 1999, Huang *et al.*, 2012b). However, for the purpose of this study, we direct our focus on the main transport proteins associated with airway Cl^- secretion,

namely CFTR, CaCC, NKCC1 and basolateral K^+ channels or the proteins associated with Na^+ absorption, namely ENaC and Na^+/K^+ ATPase.

1-4.1 Cystic Fibrosis Transmembrane Conductance Regulator (CFTR)

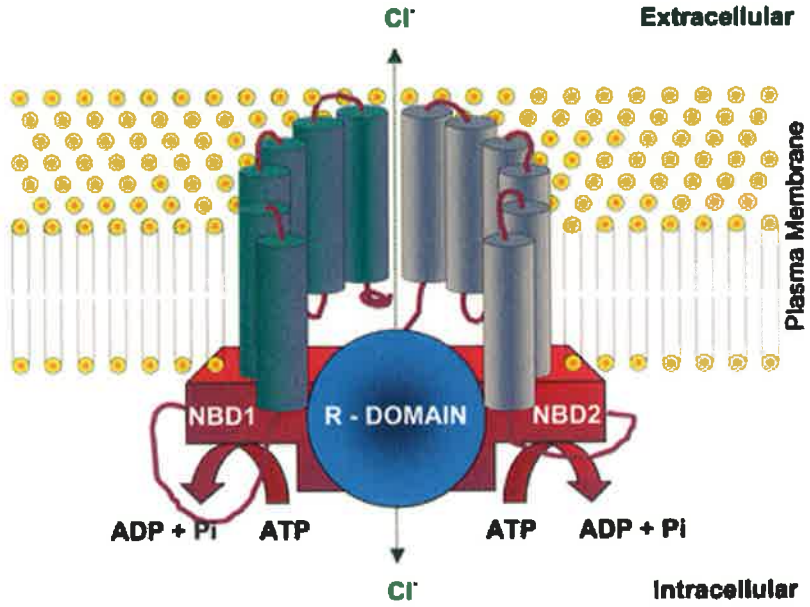

Fig 1.7 The Structure of the Cystic Fibrosis Transmembrane Conductance Regulator (CFTR) CFTR contains two transmembrane spanning domains, each comprised of 6 membrane-spanning regions, and two nucleotide-binding domains (NBDs) that bind and cleave ATP. CFTR also has a highly charged central domain (regulatory "R" domain), which contains a number of serine residues that are targets for phosphorylation. Phosphorylation of the serine residues on the R domain by cAMP-dependent PKA or by PKC is required for the channel to open. Once the R domain is phosphorylated, intracellular ATP interacts with the NBDs to regulate channel activity.
Image: *http://users.ox.ac.uk/~genemed/cysticfibrosis/protein.html*

CFTR has been identified as a member of the superfamily of transporters known as the ATP binding-cassette (ABC) transporters (Hyde *et al.*, 1990). It contains two transmembrane spanning domains and two nucleotide-binding domains (NBDs) that bind and cleave ATP, providing the energy source for transport (Hyde *et al.*, 1990). Even though ATP is required for activation of CFTR, Cl^- secretion through CFTR is not classed as active transport. In fact, Cl^- passes out of the cell according to its electro-chemical gradient, without any stoichiometric relationship between molecules of ATP cleaved and numbers of ions that pass through CFTR (Collins, 1992).

CFTR also has a highly charged central domain (regulatory "R" domain), which contains a number of serine residues that are targets for phosphorylation (Riordan *et al.*, 1989). Phosphorylation of the serine residues on the R domain by cAMP-dependent PKA or by PKC is required for the channel to open (Cheng *et al.*, 1991, Carson *et al.*, 1995). PKC results in weak activation of CFTR when added alone but it potentiates the response to PKA (Billet *et al.*, 2013). Once the R domain is phosphorylated, intracellular ATP interacts with the NBDs to regulate channel activity.

In addition to functioning as a Cl^- channel, CFTR has also been implicated in the regulation of another apical membrane conductance via interaction with ENaC. Gentzsch *et al* (Gentzsch *et al.*, 2010) have shown that CFTR physically associates with ENaC in primary human airway epithelial cells and reported that CFTR markedly impedes ENaC stimulation by suppressing proteolysis of its extracellular domains. ENaC inhibition via a cAMP/PKA activation of CFTR is physiologically appropriate since, for effective Cl^- secretion, ENaC must be inhibited in order to maintain the driving force for Cl^- exit from the cell.

Mutation of the CFTR channel leads to severe lung disease in the form of cystic fibrosis (CF), with over 1000 mutations for the channel having been identified to date. The most common mutation of CFTR, which occurs on 70% of all CF chromosomes, is the deletion of a single phenylalanine residue at position 508 in the CFTR protein called the F508del mutation (formerly known as △F508), and has a deleterious effect on protein processing through endoplasmic reticulum under-glycosylation (Rommens *et al.*, 1989, Riordan *et al.*, 1989). The G551D missense mutation of CFTR (Gly to Asp at position 551), unlike F508del- CFTR, escapes the endoplasmic reticulum to become fully glycosylated and enter the plasma membrane, but has little or no functional activity and is associated with severe disease (Riordan *et al.*, 1989).

In the human CF lung, thick, tenacious secretions obstruct the distal airways and submucosal glands, which express CFTR (Engelhardt *et al.*, 1992). CF epithelia absorb excessive liquid, resulting in a depletion of the PCL, resulting in mucus layer tethering to epithelial mucins and impaired ciliary beating (Knowles and Boucher, 2002). This defect in mucociliary clearance facilitates colonization of the airways by opportunistic pathogens leading to chronic inflammation. For years excessive functioning of the epithelial sodium channel (ENaC) was believed to be characteristic of airway surface dehydration seen in the CF lung phenotype (Mall *et al.*, 2004). However, recent studies using a porcine model have shown that CF airway epithelia lack anion conductance but do not hyperabsorb sodium (Itani *et al.*, 2011). According to current statistics by the World Health Organisation, CF is predominantly a Caucasian disease and has high incidences in North America (1:3500), Europe (1:2000-3000) and Australia (1:2000). Ireland has the highest incidence of CF worldwide (1:1461). Fortunately, recent developments in the understanding of the genetics and molecular mechanisms of CF, have led to new targets for treatment and an increasingly positive outlook.

1-4.2 Calcium-activated Chloride Channel (CaCC)

It was first reported almost three decades ago that, in addition to CFTR, calcium-activated chloride channels (CaCC) capable of stimulating Cl^- secretion are present in the airways (Frizzell *et al.*, 1986, Knowles *et al.*, 1991). CaCC channels are of particular interest under pathological conditions where CFTR loss of function occurs, eg. CF, as they become the primary route for Cl^- secretion. Investigators found that Cl^- channels could be activated in excised membrane patches from CF cells, when they were placed in solutions with sufficient extracellular free calcium (Frizzell *et al.*, 1986).

Recently members of the anoctamin 1 (Ano1) family of proteins, also known as the transmembrane protein 16 (TMEM16), have been identified as essential components of CaCCs (Caputo *et al.*, 2008, Schroeder *et al.*, 2008, Yang *et al.*, 2008). Ano1/TMEM16 is highly expressed in secretory epithelial tissues including ductal glands, where it has been implicated to play an important role in calcium stimulated Cl^- secretion. However the role played by

TMEM16A in the airways remains controversial. Studies by Namkung *et al* (Namkung *et al.*, 2011) had suggested that while TMEM16A carries nearly all CaCC current in salivary gland cells, it is only a minor contributor to CaCC currents in airway and intestinal epithelia. In contrast, Huang *et al* reported in 2012 that in fact TMEM16A is expressed in the airway epithelium and airway smooth muscle cells and that expression of TMEM16A is increased in the secretory cells of asthmatic airways (Huang *et al.*, 2012a), indicating that TMEM16A is the primary channel for Ca^{2+} activated Cl^- secretion in the airways.

In general cAMP/CFTR dependent Cl^- secretion is much more sustained than Ca^{2+}/TMEM16A-dependant secretion, due to the transient nature of the intracellular Ca^{2+} signal (Kunzelmann *et al.*, 2012). Therefore, Cl^- secretion through TMEM16A-CaCC must be highly sensitive to changes in intracellular Ca^{2+} levels. ATP, interacting with apical purinergic receptors ($P2Y_2$-R) can inhibit Na^+ absorption and initiate/accelerate Cl^- secretion via PKC-mediated actions on ENaC and Ca^{2+}-mediated actions on calcium activated chloride channels (CaCC) (Chambers *et al.*, 2007). The quantities of ATP, and its metabolic product adenosine, on airway surfaces are determined by the mechanical stresses imparted to airway epithelia during breathing that regulate the rate of ATP release from epithelial cells into ASL (Tarran *et al.*, 2006).

1-4.3 $Na^+/K^+/2Cl^-$ Cotransporter

Transporters are distinguished from channels because they mediate the transport of ions and molecules by physically binding to and moving the substance across the membrane. The $Na^+/K^+/2Cl^-$ cotransporters are a class of ion transporters that transport Na^+, K^+ and Cl^- into and out of the cell in an electrically neutral manner with a stoichiometry of $1Na^+:1K^+:2Cl^-$ (Haas and Forbush, 2000). NKCC2 is present only in the kidney while NKCC1 is distributed throughout a wide variety of secretory epithelia (Lionetto and Schettino, 2006). It plays an important role in maintaining the water and electrolyte content of individual cells and in promoting salt and water movement across polarized cells. In particular, it provides the major chloride

entry mechanisms present in most chloride absorptive and secretory epithelia (Lionetto and Schettino, 2006).

In most cell types studied to date, $Na^+/K^+/2Cl^-$ cotransport is activated by cell shrinkage and as such plays a potential role in the regulation of cell volume (Haas and Forbush, 2000). $Na^+/K^+/2Cl^-$ cotransport in all cells and tissues is inhibited by the 5-sulfamoylbenzoic acid loop diuretics, which include (in order of increasing potency) furosemide, bumetanide, and benzmetanide, although the inhibitory potency of these drugs for $Na^+/K^+/2Cl^-$ cotransport varies significantly between tissues and species (Haas and Forbush, 2000, Haas, 1989, Palfrey *et al.*, 1980). Cl^- secretion can be abolished in most airway epithelial cell types by inhibition of the NKCC1 cotransporter indicating that NKCC1 plays a vital role in Cl^- entry into the cell.

1-4.4 Na^+/K^+ ATPase

ATPases are a family of transporters that transport molecules against a concentration gradient in a thermodynamically unfavourable process and so must be coupled to an exergonic process, in this case hydrolysis of ATP (Kaplan, 2002). The Na^+/K^+ ATPase was discovered by Jens C. Skou in 1957, and is an important regulator of intracellular electrolyte levels in almost all animal cells (Skou, 1957). It maintains low intracellular Na^+:K^+ ratio essential for the normal cell function by catalysing the active uptake of K^+ and extrusion of Na^+ at the expense of hydrolysing one ATP unit with a stoichiometry of $3Na^+$ for $2K^+$, which establishes and electrochemical gradient in the cell (Mobasheri *et al.*, 1997).

The Na^+/K^+ ATPase is a P-type ion transporter, found in the plasma membrane, that consists of a catalytic α subunit and a glycosylated β subunit, both of which contain several membrane spanning segments (Kaplan, 2002). The α subunit is a large, ~ 1000 amino acid complex that contains the Na^+ and K^+ antiporter function coupled to the ATPase activity. The β subunit is a small 330 amino acid single transmembrane spanning protein thought to act as a chaperone to traffic the α subunit to the membrane from the endoplasmic

reticulum and to modulate ion transport (Geering, 2001). Mobasheri *et al* (Mobasheri *et al.*, 1997) have characterized multiple isoforms of α and β subunits of the Na^+/K^+ ATPase that exhibit different kinetic parameters and tissue distribution. Additional regulatory subunits of the Na^+/K^+ ATPase belong to a family of seven single-span transmembrane proteins containing an FXYD (γ) motif in the transmembrane region (Vagin *et al.*, 2011). However, it is believed that the γ-subunit is not essential to the function of the Na^+/K^+ ATPase in many tissues (Therien and Blostein, 2000).

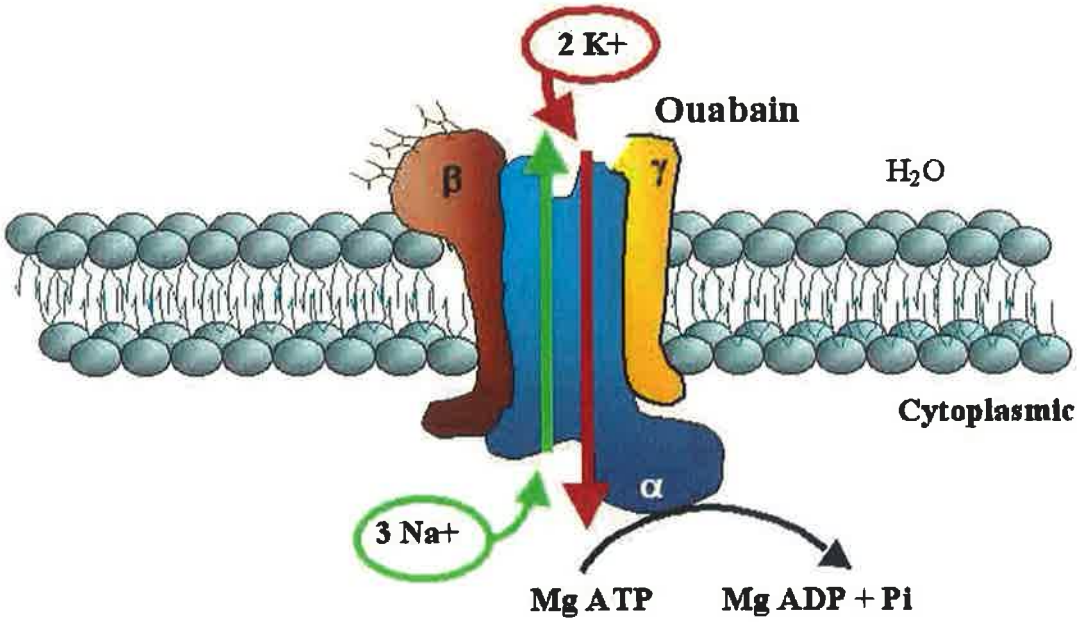

Fig 1.8 The structure of Na^+/K^+ ATPase. The Na^+/K^+ ATPase consists of 3 membrane spanning subunits, α, β, γ. The α subunit is the largest subunit, responsible for the transport of Na^+ and K^+, which is coupled to the ATPase activity. The β subunit is a small single transmembrane spanning protein thought to act as a chaperone to traffic the α subunit to the membrane and to modulate ion transport. The smallest subunit is the γ subunit, thought to regulate pump activity but is not considered essential to the function of Na^+/K^+ ATPase. **Image from:** *http://www.bioscience.org/2001/v6/d/watson/figures.htm*

When Na^+/K^+ ATPases have ATP bound they can bind Na^+ and the phosphorylation of the pump results in a conformational change that exposes Na^+ ions to the outside of the cell and they are released (Kaplan, 2002, Jorgensen and Pedersen, 2001). Na^+/K^+ ATPase then binds to extracellular K^+ ions causing dephosphorylation of the α-subunit, resulting in a return to its

original conformation, exposing K^+ to the inside of the cell and they are released, allowing ATP to bind again. In addition to autophosphorylation in the P-domain of Na^+/K^+ ATPases, these pumps are also subject to additional regulatory events catalysed by PKA and PKC (Therien and Blostein, 2000, Beguin *et al.*, 1994). PKC and PKA phosphorylation of the α-subunit has been implicated in the inhibition of Na^+/K^+ ATPase activity.

The basolaterally located Na^+/K^+ ATPase works together with the apically located ENaC to generate a transepithelial osmotic gradient which drives fluid absorption (Factor, 2001). It has been shown that low concentrations of extracellular Na^+ (0 – 10 mM) have an inhibitory effect on the Na^+/K^+ ATPase activity while increasing concentrations of Na^+ up to 100 mM have a stimulatory effect on the rate of Na^+/K^+ exchange (Kaplan and Hollis, 1980).

1.4.5 Basolateral K^+ Channels

During Cl^- secretion, Cl^- ions enter the secreting cells via the $Na^+/K^+/2Cl^-$ cotransporter and leave the luminal surface through apical Cl^- channels resulting in an accumulation of K^+ by the secreting cell (McNamara *et al.*, 1999). This K^+ must exit the cell in order to maintain the driving force for further Cl^- secretion and therefore the basolateral K^+ channels (KCNQ1/KCNE3 and KCNN4) play a very important role within the cell (Kunzelmann *et al.*, 2012, McNamara *et al.*, 1999). In epithelial fluid secretion there is a simultaneous opening of K^+ channels and an associated flux of K^+ into the interstitial fluid, resulting in a transepithelial electrical potential that in turn drives paracellular transport, which finally generates the osmotic gradient that drives water secretion (Begenisich and Melvin, 1998).

In most secretory epithelia that exhibit hormone stimulated transepithelial secretion, such as those of the airways and intestines, Cl^- channels in the apical membrane appear to represent the primary site of hormone action, although in some cases (particularly with some secretagogues using $[Ca^{2+}]$ instead of cAMP as second messenger) basolateral K^+ channels may also be directly activated (Haas and Forbush, 2000). ATP regulated K^+ channels that

are involved in the recycling of K^+ in parallel with the Na^+/K^+ ATPase have also been shown to play an important role in regulation of epithelial ion transport (Urbach *et al.*, 1996). It has been shown that voltage gated K^+ channels encoded by the KCNQ family of genes, usually associated with the KCNE3 proteins are important regulators of airway epithelial activity (Greenwood *et al.*, 2009). KCNQ channels are themselves regulated by intracellular cAMP levels and are responsible for stabilizing resting membrane potential in many cell types.

Although controversial, there have also been reports in the literature to indicate the presence of apical K^+ channels in the airway (Zhao *et al.*, 2012). Functional large conductance Ca^{2+} -activated and voltage dependent K^+ (BK) channels have been shown to be apically expressed in freshly isolated and cultured primary human airway epithelial cells, grown at an air-liquid interface with tight junctions intact (Manzanares *et al.*, 2011). It has been suggested that these channels could contribute to the osmotic gradient by moving K^+ out from the apical membrane, partially substituting for the paracellular movement of Na^+.

1.4.6 ENaC

The epithelial sodium channel (ENaC) is expressed at the apical membrane of several ion-transporting epithelia throughout the body, including principal cells in the distal nephron of the kidney, urinary bladder, distal colon, lung airways and ducts of salivary glands and sweat glands (Bhalla and Hallows, 2008). In proximal lung airways, ENaC has a distinct role in controlling fluid reabsorption at the air-liquid interface, thereby determining the rate of mucociliary transport (Randell and Boucher, 2006).

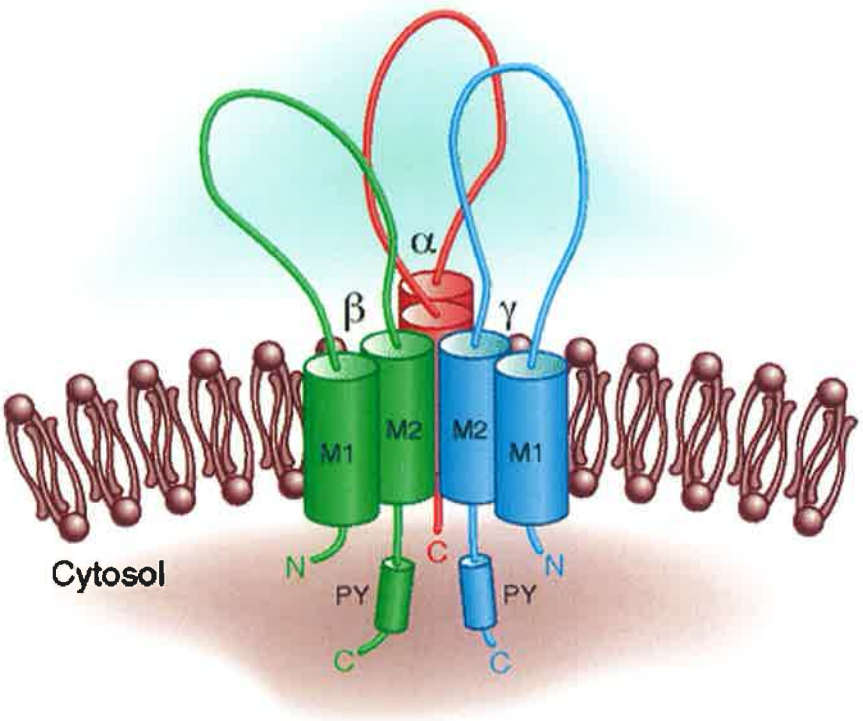

Fig 1.9 The Structure of the Epithelial Sodium Channel (ENaC) (Bhalla and Hallows, 2008) ENaC is a membrane bound Na^+ selective ion channel made up of three subunits, each (α,β,γ) that are 30% homologous at the protein level. Each of the subunits consists of 2 transmembrane helices (M1 and M2) and an extracellular loop. All 3 subunits also contain an intracellular N- domain and intracellular C- domain. The β and γ subunits each contain a proline rich PY motif in their C-termini, which functions to regulate channel activity. Post-translational modifications such as, glycosylation or proteolytic cleavage of specific subunits, play an important role in the regulation of ENaC activity and expression. Maximal sodium transport occurs when ENaC is preferentially assembled into heteromeric α,β,γ complexes.

The highly sodium-selective epithelial sodium channel (ENaC) is a membrane bound ion channel made up of three subunits (α,β,γ) that are 30% homologous at the protein level (Grunder *et al.*, 2001). Each subunit is approximately 85-95 kDa in size in their unmodified state, however, glycosylation, proteolytic cleavage and other post-translational modifications play an important role in the regulation of ENaC activity and expression (Bhalla and Hallows, 2008). It has been shown that maximal sodium transport occurs when ENaC is preferentially assembled into heteromeric α,β,γ complexes (Bonny *et al.*, 1999, Harris *et al.*, 2008). Studies demonstrate that the α subunit plays an important role as a chaperone bringing the β and γ

subunits to the membrane but that the β and γ subunits are essential for optimal function of the channel (Bonny *et al.*, 1999).

Regulation of ENaC in the airways is very important, especially in the newborn where large volumes of fluid need to be rapidly cleared from the airways to prevent alveolar flooding during breathing. The external environment of the lung is constantly changing in response to inhaled insults and so there is constantly a need for rapid dynamic changes in salt and water reabsorption and secretion. Several intrinsic and extrinsic factors which have evolved to regulate ENaC include; hormonal regulation such as aldosterone, mechanical and cytoskeletal activity, proteolytic cleavage by channel activating proteases (CAPs), ubiquitination, self-feedback inhibition, regulation of ENaC trafficking, phosphorylation and pH (Bhalla and Hallows, 2008).

1-5. Regulators of Epithelial Ion Transport

Airway epithelial cells have evolved a number of signalling pathways that tightly regulate ion transport and that can quickly respond to changes in their environment. This is a key feature of lung defence in order to ensure that the airways have adequate apical fluid for effective removal of pathogens. Cells can easily switch from an absorptive to secretory phenotype, and vice versa, in response to various endogenous stimuli such as hormones (including gluco-and mineralocorticoids), inflammatory mediators, channel activating proteases, shear stress, nucleotides or in response to inhaled pathogens or irritants. Each of these stimuli can induce signalling via many different kinase pathways, such as serum and glucocorticoid induced protein kinase (SGK1), mitogen activated protein (MAP), extracellular signal-regulated kinase (ERK), protein kinase A (PKA), protein kinase C (PKC), usually through the mobilization of a number of key 2nd messengers such as Ca^{2+} or cAMP, which we will focus on in this study.

Changes in the levels of cytoplasmic cAMP and Ca^{2+} have been described as important 2nd messengers involved in the epithelial response to secretagogues. Rapid intracellular cAMP and Ca^{2+} signals are usually elicited

through stimulation of purinergic ($P2Y_{2,4,6}$ and A2B) receptors, or basolateral hormonal stimulation (prostaglandin, muscarinic and other receptors) (Kunzelmann *et al.*, 2012). For almost the past 30 years it has been known that both apical Cl^- conductance and basolateral K^+ conductance, two key features of airway secretion, are regulated by cAMP and Ca^{2+} in tracheal epithelial cells (Welsh and McCann, 1985).

1-5.1. Intracellular Calcium

Calcium acts as a universal 2nd messenger in a variety of cells. These cells contain binding proteins that act as links between the Ca^{2+} messenger and various cellular phenomena. By itself Ca^{2+} is a metal ion that can be extremely toxic to cells and so the concentration of intracellular Ca^{2+} ($[Ca^{2+}]_i$) is tightly regulated. The $[Ca^{2+}]_i$ is usually kept at a very low concentration (~100 nM) while the Ca^{2+} levels of the extracellular environment or the calcium stores within the endoplasmic reticulum can reach more than 1000 times higher at ~ 1 mM (Mikoshiba, 2007). Therefore cytoplasmic Ca^{2+} levels can rise very quickly in response to agonists that mobilize Ca^{2+} from intracellular stores or stimulate Ca^{2+} influx from the extracellular environment. This results in the evocation of rapid and transient Ca^{2+} signalling cascades.

Cells tightly control intracellular Ca^{2+} concentration ($[Ca^{2+}]_i$) with several Ca^{2+} regulatory mechanisms such as Ca^{2+} pumps, Ca^{2+} channels and Ca^{2+} exchangers (Takahashi *et al.*, 1999). When ligands bind to G-protein coupled receptors (GPCR) in the plasma membrane, the result is often activation of phospholipase C (PLC), which in turn cleaves membrane lipids to produce inositol triphosphate (IP_3) and diacylglycerol (DAG) (Toumi *et al.*, 2011). IP_3 then releases Ca^{2+} from various intracellular stores, including the endoplasmic reticulum, while DAG activates different forms of protein kinase C (PKC). One important feature of IP_3 mobilization of Ca^{2+} is that its target, the IP_3 receptor (IP_3R), has in fact been shown to be a functional Ca^{2+} channel when incorporated into lipid bilayer (Mikoshiba, 2007).

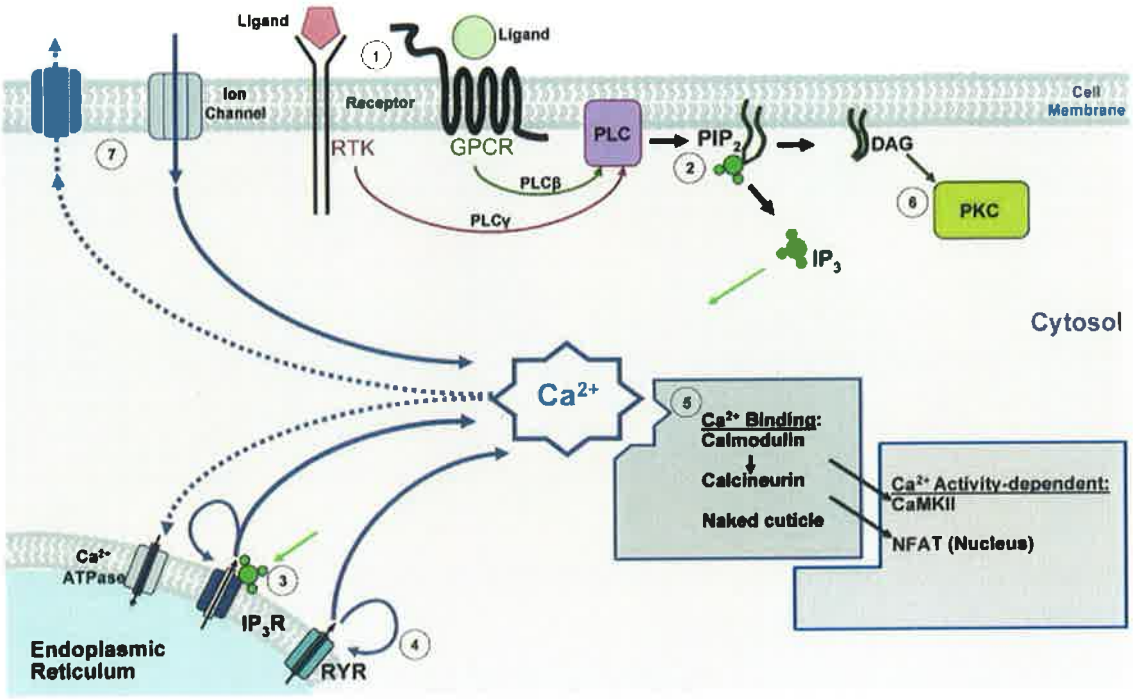

Fig 1.10 An overview of Ca^{2+} signalling in non-excitable cells . (1) Ligand binding to G-coupled protein receptors (GPCR) or receptor tyrosine kinases (RTK) leads to the activation of phospholipase C (PLC) isoforms. (2) PLC catalyzes the hydrolysis of membrane bound phosphatidylinositol (4,5) bisphosphate (PIP_2) giving rise to inositol 1,4,5 triphosphate (IP_3) and diacylglycerol (DAG). In non-excitable cells, the majority of Ca^{2+} release is through IP_3-sensitive Ca^{2+} channels in the endoplasmic reticulum (ER) (3) IP_3 binds to its receptor (IP_3R) on the ER and triggers Ca^{2+} release from the store. (4) This Ca^{2+} released from the ER can bind back to IP_3Rs and neighbouring ryanodine receptors (RYR) inducing the channels to open, stimulating Ca^{2+} induced Ca^{2+} release. (5) The free intracellular Ca^{2+} is then rapidly bound by Ca^{2+} binding proteins, eg calmodulin, which leads to the induction of signalling cascades such as, Ca^{2+}calmodulin-dependent kinase II (CaMKII) or nuclear factor of activated T cells (NFAT),as shown here. (6) At the same time, DAG can act as an additional second messenger to activate further downstream targets such as PKC. (7) Clearance of cytoplasmic Ca^{2+}, shown by dashed lines, occurs by Ca^{2+} extrusion via pumps and Na^{+}/ Ca^{2+} exchange in the plasma membrane, as well as by uptake into intracellular stores, such as the endoplasmic reticulum. **Image adapted from (Slusarski and Pelegri, 2007)**.

A variety of secretory cells respond to cholinergic stimulation by raising $[Ca^{2+}]_i$. In these cells both Ca^{2+} channels and Ca^{2+} pumps are present, which work together to maintain resting $[Ca^{2+}]_i$, restore $[Ca^{2+}]_i$ after stimulation, and mediate refilling of the intracellular calcium store (store-operated Ca^{2+} entry) (Negulescu and Machen, 1993) . There is increasing evidence emerging from the literature to indicate cross-talk between the Ca^{2+} and cAMP signalling

pathways, with particular interest in the relationship between cAMP and store-operated Ca^{2+} channels.

Namkung *et al* (Namkung, 2010) have shown that intracellular calcium also affects the activity enzymes that control intracellular cAMP levels such as adenylate cyclase and phosphodiesterase, concluding that CFTR is the principal Cl^- secretory pathway in non-CF airways for both cAMP and Ca^{2+} agonists. This is further supported by a recent study demonstrating that activation of the M3 muscarinic receptor in airway submucosal glands can activate CFTR by a Ca^{2+} dependent increase in cAMP and phosphorylation of PKA, through inhibition of the phosphatase PPA2 and through direct phosphorylation of CFTR by tyrosine kinases (Billet *et al.*, 2013). In addition to the effects on CFTR, mobilization of Ca^{2+}_i also results in the stimulation of Cl^- secretion in epithelial cells via activation of both the apical CaCC channels and the basolateral K^+ channels that hyperpolarize the cell, providing the driving force for further Cl^- secretion (Manzanares *et al.*, 2011, Haas and Forbush, 2000, Caputo *et al.*, 2008, Mroz and Keely, 2012a).

1-5.2 Cyclic Adenosine 3', 5' Monophosphate (cAMP)

Cyclic AMP is an important intracellular 2nd messenger discovered by Earl W. Sutherland Jr and Theodore W Rall in 1956 (Sutherland and Rall, 1958), that has since been shown to modulate a wide range of cellular events that are crucial to airway function, such as relaxation of the airway smooth muscle, mucin secretion, anion transport, proliferation, and wound healing. Activation of cAMP is induced by ligand binding to a G-protein coupled receptor, which in turn through G-proteins that regulate various different isoforms of adenylate cyclase, results in the generation of cAMP (Tasken and Aandahl, 2004). Intracellular levels of cAMP are controlled by differential expression and regulation of the adenylate cyclase and phosphodiesterase families of enzymes. Phosphodiesterases are enzymes that break down cyclic nucleotides and play an important and highly regulated role in maintaining resting cAMP concentrations within the cell (Jin *et al.*, 1999). Since the identification of forskolin as a specific and potent reversible activator of adenylate cyclase in 1981 (Seamon *et al.*, 1981), there have been many

studies conducted which greatly improve our understanding of the relationship between cAMP concentrations and physiological function in various tissues. It has been reported that forskolin, through mobilization of cAMP, can induce fluid secretion in the submucosal cells of porcine bronchi via activation of Cl^- and HCO_3^- secretion (Ballard *et al.*, 2006). In addition, phosphorylation of the serine residues of the regulatory domain of CFTR by cAMP dependant protein kinase A (PKA), in response to cAMP agonists has been shown to be required for CFTR activation (Cheng *et al.*, 1991).

Although the cAMP signalling pathway can have many different downstream effectors, it was previously thought that the most commonly used effector by cells was activation of PKA. However, over the past two decades much attention has been drawn to the exchange protein directly activated by cAMP (Epac), highlighting the importance of this protein in cAMP signalling. Epac was characterized by de Rooij et al (de Rooij *et al.*, 1998) in 1998 as belonging to a family of guanine nucleotide exchange factors that catalyse the conversion of GDP bound to G-proteins to GTP, activating the G-Protein. The main targets for Epac are Ras-like GTPases Rap 1 and Rap 2. The discovery of this second major pathway for cAMP signalling in cells has provided a better understanding of the diverse range of cellular processes which cAMP can regulate.

It has been shown that PKA and Epac can have opposing effects on cellular processes in different tissues, eg. cell migration, thus reinforcing the need for tight regulation of the downstream effectors of cAMP mobilization (Billington and Hall, 2012). While it is important to acknowledge that agonists which result in the generation of cAMP in airway epithelial cells may have many further reaching effects than stimulation of ion transport, for the purposes of this study we are mostly interested in the stimulation of Cl^- secretion in the airway. Therefore we will focus on cAMP activation of PKA and hence stimulation of Cl^- secretion through activation of CFTR.

1-5.3 Protein Kinase A (PKA)

The PKA signalling pathway has evolved to become one of the most versatile and commonly used signalling pathways in eukaryotic cells and plays an important role in the regulation of cellular functions in all mammals. There are two different PKA isoforms, PKA I or PKA II. Each PKA isoform is composed of two different catalytic subunits, which are conserved between isoforms, and two identical regulatory subunits, which are biologically and physically different between PKA I and PKA II (Tasken and Aandahl, 2004) The relative abundance of PKA I or PKA II is determined during development and cell growth. PKA II is predominantly expressed in non-proliferating tissues and growth arrested cells whereas PKA I is often found in rapidly dividing cells and tumours but only transiently in normal cells that have been exposed to mitogenic stimuli (Ciardiello and Tortora, 1998).

An increase in intracellular cAMP facilitates the binding of two molecules of cAMP to each regulatory subunit, resulting in dissociation of the catalytic subunit and induction of catalytic activity (Billington and Hall, 2012). PKA anchoring proteins (AKAP) help to improve the specificity of the cAMP signal transduction by placing PKA close to effector or substrate locations within the cell. AKAPs also are important in regulating PKA activity by targeting PKA to adenylate cyclases (for activation) or phosphodiesterases (for negative feedback inhibition of signal) (Wong and Scott, 2004). PKA is known to activate CFTR by phosphorylation of its regulatory subunit, at a number of different serine residues. In addition Cl^- secretion in the airways has been shown to be modulated by PKA activation of basolateral K^+ channels (Fung *et al.*, 2011). This demonstrates a dual role for PKA in regulation of Cl^- secretion and hence ASL volume in the lung.

1-5.4 Protein Kinase C (PKC)

PKC belongs to a family of serine/threonine kinases first identified in 1977 (Inoue *et al.*, 1977), which contain at least twelve different isozymes. Members of the PKC family are a single polypeptide composed of a N-terminal regulatory region (20-40 kDa) and a C-terminal catalytic

region(~45kDa) (Newton, 1995). PKC isozymes show high levels of homology in their catalytic domain while differences in their regulatory domains determine different responses to activators (Kheifets and Mochly-Rosen, 2007). The N-terminal region contains the binding sites for activation by Ca^{2+} or phospholipids while the C-terminal region contains the substrate binding site responsible for kinase activity.

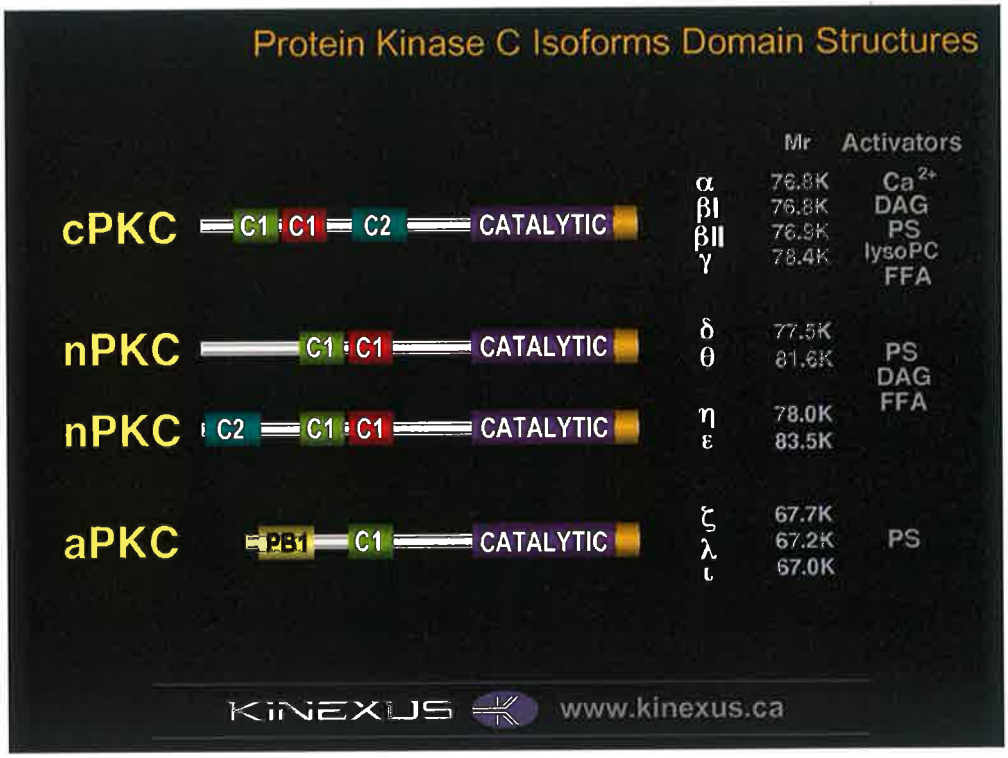

Fig 1.11 The basic structure of PKC isoforms. All PKCs contain a catalytic domain, which shows high levels of homology across isozymes, and a regulatory domain. The regulatory domain of each PKC contains some shared subregions across PKC isozymes. The C1 domain contains the binding site for DAG and phorbol esters in all PKCs except the atypical PKCs (aPKC). The C2 domain acts as a Ca^{2+} sensor but is only functional in the classical PKCs (cPKC). The aPKCs are not activated by Ca^{2+} or DAG but instead depend on phosphatidylserine activation at region PB1. **Image from: *www.kinexus.ca***

The family of classical PKC isozymes (α, βI, βII, γ) are activated by Ca^{2+}, DAG/phorbol esters and phospholipids, while the novel family of PKC isozymes (ε, δ, η, θ, μ, υ – the latter two belonging to the distant PKD family) respond only to DAG/phorbol esters and phospholipids (Kheifets and Mochly-

Rosen, 2007). Ca^{2+} promotes DAG activation of classical PKC isozymes, while phorbol esters have been shown to cause PKC to translocate to the membrane. Novel PKC isozymes are more sensitive to activation by DAG and so do not require Ca^{2+}. The least understood isozymes are the atypical PKCs (ζ, λ, ι). Atypical PKC isozymes differ significantly in structure from the classical or novel PKCs and they do not respond to phorbol esters (Newton, 1995).

It is widely accepted now that the PKC family of kinases are critical to many cellular processes, such as regulation of transcription, modulation of membrane structure events, mediating immune response and cell growth. Each member of the PKC family can often be found in the same cell but migrate to different intracellular locations upon activation, where they can have different and sometimes opposing effects (Kheifets and Mochly-Rosen, 2007). While it has been reported many times that PKC modulation of ion transport is cell and PKC isozyme specific, the most compelling evidence for a specific role of PKC on Cl^- secretion has come from studies in the airways (Liedtke *et al.*, 2005). It has been shown that while PKCε activates CFTR, Cl^- secretion is maintained by activation of NKCC1 via a complex cascade of kinases including PKCδ and protein phosphatases (PP2A). Although CFTR contains at least seven potential sites for phosphorylation by PKC, the role of PKC in activation of CFTR was unknown for many years (Jia *et al.*, 1997). In 1997, it was shown that PKC mediated-phosphorylation of CFTR not only enhances CFTR responses but is actually required for acute PKA activation of CFTR (Jia *et al.*, 1997). They suggest that under normal conditions, phosphorylation of CFTR by PKC has a constitutive role in "priming" the channel for activation by PKA. These studies therefore demonstrate how PKC isoforms can modulate the activity of both CFTR and NKCC1 to regulate Cl^- secretion in the airway epithelium.

1-5.5 Bile acids

Bile acids are physiological detergents derived from the enzymatic conversion of cholesterol into primary bile acids in the hepatocytes (Abu-Hayyeh *et al.*,

2013). The classical function of bile acids is lipid metabolism and facilitation of bile flow. In recent years however, there has been increased interest in the role bile acids play as signalling molecules and modulators of epithelial ion transport, particularly in the colon. Previous work by Keely *et al* has shown that both the conjugated and unconjugated forms of the two common dihydroxy bile acids, chenodeoxycholic acid (CDCA) and deoxycholic acid (DCA), induce Cl^- secretion in the mammalian colon (Keely *et al.*, 2007). However, the taurine conjugate of DCA, taurodeoxycholic acid (TDCA) was only able to induce secretion when applied to the basolateral side of the epithelial monolayer. This demonstrated that bile acid stimulation of Cl^- secretion was specific to the structure of the bile acids and could be modulated by bacterial dehydroxylation of primary bile acids into secondary bile acids, or by microbial enzymatic removal of the conjugated glycine or taurine from the bile acid (Keely *et al.*, 2007).

Keating *et al* have observed that high concentrations of DCA (0.5 - 1 mM) acutely stimulate colonic epithelial Cl^- secretion and reduce transepithelial electrical resistance (TEER) (Keating *et al.*, 2009). In contrast, they found that chronic exposure to low levels of DCA (>200 μM) decreased epithelial Cl^- secretion without causing apparent cell damage. These findings were physiologically relevant in the gut as they indicate that under normal conditions, low concentrations of bile acids (~50 – 200 μM) promote absorption to conserve the large volumes of fluid that enter the intestine each day. However, under conditions of bile acid malabsorption, high concentrations of bile acids (>500 μM) enter the colon and stimulate Cl^- and fluid secretion, thereby causing diarrhoea (Keating *et al.*, 2009). Bile acids have also been shown activate phospholipase C in colonic epithelium, increasing IP_3 and intracellular Ca^{2+}, further supporting bile acid stimulation of epithelial Cl^- secretion (Kanchanapoo *et al.*, 2007). In 2013, it was also demonstrated that CDCA can activate CFTR via cAMP/PKA pathway in T_{84} cells (Ao *et al.*, 2013).

In addition, it has recently been reported that the metabolite of CDCA, ursodeoxycholic acid (UDCA), formed by the colonic bacteria, also modulates colonic Cl^- secretion (Kelly *et al.*, 2013). Kelly *et al* demonstrate that UDCA attenuates the activity of the Na^+/K^+ ATPase and basolateral K^+ channels, without changing surface expression of either, resulting in decreased overall Cl^- secretion. However, *in vivo* studies of UDCA in mice resulted in enhanced colonic secretory response to agonists, likely due to bacterial conversion of UDCA to lithocholic acid (LCA) within the mouse colon (Kelly *et al.*, 2013). This provides further evidence to support the importance of bile acid structure in modulating Cl^- secretion. Taken together, these studies suggest a novel role for bile acids as regulators of epithelial secretion since patho-physiologically high concentrations of bile acids induce secretion while lower, physiologically relevant concentrations of bile acids chronically down-regulate colonic epithelial secretion (Keating and Keely, 2009a, Keely *et al.*, 2007, Keating *et al.*, 2009). They also provide a strong basis for the hypothesis that bile acids modulate ion transport in the airway epithelium.

Acidification of the airways can occur under certain conditions, such as in CF, where the pH has been reported to be approximately 6 (Pezzulo *et al.*, 2012) or in patients who experience gastroesopageal acid reflux (Vic *et al.*, 1995, Ledson *et al.*, 1998, Blondeau *et al.*, 2010). Using a model of normal bronchial epithelium grown at air-liquid interface, it has been shown that under acidic conditions (pH 6), bile acids were able to disrupt the squamous epithelial barrier function partly by modulating the levels of tight junction proteins claudin-1 and claudin-4, however the underlying mechanisms for such disruption of the tight junctional proteins remains unclear (Chen *et al.*, 2011). This report suggests that the presence of bile acids in the lungs of patients, where airway acidification has already occurred, might result in disruption of the epithelial barrier function. Most recently, it has been shown that CDCA increases alveolar permeability via degradation of junctional proteins resulting in reduced TEER (Su *et al.*, 2013). Disruption of the integrity of the epithelial layer would establish more "leaks" in the tissue as flow of ions through the paracellular pathway increases, resulting in deregulation of airway epithelial ion transport. Therefore in this thesis, it was important to establish the effects

of bile acids on airway transepithelial resistance, in addition to modulation of airway epithelial ion transport, in order to get a clearer insight into how bile acids might affect fluid transport, leading to pulmonary edema and impaired mucociliary clearance in the airways.

1-6. Bile Acids

Bile is both a digestive and secretory fluid that is secreted by the liver into the intestine in vertebrates (Hofmann, 1999a). It contains bile acids/salts, acidic steroids synthesized by the liver from cholesterol through several complementary pathways (Monte *et al.*, 2009). The most important physiological properties of bile acids are lipid transport as mixed micelles in the biliary tract and small intestine and the excretion of cholesterol into the intestinal tract, where it is poorly absorbed (Abu-Hayyeh *et al.*, 2013, Hofmann, 1999a, Monte *et al.*, 2009). The enterohepatic circulation of bile acids is a closed system that encompasses the flow of bile from the liver, through the biliary tract to the intestine and back to the liver. Recycled bile is stored in the gall bladder where it is released in approximately two bursts after each meal, up to eight times per day in total (Borgstrom *et al.*, 1957).

Most of the bile acids released into the intestine are reabsorbed in the ilium, however, with each cycle of the enterohepatic circulation, a small proportion (~3-5%) of the bile acid pool enters the large intestine (Keely *et al.*, 2007). It is therefore well-accepted that the enterohepatic circulation is an extremely efficient method of bile recycling, facilitating repeated access to a large pool of bile acids each day, rather than re-synthesis of new bile acids by the liver after every meal. It is also possible that the reason for such an efficient closed system of bile acid circulation may be to prevent bile acid accumulation in tissues where they may have pathophysiological effects, such as in the lungs.

1-6.1 Formation of Bile Acids

In humans, the major primary bile acids, cholic acid (CA) and chenodeoxycholic acid (CDCA), are synthesized from cholesterol in the

hepatocyte, after which they are secreted into bile and enter the colon (Zabin and Barker, 1953, Dawson, 1967, Hofmann, 1999a, Monte *et al.*, 2009). Cholesterol modulates its own catabolism to bile acids, mainly at the transcriptional level and some hormones and exogenous compounds may also affect bile acid synthesis (Monte *et al.*, 2009). The rate limiting step for the classic bile acid synthesis pathway is catalysed by cholesterol 7-α hydroxylase. Secondary bile acids are formed by bacteria in the intestine by removal of a hydroxyl group at C-7 from a primary bile acid (Hofmann, 1999a). Bacterial hydroxylation converts CA into deoxycholic acid (DCA) and CDCA into lithocholic acid. Secondary bile acids can then re-enter the bloodstream and enterohepatic circulation.

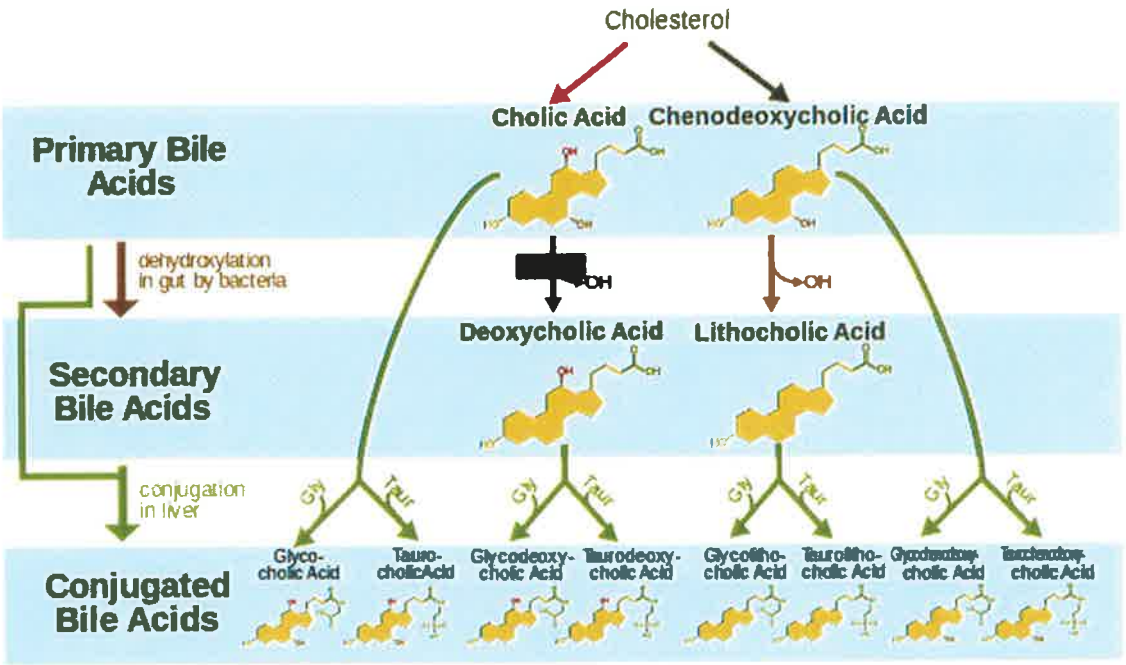

Fig 1.12 The classical pathway for formation of bile acids. In human hepatocytes, the two primary bile acids, cholic acid (CA) and chenodeoxycholic acid (CDCA), are synthesized as result of cholesterol metabolism. CA and CDCA differ in their hydroxylation at C-12. These primary bile acids are usually conjugated to glycine or taurine before they enter biliary flow. Once they reach the digestive tract, microbes in the gut can remove the conjugated glycine or taurine and they can transform the primary bile acids into secondary bile acids via hydroxylation at C-7. CA is transformed in deoxycholic acid (DCA) and CDCA is transformed into lithocholic acid (LCA). Most bile acids then re-enter enterohepatic circulation, returning to the liver where they are re-conjugated to taurine or glycine.

Image from: *https://en.wikipedia.org/wiki/File:Bile_acid_differentiation.svg*

Under normal circumstances the majority of bile acids in circulation are conjugated to glycine or taurine by the hepatocytes before leaving the liver. Unconjugated bile acids are usually only found in the colon, where the taurine or glycine conjugate has been removed by the native bacteria. However, proton pump inhibitor therapy in patients with gastro-esophageal reflux disease (GERD) can result in bacterial overgrowth in the intestine, causing deconjugation of bile acids and thus an increase in circulating unconjugated bile acids (Theisen *et al.*, 2000).

1-6.2 Conjugation status

After bile acid synthesis in the liver, the majority of bile acids in humans are conjugated to either glycine or taurine at their terminal side chain carboxylic acid. Bile acid conjugation is carried out by the enzyme, bile acid CoA amino acid N- acetyltransferase (BAAT), which has been reported to be present in both the peroxisomes and the cytosol (Solaas *et al.*, 2000). The main purpose of bile acid conjugation is to increase bile acid water solubility and to reduce membrane permeability or Ca^{2+} precipitation of the bile acids, hence keeping the bile acids in the gastrointestinal tract all the way to the ilium, facilitating increased lipid digestion.

The majority of bile acids found in circulation are conjugated bile acids since unconjugated bile acids are usually restricted to the colon, where microbial modification removes the glycine or taurine subunits from the bile acid. This process is catalysed by bile salt hydrolases from the cholololylglycine hydrolase family of enzymes found only in gut microbes and not by mammalian enzymatic cleavage (Monte *et al.*, 2009, Midtvedt, 1974). Most of the microbes in the intestine generally are capable of cleaving both glycine and taurine conjugated bile acids. Bile acids in the chemical form of their conjugates are hydrophilic molecules that cannot cross the plasma membrane. Alternatively, if they are deconjugated by bacterial enzymes they become membrane permeable and can therefore act intracellularly (Keely, 2010).

Song *et al* have reported that in human esophageal epithelial cells, conjugated bile acids are potent inducers of MUC5AC expression, a mucin that is usually only produced in the stomach and the tracheobronchial epithelium (Song *et al.*, 2010). They demonstrated that the conjugated bile acids glycochenodeoxycholate, taurocholic acid, glycocholic acid and taurodeoxycholate, which are major components of bile refluxate in the esophagus, are strong inducers of MUC5AC apomucin expression in the esophagus. Since MUC5AC is an important mucin in the airways, this finding may be relevant for understanding how bile acids could affect mucin secretion and hence mucociliary clearance in the lung

1-6.3 Bile Acid Function

As previously mentioned, the most classical physiological functions of bile acids are facilitation of lipid transport as mixed micelles in the biliary tract and small intestine and the excretion of cholesterol into the intestinal tract. Bile salts reach a critical concentration, known as critical micellar concentration (CMC), at which point, rather than precipitating out of solution they form micelles capable of encapsulating soluble lipid molecules (Dawson, 1967). The CMC is influenced by side chain and nuclear structure. Bile acids affect primarily cell membranes and intracellular organelles (Kauer *et al.*, 1997). Upon completion of their digestive tasks, most intestinal bile acids (95%) are recovered by active transport in the intestine, mainly in the ileum (Monte *et al.*, 2009).

The physical behaviour of the acids depends on their degree of hydroxylation and the type and presence of conjugation of the basic steroid nucleus. Conjugation of bile acids improves their solubility in water and hence makes them more efficient at micelle formation. In addition, conjugation reduces membrane permeability or Ca^{2+} precipitation of the bile acids, keeping the bile acids in the gastrointestinal tract all the way to the ilium, facilitating increased lipid digestion (Monte *et al.*, 2009). Bile acids that are deconjugated by bacteria become more lipophilic increasing their capacity to permeate the epithelial membrane and interact with intracellular bile acid receptors such as

FXR (Keely, 2010). Conjugated bile acids, on the other hand, require cellular uptake by bile acid transporters such as the apical bile salt transporter (ABST). Both conjugated and unconjugated bile acids are recycled across the ilium, with bacterial modification of bile acids increasing passive re-absorption of unconjugated secondary bile acids (Hofmann, 1999b). Unconjugated dihydroxy bile acids such as DCA are more rapidly absorbed than the trihydroxy bile acid, CA, which is less hydrophobic, with the magnitude of bile acid hydrophobicity in the order of UDCA <CA <CDCA <DCA <LCA (Perez and Briz, 2009). The unconjugated bile acids are then re-conjugated to glycine or taurine in the liver, so that the majority of bile acids in circulation are conjugated. Conjugated bile acids are hydrophilic and usually not cytotoxic until their concentrations approach CMC.

Bile acids have been reported to act as cell signalling molecules that regulate many biological processes such as inflammation, proliferation, and epithelial ion transport. The signalling pathways modulated by bile acids include calcium mobilization, cAMP synthesis and activation of PKA and PKC. However, these effects are not induced by all bile acids as responses are affected by the respective bile acids hydrophobicity and/or degree of hydroxylation (Nguyen and Bouscarel, 2008). It has been reported that the more hydrophobic the bile acid, the higher the concentration required to stimulate an increase in intracellular Ca^{2+}, eg 50 μM DCA compared with 10 μM UDCA mobilizes Ca^{2+} in hamster hepatocytes (Nguyen and Bouscarel, 2008). On the other hand, lower concentrations of taurine conjugated bile acids were required to increase intracellular cAMP when compared with unconjugated bile acids, which may be due to a higher affinity of taurine conjugates for TGR5 activation.

There are also marked differences in behaviour of bile acids depending on the pH of the solution in which they reside (Kauer *et al.*, 1997). Bile acids are usually confined to the enterohepatic circulation but they can also often be found in low concentrations in the systemic circulation. Although the total bile acid concentration in serum is approximately 1-5 μM in fasting individuals, bile

acid levels in systemic circulation can increase rapidly upon ingestion of food or during pregnancy and at different stages in the menstrual cycle, although the exact reason for this menstrual fluctuation is unknown (Pennington *et al.*, 1981, Keely, 2010). This provides evidence that bile acids may have further reaching effects than just the intestine, as higher concentrations of bile acids travel through the blood to various tissues throughout the body.

1-6.4 Bile Acid Receptors

Bile acids have been shown to elicit their response through two distinct classes of receptors, nuclear receptors and gPCRs. Bile acid activation of nuclear receptors such as farnesoid x receptor (FXR), pregnane x receptor (PXR), constitutive androstane receptor (CAR) along with the vitamin D receptor, is known to modulate genomic effects that are essential to the regulation of cholesterol, lipid and bile acid homeostasis, immune responses and insulin signalling (Cipriani *et al.*, 2011). Although an increasing number of bile acid receptors have been identified, the two main receptors that we are interested in for the purpose of this study are FXR and the G-protein coupled receptor, TGR5, as they have been implicated in regulation of transport proteins or epithelial secretion (Ward *et al.*, 2013, Toumi *et al.*, 2011, Holt *et al.*, 2003, Keating and Keely, 2009b, Mroz *et al.*, 2013). FXR belongs to the first class of nuclear receptors through which bile acids can regulate long-term changes in cell function mediated by gene transcription (Makishima *et al.*, 1999). The second class of bile acid receptor belongs to the g-protein coupled family of receptors present at the surface of the cell, which is internalised in response to bile acid agonists. This receptor is designated as GpBAR1 (or TGR5) and can mediate more rapid responses (Keely, 2010).

1-6.5 Farnesoid X Receptor

In 1999, Makishima *et al* identified FXR (also known as NR1H4) as an endogenously expressing bile acid nuclear receptor (Makishima *et al.*, 1999). Bile acids regulate their own synthesis and metabolism by activation of FXR, which is a transcription factor containing a ligand binding domain that is sensitive to bile acids and a DNA binding domain (Abu-Hayyeh *et al.*, 2013). It

is now widely acknowledged that FXR plays an important role in the regulation of enterohepatic recycling of bile acids and in the feedback regulation of bile acid biosynthesis in the liver and intestine. Zhang *et al.* have shown that FXR plays a critical role in suppressing the inflammatory response in the lung and promoting lung repair after injury (Zhang *et al.*, 2012). It has previously been shown that bile acids activate FXR with the following magnitude of potency CDCA > DCA > CA > LCA > UDCA, where the EC_{50} of CDCA is 2 -5 μM, while 200 μM UDCA is required for FXR activation (Lew *et al.*, 2004, Claudel *et al.*, 2005).

Upon activation, FXR binds DNA in a complex with the retinoid x receptor and initiates transcription of a cohort of genes involved in decreasing bile acid levels in hepatocytes, specifically transporters such as ABC transporters that facilitate bile acid movement from hepatocytes into the bile (Holt *et al.*, 2003). Since CFTR is also a member of the ABC family of transporters, it was therefore hypothesized that activation of FXR could regulate CFTR expression in epithelial cells, thus modulating chronic secretion, which has recently been confirmed (Mroz *et al.*, 2013). It had previously been shown that activation of FXR chronically downregulates Cl^- secretion in colonic epithelium in a manner which appears to be mediated by inhibition of Na^+/K^+ ATPase (Keating and Keely, 2009b).

1-6.6 TGR5

In 2002, the discovery of TGR5 (also known as M-BAR or BG37 or GPBAR1), a GPCR for bile acids, lead to the establishment of non-genomic functions of bile acids (Maruyama *et al.*, 2002, Kawamata *et al.*, 2003). TGR5 was shown to be expressed on the plasma membrane and internalized in response to direct activation by bile acid agonists, resulting in an increase in cAMP production and induction of MAP kinase signalling (Kawamata *et al.*, 2003). It was soon found that this new receptor differed from previously identified receptors, as potent agonists for the bile acid nuclear receptors, FXR, PXR, and liver X receptor had little or no effect on the activation of TGR5 (Tiwari and Maiti, 2009). This demonstrated an independent signalling pathway for

bile acids to elicit rapid responses through TGR5. In addition, the effective doses of bile acids required to elicit response were lower for TGR5 than for nuclear receptors (Kawamata *et al.*, 2003). In chinese hamster ovary (CHO) cells transfected with TGR-5, TLCA, LCA, DCA, CDCA and CA were found to dose-dependently increase cAMP production at the median effective concentrations (EC_{50}) of 0.33, 0.53, 1.01, 4.43 and 7.72 μM respectively (Kawamata *et al.*, 2003). These responses were abolished in CHO cells that had not been transfected with TGR5, indicating that bile acid activation of TGR5 was responsible for the increase in intracellular cAMP. Furthermore, conjugated bile acids were observed to be agonists for TGR5, without the requirement for a specific transporter as is needed with most nuclear receptors.

In recent years there have been increasing reports in the literature indicating that TGR5 plays a role in bile acid induction of Cl^- secretion in colonic epithelium (Toumi *et al.*, 2011, Ward *et al.*, 2013). TGR5 has been described as an important regulator of both basal colonic secretion and also secretion in response to cholinergic stimulation in the rat colon (Ward *et al.*, 2013). In addition, TGR5 involvement has been implicated in in CDCA activation of CFTR via cAMP/PKA pathway in T_{84} cells (Ao *et al.*, 2013).

1-6.7 Evidence for the presence of bile acids in the airway

Over the past decade there has been steady increase in reports emerging from the literature to indicate the presence of bile acids in the airways, while observing that bile acids are usually associated with a decrease in lung function. Bile acids may reach the lung by aspiration during episodes of gastroesophageal reflux, or have been taken up from the blood under conditions where circulating bile acids levels are increased. Evidence for both entry pathways have been reported and it has been shown that bile acid aspiration produces severe chemical pneumonitis in a porcine lung model, while injected bile acids have been shown to produce severe pulmonary edema in rabbits (Kaneko *et al.*, 1990, Porembka *et al.*, 1993, Perez and Briz, 2009). In the adult, lung injury may occur because of bile aspiration after

gastroesophageal reflux (GER). GER in lung transplant patients may potentially be induced by immunosuppressive drugs or iatrogenic vagal nerve injury at surgery or it may even be present as a preoperative condition (D'Ovidio *et al.*, 2006). Bile acid aspiration is prevalent after lung transplantation, and is associated with the development of bronchiolitis obliterans syndrome (BOS), which is characterized by fibrosis with inflammatory cell infiltrates in and around the airway walls (D'Ovidio *et al.*, 2005). In patients with BOS, who have had lung transplantation, bile acid levels in bronchoalveolar lavage (BAL) fluid can reach levels as high as 32 μmol/L (D'Ovidio *et al.*, 2005).

Serum bile acid levels in fasting individuals have been reported to be in the range of 1-5 μM, but can increase rapidly upon ingestion of food or under certain conditions such as intrahepatic cholestasis of pregnancy (ICP), which occurs during late pregnancy. This results from an imbalance of hormones during pregnancy, which leads to impaired clearance of bile acids from serum. ICP can often persist until delivery leading to a dangerous accumulation of foetal bile acid compounds within the foetus and the new-born. During ICP, circulating bile acid concentrations can reach 40 - 60 μM in the mother and 60 – 120 μM in the newborn (Keely, 2010, Zecca *et al.*, 2004, Zecca *et al.*, 2008). Bile acids have been shown to be present in the BAL of ICP neonates with respiratory distress syndrome (RDS) but were absent in non-lung disease and RDS-non-ICP control groups (Zecca *et al.*, 2008). Elevated serum bile acid levels in these infants suggest that bile acids reach the lung after uptake from circulation.

In children, GER has been associated with respiratory symptoms such as chronic cough and wheezing (Bauman *et al.*, 1996). Children with neurodisability (ND) commonly experience recurrent respiratory problems that often require multiple prolonged hospital admissions (Trinick *et al.*, 2012). In these children, a high incidence of GER is also a well-recognized phenomenon, with aspiration occurring both directly and from reflux. However, much is still unclear regarding the interactions among GER, aspiration, and

respiratory symptoms, with casual relationships often difficult to prove conclusively.

One study has shown that significantly higher levels of bile acids were found in the airways of patients with suspected ventilator-associated pneumonia (VAP) as compared to those without suspected VAP (Wu *et al.*, 2009). They demonstrated that bile acid aspiration may contribute to neutrophilic inflammation in the airways of patients with suspected VAP through CDCA induced interleukin (IL)-8-production, via the activation of mitogen-activated protein (MAP) kinase (Wu *et al.*, 2009). Studies by Perng *et al* have also proposed a mechanism to explain the consequences of exposing airway epithelium to bile acids. Their results indicate that bile acid exposure may induce airway epithelium to produce transforming growth factor β (TGF-β), and connective tissue growth factor (CCN2), which in turn activate autocrine pathways that contribute to the pathogenesis of airway fibrosis (Perng *et al.*, 2007, Perng *et al.*, 2008).

Acid GER is common both in children and adults with Cystic Fibrosis (CF) and has been associated with reduced pulmonary function (Navarro *et al.*, 2001). Bile acids have been reported to be present in the lower airways and sputum of patients with cystic fibrosis (Blondeau *et al.*, 2010, Ledson *et al.*, 1998, Pauwels *et al.*, 2012, Aseeri *et al.*, 2012). Accumulation of intraluminal secretions and chronic destruction of the airway wall together with bronchiolitis are associated with a progressive reduction of lung function in patients with CF (Rowe *et al.*, 2005). As a consequence, the need for antibiotics and bronchodilators increases and this may further affect the gastric and duodenal flora and may impair lower oesophageal sphincter (LES) function, leading to the worsening of GER (Blondeau *et al.*, 2010). The relationship between GER, aspiration, and respiratory symptoms in CF patients has never been fully clarified. There continues to be much debate over whether GER is a primary phenomenon of CF, or secondary to cough or physiotherapy (Blondeau *et al.*, 2010, Vic *et al.*, 1995, Ledson *et al.*, 1998).

Unfortunately, our current knowledge of bile acids in the airways is limited by the lack of reports to identify and quantify specific bile acid levels present in the lungs, due to sampling difficulties and reliability of bile acid assays. Most investigations so far have involved BAL studies (Zecca *et al.*, 2008, Aseeri *et al.*, 2012, Perng *et al.*, 2008), which have limitations as airways are perfused with ~10 ml of fluid and as a result, the concentrations of bile acids present in the BAL may be much more dilute than those which the airways are actually exposed to. In addition, there are many different types of bile acids, which may be differentially conjugated but it is so far unknown which bile acids are more prevalent in the lungs. Furthermore, the type of bile acid that is most abundant in circulation can change with age, diet or drug treatment, and might result in an increase in the ratio of taurine-conjugated secondary bile acids. It could also be hypothesized that colonization of the airways by opportunistic pathogens might result in microbial transformation of conjugated primary bile acids, increasing the presence of unconjugated secondary bile acids in the lung. Nonetheless, most studies to date have investigated only the major bile acids which are most likely to be found in circulation, such as CA, CDCA or DCA, as possible contenders to be present in the airway.

1.7. Aim of the Study

Taken together, the studies described in the previous section provide strong evidence to support the existence of bile acids in the airways. However, although bile acids are present and can sometimes be associated with decreasing lung function, no direct correlation has yet emerged to indicate whether bile acids play a pathophysiological role in the airways. Much of the research previously performed on bile acids in the lung has focused on bile acid induced inflammation leading to airway fibrosis and VAP (Wu *et al.*, 2009, Vos *et al.*, 2008, Perng *et al.*, 2008). However, bile acids are also well established mediators of epithelial ion transport in many tissues such as the colon and gallbladder (Devor *et al.*, 1993, Keating *et al.*, 2009, Keitel *et al.*, 2009), but to the best of our knowledge the role played by bile acids in modulation of airway epithelial ion transport has not yet been investigated. Given that for almost 2 decades, under the supervision of Prof. Brian Harvey,

one key area of research in our group has been to improve our knowledge in the field of airway epithelial ion transport, we hoped to build on this experience during our investigation of bile acids in the lung.

The primary aim of this study was to determine whether low levels of bile acids present in the airways can modulate airway epithelial ion transport and to elucidate the ion transport proteins and signalling molecules involved in this process. Therefore, it is hoped that this thesis will provide novel data to explain the processes by which bile acids modulate Cl^- secretion and to elucidate how their role in modulation of epithelial ion transport may participate in lung disease.

Specifically, in the following chapters we investigated:

1) Whether each of the bile acids, DCA, UDCA and the taurine conjugate of DCA (TDCA) can modulate airway epithelial ion transport at concentrations likely to be found in the airways.
2) The epithelial ion transporters modulated by TDCA
3) The signalling molecules involved in TDCA stimulation of airway epithelial secretion
4) The role of bile acid receptors in TDCA mediated airway secretion.

Chapter 2

Materials & methods

2-1 Cell Culture

2-1.1 NuLi-1/ CuFi-1 Cell Culture

NuLi-1 / CuFi-1 bronchial cell lines were kindly donated by Prof Zabner & Prof. Welsh from the University of Iowa and were cultured according to the protocol by Zabner et al (Zabner *et al.*, 2003). The NuLi-1 cell line was derived from a male non-Cystic Fibrosis lung, while the CuFi-1 cell line was derived from the lung of a female patient homozygous for the F508del CFTR mutation. These cell lines have been shown to represent a good model of bronchial airway epithelium for ion transport studies, when grown in air-liquid interface (Zabner *et al.*, 2003). All flasks and inserts were pre-coated with 1X collagen VI for 24 hr and washed x 3 with PBS prior to seeding

Collagen VI: 50 mg of Human Placental Collagen type VI (Sigma-Aldrich, St.Louis.MO, USA) was dissolved in 83.3 ml of distilled H_2O (dH_2O) + 166.7 µl of glacial acetic acid to yield 0.6 mg/ml, 10X stock. This was diluted 1:10 with dH_2O before use to give a final working volume of 60 µg/ml, 1X collagen VI. Both 10X and 1X collagen VI were stored at 4°C.

Cells were grown to confluency in T75 flasks in BEGM (Lonza, Basel, Switzerland), supplemented with BEGM bullet kit™ (epidermal growth factor, hydrocortisone, bovine pituitary extract, transferrin, bovine insulin, triiodothyronine, epinephrine, retinoic acid), 1% Pen/Strep,1.25 µg/ml Amphotericin B, and 10 µg/ml Gentamycin. NuLi-1/ CuFi-1 cells up to passage 17 were grown on semi-permeable hanging inserts and Costar Transwell™ permeable supports pre-coated with collagen VI. Cells were grown on inserts in BEGM for 2 days and then switched to Day 2 Media - 1000mls of 1:1 DMEM: F12 (Sigma-Aldrich, St.Louis.MO, USA), 2% Ultroser G (Biosciences, Dublin, Ireland) 10 µg/ml Gentamycin, and 1.25 µg/ml Amphotericin B. All media was filtered using Steritop-GP, 0.22 µm filters (Millipore, Billerica, MA01821, USA). Cell culture media was changed every 2-3 days. Cells were switched to air-liquid interface after 7 days to aid differentiation. Transepithelial resistance (TEER) was measured every 4/5 days and mucus was washed from the apical surface once a week. Cells were considered confluent and fully differentiated when the TEER was ~1000

Ohms*cm^2 and cells were under air-liquid interface, which usually occurred after 21-28 days.

2-1.2 Calu-3 Cell Culture

The Calu-3 cell line is a well-differentiated and characterized cell line derived from the secretory serous cells of the human bronchial submucosal glands of a male patient with lung cancer. Calu-3 cells grown under air-liquid interface demonstrate many characteristics of bronchiolar epithelium and are often used for ion transport studies (Pezzulo *et al.*, 2011, Devor *et al.*, 1999). Calu-3 cells were purchased from the ATCC at passage 18 and stocks were frozen up to passage 23. Cells were grown in DMEM:F12 (Sigma-Aldrich, St.Louis.MO, USA), supplemented with 10% Fetal Bovine Serum, 1% Pen/Strep, 10 μg/ml Gentamycin. Calu-3 cells from passage 24 - 34 were grown on semi-permeable hanging inserts and Costar Transwell^{TM} permeable supports. Cells were grown on inserts in liquid/liquid interface for 2 days after which cells were switched to air / liquid interface. Cell culture media was changed every 2 – 3 days. Transepithelial electrical resistance (TEER) was measured every 4/5 days and mucus was washed from apical surface once a week. Cells were considered confluent and fully differentiated when the TEER stabilized at ~ 500 - 1000 Ohms*cm^2 and cells were in air-liquid interface, which usually occurred after 9 – 11 days. Cells were not used for experiments after 12 days in culture due to the formation of thick overlying mucus that was difficult to remove without disrupting the cell layer.

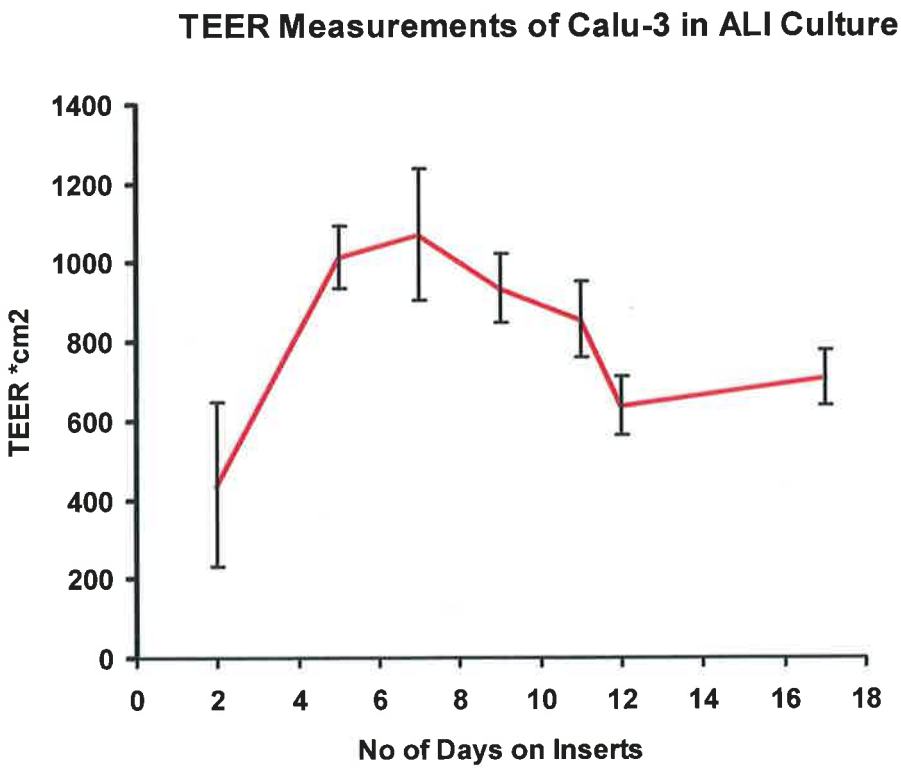

Fig. 2.1. Transepithelial electrical resistance (TEER) recordings for Calu-3 cells grown under air/liquid interface. In order to determine the rate of polarization of Calu-3 cells grown on Costar Transwell^{TM} permeable supports under air/liquid interface, the TEER was initially measured every 2 days. TEER recordings of 500-1000 Ohm*cm^2 represented optimum differentiation and indicated suitability for Ussing chamber experiments. As previously reported, Calu-3 TEER rose steadily for 7 days, levelled off between days 8-11 and began to decrease after day 12, by which time a thick mucus layer that was difficult to remove had formed (n = 8). Based on this result, days 9-11 were chosen as the optimum time for Calu-3 experiments and all investigations were performed during this period post-seeding.

2-1.3 Bronchoscopy Brush Sampling for in vivo Bronchial Epithelial Cells

Ethical approval for the study was obtained from the Ethics (Medical Research) Committee of Our Lady's Hospital for sick children, Dublin, under the Study of Host Immunity and Early Lung Disease in Children with Cystic Fibrosis (SHIELD CF) (Committee approval number GEN228/11). In this thesis, bronchial brushings were obtained from 5 children with CF and one non-CF, as described in table 2.1.

Table 2.1. Patient description for bronchial brushings obtained in this thesis.

Patient Sample	CF	Non-CF	Age	Gender
1	F508del/F508del	----------	4	F
2	F508del/1766+1G>A	----------	4	F
3	F508del/1766+1G>A	----------	6	F
4	F508del/X	----------	?	M
5	F508del/X	----------	3	F
6	----------	Haemoptysis	2	M

All patients were undergoing diagnostic or therapeutic fiberoptic flexible bronchoscopy as part of routine care. Full informed written consent was obtained from the parents pre-procedure and appropriate approval was obtained from our institutional review board. After completion of the procedure and before withdrawal of the bronchoscope, an area 2 cm distal to the carina (medially located) in either the right or left main bronchus was selected and washed twice with 10 ml sterile 0.9% NaCl. After this, a sterile 10 3 1.2 mm bronchial brush (Olympus Medical Systems, Tokyo, Japan) was inserted through the appropriate port on the bronchoscope and the chosen area sampled with two consecutive brushes by scraping the chosen area gently. The brush was withdrawn and immediately placed into 5 ml of transport media DMEM (Sigma-Aldrich, St.Louis.MO, USA), supplemented with 1% Pen/Strep (Biosciences, Dublin, Ireland), 1% Amphotericin B (Lonza, Basel, Switzerland), and 10 μg/ml Gentamycin (Invitrogen, Carlsbad, CA 92008.USA) on ice.

The brushings were transferred to 5 ml of warm culture media BEGM (Lonza, Basel, Switzerland) supplemented with BEGM bullet kit™(Lonza, Basel, Switzerland),1% Pen/Strep, 1% Amphotericin B, 10 μg/ml Gentamycin, and 80 μg/ml Tobramycin (Sigma-Aldrich, St.Louis.MO, USA) and placed on rollers at 4°C for 90 min. Transport tubes were centrifuged at 1000 rpm, 4°C for 5 min. Supernatant was removed, cells were resuspended in warm culture

media and placed on rollers at 4°C for 90 min. Brushes were then transferred to fresh culture media, swirled and tapped vigorously on the tube to detach any remaining cells. This was repeated as necessary until brushes appeared free from cells. All tubes were centrifuged at 1000 rpm, 4°C for 5 min. Cells were resuspended in a final volume of 2 ml culture media and used to seed one T25 flask pre-coated with 1X collagen VI (Sigma-Aldrich, St.Louis.MO, USA) for 24 hr (collagen washed x 3 with PBS prior to seeding). Flasks were incubated at 37°C, 5% CO_2 for 24 hr after which media was changed. Cell culture media was changed every 2 – 3 days until cells reached 70% confluency at which stage they were expanded to one T75 at passage 1.

2-1.4 Bronchial Epithelial Cell Culture

Primary cells obtained from bronchoscopy brush sampling were cultured using a protocol similar to that for NuLi-1 and CuFi-1 cell culture. Cells were grown to confluencey in T75 flasks in BEGM (Lonza, Basel, Switzerland) supplemented with BEGM bullet kit™(Lonza, Basel, Switzerland),1% Pen/Strep (Biosciences, Dublin, Ireland), 1.25 μg/ml Amphotericin B (Lonza, Basel, Switzerland), 10 μg/ml Gentamycin (Invitrogen, Carlsbad, CA 92008.USA), 80 μg/ml Tobramycin (Sigma-Aldrich, St.Louis.MO, USA). Primary cells from passage 2 to passage 5 were grown on semi-permeable hanging inserts (Millipore, Billerica, MA01821, USA) and Costar Transwell™ permeable supports (VWR Labshop, Batavia, IL 60510, USA) pre-coated with 1X collagen VI for 24 hr and washed x 3 with PBS prior to seeding. Media used for cells grown on inserts was 50/50 media -500 ml of BEGM supplemented as above but without tobramycin + 500 ml of DMEM supplemented with BEGM bullet kit™, 10 μg/ml Gentamycin, 1.5 mg/L BSA (Sigma-Aldrich, St.Louis.MO, USA), and 1 μM retinoic acid. All media was filtered using Steritop-GP, 0.22 μm filters (Millipore, Billerica, MA01821, USA). Cell culture media was changed every 2 – 3 days. Cells were switched to air-liquid interface after 7 days to facilitate differentiation. Transepithelial electrical resistance (TEER) was measured every 4/5 days and mucus was washed from apical surface once a week. Cells were considered confluent and fully

differentiated when the TEER was 500 – 1000 Ohms*cm^2 and cells were in air-liquid interface, usually after 21 – 28 days.

2-2 Electrophysiological Measurements

2-2.1 Ussing chamber

Measurement of transepithelial ion transport was performed using Ussing chambers and the short circuit current technique, which was first devised by the Danish physiologist, Hans Ussing, in the 1950s. Using this technique, cells cultured on snapwell inserts (Costar, Corning) were placed into hemi-chambers (p2300 Physiologic Instruments) that perfused each surface of the epithelium independently with equal volumes of a defined medium, typically a bicarbonate buffered Krebs solution, and the tissues were continuously gassed with 5% CO_2 / 95% O_2 mix, while the temperature was maintained at 37°C (Easymount Ussing chamber system, Physiologic Instruments). Thus in Ussing chambers it was possible to isolate the apical side of epithelial monolayers from the basolateral side.

Under normal circumstances in any epithelia at a given time there is ion transport taking place across the epithelium, whether it is from apical to basolateral or vice versa, creating a potential (voltage) difference across the epithelium (PD or V_t). The V_t generated was measured using two voltage electrodes that were placed near the epithelium in the Ussing chambers. Due to the active absorption of cations and /or the active secretion of anions by the epithelium, the Vt was generally apically negative with respect to the basolateral side under normal conditions.

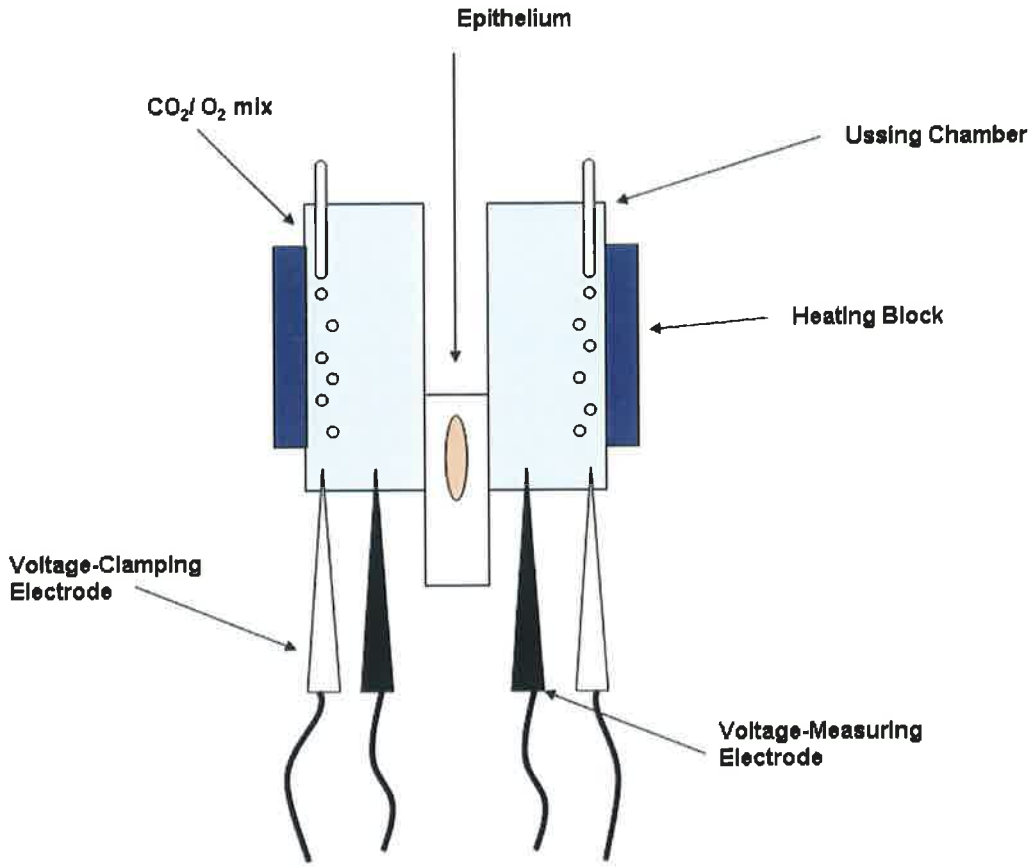

Fig 2.2. Schematic representation of the Ussing chamber. Calu-3 cells cultured inserts were placed into hemi-chambers that facilitated separation of the apical and basolateral compartments. Each surface of the epithelium was perfused independently with equal volumes of a defined medium, typically a bicarbonate buffered Krebs solution, and the tissues were continuously gassed with 5% CO_2 / 95% O_2 mix, while the temperature is maintained at 37°C. The spontaneous V_t generated by the epithelial layer was measured using two voltage electrodes that were placed close to the cells. Two electrodes placed further from the cells then passed enough current to reduce the V_t across the epithelium to zero (voltage clamping). The current required to clamp the voltage to zero was called the short-circuit current (I_{sc}). Changes in I_{sc} induced by secretagogues or inhibitors were then taken to represent changes in transepithelial ion transport.

In this procedure the spontaneous V_t across an epithelium was reduced to zero by the passage of current from two electrodes placed an 'infinite' distance from the epithelial surfaces. The current required to clamp the V_t to zero was called the short-circuit current (I_{sc}). If this was performed with identical solutions on both sides of the tissue, it was clear that there was neither a potential gradient nor a concentration gradient for any of the

molecular species in solution. Therefore, any current measured must have originated from active transport of ions. The I_{sc} would have therefore been similar and of opposite charge to the current moved actively through the epithelium in order to maintain the voltage at 0 mV. Cells were allowed to equilibrate for 15 min after being placed in the Ussing chamber before beginning the experiment. Changes in transepithelial ion transport were recorded as $\triangle I_{sc}$ (μAmps/cm^2), where $\triangle I_{sc}$ represents the peak value for I_{sc} recorded after treatment with a bile acid or secretagogue minus the basal I_{sc} recorded before treatment

Another important electrical parameter that was able to be measured using Ussing chambers was the transepithelial resistance R_t, an important indicator of cell integrity. R_t included both the resistances of the apical and basolateral membranes to ion flow plus the resistance by the paracellular pathway. Due to the presence of tight junctions between adjacent cells of tight epithelia, the resistance was highest via the paracellular pathway. Therefore, active ion transport through the cell was favoured. Using Ohm's law, the overall R_t was be calculated from the short- circuit technique using the following equation:

$$R_t = V_t / I_{sc}$$

Table 2.2. Ionic composition of physiological solutions used for electrophysiological measurements. For most of the Ussing chamber experiments performed in this study, normal Krebs solution was used, unless otherwise stated. All buffers were made fresh on the day of the experiment. After bubbling through the Krebs solution with 5% CO_2/ 95% O_2 mix, the pH was adjusted to 7.4 with HCl or NaOH. The osmolarity was recorded in the range 290-300 mOsm. Cl^- free Krebs was used for determination of Cl^- currents, basolateral cAMP Cl^- Krebs was used in experiments to isolate CFTR currents, while apical K^+ Krebs was used in experiments to isolate basolateral K^+ channel activity. Na^+/K^+ ATPase Krebs and CaCC Krebs were used in experiments to isolate Na^+/K^+ ATPase activity or CaCC activity respectively.

Krebs Solutions Ionic Concentrations (mM)							
	Krebs	**Cl^- Free Krebs**	**CFTR basolateral solution $^-$**	**K^+ channel Apical solution**	**Na^+/K^+ ATPase Apical + basolateral solutions**	**CaCC Apical solution**	**CaCC Basolateral solution**
$CaCl_2$	1.2	0	1.2	1.2	1.2	1.25	1.25
$MgCl_2$	1.2	0	1.2	1.2	1.2	0	0
K_2HPO_4	2.4	2.4	2.4	2.4	2.4	0	0
KH_2PO_4	0.4	0.4	0.4	0.4	0.4	0	0
NaCl	115	0	25	0	0	0	0
$NaHCO_3$	25	25	25	25	25	25	25
Glucose	10	10	10	10	10	10	10
Ca^{2+} - gluconate	0	1.2	0	0	0	0	0
Mg^{2+} - gluconate	0	1.2	0	0	0	0	0
Na^+ - gluconate	0	115	95	0	0	0	0
K^+ - gluconate	0	0	0	0	0	107	0
KCl	0	0	0	115	0	4.5	111.5
NMDG-Cl^-	0	0	0	0	115	0	0
Na_2HPO_4	0	0	0	0	0	1.8	1.8
NaH_2PO_4	0	0	0	0	0	0.2	0.2
$MgSO_4$	0	0	0	0	0	1	1

Table 2.3. Pharmacological inhibitors and secretagogues used for electrophysiological measurements. This table lists all of the pharmacological inhibitors, secretagogues or agonists that were used for elucidation of channel activity or signalling molecules involved in TDCA stimulation of airway epithelial Cl^- secretion. With the exception of GW4064, which was used both chronically (24hr) and acutely (10min), all other treatments with these agents were acute (up to 1 hr).

Pharmacological Inhibitors and Secretagogues used for Electrophysiological Measurements				
Compound Name	**Function**	**K_i**	**Final Conc**	**Application**
Amiloride	Inhibitor of ENaC	7μM	10 μM	Apical
Amphotericin B	Membrane Permeabilization	130 μM	25 μM	Apical
Bumetanide	Inhibitor of NKCC1	0.1 μM	10 μM	Basolateral
Bis 1	General inhibitor of PKC	10 nM	500 nM	Bi-lateral
Carbachol	Activation of muscarinic receptors to stimulate Ca^{2+} release	90 μM	100 μM	Basolateral
$CFTR_{inh172}$	Inhibitor of CFTR	0.3-5 μM	10 μM	Apical
Clotrimazole	K^+ Channel Blocker	899-1755 nM	10 μM	Basolateral
Forskolin	Activator of adenylate cyclase increasing intracellular cAMP	29.4 nM	10 μM	Basolateral / Apical
GW4064	Activator of FXR	1000-1100 nM	5 μM	Bi-lateral
H 89	Inhibitor of PKA	48 nM	10 μM	Bi-lateral
Nystatin	Membrane Permeabilzation	50 μg/ml	200 μg/ml	Basolateral
Ouabain	Inhibitor of the Na^+/K^+ ATPase	2.9-3.2 μM	100 μM	Basolateral
Thapsigargin	Inhibitor of Ca^{2+} ATPase, preventing Ca^{2+} entry into the stores of the endoplasmic reticulum	146 nM	2 μM	Bi-lateral

2-2.2 Measurement of Apical cAMP Cl^- currents

Intact monolayers of Calu-3 cells with TEER recordings of ~500-1000 Ohm*cm^2 were placed into Ussing chambers perfused by normal Krebs solution in the apical compartment and low Cl^- Krebs solution in the basolateral compartment (Table 2.2) generating an apical to basolateral Cl^- gradient, which favoured Cl^- transport and prevented cell swelling due to increased Cl^- permeability at the basolateral membrane. The basolateral membrane was permeabilized with 200 μg/ml nystatin, so that the apical membrane provided the only resistance to transcellular flow of ions. This protocol for measurement of apical cAMP Cl^- currents was based on one previously described (Hallows *et al.*, 2003). Under these conditions, forskolin or bile acid induced changes in I_{sc} were due to increased Cl^- movement through CFTR. In each experiment, one insert was pre-treated with $CFTR_{inh172}$ (10 μM) before acute bile acid treatment, as a control to confirm that observed changes in I_{sc} were due to Cl^- secretion through CFTR.

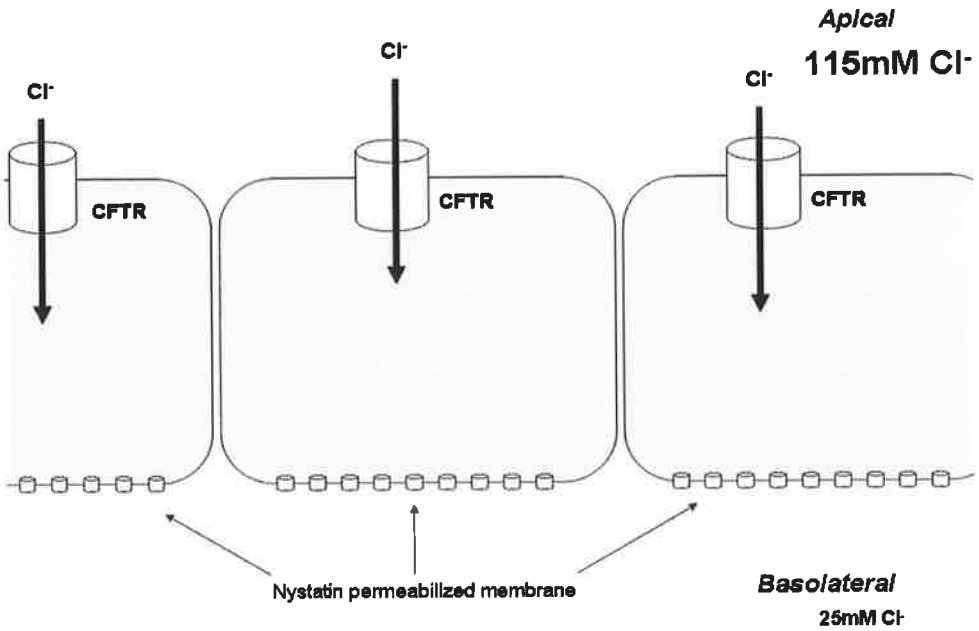

Fig 2.3 Diagram representing the technique used to isolate of CFTR currents in the Ussing chamber. Calu-3 cells were exposed an apical to basolateral Cl^- gradient to favour Cl^- transport, while the basolateral membrane was permeabilized with 200 μg/ml nystatin. Under these conditions, secretagogue induced changes in I_{sc} are due to increased Cl^- movement through CFTR. In order to confirm this, pre-treatment of one insert with $CFTR_{inh172}$

(10 μM) before secretagogue treatment, inhibited I_{sc} changes indicating that observed changes in I_{sc} were due to Cl^- secretion through CFTR.

2-2.3 Measurement of Basolateral K^+ currents

Tight monolayers of Calu-3 were mounted in Ussing chambers perfused by normal Krebs solution in the basolateral compartment and high K^+ Krebs solution in the apical compartment (Table 2.2) generating an apical to basolateral K^+ gradient, which favoured K^+ transport through the epithelium. This protocol for measurement of basolateral K^+ currents was based on one previously described (Wong *et al.*, 1990, Kirk and Dawson, 1983). The apical membrane was permeabilzed with 25 μM amphotericin B, which facilitated an influx of K^+ into the cell according to its concentration gradient, with the basolateral membrane providing the only resistance to this K^+ flux. The contribution of the Na^+/K^+ATPase to I_{sc} was then abolished by the inhibition of the Na^+/K^+ pump with 100 μM ouabain. Under these conditions, secretagogue or bile acid-induced changes in I_{sc} were reflective of increased K^+ movement through basolateral K^+ channels.

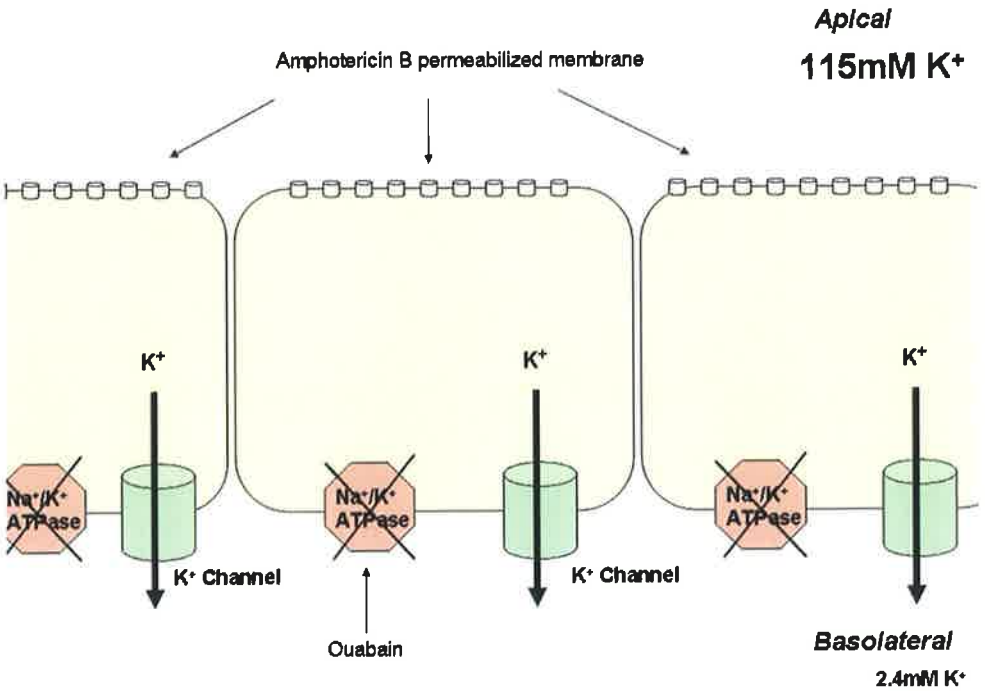

Fig 2.4 Diagram representing the technique used to isolate basolateral K^+ currents in the Ussing chamber. Calu-3 cells mounted in Ussing chambers were exposed to an apical to basolateral K^+ gradient, favouring K^+ transport through the epithelium. The apical membrane was permeabilized with 25 μM amphotericin B, allowing an influx of K^+ into the cell according to its concentration gradient, with the basolateral membrane providing the only resistance to this K^+ flux. The contribution of the Na^+/K^+ATPase to I_{sc} was abolished by inhibition of the Na^+/K^+ pump with 100 μM ouabain. Under these conditions, secretagogue induced changes in I_{sc} were reflective of increased K^+ movement through basolateral K^+ channels.

2-2.4 Measurement of Na^+/K^+ ATPase Pump Current

Calu-3 monolayers were mounted in Ussing chambers perfused by low Na^+ Krebs solution in both the apical and basolateral compartments (Table 2.2), which more closely resembled physiological cytosolic Na^+ concentrations. Each side of the epithelium also contained equimolar concentrations of K^+ and Cl^-. This ensured that ions were not moving passively along a concentration gradient. The apical membrane was then permeabilized with 25 μM amphotericin B, allowing an influx of ions into the cell through the apical membrane with active transport occurring through the basolateral membrane alone. The driving force for K^+ efflux from the cell through the basolateral K^+

channels was abolished under these conditions and so responses to bile acids or secretagogues were reflective of changes in Na^+/K^+ ATPase current. Again, in each experiment, one insert was pre-treated with ouabain (100 μM) prior to acute bile acid treatment, as a control to confirm that observed changes in I_{sc} were due to activation of the Na^+/K^+ ATPase.

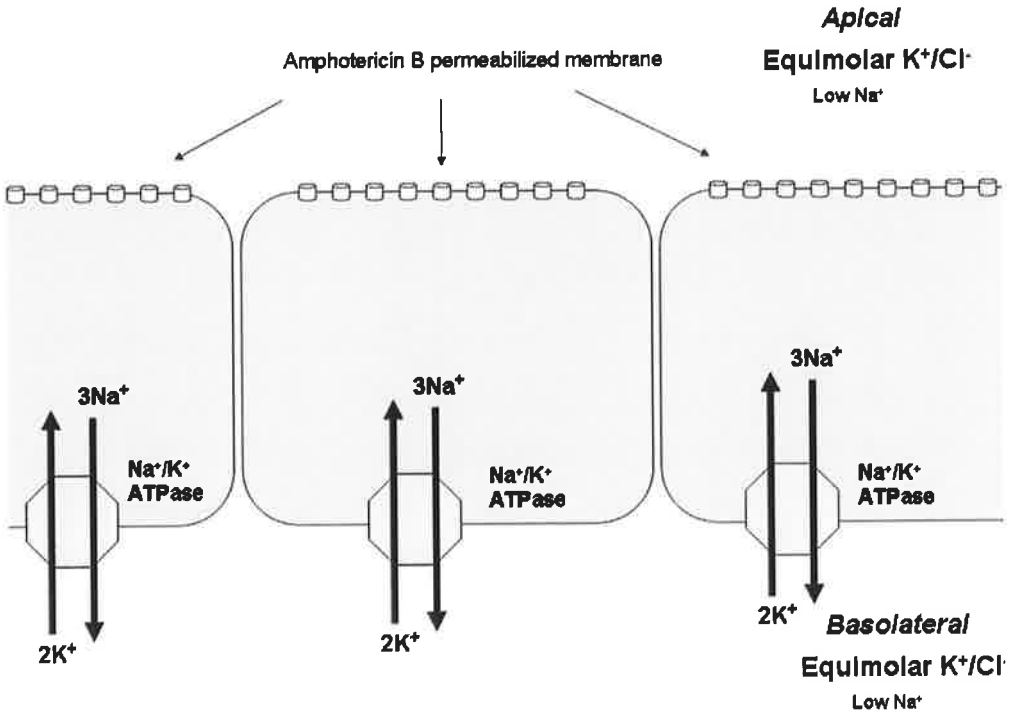

Fig 2.5 Diagram representing the technique used to isolate Na^+/K^+ ATPase generated currents in the Ussing chamber. Calu-3 cells were exposed to low Na^+, and equimolar concentrations of K^+ and Cl^- on both sides of the epithelium to ensure that ions were not moving passively along a concentration gradient. The apical membrane was then permeabilzed with 25 μM amphotericin B, allowing an influx of ions into the cell through the apical membrane with active transport occurring through the basolateral membrane alone. The driving force for K^+ efflux from the cell through the basolateral K^+ channels was abolished under these conditions and so responses to bile acids or secretagogues were reflective of changes in Na^+/K^+ ATPase current. In order to confirm this pre-treatment of one insert with ouabain (100 μM) prior to secretagogue treatment, demonstrated that observed changes in I_{sc} are due to activation of the Na^+/K^+ ATPase.

2-2.5 Measurement of Calcium-Activated Cl^- currents (CaCC)

This protocol for measurement of calcium-activated Cl^- currents was based on one previously described (Mroz and Keely, 2012a, Schultheiss *et al.*, 2005). Calu-3 monolayers were mounted in Ussing chambers perfused with Krebs solution containing high concentrations of K^+ on the apical side and high concentrations of both K^+ and Cl^- on the basolateral side. This established a basolateral to apical Cl^- gradient favouring Cl^- secretion from the apical membrane, while high basolateral K^+ resulted in depolarization of the membrane due to elimination of the driving force for K^+ exit through the basolateral K^+ channels. Under these conditions bile acid or carbachol induced changes in I_{sc} were due to increases in Cl^- secretion. In order to eliminate any contribution made by CFTR to I_{sc}, each insert was pre-treated with $CFTR_{inh172}$ (10 μM) prior to any treatment with bile acids or secretagogues. The remaining I_{sc} was therefore a representation of Cl^- secretion through the calcium-activated Cl^- channel

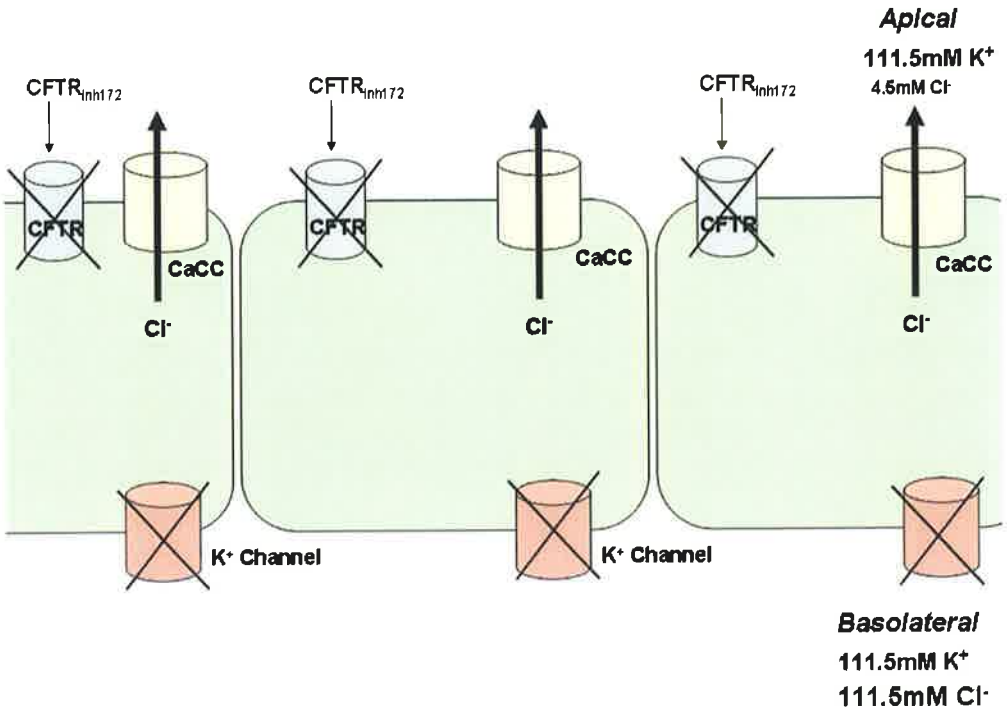

Fig 2.6 Diagram representing the technique used to isolate calcium-activated Cl^- currents in the Ussing chamber. Calu-3 monolayers were exposed to high concentrations of K^+ on the apical side and high concentrations of both K^+ and Cl^- on the basolateral side. This established a basolateral to apical Cl^- gradient favouring Cl^- secretion from the apical membrane, while high basolateral K^+ results in depolarization of the membrane due to elimination of the driving force for K^+ exit through the basolateral K^+ channels. Under these conditions secretagogue induced changes in I_{sc} are due to increases in Cl^- secretion. In order to eliminate any contribution made by CFTR to I_{sc}, cells were pre-treated with $CFTR_{inh172}$ (10 μM) prior to any treatment with secretagogues. The remaining I_{sc} is therefore a representation of Cl^- secretion through the calcium-activated Cl^- channel

2-3 Protein Chemistry

2-3.1 Protein Extraction

Cells were seeded on 6-well hanging inserts (millicell hanging insert, PIRP30R48, Millipore, Billerica, MA, USA,) and grown in air / liquid interface until the TEER reached a resistance of ~ 500-1000 Ohms*cm^2. All protein extractions were carried out on ice to slow down cellular interactions and to prevent degradation of proteins. Each insert was first washed x 3 with ice cold PBS (Sigma-Aldrich, St.Louis.MO, USA). Lysis buffers used were as follows:

Table 2.4. Composition of Lysis buffers used for protein extraction. Soft lysis buffer was used for all protein extractions unless otherwise stated. This buffer did not contain SDS and was preferential to RIPA buffer for extraction of proteins where phosphorylation status of the protein was to be investigated. Membrane protein lysis buffer was only used for extraction of biotinylated proteins from the cell membrane.

Soft Lysis Buffer		**Membrane Protein Lysis Buffer**	
Reagent	**Concentration**	**Reagent**	**Concentration**
Tris HCl	50 mM	**Tris HCl**	50 mM
NaCl	150 mM	**NaCl**	150 mM
NP-40	1%	**NP-40**	1%
Glycerol	3%	**PMSF***	0.1 mg / ml
EDTA	2 mM	**Na_3VO_4***	100 mM
EGTA	2 mM		
Complete mini-EDTA free protease inhibitor tablets*	1 tablet / 10 ml	**Complete mini-EDTA free protease inhibitor tablets***	1 tablet / 10 ml
Phosphatase Inhibitor Cocktail 2*	1% v/v		

*** added fresh prior to use**

300 µl of soft lysis buffer was added to each well and incubated on ice for 15 min. Cells were scraped and transferred to microtubes which were placed on a rotator at 4°C for minimum 30 min. Cells were lysed further by sonification in ice-cold water using SoniPrep 150 (MSE, London SE265AZ, UK) with an amplitude of 10 microns for 2 x 10 sec and then centrifuged at 14,000 rpm at 4°C for 15 min to remove any insoluble cell debris. The supernatant was

removed and transferred to a new microtube which could then be stored at -80°C.

2-3.2 Protein Quantification

Proteins were quantified using the Bio-Rad protein assay (BioRad Life Sciences, CA 94547, USA), based on the Lowry method, which is a simple and accurate procedure for determining concentration of solubilised protein. It involves the reaction of proteins with copper tartrate and Folin reagent producing a blue colorimetric product, the absorbance of which can be measured at 750 nm with a spectrophotometer or microplate reader. 96-well plates were set up as follows:

Table 2.5. Composition of each well for protein quantification using BSA (1 – 20 μg) to create a standard curve. A standard BSA curve was set up to quantify protein content of unknown samples of interest using a BioRad protein assay. 2 μg of each sample was assayed and the plate was read at 750 nm.

	Volume per Well (μl)							
Protein Concentration	**0μg BSA**	**1μg BSA**	**2μg BSA**	**5μg BSA**	**10μg BSA**	**15μg BSA**	**20μg BSA**	**? μg sample**
Protein vol: BSA 1mg/ml or sample	0	1	2	5	10	15	20	2
$_dH_2O$	23	22	21	18	13	8	3	23
Lysis Buffer	2	2	2	2	2	2	2	---------
Bio-Rad Solution A*	25	25	25	25	25	25	25	25
Bio-Rad Solution B	200	200	200	200	200	200	200	200

2 μl of each protein sample was used for quantification using bovine serum albumin (BSA 1 mg/ml) (Sigma-Aldrich, St.Louis.MO, USA) as a standard with Bio-Rad protein assay. The plate was incubated in the dark for 15 min in order to allow the reaction to occur and then the luminescence was read at 595 nm using a multiscan EX multiplate reader (Thermo Scientifc, Basingstoke, UK). A standard curve was prepared using varying concentrations of BSA (1 – 20 μg) and sample concentrations were calculated by plotting absorbance values against the standard curve for BSA.

2-3.3 Protein separation by SDS-PAGE

Once the proteins had been quantified, a fixed concentration of protein, usually 30 – 50 μg (depending on the total protein concentrations of the samples) was diluted in an equal volume of 2 x Laemmli buffer (Sigma-Aldrich, St.Louis.MO, USA), and made up to 40 μl with $_dH_2O$. Each sample

was boiled for 5 min at 95°C to denature the proteins so that they could be separated according to size using sodium-dodecyl-sulphate polyacrylamide gel electrophoresis, SDS-PAGE.

Table 2.6 Composition of polyacrylamide gels used for SDS-PAGE. Gels were either made up fresh on the day or pre-cast up to 5 days before experiment and stored at 4°C. The concentration of resolving gel required was determined by the size of the protein of interest. In general, the bigger the protein, the lower the % of acrylamide used in the gel and vice-versa.

Reagent	**Concentration (ml)**			
	8% resolving	**10% resolving**	**12% resolving**	**Stacking**
30% (v/v) acrylamide/bis-acrylamide mix	2.7	3.3	4.0	1.7
1.5 M Tris (pH = 8.8)	2.5	2.5	2.5	----------
0.5 M Tris (pH = 6.8)	----------	----------	----------	1.25
10% (w/v) SDS	0.1	0.1	0.1	0.1
TEMED	0.006	0.004	0.004	0.01
10% (w/v) APS	0.1	0.1	0.1	0.1
H_2O	4.6	4.0	3.3	6.8

*** Per 10mls gel required**

The concentration of acrylamide mix used for each gel varied depending on the molecular weight of the protein under investigation, in general the smaller the protein the more acrylamide used and vice versa. Proteins in the range 40-100 kDa were run on a 10% gel, proteins smaller than 40 kDa were run on a 12% gel and proteins larger than 100 kDa were run on an 8% gel.

After polymerisation, the gels were placed tightly into mini-protein chambers in an electrophoresis apparatus forming an internal chamber, containing the

cathode, and an external chamber where the anode is located. The internal chamber was filled with running buffer (Table 2.7) first to ensure that there was no leakage between the chambers and then running buffer was added to the external chamber to cover the electrodes and allow flow of electric current from the internal chamber, through the gel to the external chamber.

Table 2.7 Composition of buffers used for SDS-PAGE and Western blot. 10X stock of Tris-Glycine or TBS was made up and stored for up to 6 months at room temperature. Running buffer and transfer buffer were usually made up fresh on the day of experiment.

Buffer Compositions (per 1000ml)					
Reagents	10X Tris -glycine	10X TBS	Running Buffer	Transfer Buffer	1X TBS-T
Tris Base	30.3 g	12.1 g	----------	----------	----------
Glycine	144.4 g	----------	----------	----------	----------
NaCl	----------	86.6 g	----------	----------	----------
10X Tris-glycine	----------	----------	100 ml	100 ml	----------
10% SDS	----------	----------	10 ml	----------	----------
100% Ethanol*	----------	----------	----------	200 ml	----------
10X TBS	----------	----------	----------	----------	100 ml
Tween 20	----------	----------	----------	----------	2 ml
$_dH_2O$	**Make up to 1 L with deionised water, pH 7.4**				

* Ethanol switched to methanol if PVDF membranes are used for transfer

15 µl of Benchmark pre-stained protein ladder (Invitrogen, Carlsbad, CA 92008.USA) was loaded into the 2nd well of each gel, (1st well left empty). Benchmark is a commercially available protein size ladder stained for 10 standard proteins ranging in size from 10-190 kDa, which enables determination of protein size bands after migration through the gel. 40 µl of protein sample was loaded into each of the other wells in a pre-determined order. Protein migration was performed by application of an external voltage to each gel so that all proteins migrate in the same direction but speed is

determined by the size of the protein. Samples were initially run through a stacking gel at 75 V for 30 min until they reach the top of the resolving gel. The stacking gel was slightly acidic and contained a lower % of acrylamide, creating a porous gel, which favoured the formation of thin, sharply defined protein bands. Samples were then run at 150 V for 1 hr through the resolving gel until they reach the bottom of the gel. The resolving gel was more basic, with a higher concentration of acrylamide, resulting in a gel with narrower pores. Therefore as the proteins, concentrated into thin bands by the stacking gel, travelled through the resolving gel, the narrower pores had a sieving effect, allowing smaller proteins to travel more easily and rapidly than larger proteins.

2-3.4 Western Blotting

After electrophoresis, gels were removed from the electrophoresis apparatus and the stacking gel, tracking dye and empty wells were cut away. Protein transfer packs (trans-blot SD, semi-dry transfer cell, Bio-Rad Life Science,CA 94547, USA) were prepared with Whatmann filter paper and Hybond -C Extra Nitrocellulose membranes (GE Healthcare, BUCKS, HP84SP, UK) that had been pre-soaked in transfer buffer (Table 2.7). Gels were placed in transfer machines onto the nitrocellulose membrane and sandwiched between two pre-soaked pieces of blotting paper, making sure that there were no bubbles between the membrane and the gel. Protein transfer was performed by applying a voltage of 15 V for 45 – 90 min, depending on the protein size.

After this time, the Benchmark size ladder could be clearly seen on the nitrocellulose membrane indicating transfer efficiency. The membranes were placed into trays and covered with red Ponceau S dye (0.5% w/v ponceau in 10% acetic acid v/v) for 2-3 min, to stain protein bands on the membrane. Membranes were cut along appropriate size bands for the protein ranges of interest, and red Ponceau S was washed off with distilled water. One final wash with 1 X TBS-T for 15 min was performed to ensure that all acrylamide was washed off the membrane.

The membranes were then incubated with appropriate blocking agent for 1 hr on a shaker at room temperature to ensure that all non-specific binding sites on the membrane were occupied prior to addition of the antibodies. The blocking agents used were either 5% BSA in 1X TBS-T (Table 2.8) or 5% Marvel skimmed milk solution resuspended in 1X TBS-T, depending on the 1^{o} antibody that was to be used. In general, 5% BSA was used for investigation of phosphorylated proteins, while 5% milk was used for investigation of endogenous protein levels. Primary and corresponding secondary antibodies used for this study are listed in Table 2.8.

Table 2.8 Primary and secondary antibodies used to identify proteins of interest by Western blot. All primary antibodies (left hand side) were from either rabbit or mouse species. In general, BSA was used as a blocking agent for phosphorylated proteins while milk was preferential for non-phosphorylated proteins (with the exception of CFTR)

Primary Antibody				**HRP-conjugated Secondary Antibody**			
1°Ab	**Supplier**	**Dilution**	**Solvent**	**2°Ab**	**Supplier**	**Dilution**	**Solvent**
Phospho-PKCα (82 kDa)	Cell Signalling	1:1,000	5% BSA	Anti-Rabbit	Cell Signalling	1:3,000	5% BSA OR 5% Milk
Farnesoid X Receptor (59 kDa)		1:1,500	5% Milk				
TGR5 (35 kDa)	Abcam	1:3,000	5% Milk				
CFTR (167kDa)	Millipore	1:3000 (1:500 Memb)	5% BSA	Anti-Mouse	Cell Signalling	1:10,000	5% BSA OR 5% Milk
Na^+/K^+ ATPase α (113kDa) β (35 kDa)	Abcam	1:10,000	5% Milk				
β-Actin (42 kDa)	Sigma	1:20,000	5% BSA OR 5% Milk				

Membranes were incubated overnight at 4°C with 1° antibodies under gentle agitation. The following day, membranes were washed x 3 in 1X TBS-T for 15 min each prior to incubation with 2° antibody for 2 hours at room temperature with gentle agitation. Again, membranes were washed x 3 in TBS-T and antibody-labelled proteins were visualized by enhanced chemiluminescence detection method using ECL prime kit (Amersham Bioscience, Sweden) according to the manufacturers' instructions. After performing the ECL reaction, the membrane was placed under a transparent plastic sheet in a hyper-cassette. In the darkroom Kodak X-Omat LS Film (Sigma-Aldrich, St.Louis.MO, USA) was placed over the plastic covered membranes and closed in the hyper-cassette for fixed intervals, depending on the intensity of the protein bands. The film was removed and placed in 1. Kodak GBX developer (Sigma-Aldrich, St.Louis.MO, USA) 2. water 3. Kodak GBX fixer (Sigma-Aldrich, St.Louis.MO, USA) 4. water and allowed to dry. Once dry, the film was superimposed on the membrane in the hyper-cassette to locate the different bands on the Benchmark size ladder and the bands were drawn onto the film using a black felt pen. This enabled estimation of the size of the bands revealed on the film by comparison with the standard molecular weight markers. The film was then scanned and the proteins were quantified using Photoshop. Relative intensity of each protein band was determined using β-actin as the standard.

2-4 Isolation of membrane proteins using biotin labelling

Many of the proteins involved in ion transport are located at the apical or basolateral membranes of epithelial cells. However, in spite of their importance, membrane proteins have often escaped a systematic analysis and quantification in biological systems due to their limited solubility in water and their relatively low abundance (Scheurer *et al.*, 2005). Covalent attachment of active chemical derivatives of biotin to surface proteins, followed by purification on streptavidin beads, has been investigated as a method to restrict proteomic analysis to membrane proteins. Biotinylation is rapid, specific and unlikely to perturb the natural function of the molecule due to its small size (MW = 244.31). Biotin binds to avidin and streptavidin with an

extremely high affinity, allowing biotin-containing molecules in a complex mixture to be discreetly bound with avidin conjugates, making capture of biotinylated molecules possible in a wide variety of environments.

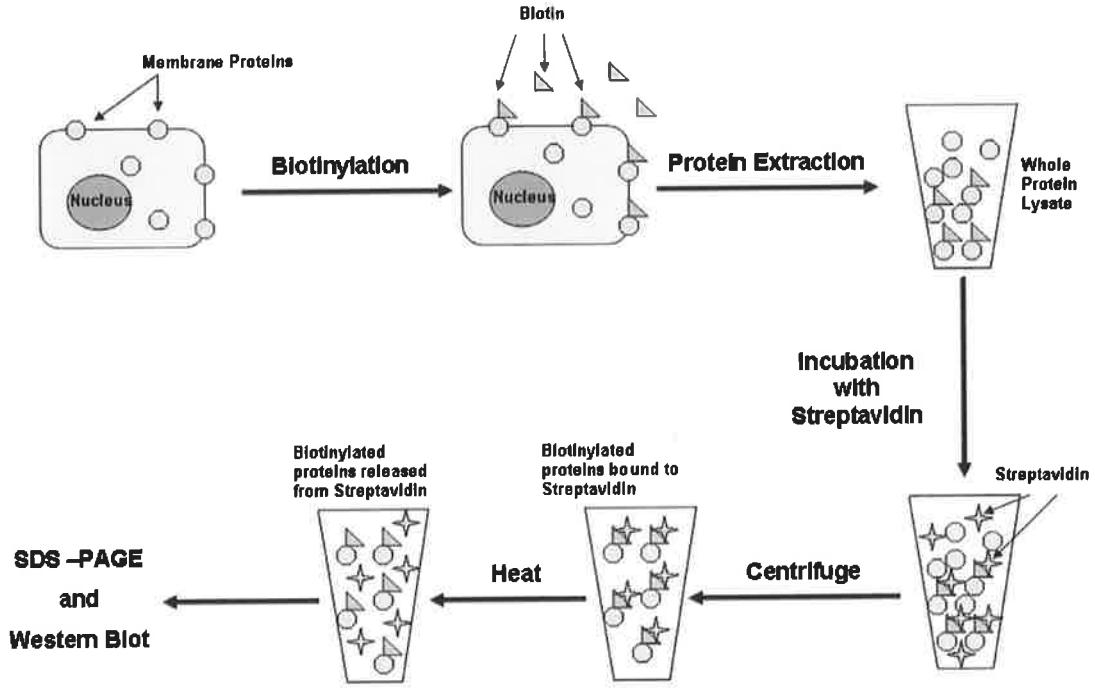

Fig. 2.7 Isolation of membrane proteins using the biotinylation technique. Cells were incubated with apical or basolateral 1 mg / ml biotin for 30 min which covalently binds to the membrane proteins. Cells were then lysed and 250 μg of whole protein lysate was incubated overnight with streptavidin beads on at rotator at 4°C. Biotinylated proteins bind to the streptavidin beads with high affinity and can be separated from all other proteins by centrifugation. The biotinylated proteins were then released the from the streptavidin beads by heating to 40 °C for 2 hr, prior to separation by SDS-Page and Western blot analysis for Na^+/K^+ ATPase or CFTR.

Biotinylation was used in this study to determine whether TDCA was having an effect on Na^+/K^+ ATPase or CFTR trafficking to the membrane. Calu-3 cells grown on inserts in an air/liquid interface were treated basolaterally with 25 μM TDCA for 5 min. Cells were immediately placed on ice and all biotinylation steps were carried out at 4°C. Cells were washed x 2 with ice-cold PBS (Sigma). PBS was left on the side of the membrane that did not contain the protein of interest (ie, basolateral for CFTR, apical for Na^+/K^+ ATPase) and 1 ml of ice-cold 1 mg/ml biotin (EZ-link Sulfo- NHS-biotin,

Thermo Scientific) dissolved in PBS was added to the side of each membrane that was under investigation and incubated at 4°C on a shaker for 30 min. After 30 min, the biotin was removed and each biotinylated side was washed x 2 with PBS before 2 ml of 100 mM glycine (Sigma) was added to quench the reaction. Cells were incubated with glycine on a shaker at 4°C for 15 min before inserts were washed again x 2 with PBS. After covalent modification with biotin, cells were lysed with 300 μl of membrane protein lysis buffer (Table 2.4) for 30 min, scraped from the filters and centrifuged at 12000 rpm for 15 min to remove insoluble material. Proteins were quantified using Bio-Rad (Bio-Rad, Hercules, C.A, USA) protein assay as per section 2.7.

40 μg of protein was removed from each sample to represent total protein and stored at -80°C overnight. 50 μl of streptavidin beads (streptavidin agarose resin, Pierce) per sample was washed x 2 with PBS at 4000 rpm and 4°C for 2 min. 250 μg of each protein sample was diluted to 400 μl in membrane protein lysis buffer and was then incubated with the washed streptavidin beads at 4°C overnight. The following day, each tube was centrifuged at 4000 rpm and 4°C for 2 min. The supernatant was saved as it contained all of the proteins that did not bind streptavidin and therefore this fraction represented the intracellular proteins. The pellet contained the biotinylated proteins bound to the streptavidin beads and was washed a further 3 times with membrane protein lysis buffer at 4000 rpm and 4°C for 2 min. After the final wash, 40 μl of loading buffer containing 100 mM Tris, 4% SDS, 0.2% bromophenol blue, 20% glycerol and 100 μM DTT, was added to the pellet and each of the total protein fractions. 30 μl of loading buffer was added to 30 μg of cellular protein fraction.

Each sample was then heated to 40°C for 2 hr to release the biotinylated proteins from the streptavidin beads before being separated by SDS-PAGE run at 75 V for 30 min through the stacking gel and 150 V for 60 min through an 8% acrylamide gel. Proteins were transferred to a nitrocellulose membrane (Hybond C extra nitrocellulose membranes, GE Healthcare, BUCKS, HP84SP, UK) using a semi-dry transfer pack at 15 V for 90 min. Ponceau Red

was used to determine protein transfer to the membranes and each membrane was cut just above the 64 kDa size band. Each membrane was blocked (5% milk for Na^+/K^+ ATPase, 5% BSA for CFTR) for one hour. Membranes were incubated overnight at 4°C on rotator with Na^+/K^+ ATPase α (113kDa) or β (35 kDa) 1° antibody, with a 1:10,000 dilution used for each in 5% milk or with CFTR 1° antibody, with a 1:3000 dilution used for total and cellular fraction and 1:500 dilution used for membrane fraction in 5% BSA.

The next day, membranes were washed x 3 in TBS-T and incubated at room temperature for 2 hr on a shaker, with anti-mouse horseradish-peroxidase conjugated 2° antibody (IgG HRP-linked antibody, Cell Signalling Technology Inc, MA 01923 USA), diluted 1:10,000 in 5% milk/BSA. Membranes were washed x 3 in TBS-T and antibody-labelled proteins were visualized by enhanced chemiluminescence detection method using ECL prime kit (Amersham Bioscience, Sweden) according to the manufacturers' instructions. After performing the ECL reaction, the membrane was placed under a transparent plastic sheet in a hyper-cassette. In the darkroom Kodak X-Omat LS Film (Sigma-Aldrich, St.Louis.MO, USA) was placed over the plastic covered membranes and closed in the hyper-cassette for fixed intervals, depending on the intensity of the protein bands. The film was removed and placed in 1) Kodak GBX developer (Sigma-Aldrich, St.Louis.MO, USA) 2) water 3) Kodak GBX fixer (Sigma-Aldrich, St.Louis.MO, USA) 4) water and allowed to dry.

Membranes probed for Na^+/K^+ ATPase β (35 kDa) were washed x 3 in TBS-T before being stripped for 30 min in Restore Western Blot Stripping Buffer (Pierce Chemical Company, Rockford, IL, USA). Membranes were washed x 3 in TBS-T and blocked overnight in 5% milk in TBS-T at 4°C on rotator. The next day, membranes were incubated at 4°C temperature for 1 hour on a shaker, with β-actin (42 kDa) 1° antibody, diluted 1:20,000 in 5% milk in TBS-T. Following this, membranes were washed x 3 in TBS-T and incubated at room temperature for 2 hr on a shaker, with anti-mouse horseradish-peroxidase conjugated 2° antibody, diluted 1:10,000 in 5% milk in TBS-T. Membranes were washed x 3 in TBS-T and antibody-labelled proteins were

visualized by enhanced chemiluminescence detection method using ECL prime kit. β-actin is not a membrane protein and so should not be detectable in the membrane fraction of proteins on the film, if the biotinylation process has worked properly.

2-5 Measurement of Intracellular Calcium

Calcium imaging is a common technique that is useful for measuring calcium signals in cultured cells. The calcium indicator used in this technique was the ratiometric dye Fura-2, first developed by Grynkiewicz et al (Grynkiewicz *et al.*, 1985), which has an emission peak at 510 nm and changes its excitation peak from 340 nm to 380 nm in response to calcium binding. The acetoxy-methylester form of Fura-2 (Fura-2-AM) facilitates entry of the dye across the cell membrane. Once inside the cell, the AM ester is cleaved by cytosolic esterases rendering the Fura-2 trapped within the cell where it forms complexes with Ca^{2+}.

Calu-3 cells were grown on 35 mm gamma irradiated glass bottom culture dishes (MatTek Corp, 200 Homer Ave. Ashland, MA 01721, USA) pre-coated with Collagen VI for 18-24 hr prior to seeding. The use of glass dishes provided better optical resolution and higher quality images while pre-coating with collagen helped to prevent cells from detaching during imaging. Glass dishes were seeded 1-2 days before each experiment to allow enough time for cells to attach and grow without becoming confluent. Cells were washed twice with physiological perfusion solution (PPS) before being loaded with 5 μM of Fura-2 acetoxy-methylester (Fura-2-AM) (Invitrogen) for 30 min at 37°C in the dark. Cells began to detach after Fura-2 incubations longer than 30 min.

Table 2.9 Ionic composition of physiological solutions used for calcium imaging with Fura-2. For most of the calcium imaging performed in this study normal PPS was used, unless otherwise stated. All buffers were made fresh on the day of the experiment. Zero calcium PPS was used for investigation of calcium entry into the cell.

Physiological Perfusion Solution (PPS)	Zero Calcium PPS
28 mM NaCl	28 mM NaCl
5 mM KCl	5 mM KCl
10 mM HEPEs/ TMA	10 mM HEPEs/ TMA
10 mM Glucose	10 mM Glucose
3 mM $MgCl_2$	3 mM $MgCl_2$
1 mM $CaCl_2$	10 mM EGTA
pH 7.4	pH 7.4

Cells were then washed twice with PPS before being mounted on the stage of a Nikon fluorescent microscope. The fluorescence was obtained at each excitation wavelength (340 nm for Ca^{2+}-bound Fura-2 and 380 nm for unbound Fura-2), depending on the level of calcium binding to Fura-2 AM, while emission was measured at 510 nm. Images were captured using a CCD camera connected to the microscope and between 10 and 15 regions of interest were chosen at random within the live image to measure cytosolic Ca^{2+} levels. One region containing no cells was selected and subtracted from the values of each region of interest to correct for background fluorescence. Changes in the $[Ca^{2+}]_i$ were determined from the F340/F380 ratio. The maximum ratio increase was calculated by the variation between the mean ratio recorded for the 2 min prior to bile acid treatment and the maximum ratio peak recorded after treatment. In order to study calcium entry into the cells, a zero-calcium PPS was used containing 0 mM $CaCl_2$ and 10 mM EGTA

2-6 Measurement of Intracellular cAMP

Cyclic AMP (cAMP) levels were measured in Calu-3 cells using the EIA direct cyclic AMP kit from Sigma-Aldrich. Using this method, a polyclonal antibody to cAMP competitively binds either cAMP in the sample of interest or an alkaline phosphatase molecule that has cAMP covalently attached to it. The samples, standards and alkaline phosphatase conjugates were all simultaneously incubated at room temperature on a 2^{o} antibody-coated multiwell plate. All wells were then washed thoroughly before addition of the substrate. Upon incubation with the substrate, the alkaline phosphatase generated a yellow colour that could be read at 405 nm. The intensity of the colour product was inversely proportional to the concentration of cAMP present as increased concentrations of free cAMP in standards and samples reduced alkaline phosphatase conjugate binding to the 2^{o} antibody-coated multiwell plate. Using a defined set of standards, the concentration of cAMP in each sample could then be calculated.

The kit contained two variations of the assay; acetylated and non-acetylated. The acetylated version of the kit was more sensitive and allowed detection of cAMP in the concentration range of 20-0.27 pmol/ml, while the non-acetylated version enabled detection of cAMP in the range 200-2.64 pmol/ml. In order to first determine the basal levels of cAMP in Calu-3 cells, the acetylated version of the kit was used and samples were serially diluted to ensure detection within the standard curve range. After establishing that Calu-3 cells have relatively high basal levels of cAMP, ~20-50 pmol/ml, the non-acetylated version of the kit was then used for all further assays.

Calu-3 cells grown on 30 mm inserts were treated basolaterally with 25 μM TDCA or 10 μM forskolin for 5 min before cell lysis. The media was removed and 200 μl of 0.1 M HCl was added to each insert. Cells were incubated at room temperature for 20 - 30 min until detachment could be visualized. Cells were then harvested and centrifuged at 600 g for 10 min at room temperature. 100 μl of each sample was diluted 1:10 before being added to the antibody-coated plate along with the standards. This was to ensure detection of

forskolin treated samples, the positive biological controls, within the standard curve range. 50 μl of cAMP-conjugated alkaline phosphatase and anti-cAMP antibody were then added to the plate, which was incubated at room temperature on a shaker for 2 hr.

During this time, the protein concentration of each undiluted sample was quantified using the BioRad protein assay as described in section 2-3.2. After 2 hr, the wells were emptied and washed thoroughly before 200 μl of the *p*-Nitrophenyl phosphate substrate solution was added. The plate was incubated for 1 hr without shaking at which point 50 μl of "stop solution" was added to each well and the plate was read immediately at 405 nm, with correction at 570 nm. The optical density of the blank wells was subtracted to correct for background and a standard curve was plotted of bound cAMP versus concentration in the standards solutions according to the Sigma protocol. The concentration of cAMP in the unknown samples was calculated from the standard curve. The values were then multiplied by 10 to account for the dilution factor and the concentration of cAMP in each sample was normalized to its total protein concentration.

2-7 PKA Assay

The activity of the cAMP-dependent protein kinase (PKA) after acute TDCA treatment (5 or 20 min) or acute treatment with 10 μM Forskolin, was assayed using the Peptag® Non- Radioactive PKA assay kit (Promega, Wisconsin, USA). This kit uses a brightly coloured pink fluorescent peptide substrate, kemptide, that is highly specific for PKA. Phosphorylation of this substrate by PKA results in a change in net charge of the peptide from +1 to -1. This change in the net charge of the peptide allows for the separation of the phosphorylated and non-phosphorylated forms of the substrate by electrophoresis on an agarose gel. The phosphorylated species migrates towards the positive electrode while the non-phosphorylated species migrates towards the negative electrode.

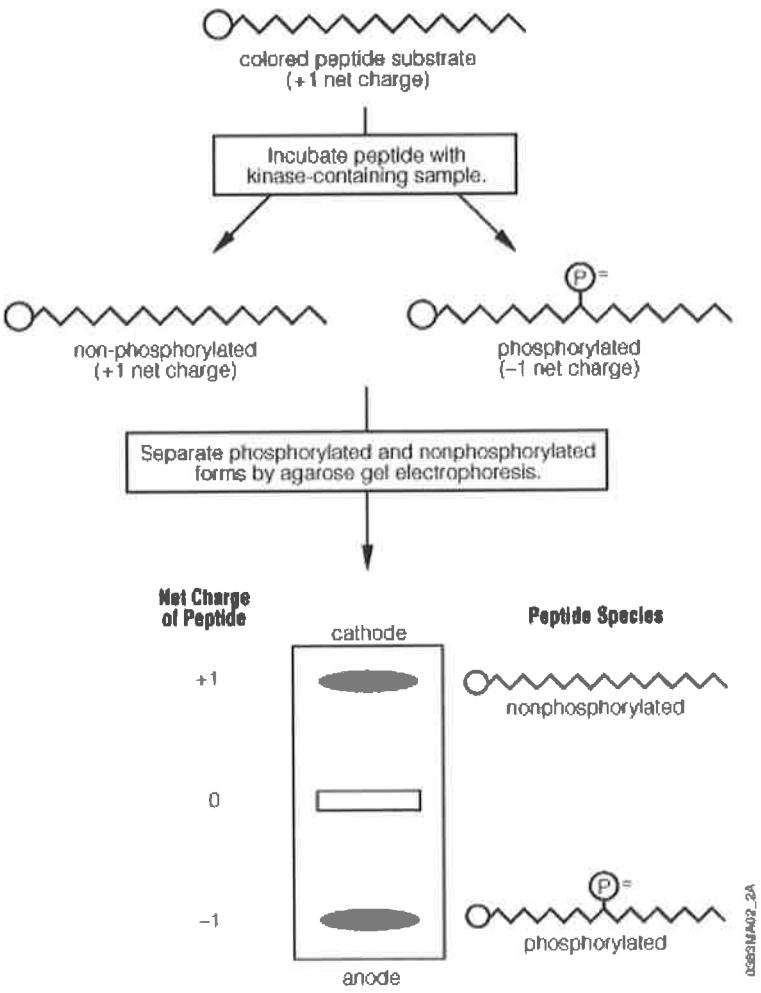

Figure 2.8 Schematic diagram of the PepTag® Non-Radioactive Protein Kinase Assay procedure. This kit uses a brightly coloured pink fluorescent peptide substrate, kemptide, that is highly specific for PKA. Phosphorylation of this substrate by PKA in the samples of interest results in a change in net charge of the peptide from +1 to -1. This change in the net charge of the peptide allows for the separation of the phosphorylated and non-phosphorylated forms of the substrate by electrophoresis on an agarose gel. The phosphorylated species migrates towards the positive electrode while the non-phosphorylated species migrates towards the negative electrode. **Taken from Promega protocol:** ***http://worldwide.promega.com/~/media/Files/Resources/Protocols/Technical%20Bulletins/0/PepTag%20Assay%20for%20NonRadioactive%20Detection%20of%20Protein%20Kinase%20C%20Protocol.pdf***

Soft lysis buffer was added to the treated or control cells grown in an air/liquid interface, and proteins were extracted and quantified as described in sections 2.5.1 and 2.5.2. Proteins were stored at -80°C or used for PKA assay straight

away. The assay was carried out according to the manufacturer's protocol. Peptag® components were combined on ice in labelled tubes to yield a 21 μl final volume and the tubes were incubated at 30°C for 1 min to start the reaction. 30 μg of each protein sample was then added to the appropriate tube and incubated for 30 min at room temperature. The reaction was stopped by incubating the tubes at 95°C for 10 min and they were then immediately placed back on ice and stored in the dark until the gel was ready to be loaded.

Samples were run on a 0.8% agarose gel (0.8 g agarose in 100 ml 1X TAE buffer (4.84 g/L Tris-base, 1.14 ml/L glacial acetic acid, 2 ml/L 0.5 M EDTA)). The wells were placed in the middle of the gel and it was completely submerged in 1X TAE buffer in an electrophoresis tank. A kit control was run alongside the samples to be assayed to ensure that the components were working properly and to confirm a negative result. The PKA catalytic subunit was added as a positive control and replaced with water as a negative control in every experiment. 1 μl of 80% glycerol was added to each sample to increase the density of the sample, facilitating loading into the wells.

A voltage of 120 V was applied to the samples after loading onto the gel and samples began to separate and migrate towards the anode or cathode depending on the phosphorylation of the peptide. After ~30 min, when 2 distinct bands could be seen on the gel, the gel was removed from the tank and imaged under UV light using Syngene Gene Snap® software. Densiometric analysis of the bands was performed using Photoshop software, and the intensity of each sample was normalized to % of control.

2-8 TGR5 siRNA Knockdown

Short interfering RNAs (siRNAs) are small double stranded molecules of non-coding RNA, approximately 20-25 bp in length that can bind to messenger RNA (mRNA) and inhibit mRNA translation into protein. siRNAs can occur endogenously within the cell or exogenous siRNAs targeting genes of interest can be transfected into cells to silence protein expression. The effect of siRNA knockdown by exogenous siRNA transfected into cells is transient in nature,

usually appearing ~24 hr after transfection and lasting no longer than 72 hr post transfection. siRNAs can also be formed intracellularly when anti-sense RNA is introduced into the cell, binds with its complementary sense RNA and results in long double stranded RNA molecules that are then cleaved into small siRNA fragments by dicer enzymes. The siRNA then binds to the RNA-induced silencing complex (RISC), which becomes activated by the unwinding of the siRNA and facilitates binding of the complex to the corresponding mRNA. The RISC contains an enzyme that cleaves the mRNA, resulting in degradation of the mRNA and inhibition of the protein translation.

To establish whether the G-protein bile acid receptor TGR5 (GPBAR1) was involved in TDCA stimulation of Cl^- secretion in Calu-3, siRNA knockdown of TGR5 was performed using commercially available pre-designed siRNA from Qiagen (Flexi-tube siRNA). In order to increase the probability of achieving relative knockdown of siRNA, cells were transfected with a mix of 3 different siRNAs, targeting sequences located spatially apart from one another along the TGR5 gene (hs_GPBAR1_1, hs_ GPBAR1_4, hs_GPBAR1_8). The Poly(ethyleneimine)-Poly(ethylene) glycol (PEI-PEG) vector developed by Hibbitts *et al* from RCSI school of Pharmacy was used as a transfection vector for these knockdown experiments, as it has been shown to increase siRNA nanoparticle uptake and luciferase knockdown in Calu-3 cells when compared with commercially available unmodified PEI (Hibbitts *et al.*, 2011). The concentration of vector used was determined by the ratio of the positively charged amine groups of the polymer (N) to the negatively charged phosphate groups of the nucleic acid (P), termed the N/P ratio. In general, the higher the N/P ratio, the more positively charged and smaller the nanoparticle containing the siRNA formed. N/P 15 was the highest concentration of vector with which Hibbitts *et al* observed efficient transfection of Calu-3, beyond this level, aggregation of particles and cell toxicity occurred.

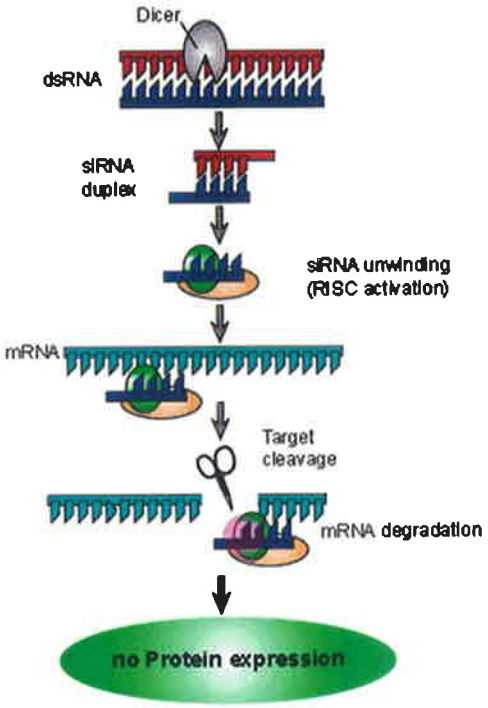

Figure 2.9 Schematic representation of how siRNA interferes with protein expression within the cell. When anti-sense RNA is introduced into the cell, it binds with its complementary sense RNA and results in long double stranded RNA molecules that are then cleaved into small siRNA fragments by dicer enzymes. Alternatively exogenous, synthetic siRNAs can be transfected directly into the cell. The siRNA then binds to the RNA-induced silencing complex (RISC), which becomes activated by the unwinding of the siRNA and facilitates binding of the complex to the corresponding mRNA. The RISC contains an enzyme that cleaves the mRNA, resulting in degradation of the mRNA and inhibition of the protein translation ***(http://www.scq.ubc.ca/antisense-rna/)***

Fully differentiated Calu-3 cells that had been grown on Costar Transwell snapwell permeable supports under air/liquid interface, as described in section 2-1.2, were used for TGR5 knockdown experiments. 300 μl of media was added apically for 30 min to each insert and TEER was recorded before transfection. During this time 360 nM of each TGR5 siRNA complex or negative siRNA control (Qiagen) was combined with N/P 10 PEI-PEG polymer in PBS and incubated at room temperature for 20-30 min. All media was then

aspirated from the cells and each insert was washed bi-laterally with sterile PBS to remove all traces of antibiotics. Serum-containing but antibiotic –free (AB-free) media was then added basolaterally, while the siRNA/vector complexes were combined with AB-free media and 275 μl of this was added apically to each insert. For each experiment, one insert was treated with AB-free media only as an untreated control, while another insert was treated with vector that had not been combined with siRNA as a vector control.

Transfected cells were incubated at 37°C for 24, 48 or 72 hr before measuring TEER and using cells for Ussing chamber experiments with acute 25 μM TDCA. After each Ussing experiment, inserts containing transfected cells were placed directly on ice, rinsed with ice-cold PBS prior to addition of 50 μl of soft lysis buffer to each insert. After 30 min inserts were scraped and cells + buffer were centrifuged at 10,000 rpm for 10 min at 4°C. Proteins were then quantified using a BioRad BSA assay, as per section 2-3.3. TGR5 knockdown efficiency was determined by using these protein samples for Western blot for TGR5 as described in section 2-3.4. Due to the small size of TGR5 (35 kDa) proteins were only transferred to nitrocellulose for 45 min at 15 V. Proteins were normalized to β-Actin and TGR5 knockdown was determined as % of untreated TGR5.

2-9 Reverse Transcriptase PCR (RT-PCR)

It has been well-documented in the literature that GW4064 is a specific agonist for the bile acid receptor FXR and activation of FXR has been shown to result in increased expression of fibroblast growth factor (FGF) 19 (Li *et al.*, 2004). Therefore, in order to determine whether GW4064 activates FXR in our Calu-3 cells, we performed RT-PCR on RNA extracted from Calu-3 cells that had been treated with 5 μM GW4064 bi-laterally for 2 or 24 hr.

2-9.1 RNA Extraction

After GW4064 treatment, cells were washed with ice-cold PBS, scraped and centrifuged at 4000 rpm for 4 min. Supernatant was removed and cells were then either immediately frozen at -80°C or used for RNA extraction. RNA was extracted from each sample using the RNeasy ® mini-kit (Qiagen) according to the manufacturer's protocol. All steps of the RNA extraction were carried out at room temperature. RNA was finally eluted using 50 µl of RNAse-free water supplied with the kit and was DNAse treated using DNAse I, in order to eliminate contamination with genomic DNA (Ambion, Tx, USA). Total RNA concentration of each sample was assayed by using a nano-drop spectrophotometer to measure UV absorbances at 260 nm. The quality of RNA was determined by monitoring ratio at 260/280 nm (ratios of 1.8 – 2.1 were indicative of high quality). Using the formula: *RNA concentration (µg/ml) = 44 µg/ml x* Abs_{260nm} *x dilution factor,* the quantity of extracted RNA in each sample can be calculated from the absorbance readings.

2-9.2 cDNA Synthesis

In order to perform RT-PCR on the samples, single strand complementary DNA (cDNA) needed to first be synthesised from the extracted RNA. The Improm-II reverse transcription kit (Promega) was employed to generate cDNA from 750 ng of RNA from each sample following the manufacturer's instructions, using a mix of reverse transcriptase, $MgCl_2$, recombinant RNAsin ribonuclease inhibitor, dNTPs, oligo dT primers and 5X reaction buffer. The amount of cDNA synthesised was quantified by measuring the absorbance at 260 nm and using the following equation: *cDNA (µg/ml) = 33 µg/ml x* Abs_{360nm} *x dilution factor.*

2-9.3 Real-time qRT-PCR

The cDNA (0.5 – 1 µg) was then used to perform real-time qRT-PCR on the samples, using GAPDH and FGF19 primers that had been pre-designed and optimized by Dr. Stephen Keely's group for use in the colon. These primers

had been primer-blasted to determine specificity of the sequences and ensure that the product size was under 200 bp, as required for effective qRT-PCR.

FGF19 Primer sequences were as follows:

Forward- 5' CTACAATGTGTACCGATCCGAG 3'
Reverse- 5' TCCGGTGACAAGCCCAAATG 3'

Glyceraldehyde-3-phosphate dehydrogenase (GAPDH), which is widely expressed in many different tissues, was used as a standard control to normalise gene expression data for differences in sample concentration or loading. The GAPDH primers used were follows:

Forward- 5' GTCATCATCTCTGCCCCCTCTGC 3'
Reverse- 5' CGACGGCTGCTTCACCACCTTCT 3'

Using this method, the production of amplification product during each PCR cycle is monitored using fluorescent reporter molecules. Gel electrophoresis is no longer required to detect amplification products as qRT-PCR combines both detection and amplification into one homogenous assay. Both FGF19 and GAPDH were amplified using SYBR Green® I master mix (Roche) according to the manufacturer's instructions with the following PCR program: a pre-incubation step @ 95°C for 10 min, followed by 45 cycles of denaturation @ 95°C for 10 sec, annealing @ 58°C for 10 sec and elongation @ 72°C for 10 sec. The melting curves for each primer set were analysed to confirm specificity. Using LinRegPCR software the efficiencies for each primer set were calculated from the PCR kinetic curve and used to measure relative quantification of gene expression with the comparative CT method. All samples were normalised to control gene expression using GAPDH.

2-10 Statistical Analysis

All data are expressed as mean ± Standard Error of the Mean (S.E.M), and n represents the number of repeat experiments performed on different passages. The sample size required to determine statistical significance of data generated was calculated by performing power calculations using Statistical Solutions LLC Power and Sample Size Calculator. Statistical analyses were performed with GraphPad software, using unpaired Student's t-tests for comparison between 2 groups. For experiments comparing 3 or more matched groups, repeated measures one-way analysis of variance (ANOVA) was used followed by Tukey's post-hoc test which compares all pairs of groups. P values of ≤ 0.05 were considered to be statistically significant.

RESULTS

Chapter 3

Bile acid modulation of airway epithelium ion transport

3-1 Introduction

In recent years, there has been an increase in reports indicating the presence of bile acids in the airways under many different pathophysiological conditions such as cystic fibrosis (CF), ventilator associated pneumonia (VAP), bronchiolitis obliterans syndrome (BOS), idiopathic pulmonary fibrosis (IPF) and respiratory distress syndrome (RDS) (Zecca *et al.*, 2004, D'Ovidio *et al.*, 2005, Pauwels *et al.*, 2012, Savarino *et al.*, 2013, Zecca *et al.*, 2008). Often times the presence of bile acids in the lungs can be associated with a worsening prognosis but no direct correlation between the two has yet been elucidated. As previously mentioned, the limitation to such investigations lies with the lack of adequate assays to assess the quality and quantity of specific bile acids, present in human airways (Parikh *et al.*, 2013). Since very few reports identifying bile acids in the airways exist, most research to date has investigated the effects of the most common bile acids in circulation eg. cholic acid (CA), chenodeoxycholic acid (CDCA) or deoxycholic acid (DCA).

It is likely that bile acids present in the airways have either been aspirated during episodes of gastroesophageal reflux, or have been taken up from the blood under conditions where circulating bile acids levels are increased e.g. in ICP. Bile acid concentrations as high as 32 μmol/L in BAL from patients that developed BOS after lung transplant have previously been reported, and this was used as a benchmark for the physiological range of bile acids present in the lungs (D'Ovidio *et al.*, 2005). Furthermore, serum bile acid levels in fasting individuals has been reported to be in the range of 1-5 μM, but can increase rapidly upon ingestion of food or under certain conditions such as intrahepatic cholestasis of pregnancy, where circulating bile acid concentrations can reach 40-60 μM in the mother and 60 – 120 μM in the newborn (Keely, 2010, Zecca *et al.*, 2004, Zecca *et al.*, 2008). Under these conditions, bile acids present in the airway are likely to have been taken up by the lung from the blood.

Until now, the majority of investigations of bile acids in the lung have focused on inflammatory responses or signalling pathways which are thought to modulate airway fibrosis or BOS. Interestingly, the conjugation status of bile

acids has been reported to differentially affect airway fibrosis. The taurine conjugate of CDCA, TCDCA has been shown to increase expression of matrix metalloproteinase 9 (MMP9), while decreasing tumour necrosis factor α (TNFα) expression in airways thus helping to prevent airway fibrosis in mice (Zhou *et al.*, 2013). On the other hand, CDCA has been reported to increase transforming growth factor (TGF)-β production, activating MAP kinase which leads to fibroblast proliferation and airway fibrosis (Perng *et al.*, 2007). In addition, a recent study by Reen *et al* has shown that the presence of bile in the airways can lead to biofilm formation, which may be an important factor in CF lungs, where the airways become colonized by opportunistic microorganisms, exacerbating lung disease (Reen *et al.*, 2012). It has also been demonstrated that bile acids are capable of increasing epithelial permeability in the human alveoli via degradation of junctional proteins, which may contribute to bile acid-associated lung injury (Su *et al.*, 2013). However, to the best of our knowledge, the ability of bile acids to modulate airway epithelial ion transport has not yet been investigated.

One key area of research for our group for almost two decades has been the study of airway epithelial ion transport and how it regulates ASL height and hence mucociliary clearance. Building on this experience, along with emerging evidence from the literature indicating that bile acids can modulate Cl^- secretion in colonic epithelium has provided a strong hypothesis for this investigation of bile acid modulation of airway epithelial ion transport (Ao *et al.*, 2013, Kelly *et al.*, 2013, Keely *et al.*, 2007, Keating and Keely, 2009a). Classical bile acid synthesis and function has been described in detail in chapter 1 (section 1-6), and conjugates of cholic acid (CA), chenodeoxycholic acid (CDCA) and deoxycholic acid (DCA) are known to be the major biliary bile acids in humans. However, as the identity of the most prominent bile acid in the airways is still unknown, this study was focused on the most abundant secondary bile acid in circulation, deoxycholic acid (DCA) and its taurine conjugate, taurodeoxycholic acid (TDCA).

DCA is formed as a result of bacterial modification of the primary bile acid, cholic acid (CA), which catalyses the removal of a hydroxyl group from CA at C-7, shown in brown in fig 3.1 (Monte *et al.*, 2009). Almost 80% of all secondary bile acids in circulation are derivatives of cholic acid rather than chenodeoxycholic acid. It is thought the evolutionary reason for this is that lithocholic acid (LCA), the secondary bile acid derived from CDCA, contains only one hydroxyl group and as such is poorly water soluble and toxic to most cells. DCA is a membrane permeable unconjugated secondary bile acid, containing two hydroxyl groups (dihydroxy) - fig 3.2, and constitutes approximately 20% of biliary bile acids. However, in humans the proportion of DCA present in bile can increase with age and as a result DCA can become the dominant bile acid in some adults (Hofmann, 1999b). One factor, which may be important for our study, is the observation that patients receiving treatment for GER in the form of proton-pump inhibitors often experience bacterial overgrowth in the intestinal tract (Lombardo *et al.*, 2010). This could increase the level of bacterially modified secondary bile acids or unconjugated bile acids re-entering enterohepatic circulation, thus favouring dominance of DCA in total bile.

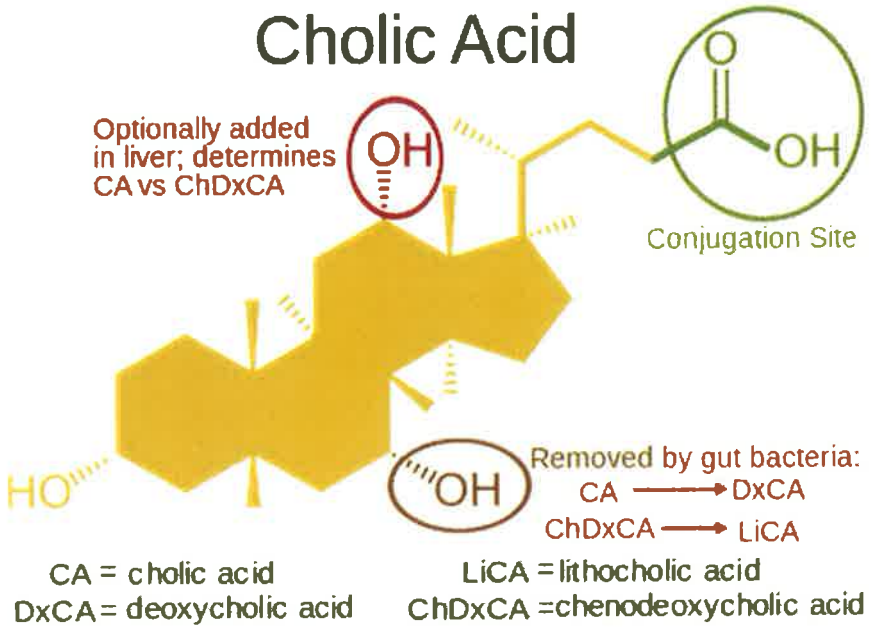

Fig.3.1 Schematic representing the basic structure of the primary bile acid, cholic acid (CA), and how it can be converted into other bile acids. All bile acids contain a steroid nucleus (shown in yellow) comprised of 4 carbon rings, and have a hydroxyl group at C-3, which was derived from cholesterol. Differential hydroxylation (at C-7 or C-12) or conjugation of this steroid nucleus determines water solubility and function of the bile acid. Omission of the hydroxyl group at C-12 (shown in red) determines synthesis of chenodeoxycholic acid (CDCA / ChDxCA), the simplest primary bile acid found in humans, rather than cholic acid. Once bile acids reach the gut, the hydroxyl group at C-7 (shown in brown) can be removed by bacteria converting primary bile acids into secondary bile acids, namely CA → DCA (DxCA), and CDCA → lithocholic acid LCA / LiCA). These secondary bile acids are then re-absorbed through the ileum, re-entering hepatic circulation and can be conjugated to either glycine or taurine at their terminal side chain carboxylic acid (shown in green), in the liver. ***https://upload.wikimedia.org/wikipedia/commons/0/06/Cholic_Acid_vs_Other_Bile_Acids.svg***

Over 40 years ago it was reported that DCA can robustly stimulate secretion in the colon of healthy human volunteers at much lower concentrations than that required for CDCA induced secretion, while CA produced no significant change in colonic absorptive capacity (Mekjian *et al.*, 1971). In addition, DCA has more recently been shown to acutely stimulate and chronically inhibit colonic epithelial Cl^- secretion in a concentration dependant manner (Keating *et al.*, 2009, Keely *et al.*, 2007). These studies further supported this initial

investigation into the effect of DCA, rather than CDCA or CA, on airway epithelial ion transport as the concentrations of bile acids likely to be found in the airway would be much lower than that of the colon.

Deoxycholic acid (DCA)

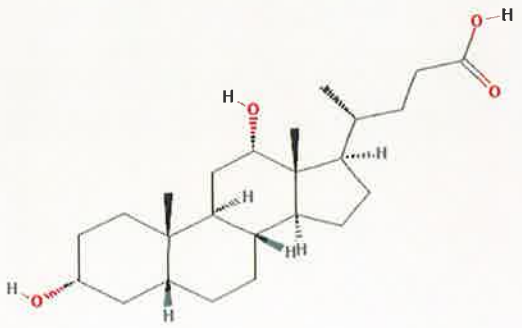

Ursodeoxycholic acid (UDCA)

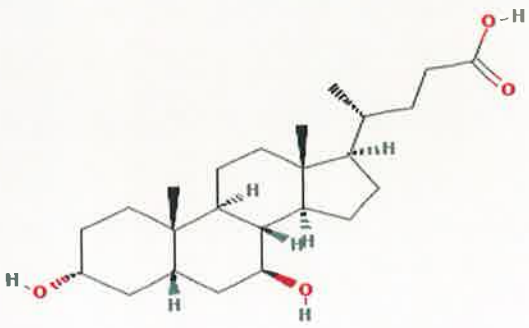

Taurodeoxycholic acid (TDCA)

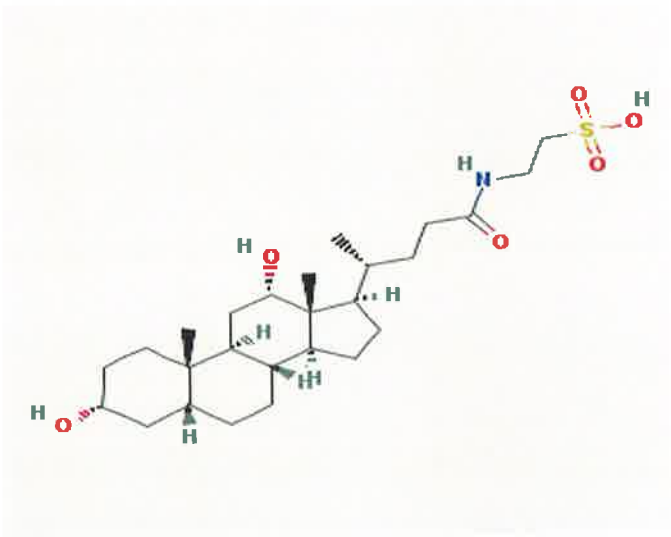

Fig.3.2. The chemical structure of DCA, UDCA and TDCA. Schematics representing the different chemical structures of the two unconjugated bile acids, DCA and UDCA, and the taurine-conjugated bile acid, TDCA. UDCA is a derivative of chenodeoxycholic acid (CDCA), while DCA is a derivative of cholic acid (CA). DCA and UDCA differ in structure by differential hydroxylation of C-7 and C-12. UDCA is almost identical to CDCA except that the hydroxyl group at C-7 in in a β- rather than α- conformation (Hofmann, 1999b). TDCA differs in structure from DCA by conjugation to a taurine group at its terminal carboxylic acid. **Images:** *http://pubchem.ncbi.nlm.nih.gov/summary/summary.cgi?cid=222528&loc=ec_rcs* *http://pubchem.ncbi.nlm.nih.gov/summary/summary.cgi?cid=31401&loc=ec_rcs*

http://pubchem.ncbi.nlm.nih.gov/summary/summary.cgi?cid=2733768&loc=ec_rcs

As previously discussed, after bile acid synthesis in the liver, human bile acids are usually conjugated to either glycine or taurine at their terminal side chain carboxylic acid, shown in green fig 3.1. Unconjugated bile acids are typically restricted to the colon, where microbial modification removes the glycine or taurine subunits from the bile acid. Therefore, since almost 90% of circulating bile acids in humans are conjugated, the taurine conjugate of DCA, taurodeoxycholic acid (TDCA) - fig 3.2, was also included in this investigation of bile acid modulation of airway epithelial ion transport. Although approximately 70% of human bile acids are conjugated to glycine rather than taurine, glycine conjugation is a relatively recent development in human evolution and many mammals, such as dogs are incapable of glycine conjugation. In addition taurine conjugates of bile acids are more water-soluble and less toxic than glyco-conjugated bile acids. Furthermore, the balance between glycine and taurine conjugated bile acids can be influenced by the type of food consumed, as diets rich in meat and fat can result in a 10-fold increase in the ratio of taurine to glycine conjugates (Hofmann, 1999b, Monte *et al.*, 2009). In support of this investigation, TDCA has been previously shown to stimulate Cl^- secretion in the epithelial layer of pancreatic ducts and the colon when added basolaterally (Keely *et al.*, 2007, Potter *et al.*, 1987, Okolo *et al.*, 2002, Devor *et al.*, 1993). In addition, a recent study has demonstrated that the taurine conjugate of CDCA may prevent airway fibrosis in mice, indicating that taurine conjugated bile acids may play a beneficial role in the airways (Zhou *et al.*, 2013).

Ursodeoxycholic acid (UDCA) is a derivative of chenodeoxycholic acid that has shown much promise for use in the treatment of diarrhoea as it has recently been reported that UDCA attenuates colonic epithelial secretory function (Kelly *et al.*, 2013). There is also evidence that UDCA may be the most effective treatment for intrahepatic cholestasis of pregnancy (ICP) (Zapata *et al.*, 2005). Taken together these reports support this investigation into the effects of UDCA on airway epithelial ion transport, given that many babies born to ICP mothers often present with respiratory distress syndrome

(RDS) and have bile acids present in their airways. UDCA may prove to be beneficial in treatment of RDS in these babies. Alternatively, if ICP mothers have been undergoing UDCA treatment, the UDCA may have an inhibitory effect on surfactant secretion in the foetus and hence exacerbate RDS in the newborn. In addition, UDCA has also been considered as therapy for liver disease in patients with CF (Kappler *et al.*, 2012). Again, it is important to understand what implications UDCA would have on airway epithelial ion transport if it were to reach the lungs in CF patients, where Cl^- secretion is already severely reduced.

The model selected for this study was the pro-secretory Calu-3 cell line, derived from human serous cells of airway submucosal glands, which were grown on permeable supports under air-liquid interface (ALI). It has been reported that, under these conditions, Calu-3 cells display many of the characteristics of fully differentiated airway epithelium and these cells have also been used by many different groups for investigation of airway epithelial ion transport (Huang *et al.*, 2012b, Devor *et al.*, 1999, Garnett *et al.*, 2013). In order to measure airway epithelial ion transport the short circuit current (I_{sc}) technique was adopted by mounting the cell layer in Ussing chambers and clamping the membrane voltage to zero. Changes in the current required to maintain the voltage at zero were taken to represent changes in transepithelial ion transport.

The specific aim of this chapter was to establish whether any of the 3 bile acids under investigation, DCA, TDCA or UDCA, could modulate either basal or secretagogue-induced changes in airway transepithelial ion transport. Although there have not been adequate reports in the literature to indicate the level of bile acids likely to be found in the airways, one study recorded bile acid concentrations as high as 32 μmol/L in BAL from patients who developed BOS after lung transplant, and therefore this was used as a benchmark for the physiological range of bile acids present in the lungs (D'Ovidio *et al.*, 2005). It has also previously been shown in the colon that bile acid modulation of secretion can exhibit sidedness and be concentration or temporally dependant

(Keely *et al.*, 2007, Kelly *et al.*, 2013, Keating *et al.*, 2009). Therefore this initial investigation of DCA, TDCA and UDCA involved treatments with concentrations of each in the range 1 – 25 μM, applied apically or basolaterally and incubation times of either 15 min or 24 hr were used. The secretagogues employed for this study were the cAMP-generating agent forskolin (Fsk) and the Ca^{2+} mobilizing analogue of acetylcholine, carbachol (CCh), which were both known to stimulate secretion in Calu-3 (MacVinish *et al.*, 2007).

3-2 Results

3-2.1 The acute effects of DCA on I_{sc} in Calu-3 Cells

Calu-3 cells grown under air-liquid interface on Costar snapwells for 9 – 12 days, until they reached a TEER of 500-1000 Ohms*cm^2, were mounted in Ussing chambers and the basal I_{sc} was recorded for 15 min prior to acute treatment with 1 – 25 μM DCA on either the basolateral or apical side. The I_{sc} was allowed to stabilize for 15 min before 100 μM CCh was added basolaterally and the transient CCh-induced Cl^- secretion was measured. The I_{sc} response to CCh was allowed to stabilize for a further 15 min before adding 10 μM Fsk and the sustained Fsk-induced Cl^- secretion was measured. Results are shown as mean ± SD and all experiments were carried out in a minimum of triplicate, where n = number of experiments performed on different passages. As can been seen in fig 3.3 A, acute basolateral treatment with 1, 10 and 25 μM DCA produced a change in basal I_{sc} respectively of 1.63 ± 1.11, 1.56 ± 1.24, 2.33 ± 1.16 μAmps/cm^2, which was not statistically significant, when compared with the 0.59 ± 0.34 μAmps/cm^2 change in basal I_{sc} observed in the untreated control (n = 6). Furthermore, acute basolateral treatment with DCA did not significantly affect subsequent CCh or Fsk induced I_{sc} responses, fig 3.3 B & C (n = 6). Taken together, these results indicate that acute basolateral treatment with physiologically relevant doses of DCA did not affect Calu-3 I_{sc}.

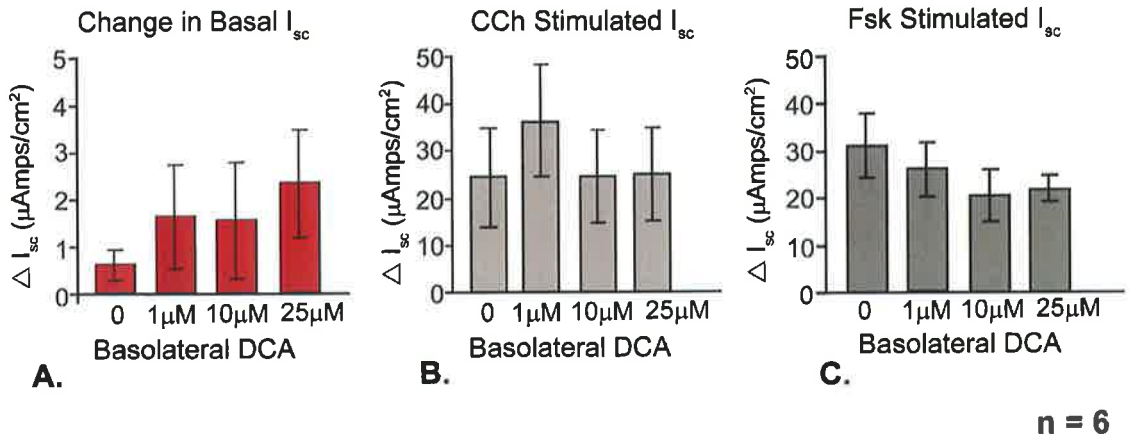

Fig.3.3 Acute basolateral treatment with DCA does not affect I_{sc} in Calu-3 cells. A. I_{sc} responses observed after treatment of Calu-3 cells with basolateral DCA. **B.** I_{sc} responses observed after treatment of Calu-3 cells with CCh. **C.** I_{sc} responses observed after treatment of Calu-3 cells with Fsk. Acute treatment with basolateral DCA did not significantly affect basal I_{sc} or subsequent CCh or Fsk- induced secretory responses in Calu-3 cells.

Preliminary experiments performed using apical 1 – 25 μM DCA treatment, indicated that 1 or 10 μM DCA had no effect on basal I_{sc} or subsequent CCh or Fsk stimulated responses. However, apical treatment with 25 μM DCA appeared to attenuate CCh stimulated I_{sc} responses. According to the power calculations performed, it was determined that n = 7 would be required to establish if DCA significantly reduced CCh stimulation of I_{sc}. Upon repeating these experiments, apical 25 μM DCA treatment was found to produce a 0.77 ± 0.63 μAmps/cm^2 change in basal I_{sc} which was similar to the 0.55 ± 0.39 μAmps/cm^2 change in basal I_{sc} observed in the untreated control (n = 7). Fsk stimulated I_{sc} by 31.96 ± 6.22 μAmps/cm^2 in control cells compared with an increase of 28.95 ± 7.01 μAmps/cm^2 after apical 25μM DCA treatment, indicating that DCA also did not significantly affect subsequent responses to Fsk. However, 25μM apical DCA significantly reduced CCh-induced I_{sc}. Under these conditions, DCA reduced the CCh increase in I_{sc} from 44.73 ± 14.95 μAmps/cm^2 to 28.45 ± 7.77 μAmps/cm^2 (n = 7, p = 0.026), as shown in fig 3.4 B.

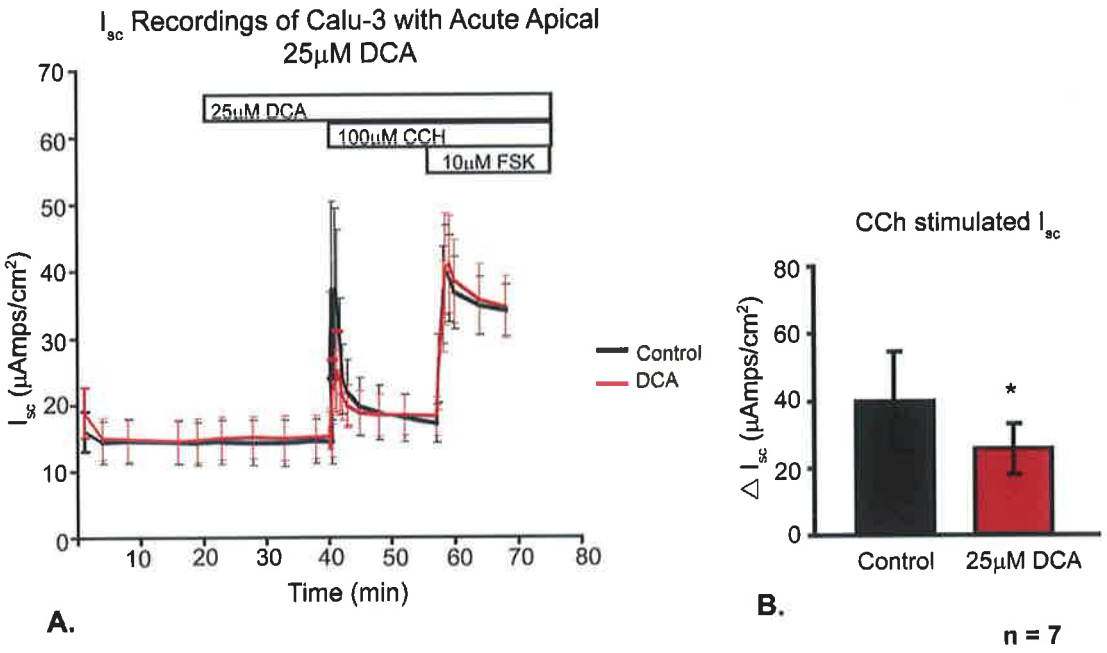

Fig.3.4 Acute apical treatment of Calu-3 cells with 25μM DCA attenuates the CCh stimulated I_{sc}. **A.** I_{sc} recorded during the experiment with Calu-3 cells treated acutely with apical 25 μM DCA. **B.** I_{sc} responses observed after treatment of Calu-3 cells with CCh. In control cells, CCh increased I_{sc} by 44.73 ± 14.95 μAmps/cm^2 while pre-treatment with 25 μM apical DCA significantly reduced CCh-induced I_{sc} responses to 28.45 ± 7.77 μAmps/cm^2 increase in I_{sc} (n = 7, p = 0.026)

3-2.2 The chronic effects of DCA on I_{sc} in Calu-3 cells

In order to determine the chronic effects of DCA on Calu-3 I_{sc}, cells grown under air liquid interface on Costar snapwells for 9 – 12 days, were pre-treated apically or basolaterally with 1 – 25 μM DCA for 24 hr prior to Ussing chamber experiments. After 24 hr incubation period, cells were mounted in Ussing chambers and the basal I_{sc} was recorded for 15 min before 100 μM CCh was added basolaterally and the transient CCh-induced Cl^- secretion was measured. Again, I_{sc} was allowed to stabilize for a further 15 min before adding 10 μM Fsk and the sustained Fsk-induced Cl^- secretion was measured. Basal I_{sc} recordings after 24 hr treatment with 1, 10 or 25 μM basolateral DCA were 9.6 ± 1.7, 8.1 ± 1.8, and 7.6 ± 0.9 μAmps/cm^2, which were not significantly different when compared with basal I_{sc} recordings of 8.9 ± 0.8 μAmps/cm^2 in control cells, as can be seen in fig 3.5 A. Carbachol alone

increased I_{sc} by 27.5 ± 11.5 μAmps/cm^2, compared with I_{sc} responses to CCh of 34.2 ± 14.0, 35.2 ± 19.6, and 31.7 ± 11.2 μAmps/cm^2 in cells treated for 24 hr basolaterally with 1, 10 and 25 μM DCA respectively (n = 3) as shown in fig 3.5 B. Furthermore, Fsk alone increased I_{sc} by 31.1 ± 13.1 μAmps/cm^2, compared with increases of 25.5 ± 11.3, 22.0 ± 10.8, and 31.7 ± 11.8 μAmps/cm^2 for cells pre-treated with 1, 10 and 25 μM DCA respectively (n = 3), fig 3.5 C. These results indicated that 24 hr basolateral DCA treatment did not affect I_{sc} in Calu-3 cells.

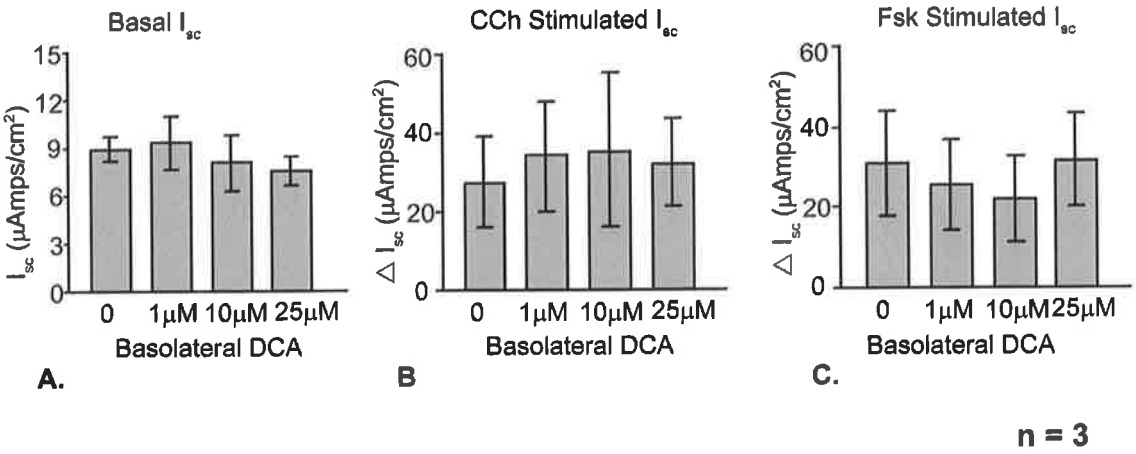

Fig.3.5 24hr Basolateral treatment with DCA does not affect I_{sc} in Calu-3 cells. A. I_{sc} recorded after 24 hr treatment of Calu-3 with 1, 10 or 25 μM DCA basolaterally. **B.** I_{sc} responses observed after treatment of Calu-3 cells with CCh. **C.** I_{sc} responses observed after treatment of Calu-3 cells with Fsk. 24 hr treatment of Calu-3 cells with basolateral DCA does not affect basal I_{sc} or subsequent CCh or Fsk induced secretory responses in Calu-3 cells (n = 3).

Preliminary experiments performed using 24 hr apical 1 – 25 μM DCA treatments, indicated that 1 or 10 μM DCA had no effect on basal I_{sc} or subsequent CCh or Fsk stimulated responses, while 25 μM DCA appeared to increase CCh stimulated responses. Upon repeating these experiments, 24 hr treatment with 25 μM apical DCA appeared to reduce basal I_{sc} to 17 ± 5 μAmps/cm^2, compared with basal I_{sc} recordings of 24 ± 5 μAmps/cm^2 in control cells, as can be seen in fig 3.6 A. In addition, as shown in fig 3.6 B,

pre-treatment with apical 25 μM DCA for 24 hr slightly increased the response to CCh, to 34 ± 14 μAmps/cm^2 compared with a CCh alone induced increase of 25 ± 11 μAmps/cm^2 in control cells. These results demonstrate that DCA exhibits sidedness and temporal dependence in modulating Calu-3 ion transport.

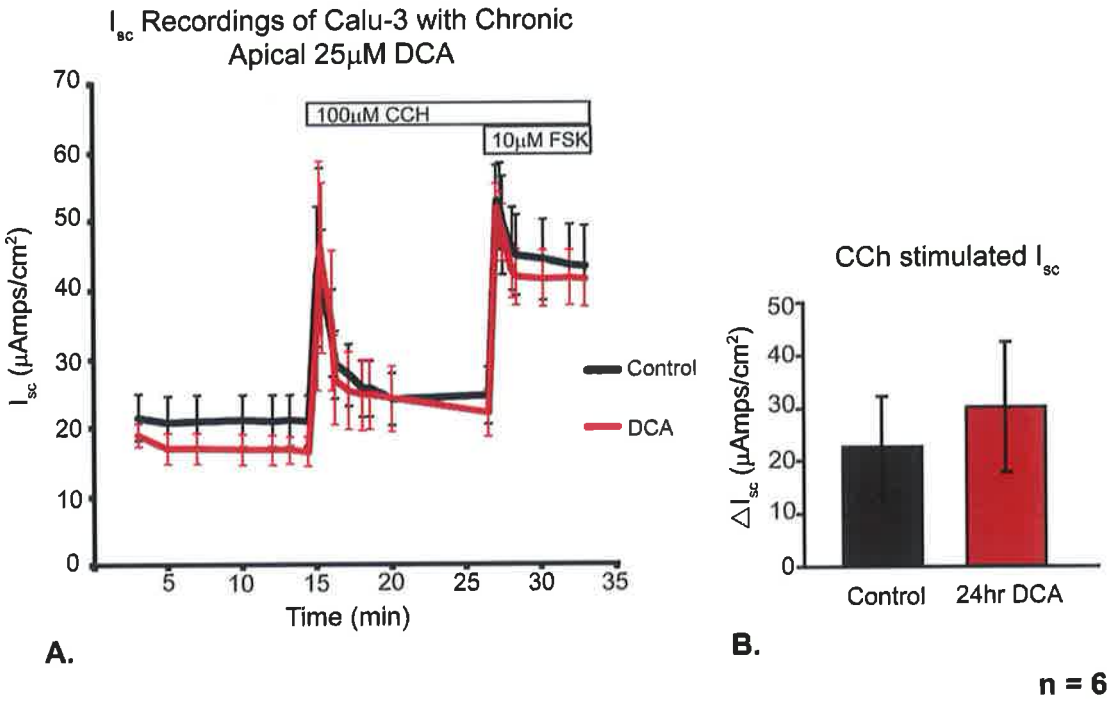

Fig.3.6 The effect of 24hr apical treatment with 25μM DCA on CCh stimulated I_{sc} in Calu-3 cells. A. Mean ± SEM I_{sc} values (μAmps/cm^2) recorded during the experiment with Calu-3 cells treated for 24 hr with apical 25 μM DCA. 24hr treatment with 25 μM apical DCA appeared to reduce basal I_{sc} to 17 ± 5 μAmps/cm^2, compared with basal I_{sc} recordings of 24 ± 5 μAmps/cm^2 in control cells. **B.** Mean ± SEM of the changes in I_{sc} (μAmps/cm^2) observed after treatment of Calu-3 cells with CCh. In control cells, CCh increased I_{sc} by 25 ± 11 μAmps/cm^2 while pre-treatment with 25 μM apical DCA slightly increased CCh-induced I_{sc} responses to 34 ± 14 μAmps/cm^2 (n = 6, p = 0.2)

3-2.3 The acute effects of TDCA on I_{sc} in Calu-3 cells

The next bile acid investigated was TDCA, the taurine conjugate of DCA. All experiments were performed in the same manner as for DCA. Once Calu-3 cells had reached a sufficiently high enough TEER in culture, the cells were

mounted in Ussing chambers and the basal I_{sc} was recorded for 15 min prior to acute treatment with 1 or 25 μM TDCA on either the basolateral or apical side. The I_{sc} was allowed to stabilize for 15 min before 100 μM CCh was added basolaterally and the transient CCh-induced Cl^- secretion was measured. Again, I_{sc} was allowed to stabilize for a further 15 min before adding 10 μM Fsk and the sustained Fsk-induced Cl^- secretion was measured. Preliminary experiments performed using acute basolateral 1 – 25 μM TDCA treatments, indicated that 1 μM TDCA had no effect on basal I_{sc} or on subsequent CCh or Fsk stimulated responses, while 25 μM TDCA appeared to increase basal I_{sc} responses. According to the power calculations performed, it was determined that n = 4 would be required to establish if TDCA significantly increased basal I_{sc} in Calu-3 cells. As shown in fig 3.7, upon repeating these experiments, acute basolateral treatment with 25 μM TDCA significantly increased basal I_{sc} by 4.54 ± 0.64 μAmps/cm^2 compared with a change in I_{sc} of 0.09 ± 0.30 μAmps/cm^2 in control cells (n = 13, p = 0.0001). CCh increased I_{sc} by 23.12 ± 5.44 μAmps/cm^2 in cells treated basolaterally with 25 μM TDCA, compared with a CCh-induced increase of 28.27 ± 7.65, μAmps/cm^2 in control cells, which was not significant (n = 13). Furthermore, 25 μM basolateral TDCA also did not significantly affect subsequent Fsk responses, with Fsk increasing I_{sc} by 22.95 ± 4.12, μAmps/cm^2 in TDCA treated cells, compared with a Fsk-induced increase of 30.03 ± 5.69, μAmps/cm^2 in control cells (n = 13).

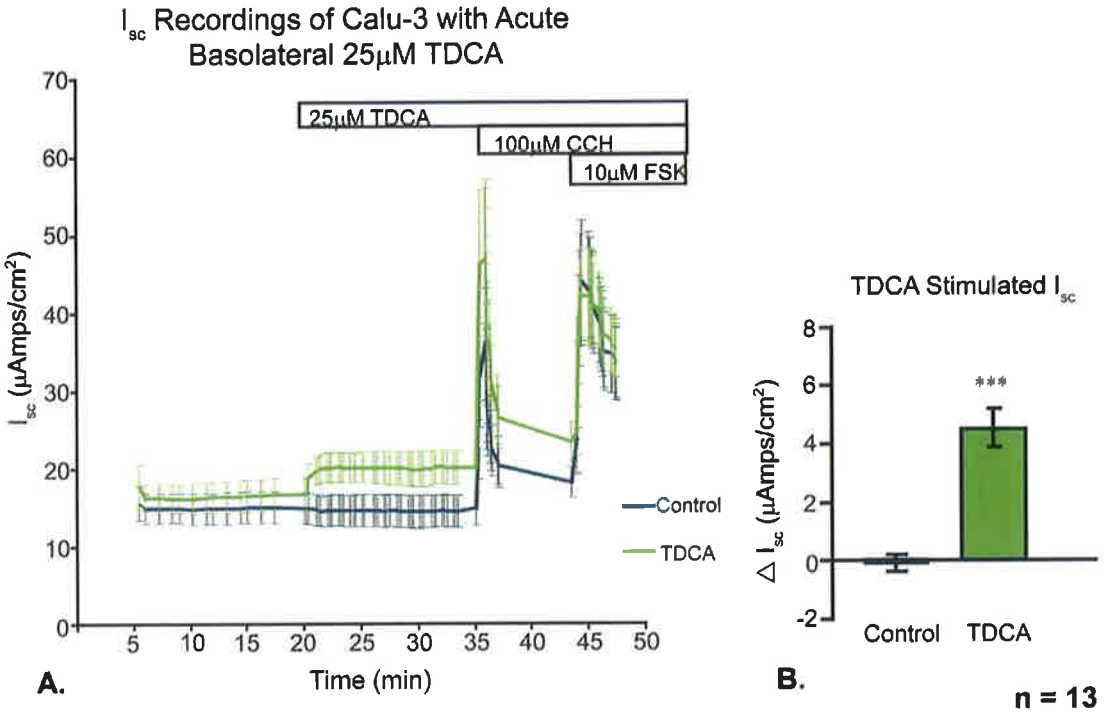

Fig.3.7 Acute basolateral treatment with 25μM TDCA increases basal I_{sc} in Calu-3 cells. **A.** Mean ± SEM I_{sc} values (μAmps/cm^2) recorded during the experiment with Calu-3 cells treated acutely with basolateral 25 μM TDCA. **B.** Mean ± SEM of the changes in I_{sc} (μAmps/cm^2) observed after treatment of Calu-3 with 25 μM TDCA basolaterally. Acute basolateral treatment with 25μM TDCA significantly increases basal I_{sc} by 4.54 ± 0.64, μAmps/cm^2 compared with a change in I_{sc} of 0.09 ± 0.30, μAmps/cm^2 in control cells in Calu-3 (n = 13, p = 0.0001), but TDCA did not significantly affect subsequent responses to CCh or Fsk.

In contrast, when these experiments were repeated using acute apical treatments of 1 or 25μM TDCA, TDCA was unable to increase basal I_{sc}. As shown in fig 3.8 A, I_{sc} responses to 1 or 25 μM apical TDCA treatment were -0.56 ± 0.39, and 0.30 ± 1.13 μAmps/cm^2 respectively, compared with a change in I_{sc} of -0.25 ± 0.69 μAmps/cm^2 in control cells (n = 4). Apical treatment with TDCA also had no significant effect on the subsequent responses to CCh or Fsk. CCh increased I_{sc} by 71.28 ± 21.74 μAmps/cm^2 in control cells, compared with CCh induced increases of 60.40 ± 20.85, and 72.29 ± 24.81 μAmps/cm^2 in cells treated apically with 1 or 25 μM TDCA respectively, while Fsk increased I_{sc} by 40.40 ± 10.62 μAmps/cm^2 in control

cells, compared with Fsk induced increases of 31.75 ± 8.69, and 36.49 ± 13.07 μAmps/cm^2 in cells treated apically with 1 or 25 μM TDCA respectively (n = 4). These results were similar to data previously reported demonstrating that taurine conjugates of bile acids only elicit secretory effects when applied basolaterally to colonic epithelium (Keely *et al.*, 2007). This suggests the presence of receptors or transporters in the basolateral membrane through which conjugated bile acids can elicit their effects.

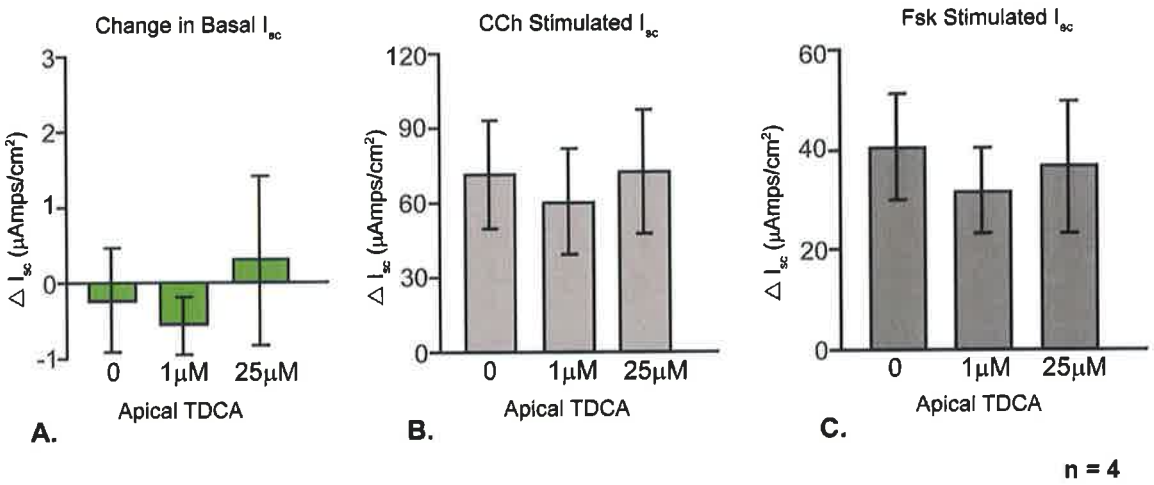

Fig.3.8 Acute apical treatment with TDCA does not affect I_{sc} in Calu-3 cells A. I_{sc} responses observed after treatment of Calu-3 with 1 or 25 μM TDCA apically. **B.** I_{sc} responses observed after treatment of Calu-3 with 100 μM CCh. **C.** I_{sc} responses observed after treatment of Calu-3 with 10 μM Fsk. Acute apical treatment with 1 or 25 μM TDCA did not affect basal I_{sc} or subsequent CCh or Fsk induced responses in Calu-3 cells.

3-2.4 The chronic effects of TDCA on I_{sc} in Calu-3 cells

Calu-3 cells were treated with 1 or 25 μM TDCA either apically or basolaterally for 24 hr prior to Ussing chamber experiments in order to assess the chronic effects of TDCA on Calu-3 I_{sc}. After 24 hr incubation period, the epithelium was mounted in Ussing chambers and the basal I_{sc} was recorded for 15 min before 100 μM CCh was added basolaterally and the transient CCh-induced Cl^- secretion was measured. I_{sc} was allowed to stabilize for a further 15 min before adding 10 μM Fsk and the sustained Fsk-induced Cl^- secretion was measured. As can be seen in fig 3.9 A, 24 hr treatment with 1 or

25 μM basolateral TDCA appeared to reduce basal I_{sc} to 13.7 ± 0.8, and 12.7 ± 1.3 μAmps/cm^2 respectively, but this was not significant when compared with control cells where basal I_{sc} recordings were 16.1 ± 4.1 μAmps/cm^2 (n = 3). In control cells CCh increased I_{sc} by 57.7 ± 25.0 μAmps/cm^2, compared with increases in I_{sc} of 46.5 ± 17.8, and 55.8 ± 23.9 μAmps/cm^2 in cells pre-treated with 1 or 25 μM TDCA respectively (n = 3). Furthermore, control responses to Fsk were 24.3 ± 4.7 μAmps/cm^2, compared with I_{sc} responses of 26.9 ± 2.9, and 25.9 ± 9.1 μAmps/cm^2 cm^2 in cells pre-treated with 1 or 25 μM TDCA respectively (n = 3). These results indicate that 24 hr basolateral treatment with TDCA did not significantly affect basal I_{sc} or subsequent CCh or Fsk stimulated I_{sc} responses.

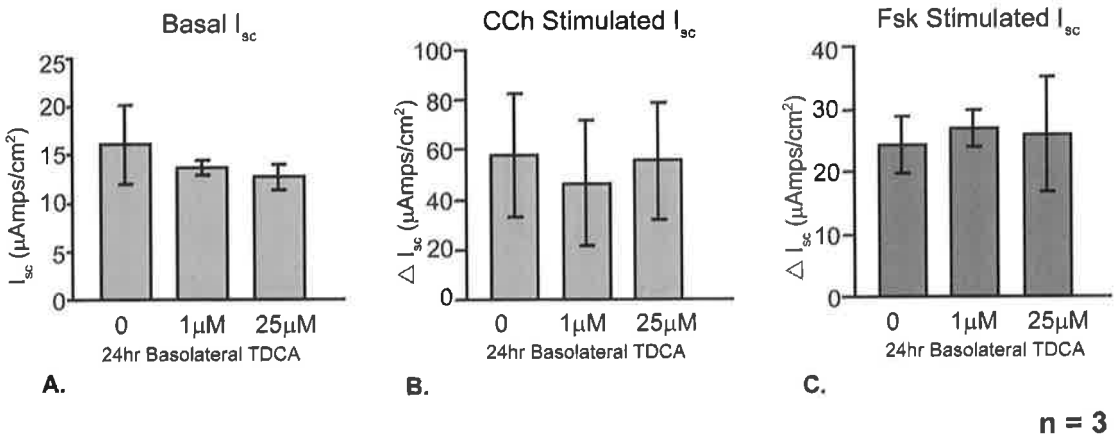

Fig.3.9 24hr basolateral treatment with TDCA does not affect I_{sc} in Calu-3 cells. A. I_{sc} recorded after treatment of Calu-3 with 24hr 1 or 25 μM TDCA basolaterally. **B.** I_{sc} responses observed after treatment of Calu-3 with 100 μM CCh. **C.** I_{sc} responses observed after treatment of Calu-3 with 10 μM Fsk. 24hr basolateral treatment with 1 or 25 μM TDCA did not significantly affect basal I_{sc} or subsequent CCh or Fsk induced responses in Calu-3 cells (n = 3).

Similarly, 24 hr apical treatment with 1 or 25 μM TDCA also did not have any significant effect on basal I_{sc} or subsequent CCh or Fsk stimulated I_{sc} responses in Calu-3 cells, fig 3.10. Basal I_{sc} recorded after 24 hr treatment with 1 or 25 μM apical TDCA was 17.2 ± 3.0, and 21.5 ± 4.6 μAmps/cm^2

respectively, but this was not significantly different to basal I_{sc} recordings of 18.2 ± 4.2 μAmps/cm^2 in control cells (n = 3). In control cells CCh increased I_{sc} by 57.7 ± 25.0 μAmps/cm^2, compared with increases in I_{sc} of 59.8 ± 18.2, and 60.9 ± 23.9 μAmps/cm^2 in cells pre-treated apically for 24 hr with 1 or 25 μM TDCA respectively (n = 3). Furthermore, control responses to Fsk were 24.3 ± 4.7 μAmps/cm^2, compared with I_{sc} responses of 20.6 ± 2.1, and 24.8 ± 12.0 μAmps/cm^2 in cells pre-treated apically for 24 hr with 1 or 25 μM TDCA respectively (n = 3). These results indicate that chronic apical TDCA does not affect basal or secretagogue-induced ion transport in Calu-3 cells.

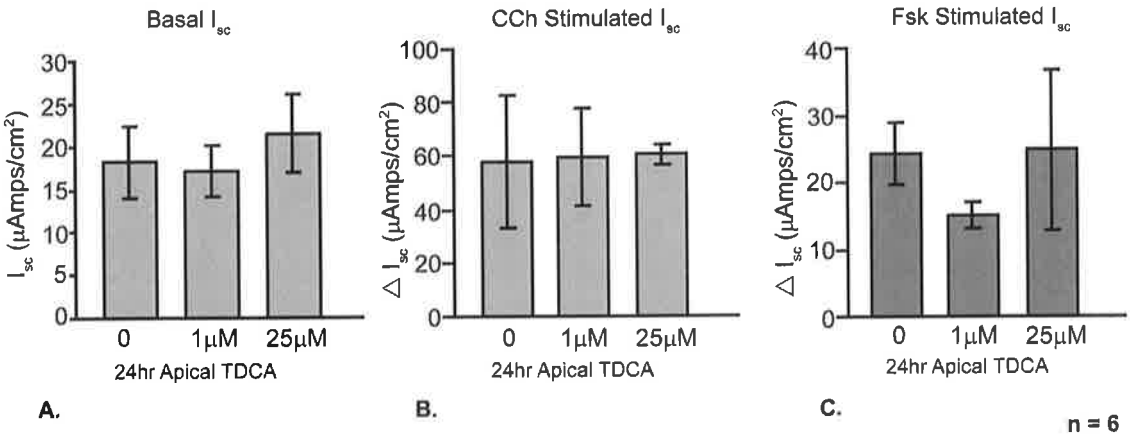

Fig.3.10 24 hr apical treatment with TDCA does not affect I_{sc} in Calu-3 cells. A. I_{sc} recorded after treatment of Calu-3 with 24 hr 1 or 25 μM TDCA apically. **B.** I_{sc} responses observed after treatment of Calu-3 with 100 μM CCh. **C.** I_{sc} responses observed after treatment of Calu-3 with 10 μM Fsk. 24 hr apical treatment with 1 or 25 μM TDCA did not significantly affect basal I_{sc} or subsequent CCh or Fsk induced responses in Calu-3 cells (n = 3).

3-2.5 The acute effects of UDCA on I_{sc} in Calu-3 cells

The third bile acid that was investigated was UDCA, and again Ussing chamber experiments were performed using the same protocol as for DCA and TDCA. High resistance cell layers were mounted in Ussing chambers and the basal I_{sc} was recorded for 15 min prior to acute treatment with 1 or 25 μM UDCA on either the basolateral or apical side. The I_{sc} was allowed to stabilize for 15 min before 100 μM CCh was added basolaterally and the transient

CCh-induced Cl^- secretion was measured. I_{sc} was allowed to stabilize for a further 15 min before adding 10 μM Fsk and the sustained Fsk-induced Cl^- secretion was measured. As can be seen from fig 3.11 A, acute basolateral treatment with 1 or 25 μM UDCA produced a 0.66 ± 0.67, and 1.35 ± 2.68 μAmps/cm^2 change in basal I_{sc} respectively, which was not statistically significant, when compared with the 2.07 ± 0.83 μAmps/cm^2 change in basal I_{sc} observed in the untreated control (n = 4). In control cells CCh increased I_{sc} by 13.08 ± 2.84 μAmps/cm^2, compared with CCh-induced increases of 13.82 ± 2.22, and 15.46 ± 4.30 μAmps/cm^2 in cells treated basolaterally with 1 or 25 μM UDCA respectively (n = 4). Furthermore, control responses to Fsk were 43.47 ± 12.55 μAmps/cm^2, compared with Fsk-induced I_{sc} responses of 40.63 ± 11.33, and 45.84 ± 7.80 μAmps/cm^2 in cells treated basolaterally with 1 or 25 μM UDCA respectively (n = 4).These results indicate that acute basolateral treatment with UDCA does not affect basal I_{sc} or subsequent I_{sc} responses to CCh or Fsk in Calu-3 cells (n = 4).

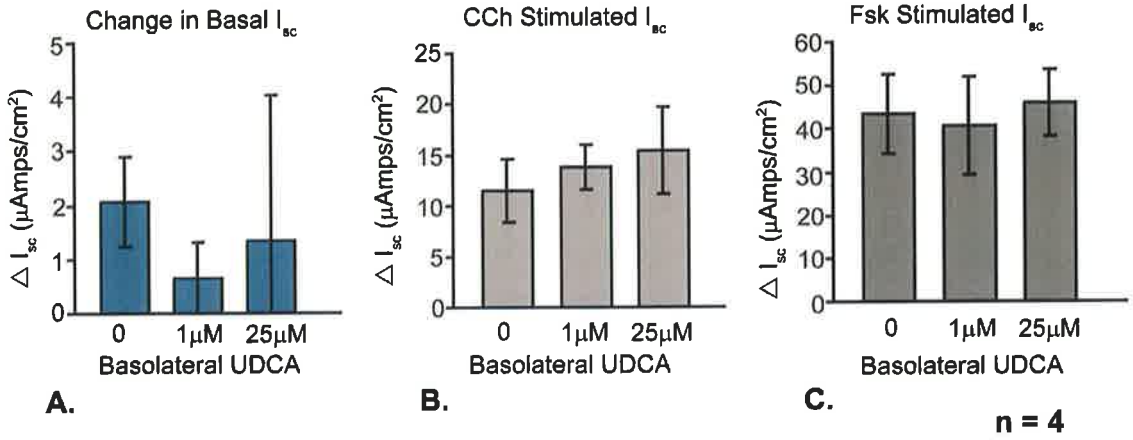

Fig.3.11 Acute basolateral treatment with UDCA does not affect I_{sc} in Calu-3 cells. **A.** I_{sc} responses observed after acute basolateral treatment of Calu-3 with 1 or 25 μM UDCA. **B.** I_{sc} responses observed after treatment of Calu-3 with 100 μM CCh. **C.** I_{sc} responses observed after treatment of Calu-3 with 10 μM Fsk. Acute basolateral treatment with 1 or 25 μM UDCA did not significantly affect basal I_{sc} or subsequent CCh or Fsk induced responses in Calu-3 cells (n = 3).

Similarly, acute apical treatment with 1 or 25 μM UDCA did not affect basal I_{sc} or subsequent I_{sc} responses to CCh or Fsk. As can be seen from fig 3.12 A, acute apical treatment with 1 or 25 μM UDCA produced a 0.98 ± 1.16, and -0.17 ± 0.85 μAmps/cm^2 change in basal I_{sc} respectively, which was not statistically significant, when compared with the 1.54 ± 2.09 μAmps/cm^2 change in basal I_{sc} observed in the untreated control (n = 4). In control cells CCh increased I_{sc} by 28.36 ± 11.13 μAmps/cm^2, compared with CCh-induced increases of 23.55 ± 9.98, and 23.15 ± 6.13 μAmps/cm^2 in cells treated apically with 1 or 25 μM UDCA respectively (n = 4). Furthermore, control responses to Fsk were 32.11 ± 10.94 μAmps/cm^2, compared with Fsk-induced I_{sc} responses of 35.93 ± 13.05, and 25.77 ± 10.63 μAmps/cm^2 in cells treated apically with 1 or 25 μM UDCA respectively (n = 4). These data indicated that UDCA did not acutely modulate Calu-3 I_{sc} within this physiological range.

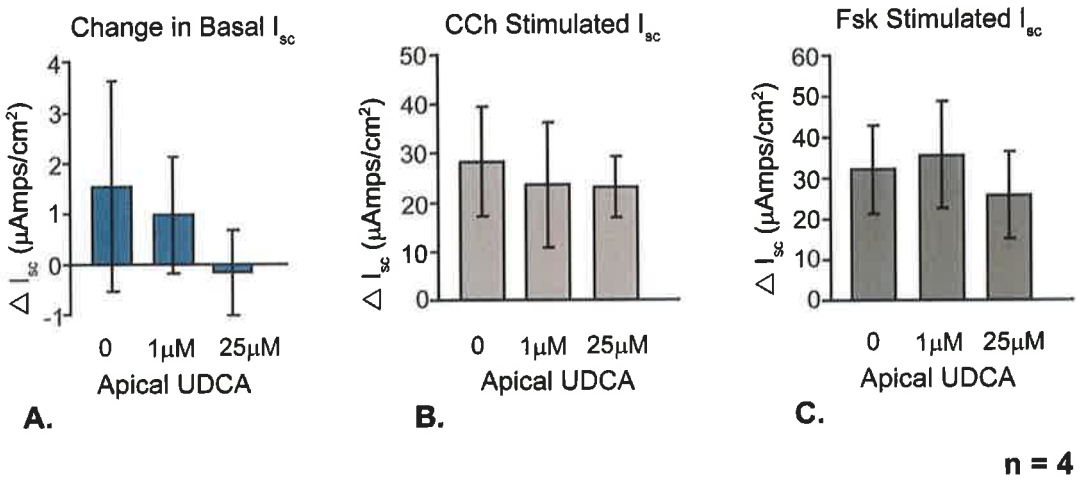

Fig.3.12 Acute apical treatment with UDCA does not affect I_{sc} in Calu-3 cells. **A.** I_{sc} responses recorded after acute apical treatment of Calu-3 with 1 or 25 μM UDCA. **B.** I_{sc} responses observed after treatment of Calu-3 with 100 μM CCh. **C.** I_{sc} responses observed after treatment of Calu-3 with 10 μM Fsk. Acute apical treatment with 1 or 25 μM UDCA did not significantly affect basal I_{sc} or subsequent CCh or Fsk induced responses in Calu-3 cells (n = 3).

3-2.6 The chronic effects of UDCA on I_{sc} in Calu-3 cells

Calu-3 were treated apically or basolaterally with 1 or 25 μM UDCA for 24 hr prior to being mounted in Ussing chambers. The experiments were performed using the same protocols as for DCA and TDCA. As can be seen in fig 3.13 A, basal I_{sc} recorded after 24 hr treatment with 1 or 25 μM basolateral UDCA was 12.66 ± 2.99, and 13.70 ± 4.01 μAmps/cm^2 respectively, but this was not significantly different to basal I_{sc} recordings of 13.62 ± 4.52 μAmps/cm^2 in control cells (n = 3). Carbachol increased I_{sc} by 18.12 ± 7.17 μAmps/cm^2 in control cells, compared with CCh induced I_{sc} increases of 19.37 ± 6.55, and 18.41± 3.77 μAmps/cm^2 in cells pre-treated basolaterally for 24 hr with 1 or 25 μM UDCA respectively (n = 3). Furthermore, Fsk-induced increases in I_{sc} were 30.18 ± 10.51 μAmps/cm^2 in control cells, compared with Fsk-induced I_{sc} responses of 30.66 ± 7.75, and 36.94 ± 7.45 μAmps/cm^2 in cells pre-treated with 1 or 25 μM UDCA respectively (n = 3). These results indicate that 24 hr basolateral treatment with UDCA did not significantly affect basal I_{sc} or subsequent CCh or Fsk stimulated I_{sc} responses.

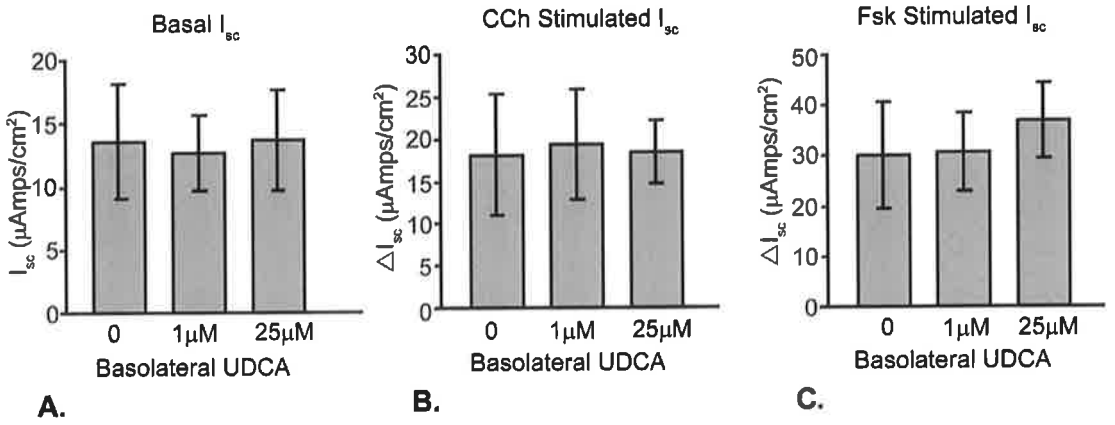

Fig.3.13 24hr basolateral treatment with UDCA does not affect I_{sc} in Calu-3 cells. A. I_{sc} recorded after 24 hr basolateral treatment of Calu-3 with 1 or 25 μM UDCA. **B.** I_{sc} responses observed after treatment of Calu-3 with 100 μM CCh. **C.** I_{sc} responses observed after treatment of Calu-3 with 10 μM Fsk. 24 hr basolateral treatment with 1 or 25 μM UDCA did not significantly affect basal I_{sc} or subsequent CCh or Fsk induced responses in Calu-3 cells (n = 3).

Preliminary experiments performed using 24 hr apical 1 – 25 μM UDCA treatments, indicated that 1 μM UDCA had no effect on basal I_{sc} or subsequent CCh or Fsk stimulated responses, while 25 μM UDCA appeared to increase CCh stimulated responses. According to the power calculations performed, it was determined that n = 3 would be required to establish if UDCA significantly increased CCh stimulation of I_{sc}. Upon repeating these experiments, 24 hr treatment with 25 μM apical UDCA slightly reduced basal I_{sc} to 13.4 ± 2.6 μAmps/cm^2, compared with basal I_{sc} recordings of 15.9 ± 4.8 μAmps/cm^2 in control cells but these changes were not statistically significant, as can be seen in fig 3.14 A. In addition, 24 hr apical incubation with 25 μM UDCA significantly increased CCh stimulated I_{sc} responses to 21.56 ± 6.35 μAmps/cm^2 compared with 13.10 ± 4.56 μAmps/cm^2 for untreated controls ($p = 0.03$, n = 6) as shown in fig 3.14, while 24 hr apical treatment with 25 μM UDCA slightly attenuated Fsk stimulated responses to 20.32 ± 5.03 μAmps/cm^2 compared with 28.52 ± 5.38 μAmps/cm^2 for untreated controls ($p = 0.07$, n = 6). Like DCA, these data indicate that UDCA also exhibits

sidedness and temporal dependency in its ability to modulate ion transport in Calu-3 cells.

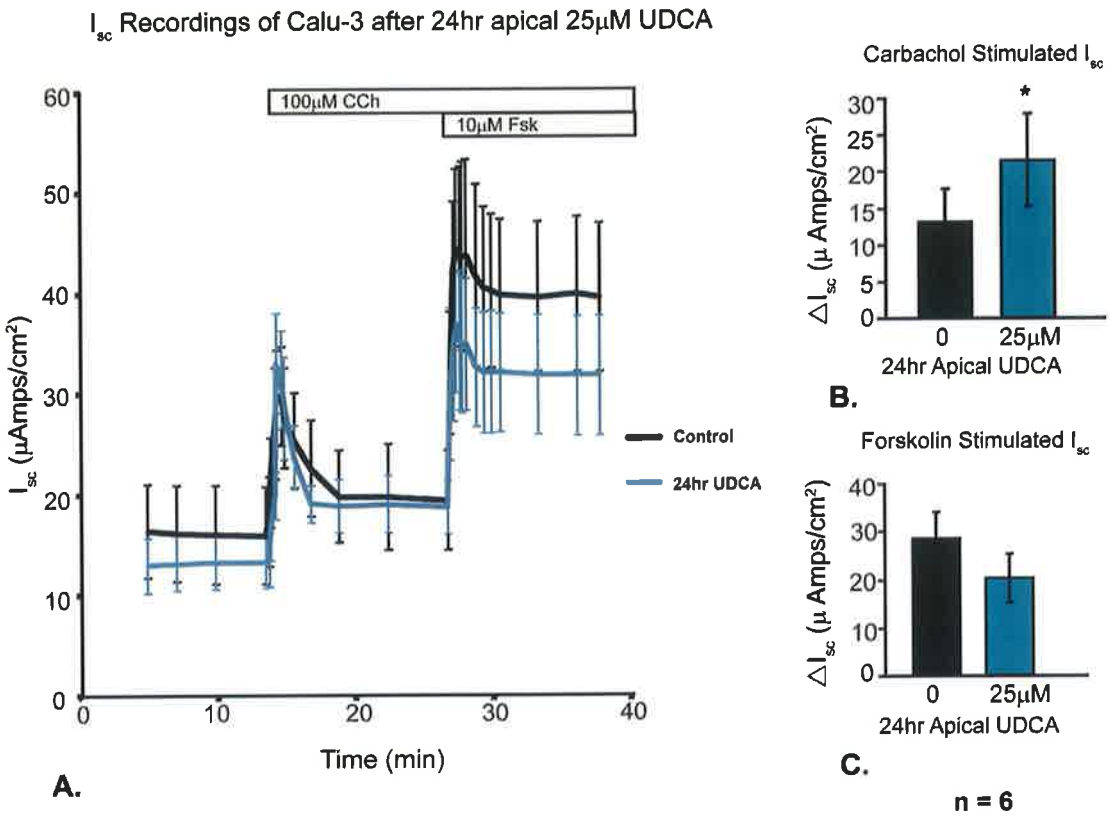

Fig.3.14 24 hr treatment with apical 25 μM UDCA increases CCH- stimulated I_{sc} in Calu-3 cells. A. I_{sc} recorded during the experiment with Calu-3 cells treated acutely with apical 25 μM DCA. **B**. I_{sc} responses observed after treatment of Calu-3 cells with CCh 24 hr treatment with UDCA significantly increased CCh-induced secretory responses to 21.56 ± 6.35 (μAmps/cm^2) compared with control responses of 13.1 ± 4.56 (μAmps/cm^2) in these experiments (p = 0.03, n = 6). **C**. I_{sc} responses observed after treatment of Calu-3 cells with Fsk. 24 hr apical treatment of Calu-3 with 25μM UDCA also significantly decreased the cAMP dependant Cl^- secretion stimulated by Fsk to 20.32 ± 5.03 (μAmps/cm^2) compared with control responses of 28.52 ± 5.38 (μAmps/cm^2) in these experiments (n = 6, p = 0.07).

3-3 Discussion

The aim of this chapter was to establish whether each of the bile acids under investigation, DCA, TDCA or UDCA, had any effect on ion transport at the low concentrations which are likely to be found in the airway. The data presented here clearly indicates that each of these bile acids, at a concentration of 25 μM, could modulate airway epithelial ion transport but that these effects varied according to bile acid structure and sidedness of application (fig 3.15).

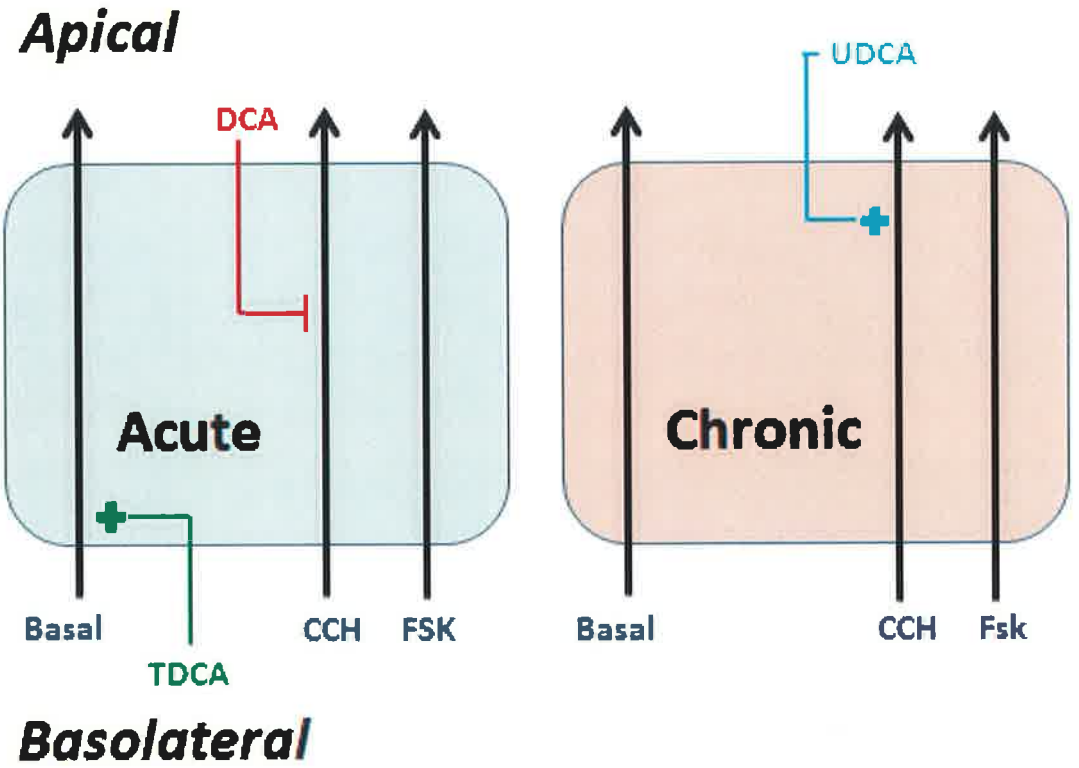

Fig.3.15 Chronic and acute modulation of I_{sc} in Calu-3 cells by DCA, UDCA and TDCA. Acute apical application of 25 μM DCA, while 24 hr apical UDCA increases CCh stimulated I_{sc}. Acute basolateral application of 25 μM TDCA stimulates basal I_{sc} in Calu-3 cells.

The unconjugated bile acids DCA and UDCA had no effect on basal I_{sc} but affected secretagogue-induced responses in a time-dependent manner, when applied apically. On the other hand TDCA, the taurine conjugate of DCA, could stimulate basal I_{sc} in Calu-3 but had no effect on secretagogue-induced responses. Again TDCA effects demonstrated temporal dependence and

sidedness as TDCA could only affect I_{sc} when applied basolaterally and had no effect after 24 hr.

Although these findings bear some similarity to bile acid effects on ion transport in colonic and gallbladder epithelia, novel observations are also reported in this chapter. Acute bilateral application of high concentrations of DCA (500 μM) has been shown to increase basal secretion in colonic epithelium in a transient fashion, with I_{sc} returning to baseline values after 15 min (Keely *et al.*, 2007). The transient nature of this secretion would suggest the involvement of intracellular calcium in stimulation of Cl^- secretion, and it has previously been reported that DCA facilitates increased Ca^{2+} entry at the plasma membrane (Lau *et al.*, 2005). Although no effect on basal I_{sc} at 25 μM DCA or UDCA concentration was observed in Calu-3 cells, acute DCA was found to significantly decrease CCh stimulated I_{sc}, while 24 hr UDCA significantly increased CCh stimulated I_{sc} (fig 3.15). Carbachol is a muscarinic agonist known to initially stimulate Cl^- secretion by mobilization of intracellular Ca^{2+} but subsequently prevents further calcium dependent Cl^- secretion without modifying Ca^{2+} mobilization, via activation of the epidermal growth factor receptor (EGFR) mediated inhibitory pathway (Keely and Barrett, 2000). The data presented here suggest that DCA and UDCA interfere with either the Ca^{2+} mobilizing ability of CCh or the negative feedback signalling mechanism of CCh, to modulate secretory responses in Calu-3 cells. In support of this conclusion, it has previously been reported that both acute and chronic activation of EGFR can differentially regulate epithelial Cl^- secretion (Keating *et al.*, 2009, Asano *et al.*, 2009, O'Mahony *et al.*, 2008), while concentrations of DCA as low as 50 μM have been shown to activate EGFR in epithelial tissues (Raimondi *et al.*, 2008). Further experiments using tyrophostin AG1478, an inhibitor of EGFR, would need to be performed in order to determine EGFR involvement in bile acid modulation of CCh responses in Calu-3 cells.

In this thesis, both DCA and UDCA have been found to have opposing acute and chronic effects on secretion. The finding that 25 μM DCA acutely inhibits

CCh stimulated secretion while UDCA was found to significantly increase CCh stimulated I_{sc} after 24 hr in Calu-3 cells would fit with the theory that bile acids acts as an "osmosignal" in colonic epithelial tissues (Keating *et al.*, 2009). This theory proposes that the physiological concentration of bile acids are maintained low to promote normal colonic absorptive function, which eventually results in dehydration of luminal contents and hence increased bile acid concentrations. When a threshold has been reached, bile acids become pro-secretory in order to rehydrate luminal contents. In turn, as bile acids become more diluted, they switch back to an anti-secretory effect. DCA may acutely inhibit secretion through acute activation of EGFR or another member of this receptor tyrosine kinase family, while chronic activation of this receptor by UDCA may in turn stimulate Cl^- secretion by increasing expression of CaCC and NKCC1, but this hypothesis would need to be investigated in detail (Mroz and Keely, 2012b, O'Mahony *et al.*, 2008).

The findings that UDCA did not acutely affect secretion in Calu-3 cells are in contrast to a recent study which demonstrated that UDCA can acutely inhibit both CCh and Fsk stimulated colonic secretion (Kelly *et al.*, 2013). However, one possible explanation for such differences in UDCA effects may be that the concentration of UDCA used in the study by Kelly *et al* was 250 μM, which was 10-fold higher than the concentration used here, and may activate different signalling pathways resulting in inhibition of Na^+/K^+ ATPase- and basolateral K^+ channel activity. Another possibility for the differences between UDCA responses observed in this study compared with that of Kelly *et al* may be due to tissue variation and hence differential expression of certain bile acid receptors such as FXR or TGR5, which will be investigated further in chapter 6.

One important observation made in this chapter, which directly contradicts previously published data from colonic epithelial studies (Keating *et al.*, 2009, Keely *et al.*, 2007, Kelly *et al.*, 2013), is that in Calu-3 cells both DCA and UDCA exhibit sidedness, with both modulating ion transport when applied apically only (Fig 3.15). This was a surprising finding given that Calu-3 cells

often have a thick overlying mucus layer, making access to the cells quite difficult. However, this was a physiologically important result for incidences where bile acids enter the airways through aspiration of gastroesophageal reflux, providing easier access to the apical than the basolateral membrane. Although unconjugated bile acids are known to be permeable to cell membranes in colonic epithelium, certain substrates involved in bile acid signal transduction, particularly signalling through tyrosine kinase receptors, may be differentially compartmentalized in polarized airway epithelial cells. It has been reported that although EGFR is predominantly expressed on the basolateral membrane of most polarised epithelial cells, overexpression of EGFR at the apical surface resulted in abnormal signal transduction due to differential regulation of EGFR mediated phosphorylation at the apical and basolateral membranes (Kuwada *et al.*, 1998). However, it is also possible that the reason for apparent sidedness exhibited by DCA and UDCA may simply be attributed to the variations between cell lines, since Calu-3 cells are often used for drug delivery studies and have shown high levels of apical permeability to aerosolized treatments (Mathia *et al.*, 2002, Mukherjee *et al.*, 2012). Therefore, this cell line may have evolved so that the apical membrane might be slightly more permeable to steroid molecules, such as DCA and UDCA, than the basolateral membrane and therefore higher concentrations of DCA and UDCA might be needed to induce secretory effects when applied basolaterally.

On the other hand, our results clearly show that TDCA stimulates basal secretion in Calu-3 cells but only when it is applied basolaterally, in accordance with previously published findings from the colon (Keely *et al.*, 2007). This indicates the presence of a receptor or transporter on the basolateral membrane of Calu-3 through which TDCA can elicit its effect. TDCA does not affect subsequent CCh or Fsk stimulated I_{sc} responses and also does not appear to have any effect on I_{sc} after 24 hr at this concentration (25 μM). The sustained nature of TDCA stimulation of I_{sc} over the course of the experiment, fig 3.7, is similar in nature, but lower in magnitude, to the sustained I_{sc} responses observed after treatment of Calu-3 cells with the

cAMP mobilizing agent Fsk. This seems to suggest the involvement of cAMP mobilization in TDCA stimulation of I_{sc}. This observation, along with the finding that TDCA does not chronically affect Calu-3 secretion, provide support to the hypothesis that TGR5, a bile acid G-protein coupled receptor which signals through cAMP, may be present in the basolateral membrane of Calu-3 cells and might perhaps be responsible for the sidedness exhibited in TDCA stimulation of I_{sc}. However, it is also possible that this sustained I_{sc} response induced by TDCA may also be due to combined mobilization of intracellular Ca^{2+} and subsequent inhibition of EGFR which is also thought to be expressed at the basolateral membrane. The role of these signalling molecules in TDCA stimulation of I_{sc} will be described in Chapter 5.

The basolateral effect of TDCA may be physiologically relevant in incidences of both elevated circulating serum bile acids, such as in intrahepatic cholestasis of pregnancy (ICP), and gastroesophageal reflux (GER) episodes. As is the case with ICP, serum bile acid levels are much higher than normal in the pregnant mother (~40 - 60 μM) due to hormonal impaired clearance of bile acids. As a result, bile acid concentrations in the blood of the newborn can reach 60 – 120 μM, with increased bile acid uptake into lungs, which is associated with development of respiratory distress syndrome (RDS) after birth (Zecca *et al.*, 2004, Zecca *et al.*, 2008). Alternatively, aspiration of bile acids during GER episodes introduces bile acids to the lung. However, in the airways of patients already experiencing increased inflammation such as CF, or other chronic airway diseases such as asthma, the integrity of the epithelial layer is compromised and the epithelial barrier function may not be as effective. Under these conditions, bile acids introduced apically to the airway epithelium may also be able to access the basolateral membrane. In addition, it has been reported that under acidic conditions bile acids are capable of disrupting the squamous epithelial barrier function (Chen *et al.*, 2011), which may be important during incidences of acid reflux where acidification of the airway could occur, facilitating bile acid access to the basolateral membrane.

In summary, this chapter provides evidence that each of the bile acids DCA, UDCA and TDCA are all capable of modulating Calu-3 ion transport, in a structurally-specific and time-dependent manner. However, as TDCA was the only bile acid to stimulate basal secretion in Calu-3 cells, the remaining chapters will focus on elucidating the mechanisms by which TDCA stimulates airway secretion. This investigation will provide a better insight into the physiological role played by bile acids in modulation of airway epithelial ion transport, rather than the effects of bile acids on secretagogue-induced secretion.

Chapter 4

TDCA stimulation of Cl^- secretion in airway epithelial cells

4-1 Introduction

Building on the results obtained in the previous chapter, the focus in this chapter was to elucidate the type of secretion stimulated by TDCA and to establish the channels involved in TDCA modulation of Calu-3 ion transport. As discussed in detail in chapter 1 (section 1.3), the airways tightly regulate epithelial ion transport in order to maintain adequate volumes of ASL bathing the surfaces of the epithelium, facilitating mucociliary clearance (MCC). This is an important feature of airway defence as impaired Cl^- secretion can lead to dehydration of the airways, reduction in MCC and hence colonization of the lung by opportunistic pathogens such as Aspergillus or Pseudomonas in CF. On the other hand, too much Cl^- secretion can also lead to defective MCC, in addition to alveolar flooding, as the level of periciliary layer (PCL) in which the cilia beat is too high and the cilia cannot make contact with the overlying mucus layer. Since it has recently been shown that CDCA can increase alveolar permeability via reduced expression of junctional proteins, including occludin, zonula occludens -1 (ZO-1) and E-cadherin, resulting in decreased transepithelial electrical resistance (TEER) (Su *et al.*, 2013), one important question that first had to be addressed in this investigation was whether TDCA stimulates secretion through the transcellular pathway or whether secretion is due to disruption of the epithelial integrity facilitating the paracellular flow of ions. It was also important to establish the type of ion secretion that TDCA could induce in these cells.

For many years there has been much controversy surrounding type of ion secretion that predominates in Calu-3 cells, ie Cl^- or HCO_3^- (Singh *et al.*, 1997, Lee *et al.*, 1998, Devor *et al.*, 1999, Cuthbert *et al.*, 2003, MacVinish *et al.*, 2007, Huang *et al.*, 2012b, Shan *et al.*, 2012, Garnett *et al.*, 2013). While there is no doubt that HCO_3^- plays an important role in ion secretion in Calu-3 cells, there is still much debate as to whether the majority of current recorded under short circuit conditions is due to direct transport of HCO_3^- or HCO_3^- -dependent Cl^- transport. It has been reported that serous cells from submucosal glands secrete HCO_3^- in response to the cAMP generating agonist, forskolin, while they secrete Cl^- in response to 1-ethyl-2

benzimidazolinone (1-EBIO), an activator of the basolateral Ca^{2+}-activated K^+ channels (Devor *et al.*, 1999). This presents a model for airway epithelium that may switch between HCO_3^- and Cl^- secretion and it has been proposed that this may be determined by the basolateral membrane potential. Recently it has been shown that HCO_3^- -dependent Cl^- secretion drives fluid transport across Calu-3 cell layers (Shan *et al.*, 2012). Furthermore, it had previously been reported that under short circuit conditions, Calu-3 cells respond to stimulation with 7,8, benzoquinoline by producing an increase in current that was completely accounted for by the net flux of Cl^- (Cuthbert *et al.*, 2003). It has been suggested that the anion exchanger AE2, expressed at the basolateral membrane of many epithelial cells may be responsible for coupling of Cl^- secretion to HCO_3^- transport in response to cAMP, as recycling of HCO_3^- is required for Cl^- loading in these cells (Huang *et al.*, 2012b). On the other hand, in contradiction to this report, it has been shown that Calu-3 cells secrete HCO_3^- in response to cAMP by a mechanism that involves inhibition of Cl^- loading through AE2, and increased apical HCO_3^- transport through exchangers such as pendrin and activation of CFTR (Garnett *et al.*, 2013). Taken together, these findings highlight the importance of determining the type of secretion induced by TDCA in our Calu-3 model, before beginning to investigate the ion transport proteins involved.

Almost 3 decades ago it was reported that concentrations of TDCA as low as 50 μM could stimulate Cl^- secretion in the distal colon of adult rabbits but not in infant rabbits lacking bile acid transporters (Potter *et al.*, 1987). It was later shown that TDCA stimulates Cl^- secretion in T_{84} colonic epithelial cells via an IP_3 – mediated Ca^{2+} release from intracellular stores (Devor *et al.*, 1993). In confirmation of this, TDCA was found to stimulate Cl^- secretion in epithelial cells from canine pancreatic ducts via Ca^{2+} activation of apical CaCC and basolateral K^+ channels (Okolo *et al.*, 2002). Taken together, these reports suggest that TDCA stimulation of I_{sc} observed in Calu-3 cells is likely due to Cl^- secretion rather than HCO_3^- secretion. The main ion transport proteins involved in Cl^- secretion in the airways are the apically located CFTR and CaCC, providing the route for Cl^- exit from the cell according to its

electrochemical gradient. The basolaterally located NKCC1 is an electroneutral symporter, which facilitates Cl^- uptake into the cell from the extracellular space along with Na^+ and K^+. The driving force for uptake of Cl^- through NKCC1 is provided by the basolateral Na^+/K^+ ATPase which establishes an inwardly directed Na^+ gradient, facilitating Na^+ entry into the cell along with Cl^- and K^+. In addition, activation of the basolateral K^+ channels further enhances Cl^- secretion by converting the resting membrane potential from positive to negative and therefore generating an electrochemical driving force for Cl^- exit through the apical membrane.

Airway epithelial ion transport is tightly regulated and cells can easily switch from an absorptive to secretory phenotype, and vice versa, in response to various endogenous stimuli such as hormones, inflammatory mediators, channel activating proteases, shear stress, nucleotides or in response to inhaled pathogens or irritants. Each of these stimuli can induce signalling via many different kinase pathways that regulate ion transporter activity by phosphorylation, and usually involve increasing intracellular concentrations of two key 2nd messengers - Ca^{2+} or cAMP, which will be investigated further in the next chapter. In addition to regulation of transporter activity by phosphorylation events, changes in ion transport can also be mediated by modulation of the trafficking of individual ion transport proteins to the membrane. Compartmentalization of proteins within the cell is a highly controlled process involving many different enzymatic steps to transport proteins from site of synthesis to where they are required, or to remove proteins from this location when they are no longer needed. Delayed trafficking of transporters to the membrane decreases the number of active transporters at the cell surface that can be stimulated under basal conditions, hence attenuating the transport of a particular ion. Similarly, increased trafficking of ion transport proteins to the membrane can increase ion transport under basal conditions. Therefore the aim in this chapter was also to determine whether observed changes in ion transporter activity after TDCA treatment were due to changes in trafficking of the transport protein to the membrane.

Finally, in order to ensure that TDCA stimulation of secretion in the airways was a feature of all epithelial cells contributing to ASL hydration rather than just the serous cells of the SMGs (Calu-3 cells), Ussing chamber experiments with the NuLi-1 cell line, a model of normal bronchial columnar epithelium, and the CuFi-1 cell line, a model of F508del CF bronchial columnar epithelium (Zabner *et al.*, 2003) were performed. In addition, these Ussing chamber experiments were repeated using primary human CF and normal epithelial cells grown under air-liquid interface (ALI) and treated acutely with TDCA. It had previously been reported that Calu-3 cells lack apical amiloride-sensitive I_{sc} and hence do not express active ENaC (Singh *et al.*, 1997), which corresponded with the findings that amiloride had no effect on Calu-3 cells in Ussing chambers in this study. Therefore, it was important to establish whether TDCA could also stimulate secretion in the presence of ENaC, or whether this increase in Cl^- secretion by TDCA could be compensated for by increased Na^+ absorption through ENaC, resulting in no overall net effect on transepithelial fluid transport.

Specifically, in this chapter the primary aim was to:

1) identify the ionic basis for secretion induced by acute TDCA treatment
2) elucidate the ion transport proteins involved in TDCA stimulated secretion, through the use of specific inhibitors and permeabilization studies in Ussing chambers
3) establish whether TDCA can stimulate secretion in all types of airway epithelial cells contributing to ASL volume, using NuLi-1, CuFi-1 and human primary epithelial cell models
4) determine whether TDCA induces secretion via modulation of ion transport protein abundance the membrane, using cell surface biotinylation technique

4-2 Results

4-2.1 TDCA stimulates I_{sc} without affecting TEER in Calu-3 Cells.

In order to establish whether TDCA stimulation of I_{sc} was due to increased transcellular ion transport or as a result of increased permeability of the paracellular pathway, the TEER of Calu-3 cells grown under ALI conditions on Costar snapwells for 9 – 12 days was measured before starting the experiment. Cells were then mounted in Ussing chambers and the basal I_{sc} was recorded for 15 min prior to acute treatment with 25 μM TDCA on the basolateral side. The I_{sc} was recorded for a further 20 min during which time changes in TEER were also recorded.

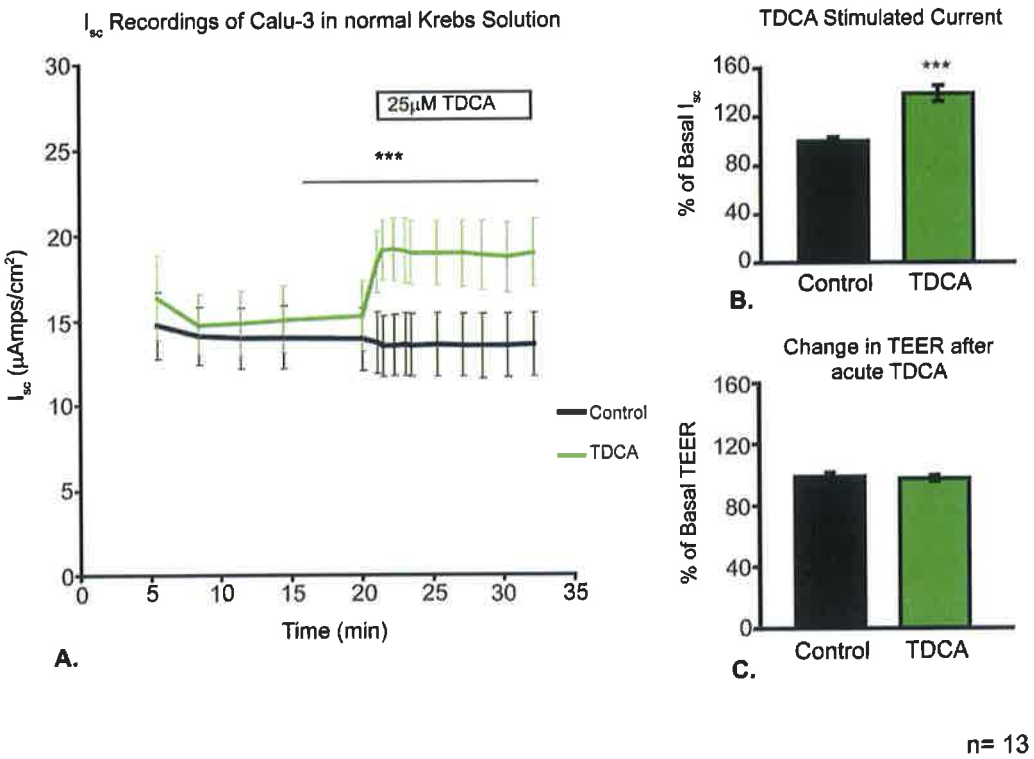

Fig.4.1 Acute treatment with 25 μM TDCA increases basal I_{sc} without affecting TEER. A, I_{sc} values recorded during Ussing chambers experiments of Calu-3 cells treated with 25 μM TDCA basolaterally **B.** Change in I_{sc} represented as % of basal I_{sc} after TDCA treatment. TDCA treatment resulted in a 39 ± 7% increase in basal I_{sc} (n = 13, p = 0.0001). **C.** Change in TEER represented as % of basal TEER after TDCA treatment. At 25 μM concentration, TDCA did not decrease TEER indicating that it does not disrupt tight junctions and hence is non-toxic to the cells.

As can be seen from fig 4.1, basolateral TDCA significantly increased basal I_{sc} in Calu-3 by 39 ± 7% (p = 0.0001) but showed no variation in TEER with respect to an untreated control during the course of the experiment (n = 13). This indicated that the integrity of the cell layer remained intact after TDCA treatment, and hence TDCA stimulation of ion transport was through the cellular pathway.

4-2.2 TDCA stimulates Cl^- secretion in Calu-3 cells.

The next step was to determine whether Cl^- or HCO_3^- contribute most to basal I_{sc} in this model of Calu-3, and hence establish whether TDCA was stimulating Cl^- secretion or HCO_3^- secretion. In order to do this a Cl^- free Krebs solution was prepared as detailed in chapter 2 (Table 2.2). Cells were mounted in Ussing chambers and two sets of experiments were performed in parallel- TDCA treatment of Calu-3 cells in normal Krebs solution and TDCA treatment of Calu-3 cells in Cl^- free Krebs solution. Once the correct perfusion solutions had been set up, the basal I_{sc} was recorded for 10 min prior to acute treatment with 25 μM TDCA on the basolateral side and the I_{sc} was recorded for a further 15 min. As can be seen in fig 4.2 A & B, removal of the Cl^- from the perfusion solution reduced basal I_{sc} values to 4.24 ± 1.89 μAmps/cm^2 compared with basal I_{sc} values of 14.75 ± 1.94 μAmps/cm^2. This indicated Cl^- secretion contributes to the majority of I_{sc} in this experimental model. As HCO_3^- was present under Cl^- free conditions but TDCA stimulation of I_{sc} was abolished, fig 4.2 A, this result suggests that TDCA stimulates Cl^- secretion in Calu-3 cells.

In order to confirm that TDCA stimulated Cl^- secretion in these cells, the experiment was repeated using normal Krebs perfusion solution and pre-treatment with 10 μM bumetanide, an inhibitor of NKCC1, before TDCA. Inhibition of NKCC1, inhibits Cl^- entry into the cell and therefore will abolish sustained Cl^- secretion. As shown in fig 4.2 C, pre-treatment with bumetanide reduced TDCA stimulation of I_{sc} to 0.7 ± 0.9 μAmps/cm^2 which was comparable to control values of 0.4 ± 0.6 μAmps/cm^2, while TDCA alone increased I_{sc} values by 2.6 ± 1.2 μAmps/cm^2 (n = 3). According to the power calculations performed, it was determined that n = 4 would be required to establish whether bumetanide significantly attenuates TDCA stimulation of I_{sc}. Taken together, these results indicate that TDCA stimulation of basal I_{sc} was due to increased Cl^- secretion in Calu-3 cells.

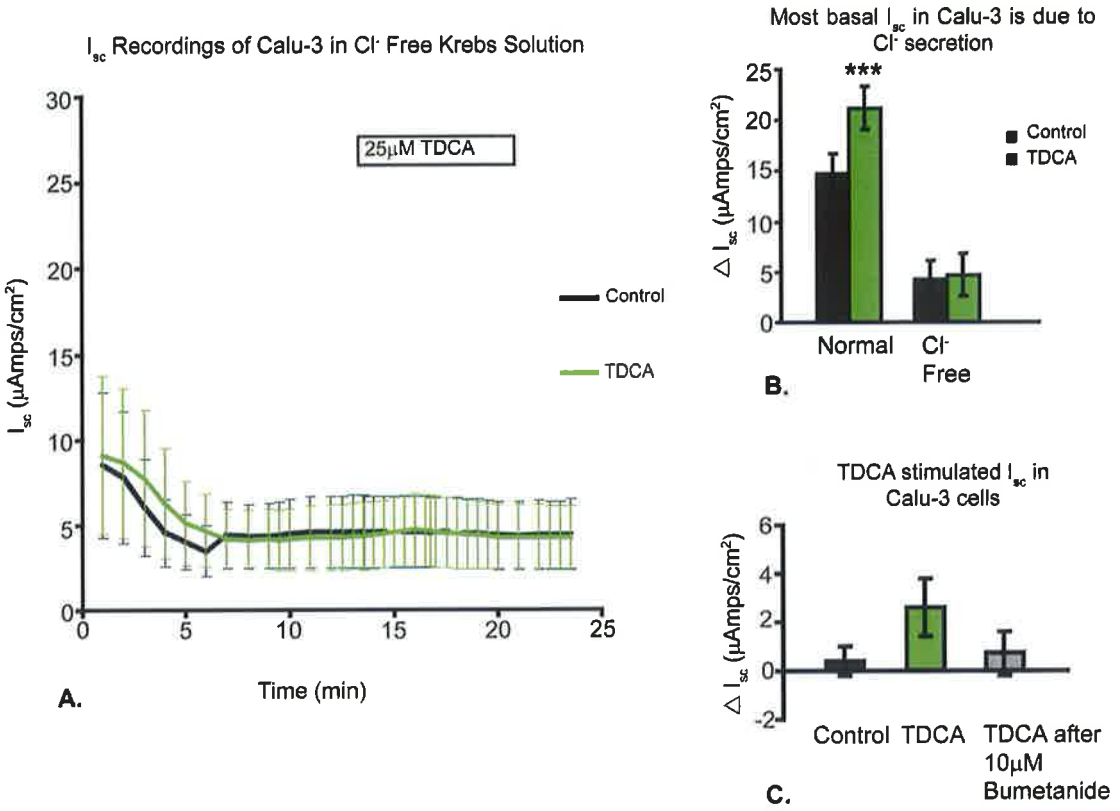

Fig.4.2 Acute treatment with 25μM TDCA stimulates Cl^- secretion in Calu-3 cells. A. I_{sc} values recorded during Ussing chambers experiments of Calu-3 cells treated with 25 μM TDCA basolaterally Cl^- free Krebs solution. **B.** Comparison between I_{sc} values recorded in normal Krebs solution or Cl^- free Krebs solution. Removal of Cl^- from the bathing solution decreased basal I_{sc} values to 4.24 ± 1.89 (μAmps/cm^2) compared with basal I_{sc} values of 14.75 ± 1.94 (μAmps/cm^2) in normal Krebs solution, suggesting that Cl^- secretion generates the majority basal I_{sc} in Calu-3 monolayers. Under chloride-free conditions the TDCA stimulation of I_{sc} was abolished, indicating that TDCA amplification of I_{sc} requires activation of Cl^- secretion (n = 4). **C.** I_{sc} responses observed after TDCA treatment in normal Krebs solution. TDCA stimulation of I_{sc} was inhibited by pre-treatment with 10 μM bumetanide further indicating that TDCA stimulates Cl^- secretion in Calu-3 (n = 3).

4-2.3 Clotrimazole does not inhibit TDCA stimulation of Cl^- secretion in Calu-3 cells.

Once it was established that TDCA induces Cl^- secretion in Calu-3, the investigation was then focused on identifying the ion transport proteins involved in Cl^- secretion. Clotrimazole is a known inhibitor of the basolateral Ca^{2+} activated K^+ channel, KCNN4, which plays an important role in the generation of a driving force for Cl^- secretion in Calu-3 cells (Waugh *et al.*,

2013). In order to investigate KCNN4 involvement in TDCA stimulation of Cl^- secretion, Calu-3 cells mounted in Ussing chambers were treated basolaterally with 10 μM clotrimazole immediately prior to treatment with TDCA. Fig 4.3 demonstrates that clotrimazole does not inhibit TDCA stimulation of Cl^- secretion, indicating that KCNN4 is not involved. However, it was possible that other K^+ channels might have been activated by TDCA and so further investigations to isolate basolateral K^+ channels in Ussing chambers were required.

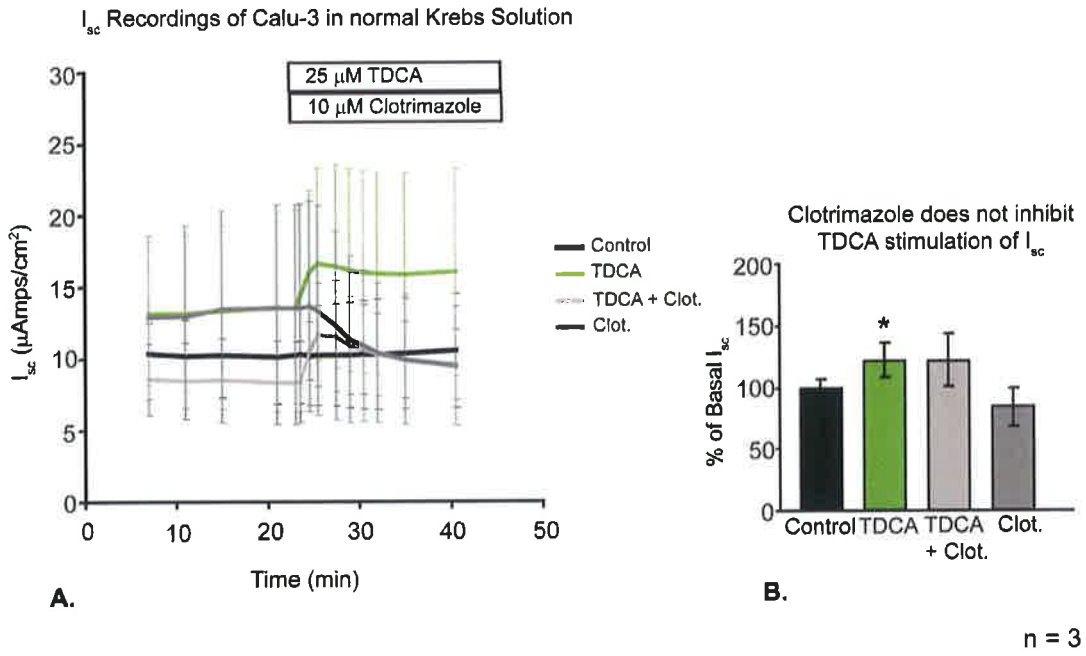

Fig.4.3 Acute treatment with the K^+ channel inhibitor clotrimazole does not inhibit TDCA stimulation of Cl^- secretion in Calu-3 cells. A. I_{sc} values recorded during Ussing chambers experiments of Calu-3 cells treated with 25 μM TDCA or 10 μM clotrimazole. **B.** Changes in I_{sc} values normalized to % of basal I_{sc}. Acute basolateral treatment of Calu-3 cells with 10 μM clotrimazole immediately before 25 μM TDCA treatment did not significantly attenuate the TDCA induced increase in basal I_{sc}. This indicates that TDCA stimulates basal I_{sc} independently of the basolateral K^+ Channel KCNN4.

4-2.4 $CFTR_{inh172}$ delays TDCA stimulation of Cl^- secretion in Calu-3 cells.

Next, the role of the apical Cl^- channel, CFTR, in TDCA stimulation of Cl^- secretion in Calu-3 cells was investigated, using $CFTR_{inh172}$, a specific

inhibitor of CFTR. Calu-3 cells mounted in Ussing chambers were treated apically with 10 μM $CFTR_{inh172}$ immediately prior to treatment with TDCA. Fig 4.4 demonstrates that $CFTR_{inh172}$ was capable of attenuating basal I_{sc} in Calu-3 but did not inhibit TDCA stimulation of Cl^- secretion. However, as can be seen from fig 4.4 A, pre-treatment with $CFTR_{inh172}$ appeared to delay TDCA stimulation of Cl^- secretion, when compared with control values. This suggested that rapid activation of CFTR by TDCA was inhibited in this experiment but that another slower component of TDCA stimulation of I_{sc} was still active, resulting in a slower increase in I_{sc} by TDCA compared to control cells. Further investigation of other ion transport proteins involved in this process, along with confirmation of CFTR activation by TDCA using permeabilization studies in Ussing chambers to isolate I_{sc} generated by specific Cl^- transporters was required.

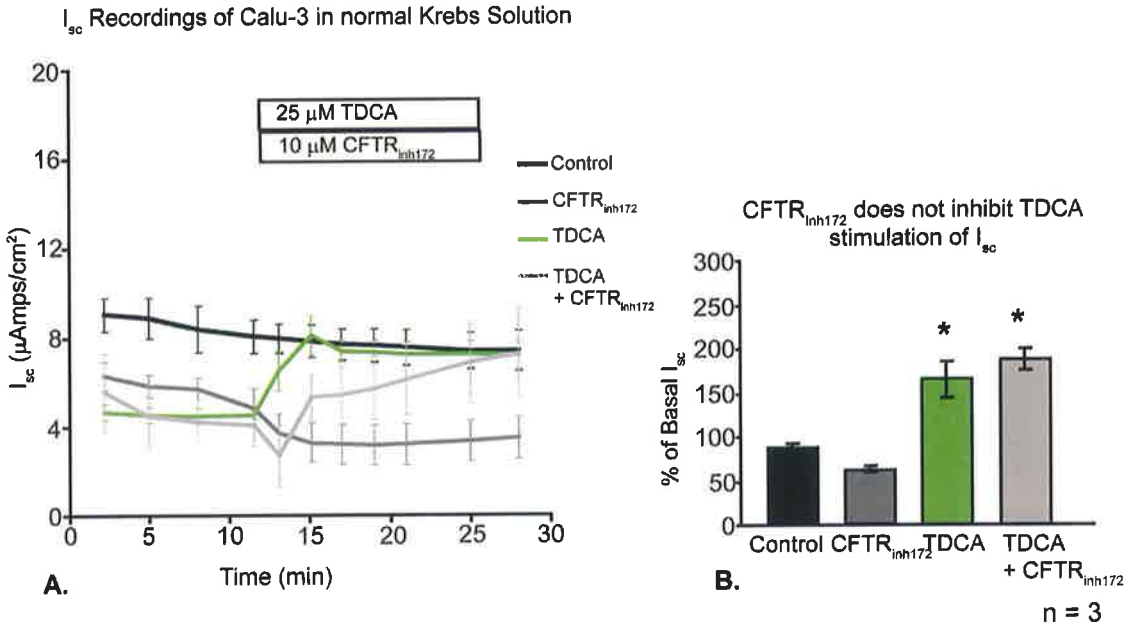

Fig.4.4 Acute treatment with $CFTR_{inh172}$ delays TDCA stimulation of Cl^- secretion in Calu-3 cells. A. I_{sc} values recorded during Ussing chambers experiments of Calu-3 cells treated with 25 μM TDCA or 10 μM $CFTR_{inh172}$. **B.** Changes in I_{sc} values normalized to % of basal I_{sc}. Acute apical treatment of Calu-3 cells with 10 μM $CFTR_{inh172}$ immediately before 25 μM TDCA treatment did not inhibit the TDCA induced increases in basal I_{sc}. However, $CFTR_{inh172}$ pre-treatment appeared to slow down TDCA stimulation of Cl^- secretion, when compared with control values. This suggested that activation of CFTR, along with other ion transporters, may be involved in TDCA stimulation of basal current.

4-2.5 TDCA attenuates CCh stimulation of basolateral K^+ channels in Calu-3 cells.

As the experiments using clotrimazole did not fully answer the question regarding the role played by K^+ channels in TDCA stimulation of Cl^- secretion, Ussing chamber membrane permeabilization experiments to isolate K^+ channel currents were performed, as described in detail in chapter 2 (section 2-2.3). Briefly, an apical to basolateral K^+ gradient was established across the Calu-3 layer mounted in Ussing chambers and the apical membrane was permeabilized using the ionophore, amphotericin B (25 μM), so that the basolateral membrane provided the only resistance to flow of K^+ ions. Once the I_{sc} had stabilized, cells were treated basolaterally with 100 μM ouabain,

the specific inhibitor of Na^+/K^+ ATPase activity. I_{sc} was once more allowed to stabilize before treatment with TDCA, CCh and Fsk. Under these conditions, changes in I_{sc} are representative of changes in K^+ transport across the basolateral membrane. Acute treatment with TDCA did not have any effect on basal K^+ I_{sc} or Fsk- induced K^+ transport in Calu-3, but significantly reduced subsequent CCh activation of K^+ channels by 58 ± 7 % compared with control values ($n = 6$, $p = 0.031$), fig 4.5. According to the power calculations performed, it was determined that $n = 4$ would be required to establish whether TDCA significantly reduced CCh stimulation of K^+ currents in Calu-3 cells. These results suggest that TDCA attenuated activation of basolateral Ca^{2+}-activated K^+ channels, but that TDCA alone did not affect basal K^+ transport.

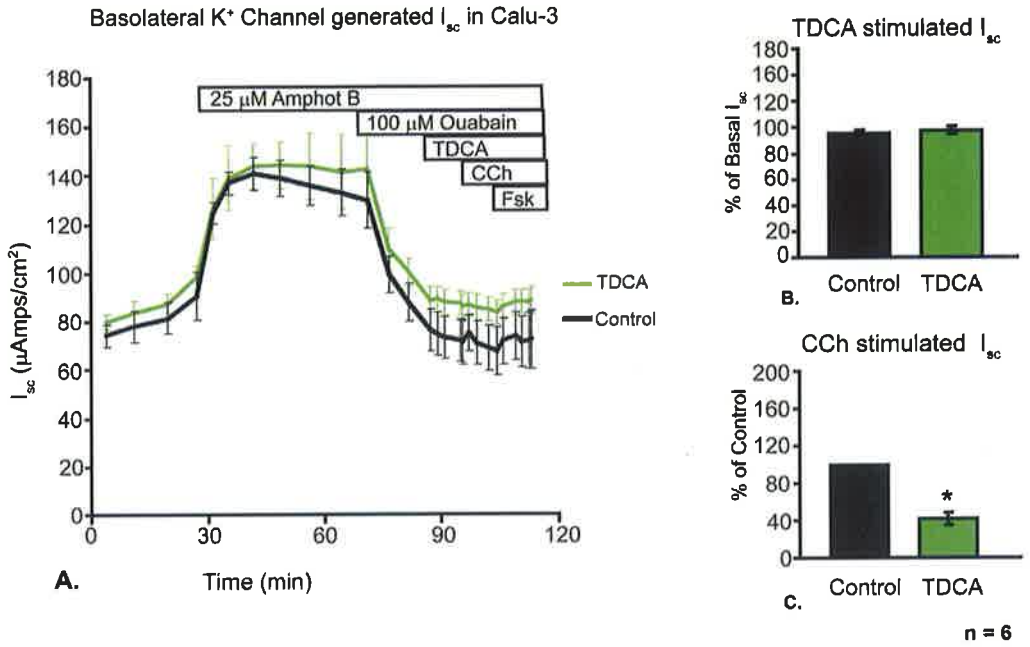

Fig.4.5 TDCA attenuates CCh stimulation of basolateral K^+ channels in Calu-3 cells. A. I_{sc} values recorded during Ussing chambers experiments of Calu-3 cells to isolate basolateral K^+ current. Basal I_{sc} values were much higher than under normal conditions due to the presence of an apical to basolateral K^+ gradient. Permeabilization of the apical membrane further increased K^+ transport through the basolateral membrane. Inhibition of the Na^+/K^+ ATPase activity using ouabain ensured that remaining I_{sc} under these conditions was representative of K^+ transport across the basolateral membrane through the basolateral K^+ channels. **B.** Changes in I_{sc} values after TDCA treatment normalized to % of basal K^+ current. TDCA had no effect on the basal activity of K^+ channels under these conditions. **C.** Changes in I_{sc} values after CCh treatment normalized to % of control. Acute treatment with TDCA significantly reduced subsequent CCh activation of K^+ channels by 58 ± 7 % compared with control values ($p = 0.031$, $n = 6$).

4-2.6 TDCA stimulates Cl^- secretion through CFTR in Calu-3 cells.

In order to confirm the results from experiments performed using pre-treatment with $CFTR_{inh172}$ in section 4-2.4, a more comprehensive examination of CFTR involvement in TDCA stimulation of Cl^- secretion was performed. In order to thoroughly investigate this, Ussing chamber membrane permeabilization experiments to isolate CFTR I_{sc} were performed, as described in detail in chapter 2 (section 2-2.2). Briefly, an apical to basolateral Cl^- gradient was established across the Calu-3 layer mounted in Ussing chambers and the basolateral membrane was permeabilized using 200 μg/ml

nystatin. Under these conditions changes in I_{sc} were representative of changes in Cl^- transport across the apical membrane. In order to ensure TDCA stimulation of I_{sc} was via activation of CFTR, one insert was pre-treated with $CFTR_{inh172}$ before TDCA, in each experiment. According to the power calculations performed, it was determined that n = 5 would be required to establish whether TDCA significantly increased CFTR currents in Calu-3 cells. As shown in fig 4.6 A & B, TDCA treatment significantly increased Cl^- transport by 20.77 ± 5.66 μAmps/cm^2 compared with an increase of 4.74 ± 2.58 μAmps/cm^2 in the $CFTR_{inh172}$ pre-treated cells and 3.93 ± 2.08 μAmps/cm^2 in the untreated control (negative values shown in fig 4.6 A due to the apical to basolateral direction of the Cl^- gradient) (n = 5, p = 0.008, p = 0.01). After TDCA treatment, the untreated control and TDCA - only cells were then treated with $CFTR_{inh172}$. It was observed that pre-treatment with TDCA significantly increased $CFTR_{inh172}$ sensitive I_{sc} responses to 29.59 ± 7.31 compared with responses of 12.19 ± 6.09 μAmps/cm^2 in the untreated control (n = 5, p = 0.04). These results therefore confirm that TDCA stimulation of Cl^- secretion involves activation of CFTR in Calu-3.

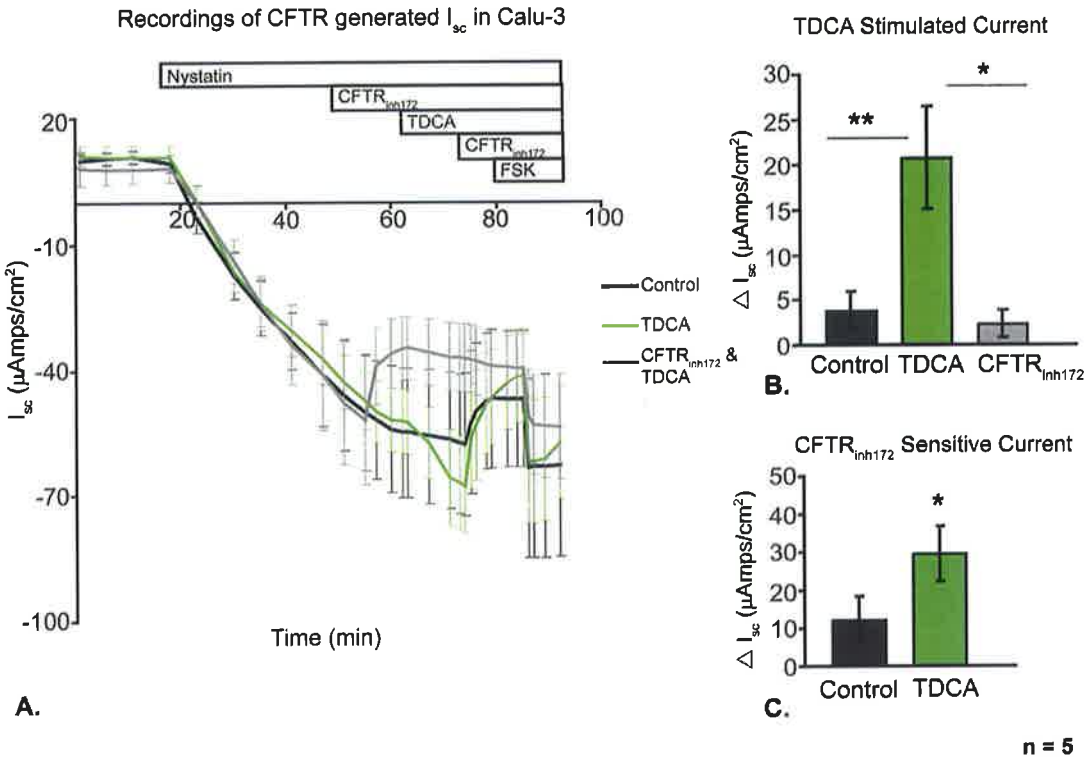

Fig.4.6 TDCA stimulates Cl^- secretion through CFTR in Calu-3 cells. A. I_{sc} values recorded during Ussing chambers experiments of Calu-3 cells to isolate CFTR generated I_{sc}. Calu-3 monolayers were exposed to an apical to basolateral Cl^- gradient in Ussing chambers. To eliminate the contribution of basolateral ion fluxes to I_{sc} responses, 200 μg/ml nystatin was added basolaterally to permeabilize the membrane. Under these conditions, I_{sc} is due to Cl^- transport through the apical membrane. In order to distinguish CFTR-generated currents, $CFTR_{inh172}$ was added either before or after TDCA. **B.** I_{sc} responses observed after TDCA treatment. Acute treatment with TDCA stimulated the CFTR-specific I_{sc} by 32 ± 9 % (n = 5, p = 0.007) and this effect was abolished by pre-treatment with $CFTR_{inh172}$ (n = 5, p = 0.008, p = 0.01). **C.** I_{sc} responses observed after $CFTR_{inh172}$ treatment. Pre-treatment with TDCA significantly increased $CFTR_{inh172}$ sensitive I_{sc} responses to 29.59 ± 7.31 compared with responses of 12.19 ± 6.09 μAmps/cm² in the untreated control (n = 5, p = 0.04). This indicates that acute basolateral TDCA treatment stimulates Cl^- secretion through CFTR.

4-2.7 TDCA stimulates Cl^- secretion through CFTR in normal ciliated bronchial epithelium but has no effect in CF epithelium.

After confirming that TDCA could stimulate Cl^- secretion via activation of CFTR, we decided to investigate whether this was only a feature of the serous cells of the airway SMGs or whether TDCA could also stimulate Cl^- secretion

in other models of airway epithelium. We therefore performed Ussing chamber experiments using NuLi-1 and CuFi-1 cell lines as models of bronchial ciliated columnar epithelium treated acutely with 25 μM TDCA. NuLi-1 and CuFi-1 were grown on Costar inserts in ALI culture for 3 - 4 weeks until TEER reached ~1000 Ohm*cm^2. The epithelia were then mounted in Ussing chambers and the basal I_{sc} was recorded for 15 min prior to acute treatment with 25 μM TDCA on the basolateral side. The I_{sc} was recorded for a further 15 min before cells were subsequently treated with 10 μM amiloride (ENaC inhibitor), and 100 μM CCh. NuLi-1 cells were further treated with 10 μM Fsk, and 10 μM $CFTR_{inh172}$. The I_{sc} was allowed to stabilize between each treatment.

As can be seen from fig 4.7, acute treatment with TDCA did not affect basal I_{sc} in either cell line, with ENaC contributing to the majority of basal I_{sc} in both NuLi-1 and CuFi-1. TDCA treatment slightly increased amiloride sensitive I_{sc} to 16.37 ± 3.51 μAmps/cm^2 compared with control values of 15.22 ± 3.02 μAmps/cm^2 in NuLi-1, but had no effect in CuFi-1. In addition, although the responses to CCh were small in both cell lines, TDCA pre-treatment appeared to attenuate subsequent CCh responses in both cell lines. In NuLi-1, CCh increased control I_{sc} by 1.97 ± 0.60 μAmps/cm^2 compared with an increase of 1.28 ± 0.60 μAmps/cm^2 after TDCA treatment, while in CuFi-1, CCh increased control I_{sc} by 0.49 ± 0.04 μAmps/cm^2 compared with an increase of 0.39 ± 0.06 μAmps/cm^2 after TDCA treatment. There did not appear to be any difference in Fsk stimulated responses in NuLi-1. However, $CFTR_{inh172}$ decreased I_{sc} by 4.77 ± 0.71 μAmps/cm^2 after TDCA treatment, which was significantly higher than the decrease of 3.49 ± 0.82 μAmps/cm^2 in control cells ($p = 0.018$, $n = 4$). According to the power calculations performed, it was determined that $n = 4$ would be required to establish whether TDCA significantly increased CFTR currents in NuLi-1 cells. Since CuFi-1 cells do not express functional CFTR and TDCA did not stimulate Cl^- secretion nor change net I_{sc} in these cells we can conclude that TDCA specifically stimulates CFTR current without affecting Na^+ absorption through ENaC.

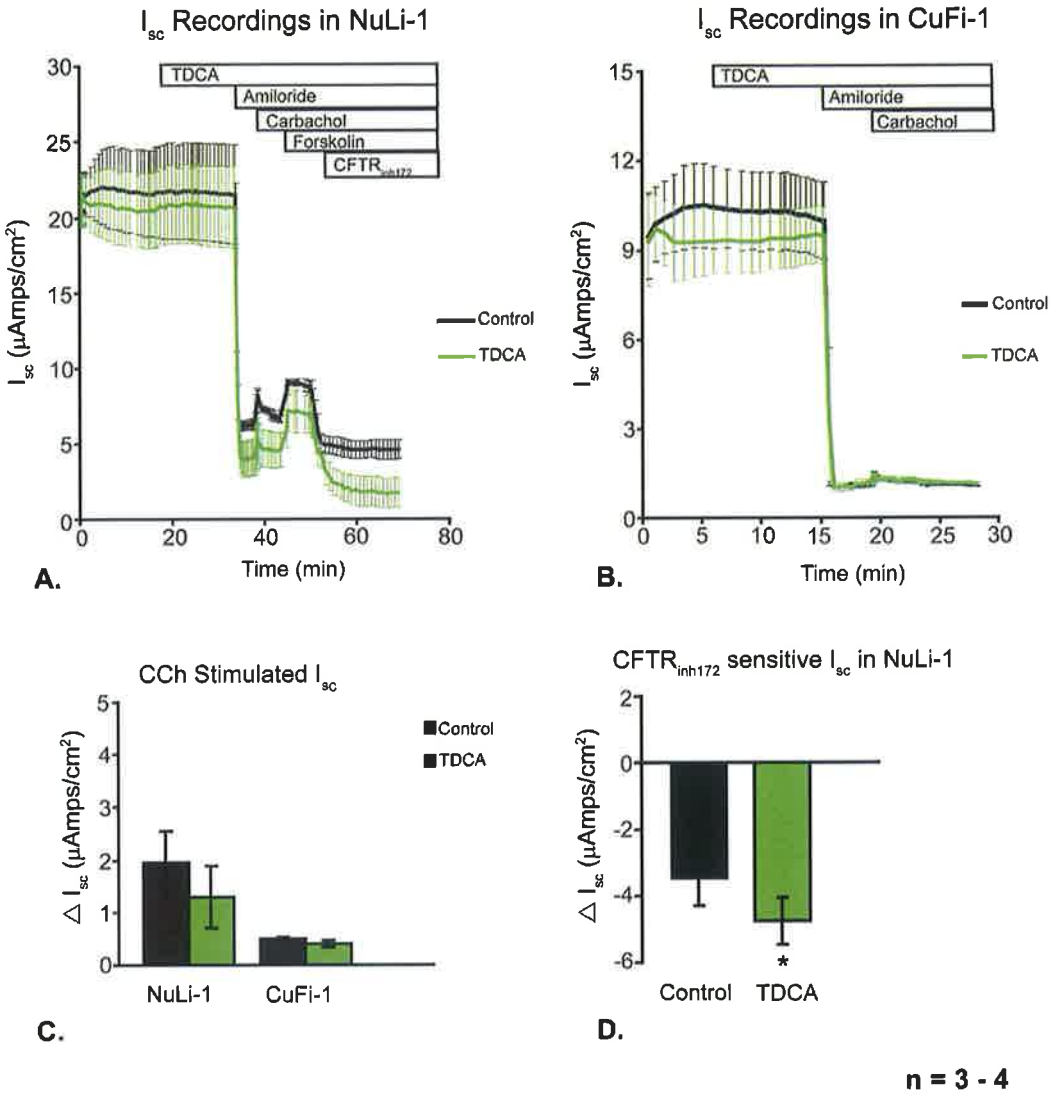

Fig.4.7 Acute treatment with TDCA increases $CFTR_{inh172}$ sensitive I_{sc} in NuLi-1 cells. A & B I_{sc} recordings of NuLi-1 and CuFi-1 monolayers mounted in Ussing chambers treated with 25 μM TDCA basolaterally **C.** I_{sc} responses observed after CCh treatment TDCA treatment appeared to decrease subsequent I_{sc} responses to CCh in both NuLi-1 and CuFi-1. **D.** I_{sc} responses observed after $CFTR_{inh172}$ treatment At 25 μM concentration, TDCA significantly increased $CFTR_{inh172}$ I_{sc} by 46 ± 13% when compared to control values ($p = 0.018$, $n = 4$).

These experiments were repeated using human primary samples of columnar epithelium isolated from CF patients, and one non-CF patient, by bronchial brushing during bronchoscopy. In these primary cells, the contribution to basal I_{sc} by amiloride-sensitive I_{sc} is lower and the responses to CCh and Fsk (non-CF only) are larger than in NuLi-1 and CuFi-1. However, as primary samples of non-CF patients are more difficult to obtain, due to a less frequent

requirement for bronchoscopy, only 1 non-CF patient sample was acquired throughout the study, while 5 CF samples, all heterozygous for F508del CFTR were obtained. As can be seen in fig 4.8, acute treatment with TDCA increased basal I_{sc} by 0.4 μAmps/cm^2 in non-CF primary tissue, and decreased basal I_{sc} by 0.4 ± 0.3 μAmps/cm^2 in the 5 CF epithelia samples. According to the power calculations performed, it was determined that n = 7 would be required to establish whether TDCA significantly reduced basal currents in CF primary cells. However, as the reduction in I_{sc} is so small, it is difficult to assess the physiological relevance of such a decrease and so investigation of ASL height should also be performed. Since this study only included one non-CF sample it is difficult to conclude whether TDCA increases Cl^- secretion in this epithelial model. However, given that TDCA was unable to induce secretion in CF epithelium and did not affect overall basal current, together with the data from NuLi-1 and CuFi-1, these results provided further support to the finding that TDCA stimulates CFTR Cl^- secretion without affecting ENaC in the non-CF airway epithelium.

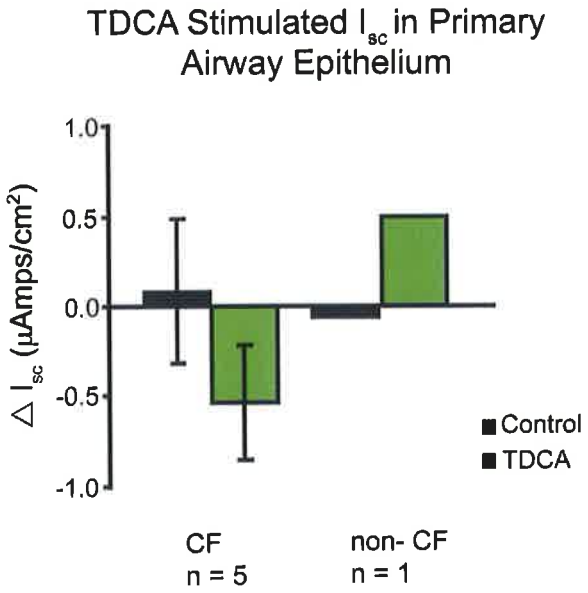

Fig.4.8 Acute treatment of CF primary bronchial epithelium with TDCA does not stimulate Cl^- secretion. Changes in I_{sc} recordings of CF and non-CF human primary epithelial monolayers mounted in Ussing chambers treated with 25 μM TDCA basolaterally. TDCA induced changes in basal I_{sc} are represented as the mean ± SEM I_{sc} values. TDCA slightly increased basal I_{sc} by 0.4 μAmps/cm^2 in non-CF primary tissue, but decreased basal I_{sc} by 0.4 ± 0.3 μAmps/cm^2 in CF epithelium.

4-2.8 TDCA does not affect abundance of CFTR at the apical membrane.

The next question addressed was the mechanism by which TDCA activates CFTR. Impaired exocytosis of CFTR from the endoplasmic reticulum/golgi network and targeting to the membrane is a well-established contributor to CF pathology. It has been reported that a significant quantity of mature, functional CFTR is localised to cellular compartments and that stimulation with cAMP/PKA can modulate CFTR localisation between these compartments and the plasma membrane (Bertrand and Frizzell, 2003). In T_{84} cells it has been shown that CFTR can undergo rapid recycling at the plasma membrane, with ~50% of CFTR retrieved within a few minutes (Prince *et al.*, 1994).

The effect of TDCA on apical abundance of CFTR was therefore investigated using a method of cell surface biotinylation. As described in detail in chapter 2 (section 2-4), biotin specifically binds to cell surface proteins, facilitating isolation of the membrane fraction by incubation with streptavidin after cell lysis. The different fractions of proteins- membrane, cellular and total, could then be separated via SDS-PAGE and changes in cell surface abundance of proteins were easily measured. In order to assess whether isolation of the cell surface fraction has been successful, membranes were also stained for β-actin, an abundant intracellular protein which should not be present in the membrane fraction. The presence of β-actin in the membrane fraction therefore indicated contamination of this fraction with intracellular proteins.

Once Calu-3 cells grown in ALI had reached a sufficiently high TEER they were incubated with 25 μM TDCA basolaterally at 37°C for 5 min before being immediately transferred to ice for biotinylation and separation via SDS-PAGE. After antibody incubation and development of the membranes, relative protein abundance was quantified using Photoshop software and cell surface abundance was normalised to % of total fraction for each sample. As can be seen from fig 4.9, acute treatment with TDCA did not affect CFTR levels at the apical membrane (n = 4). According to the power calculations performed, it was determined that n = 17 would be required to establish whether TDCA

significantly increased apical abundance of CFTR in Calu-3 cells. This result indicated that TDCA activates CFTR via pathways other than increasing channel abundance at the apical membrane.

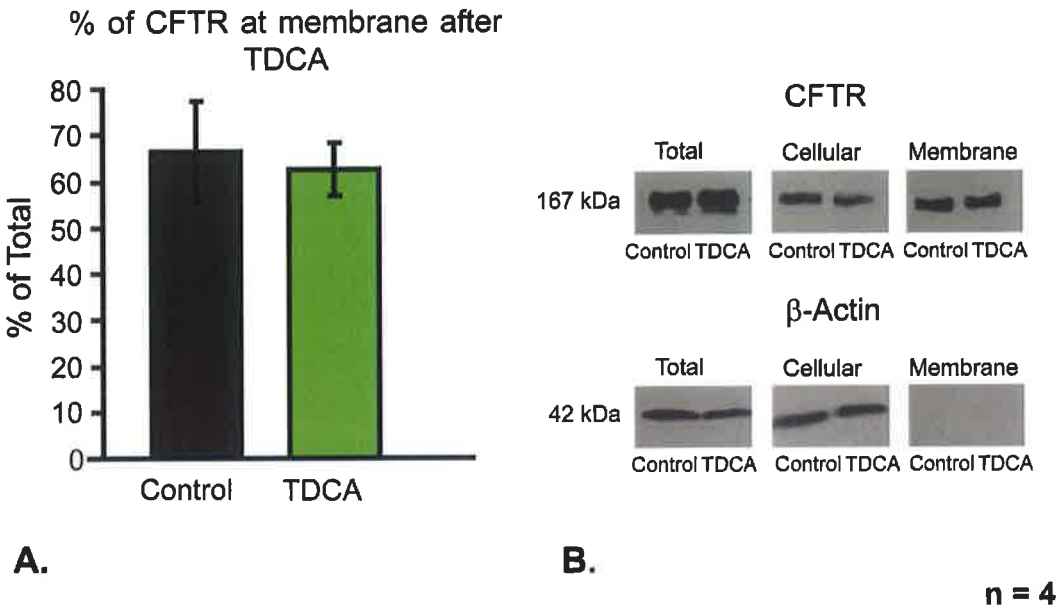

Fig.4.9 TDCA does not affect abundance of CFTR at the apical membrane. Calu-3 cells were treated basolaterally with 25 μM TDCA for 5 min prior to biotinylation and protein extraction. **A.** Relative abundance of CFTR at the apical membrane normalized to % of total for each sample. Relative abundance of CFTR after TDCA treatment was 62.6 ± 5.6 compared with 66.5 ± 10.9% for non- treated controls indicating that TDCA did not affect relative abundance of CFTR at the apical membrane. **B.** Representative Western blot for CFTR and β-actin in each fraction. The absence of β-actin in the membrane fraction indicated that the biotinylation had been successful.

4-2.9 TDCA stimulates Cl^- secretion through Ca^{2+}- activated Cl^- channels (CaCC) in Calu-3 cells.

From the experiments with $CFTR_{inh172}$ in section 4-2.4, it appeared that TDCA was capable of stimulating Cl^- secretion through the activation of another channel in addition to CFTR. Therefore the role played by CaCC in TDCA stimulation of Cl^- secretion was investigated by performing Ussing chamber membrane depolarization experiments to isolate CaCC I_{sc}, as described in detail in chapter 2 (section 2-2.5). Briefly, a basolateral to apical Cl^- gradient, in addition to high concentrations of K^+ on both sides of the epithelium, was established across the Calu-3 layer mounted in Ussing chambers. High

extracellular levels of K^+ depolarize the membrane therefore reducing the contribution to Cl^- secretion made by basolateral K^+ channels. Each insert was then treated apically with $CFTR_{inh172}$ to inhibit CFTR involvement in Cl^- secretion. Under these conditions changes in I_{sc} were representative of changes in Cl^- transport across the apical membrane through CaCC.

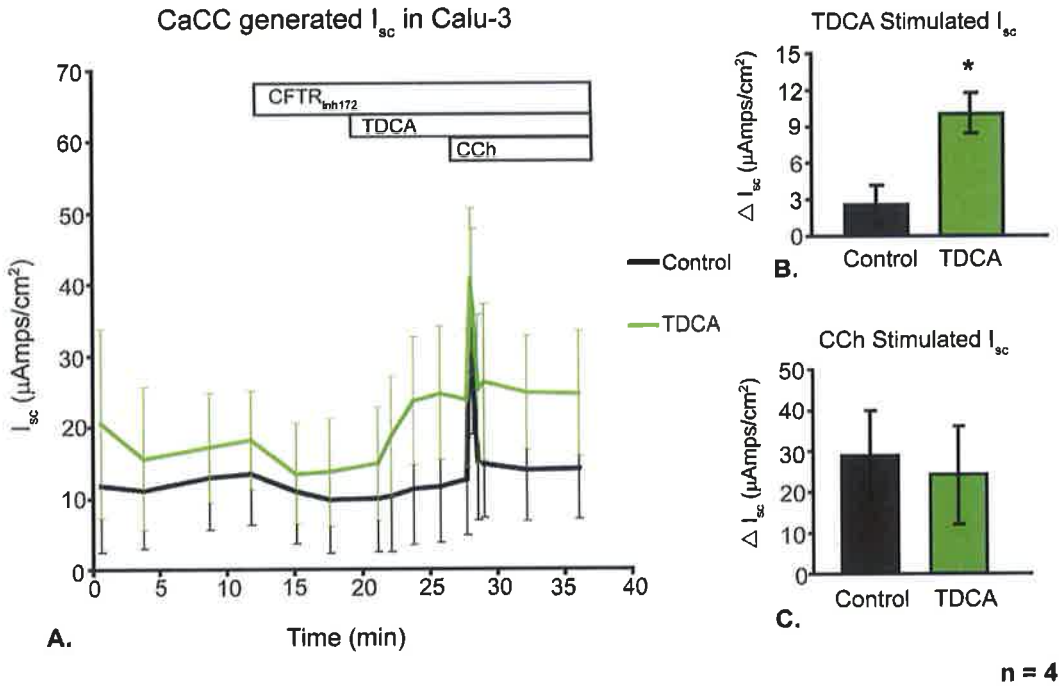

Fig.4.10 TDCA stimulates Cl^- secretion through the calcium activated Cl^- channel (CaCC) in Calu-3 cells. A. I_{sc} values recorded during Ussing chambers experiments of Calu-3 cells to isolate CaCC generated I_{sc}. Calu-3 monolayers were exposed to a basolateral to apical Cl^- gradient, and high concentrations of K^+ on both sides of the epithelium. This favoured transepithelial Cl^- transport and depolarizes the cell membrane, thus eliminating the contribution made by basolateral K^+ channels to basal I_{sc}. $CFTR_{inh172}$ was then added to the apical chamber and under these conditions, I_{sc} responses are due to Cl^- transport through apical CaCC. **B.** I_{sc} responses observed after TDCA treatment. Acute treatment with TDCA significantly increased basal CaCC currents by 10.87 ± 3.88 (μAmps/cm^2) compared with oscillations of 2.17 ± 2.74 (μAmps/cm^2) in control cells (n = 4, p = 0.017) (**C**). I_{sc} responses observed after CCh treatment. TDCA pre-treatment did not affect subsequent responses to CCh. This indicated that TDCA also stimulated Cl^- secretion through apical CaCC.

According to the power calculations performed, it was determined that n = 3 would be required to establish whether TDCA significantly increased CaCC

currents in Calu-3 cells. As shown in fig 4.10, acute treatment with TDCA significantly increased basal CaCC currents by 10.87 ± 3.88 (μAmps/cm^2) compared with oscillations of 2.17 ± 2.74 (μAmps/cm^2) in control cells (n = 4, p = 0.017) but did not affect subsequent CCh stimulated CaCC I_{sc}. Since CCh activates CaCC currents by increasing intracellular Ca^{2+} via activation of the muscarinic receptors, but TDCA did not affect CCh stimulated CaCC response, this suggests that TDCA might increase intracellular Ca^{2+} by a different process, such as inducing a cellular influx of Ca^{2+}. Furthermore, TDCA does not maximally activate CaCC, since CaCC currents are increased in response to subsequent CCh treatments. This result indicated that in addition to activating CFTR, TDCA also stimulated Cl^- secretion through CaCC which may be an important feature of CF airways lacking functional CFTR. In order to confirm the role played by CaCC in TDCA stimulation of Cl^- secretion, it would be beneficial to repeat these electrophysiological experiments using one or more of the commercially available CaCC inhibitors such as CaCCinh-A01, or DIDS. Although TMEM16A has been described a possible CaCC candidate in the airways, the identity of CaCC in this model of Calu-3 cells would need to be confirmed before the effect of TDCA on membrane abundance could be determined. Since it has repeatedly been reported that bile acids are capable of increasing intracellular Ca^{2+} it was therefore decided to pursue this line of investigation in order to assess the process by which TDCA activates Cl^- secretion through CaCC as described in Chapter 5.

4-2.10 TDCA increases Na^+/K^+ ATPase current in Calu-3 cells.

The last ion transport protein under investigation was the Na^+/K^+ ATPase, which is an important regulator of Na^+ absorption and Cl^- uptake in epithelial cells. Na^+/K^+ ATPase provides the driving force for Na^+, Cl^- and K^+ uptake by the NKCC1 and therefore is crucial to sustained Cl^- secretion as it drives increased Cl^- uptake from the basolateral space. In order to determine whether TDCA can affect Na^+/K^+ ATPase current, Ussing chamber membrane permeabilization experiments to isolate Na^+/K^+ ATPase generated I_{sc} were performed, as described in detail in chapter 2 (section 2-2.4). Calu-3

monolayers were mounted in Ussing chambers perfused by low Na^+ Krebs solution containing equimolar concentrations of K^+ and Cl^- in both the apical and basolateral compartments. This ensured that ions were not moving passively along a concentration gradient. The apical membrane was then permeabilized by 25 μM amphotericin B so that the basolateral membrane provided the only resistance to flow of ions. Equimolar concentrations of K^+, Cl^- and Na^+ on both sides of the basolateral membrane abolished the contribution made by the basolateral K^+ channels to I_{sc}.

Under these conditions, changes in I_{sc} are representative of changes in Na^+/K^+ ATPase activity. In order to ensure TDCA stimulation of I_{sc} was via activation of Na^+/K^+ ATPase, one insert was pre-treated with 100 μM ouabain before TDCA, in each experiment. According to the power calculations performed, it was determined that n = 4 would be required to establish whether TDCA significantly increased Na^+/K^+ generated currents in Calu-3 cells. Acute TDCA treatment significantly increased Na^+/K^+ pump generated I_{sc} by 1.32 ± 0.55 μAmps/cm^2, compared with decreases of 1.22 ± 0.48 μAmps/cm^2 and 0.57 ± 0.30 μAmps/cm^2 in control and ouabain treated cells respectively ($p = 0.005$, n = 9), fig 4.11. After TDCA treatment, the untreated control and TDCA - only cells were then treated with ouabain. It was observed that pre-treatment with TDCA slightly increased ouabain sensitive I_{sc} responses to 24.48 ± 6.80 μAmps/cm^2 compared with responses of 20.70 ± 5.11 μAmps/cm^2 in the untreated control, but this was not statistically significant. These results therefore indicate that TDCA increases Na^+/K^+ ATPase activity, further contributing to stimulation of Cl^- secretion.

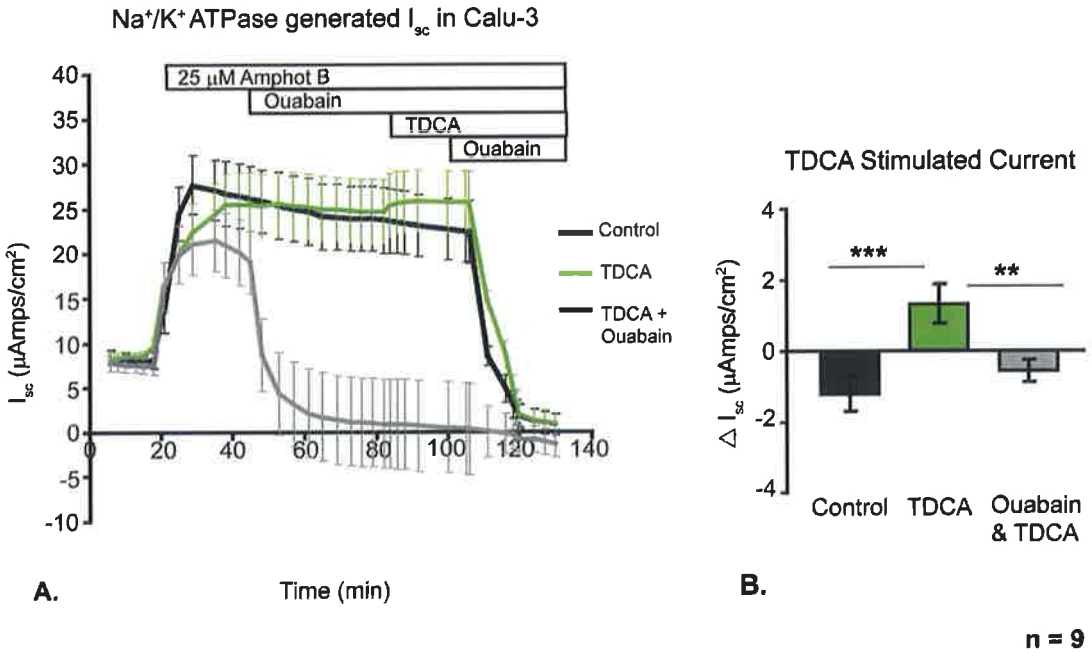

Fig.4.11 TDCA increases Na^+/K^+ ATPase current in Calu-3 cells. A. Mean ± SEM I_{sc} values recorded during Ussing chambers experiments of Calu-3 cells to isolate Na^+/K^+ ATPase generated I_{sc}. Calu-3 monolayers were exposed to low Na^+ and equimolar concentrations of K^+ and Cl^- on both sides of the epithelium. This reduced the driving force for K^+ exit through basolateral K^+ channels. The contribution made by the apical membrane to I_{sc} was removed by permeabilization with 25 µM amphotericin B. Under these conditions, I_{sc} responses were due to the activity of the Na^+/K^+ ATPase pump. To confirm this, one insert was pretreated with 100 µM ouabain in each experiment. **B.** Changes in I_{sc} values (µAmps/cm^2) after TDCA treatment Acute TDCA treatment significantly increased Na^+/K^+ pump generated I_{sc} by 1.32 ± 0.55 µAmps/cm^2, compared with decreases of 1.22 ± 0.48 µAmps/cm^2 and 0.57 ± 0.30 µAmps/cm^2 in control and ouabain treated cells respectively ($p = 0.005$, $n = 9$),

4-2.11 TDCA effects on Na^+/K^+ ATPase abundance at the basolateral membrane.

Finally the process by which TDCA activates Na^+/K^+ ATPase was investigated by first determining whether TDCA affects Na^+/K^+ ATPase abundance the membrane. Again the method of cell surface biotinylation was used as previously described in chapter 2 (section 2-4). Both the α– and β– subunits of Na^+/K^+ ATPase were investigated in this experiment. Once the relative

protein abundance for each sample had been quantified using Photoshop software, cell surface abundance was again normalised to % of total fraction for each sample.

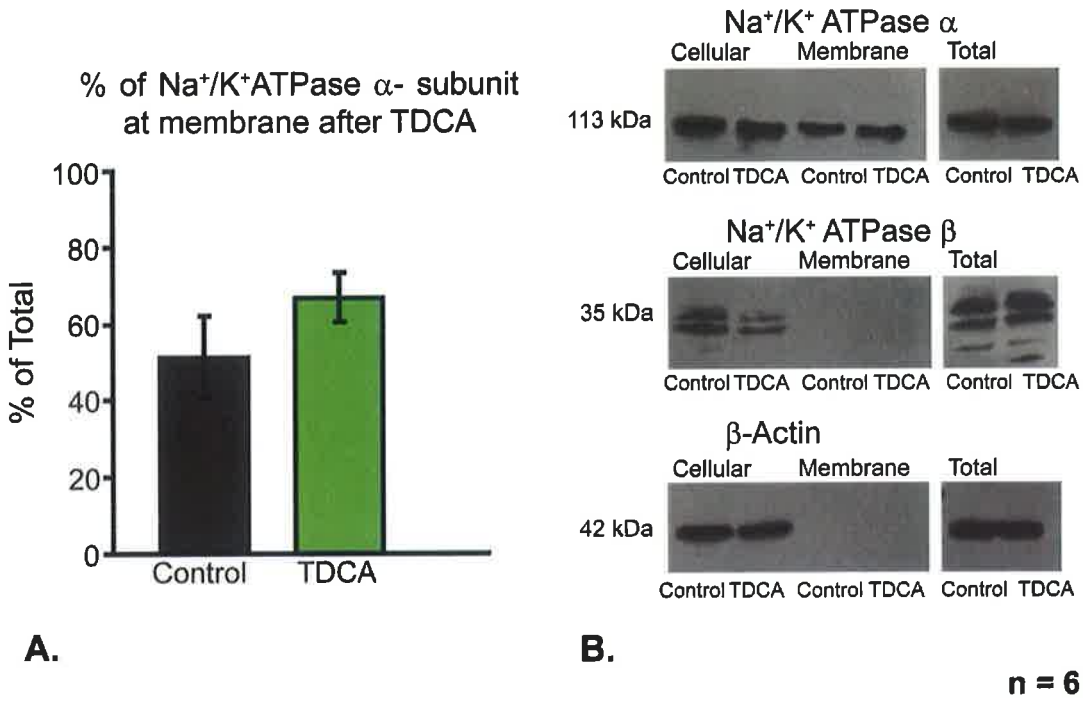

Fig.4.12 The effect of TDCA on Na^+/K^+ ATPase abundance at the basolateral membrane in Calu-3 cells. Calu-3 cells were treated basolaterally with 25 μM TDCA for 5 min prior to biotinylation and protein extraction. **A.** Relative abundance of Na^+/K^+ ATPase -α at the basolateral membrane normalized to % of total Na^+/K^+ ATPase -α for each sample. TDCA treatment appeared to produce a small increase in the abundance of α- Na^+/K^+ ATPase at the basolateral membrane, increasing relative abundance of α- subunit expressed as % of total to 66.9 ± 6.4 %, compared with 51.0 ± 10.0% control values (n = 6, p = n.s). **B.** Representative Western blot for α, β- Na^+/K^+ ATPase and β-actin in each fraction. The β- subunit could not be detected in the membrane fraction.

As can be seen from fig 4.12 B the β- subunit in the membrane fraction could not be detected, which may have been due to its low abundance in the membrane. Therefore it was difficult to determine whether TDCA affected β- Na^+/K^+ ATPase trafficking to the membrane. On the other hand, TDCA treatment resulted in a small increase in the abundance of α- Na^+/K^+ ATPase at the basolateral membrane but this change did not reach statistical significance. The relative abundance of α- subunit expressed as % of total increased to 66.9 ± 6.4 % after TDCA, compared with 51.0 ± 10.0 % control

values (n = 6). According to the power calculations performed, it was determined that n = 8 would be required to establish whether TDCA significantly increased basolateral abundance of Na^+/K^+ ATPase α-subunit in Calu-3 cells.

4-3 Discussion

In this chapter we described the ionic basis of secretion induced by TDCA and the ion transport proteins involved. The data indicate that, in the Calu-3 model of serous SMG cells, physiologically low levels of TDCA stimulate Cl^- secretion, without affecting the integrity of the junctional proteins regulating paracellular ion transport. This finding corresponds to previously published work demonstrating that TDCA stimulates Cl^- secretion in a variety of different epithelial cell types (Devor *et al.*, 1993, Okolo *et al.*, 2002, Potter *et al.*, 1987). However, in these studies the concentrations of TDCA used ranged from 50 μM to 2 mM, with the higher concentrations of TDCA shown to activate CaCC and K^+ channels. As already discussed in the previous chapter, bile acids often have opposing effects on secretion at high and low concentrations. Therefore, it was important to determine the effects of TDCA on ion transport proteins involved in secretion at a lower concentration of TDCA (25 μM), more likely to be present in the airways.

Since it had already been established in the previous chapter that TDCA does not chronically affect ion transport in the airways, it was therefore known that TDCA stimulation of Cl^- secretion was not mediated via altered expression of particular ion transport proteins. Instead the effects of TDCA on the activity of specific ion transporters were investigated by performing modified Ussing chamber experiments which facilitated the isolation of I_{sc} generated by each individual ion transporter. These experiments demonstrated that TDCA increases the activity of CFTR, CaCC and Na^+/K^+ ATPase (fig 4.13), and provided an explanation as to why pre-treatment with individual channel inhibitors did not block TDCA stimulation of Cl^- secretion as shown in sections 4.2.(3 & 4).

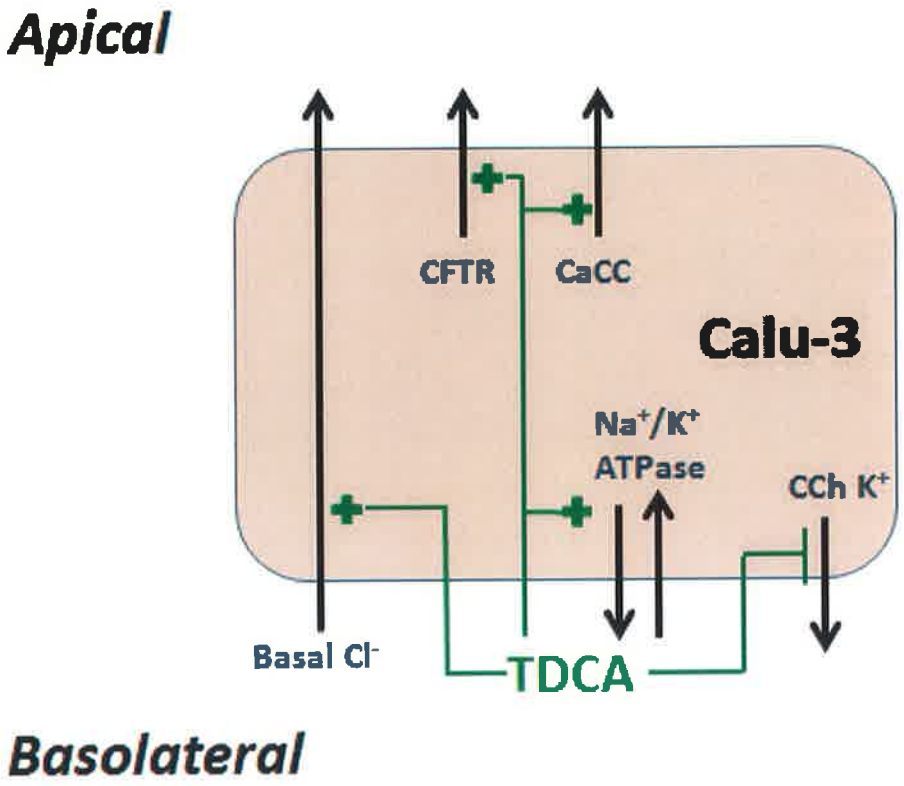

Fig.4.13 Model of TDCA stimulated Cl^- secretion in Calu-3 cells. Acute basolateral treatment with 25 μM TDCA increases basal Cl^- secretion in Calu-3 cells by increasing ion transport through CFTR, CaCC and Na^+/K^+ ATPase. TDCA also attenuates CCh induced K^+ current in Calu-3 cells.

In contrast to findings by Devor *et al*, and Okolo *et al*, our data shows that TDCA does not affect the basal activity of K^+ channels, which is likely to be accounted for by the lower concentration of TDCA used here, 25 μM compared with 0.75 - 2 mM (Devor *et al.*, 1993, Okolo *et al.*, 2002). Activation of CFTR, CaCC and Na^+/K^+ ATPase in the serous cells of airway SMGs would lead to an overall increase in fluid secretion as these cells do not express active ENaC in their apical membrane. However, in airway epithelial models where Na^+ absorption is dominated by apical ENaC, activation of the Na^+/K^+ ATPase by TDCA will increase the driving force for Na^+ entry through ENaC, and hence increase paracellular Cl^- and fluid absorption. This in turn may counteract any secretory response induced by TDCA, leading to no net change in fluid secretion across the epithelium. In order to explore this further,

the secretory (CFTR and CaCC) and absorptive (ENaC) effects of TDCA were examined in cell models of ENaC, CFTR and null CFTR expressing columnar ciliated bronchial epithelia, NuLi-1, CuFi-1 and CF-human bronchial epithelium (HBE) (fig 4.14).

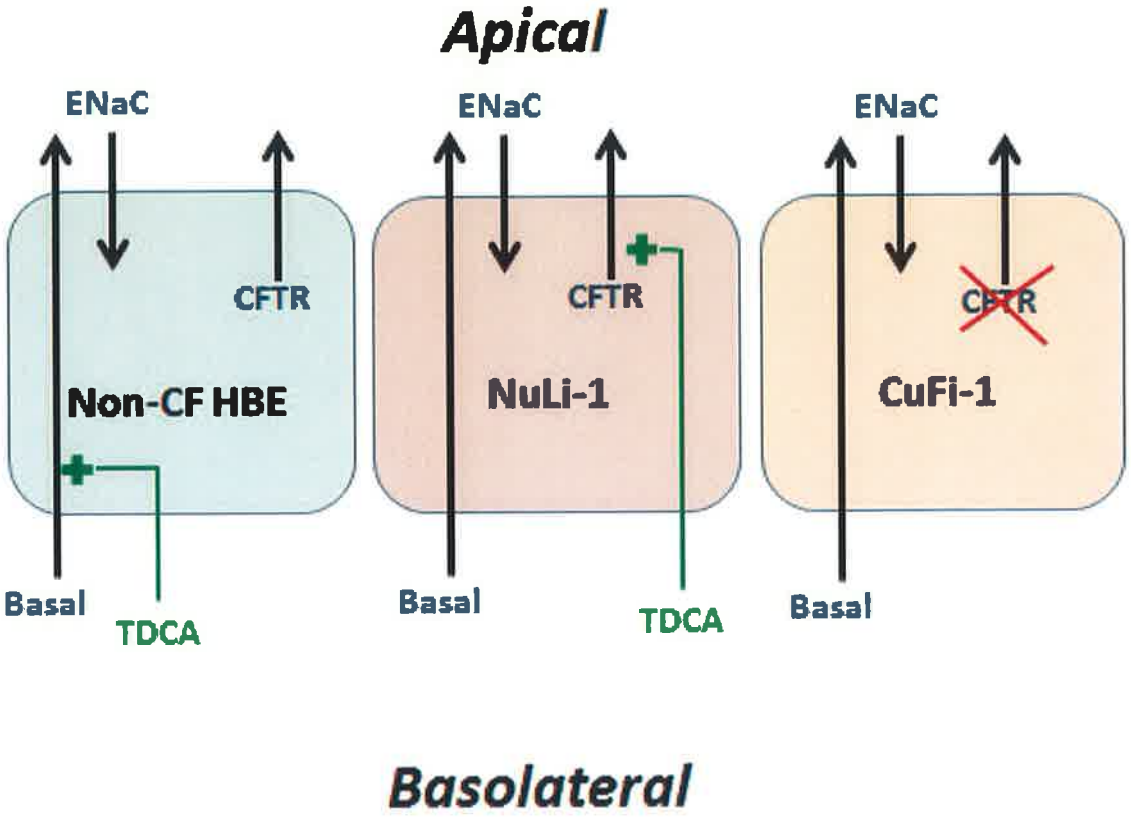

Fig.4.14 The effect of TDCA on secretion in ciliated columnar bronchial epithelial cells. Acute basolateral treatment with 25 μM TDCA increases basal I_{sc} in non-CF human primary epithelium and increases $CFTR_{inh172}$ sensitive Isc in NuLi-1. TDCA does not affect I_{sc} in CuFi-1 cells, which suggests that TDCA stimulation of Cl^- secretion is through CFTR.

TDCA was found to be unable to stimulate basal I_{sc} in NuLi-1 but did significantly increase the activity of CFTR, in agreement with the Calu-3 studies. However, TDCA was unable to significantly increase ENaC activity in either the NuLi-1 or CuFi-1 cell line, as would be expected if TDCA increases Na^+/K^+ ATPase activity in these cells. It is possible that Na^+/K^+ ATPase might be differentially regulated in these cell lines compared with the Calu-3 cells. It has been previously reported that PKA and PKC can either inhibit or activate Na^+/K^+ ATPase in a tissue-dependent manner (Gonin *et al.*, 2001, Elmedal *et*

al., 2006, Lecuona *et al.*, 2009, Han *et al.*, 2010, Lecuona *et al.*, 2013). Furthermore, due to the large amiloride sensitive I_{sc} responses observed in these cells, ENaC may already be maximally activated and therefore TDCA cannot stimulate further Na^+ entry.

In support of the findings in section 4-2.8, it had previously been shown that the main contributor to basal I_{sc} in NuLi-1 and CuFi-1 cell lines was Na^+ absorption through ENaC (Zabner *et al.*, 2003), which would make small secretory effects in these cells more difficult to detect. However, this may simply have been an artefact of immortalization in these cell lines. In agreement with previously published data (Zhao *et al.*, 2012), it was observed that in cultured primary bronchial epithelial cells, obtained via bronchial brushings, the basal I_{sc} was not completely dominated by ENaC and these cells demonstrated larger responses to secretagogues such as CCh and Fsk. This indicated that the cultured primary human bronchial cells, which were a better physiological model of airway epithelium, demonstrated a greater secretory capacity than the NuLi-1 cells. Therefore it was decided to assess the effect of TDCA on this primary human model of airway epithelium. The study included one non-CF sample and 5 CF HBE samples. The results show that TDCA was unable to stimulate Cl^- secretion in the CF samples, as was expected, but instead decreased basal I_{sc} in these cultures, while TDCA produced a small increase in basal I_{sc} in the non-CF sample (fig 4.14). As the main difference between the CF and non-CF samples is the presence of active CFTR, these results would suggest that TDCA stimulates Cl^- secretion through CFTR in this non-CF model.

Since the acute effects of TDCA on ion transporter activity were not due to changes in protein expression, other mechanisms of regulation of transporter activity were explored. In addition to its activation by cAMP/PKA phosphorylation, it has been shown that CFTR levels at the plasma membrane are regulated by endocytosis and recycling (Fu *et al.*, 2012). In the case of the most common mutation of CFTR, F508del, the mutated CFTR becomes trapped in the endoplasmic reticulum, resulting in the abolition of Cl^- secretion through CFTR. The balance between trafficking of CFTR to the

membrane and its removal from the membrane therefore plays an important role in regulating CFTR activity. Furthermore, it has been reported that elevation of cAMP in alveolar epithelial cells can increase Na^+/K^+ ATPase activity by promoting Na^+/K^+ ATPase recruitment to the plasma membrane (Lecuona *et al.*, 2009). Therefore this study first examined whether TDCA can affect CFTR or Na^+/K^+ ATPase activity by modulating protein abundance at the membrane using cell surface biotinylation. These results indicated that TDCA did not affect CFTR abundance at the apical membrane but slightly increased the α-subunit of Na^+/K^+ ATPase at the basolateral membrane. This suggested that TDCA stimulation of Cl^- secretion may require mobilization of a common intracellular 2nd messenger such as cAMP, which is known to directly activate CFTR in addition to promoting Na^+/K^+ ATPase recruitment to the plasma membrane (fig 4.15). An increase in cAMP activation of Na^+/K^+ ATPase would be expected to increase the driving force for Na^+ absorption through ENaC, however it has been reported that cAMP – dependent activation of CFTR can inhibit ENaC and hence cAMP leads to increased Cl^- secretion rather than increased Na^+ absorption (Konstas *et al.*, 2003). This might further explain why TDCA does not increase ENaC generated Isc in NuLi-1 and CuFi-1 cells.

TDCA stimulation of cAMP production will be investigated in the following chapter. Taken together, the findings in this chapter indicate that TDCA modulates Cl^- secretion in the airway epithelium by activating CFTR, CaCC and Na^+/K^+ ATPase but that the contribution of TDCA induced secretion to ASL volume may vary depending on the epithelial cell type.

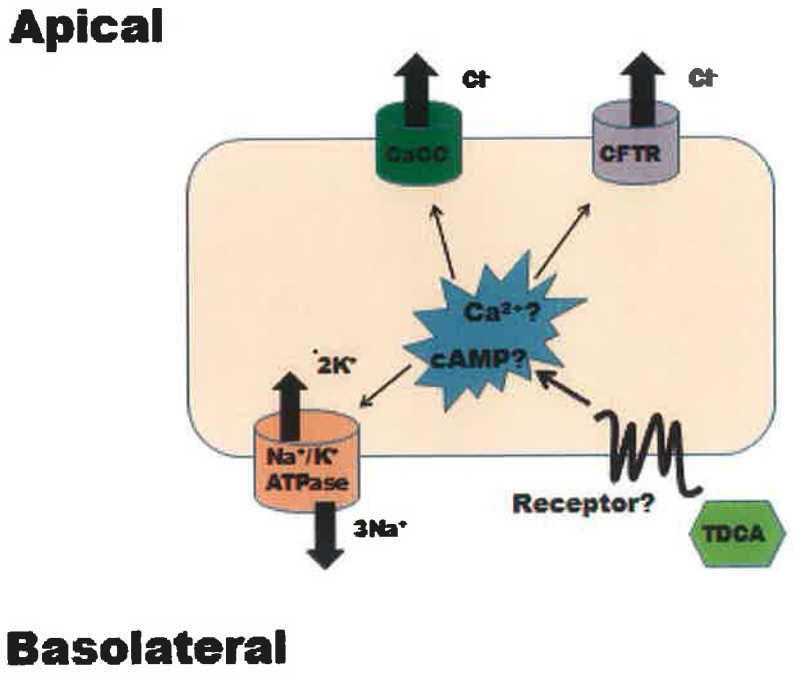

Fig.4.15 Diagram representing TDCA induced Cl^- secretion in airway epithelial cells. TDCA stimulates Cl^- secretion in airway epithelium by increasing the activity of CFTR, CaCC and Na^+/K^+ ATPase. TDCA activation of these ion transport proteins appears to involve mobilization of one or more intracellular 2nd messengers, such as Ca^{2+} or cAMP, which will be investigated further in the next chapter. Since TDCA can only stimulate Cl^- secretion when applied basolaterally to the epithelium, it would suggest that a receptor for TDCA or a bile acid transporter is present in the basolateral membrane, through which TDCA can elicit its effects. This will be explored in more detail in chapter 6.

TDCA can induce fluid secretion in the serous cells of SMGs in non-CF airways, contributing to increased ASL volume, which might be compensated for by increased fluid absorption by the surface epithelial cells to maintain ASL homeostasis and effective MCC in healthy lungs. However, in airway disease where one or more ion transporters are known to be defective such as in COPD, TDCA may exacerbate lung disease by diminishing MCC. In the case of CF, TDCA will not be able to induce Cl^- secretion through CFTR but may still be able to increase Na^+/K^+ ATPase activity. Since it is generally accepted that Na^+ hyperabsorption through ENaC also occurs in CF lungs, TDCA

stimulation of Na^+/K^+ ATPase will further increase the driving force for Na^+ absorption, thus reducing ASL volume even further. The presence of TDCA in the airways of new-born infants, especially those whose mother was diagnosed with ICP, may interfere with the absorptive capacity of the lung to clear fluid and adapt to breathing, by increasing fluid secretion and flooding the alveoli. Deficiency of this crucial early transepithelial fluid transport could result in chronic lung disease. In addition to regulation of ASL and MCC, it has been reported that increases in the activity of CFTR and TMEM16A attenuate the secretion of two pro-inflammatory cytokines, interleukin (IL) -6 and IL-8, in primary epithelial cultures of human bronchial epithelium grown under ALI but not liquid-liquid interface (Veit *et al.*, 2012). This suggests that TDCA may also play an anti-inflammatory role in airways exposed to chronic inflammation such as COPD and CF.

In summary, this chapter has helped to clarify the ionic transport mechanisms by which TDCA can increase basal I_{sc} in Calu-3 cells. It has been established that TDCA stimulates Cl^- secretion through CFTR and CaCC by a process that also involves increased Na^+/K^+ ATPase activity. As TDCA was not shown to significantly increase membrane abundance of the ion transport proteins, it was hypothesized that TDCA activation of each of these transporters is due to altered regulation of the protein by phosphorylation. Although the transporters can be activated by different kinase pathways, it is likely that they will share one or more common intracellular 2^{nd} messengers that can be stimulated by TDCA. The signalling molecules associated with TDCA stimulation of airway Cl^- secretion are described in the following chapter.

Chapter 5

Signalling molecules involved in TDCA stimulation of airway secretion

5-1 Introduction

The balance between secretion and absorption in the airways is carefully controlled by many different signalling pathways, such as serine/threonine-protein kinase 1 (SGK1), PKA, PKC, or mitogen-activated protein kinase (MAPK) depending on the stimulus. SGK1 plays a role in the response to cell swelling and is known to regulate different K^+, Cl^- or Na^+ channels, while MAPK is known to participate in secretory responses associated with inflammation and has been reported to mediate TGF-β induced Cl^- secretion in the colon (Howe *et al.*, 2002). The role of PKA and PKC in regulation of epithelial ion transport has been described in chapter 1 (sections 5.3 & 5.4), and will be discussed in more detail here, in the following sections. It was confirmed in the previous chapter that TDCA stimulates Cl^- secretion in the airway epithelium by increasing the activity of CFTR, CaCC and Na^+K^+ ATPase. Therefore, the focus here was to identify the signalling molecules involved in this process. It has been shown that allergic inflammation of the airways can induce Ca^{2+}-activated Cl^- secretion in ciliated epithelial cells, by a process that is dependent on activation of the stat-6 transcription factor (Anagnostopoulou *et al.*, 2010). Mechanical stress, such as that experienced during breathing, has been reported to induce secretion in the lung via the production of ATP, which can activate purinergic receptors and stimulate signalling cascades via mobilization of intracellular Ca^{2+} (Button *et al.*, 2008). In addition, reports indicate that inhaled corticosteroids, used in the treatment of asthma, or cytokines IL-1β and TNFα, released in response to bacterial infection, are capable of stimulating secretion through increasing intracellular levels of cAMP (Baniak *et al.*, 2012a, Mizutani *et al.*, 2012). Many other endogenous stimuli such as hormones, channel activating proteases, and nucleotides along with inhaled pathogens or irritants such as cigarette smoke have been reported to modulate airway epithelial ion transport. These stimuli can induce signalling via many different kinase pathways, usually involving the mobilization of one or more 2^{nd} messengers, such as Ca^{2+}, cAMP, cGMP, CO, NO or other reactive oxygen species. However, as Ca^{2+} and cAMP are known to activate CaCC and CFTR respectively, the involvement of these 2^{nd} messengers in TDCA stimulation of secretion was first investigated.

In support of this investigation, bile acids have previously been reported to stimulate Cl^- secretion by a process that involves increasing intracellular concentrations of either cAMP or Ca^{2+}. It was shown that CDCA can activate CFTR via cAMP/PKA pathway in T_{84} cells while TDCA has been reported to stimulate Cl^- secretion via the elevation of intracellular Ca^{2+} in T_{84} cells (Ao *et al.*, 2013, Devor *et al.*, 1993). In the epithelium of the human gall bladder, taurine conjugates of CDCA and UDCA have been shown to increase cAMP production by modulating PKC regulation of adenylyl cyclase (Chignard *et al.*, 2003). One study also revealed that UDCA stimulates CFTR-dependent ATP release, increasing intracellular Ca^{2+} levels and activating PKC, resulting in increased fluid secretion in cholangiocytes (Fiorotto *et al.*, 2007). Taken together, these findings suggest that TDCA should be able to stimulate mobilization of Ca^{2+} and cAMP, leading to the activation of CFTR, CaCC and Na^+/K^+ ATPase in airway epithelium.

As described in detail in chapter 1 (section1-5.1 & 2) changes in the levels of cytoplasmic cAMP and Ca^{2+} have repeatedly been identified as important 2^{nd} messengers involved in the epithelial response to secretagogues. Intracellular levels of cAMP are rapidly increased in response to ligand binding to a G-protein coupled receptor (GPCR), which in turn, through G-proteins that regulate various different isoforms of adenylate cyclase, controls intracellular cAMP levels (Tasken and Aandahl, 2004). This process is controlled by differential expression and regulation of the adenylate cyclase and phosphodiesterase families of enzymes (Jin *et al.*, 1999). CFTR channel activity is known to be regulated by phosphorylation of the serine residues on its R domain by PKA, which is activated by increasing cAMP levels (Cheng *et al.*, 1991, Carson *et al.*, 1995). The activity of Na^+/K^+ ATPase is tightly regulated in both the long term by differential expression of each subunit, and the short-term by altered phosphorylation and/or redistribution of the pump between the membrane and intracellular compartments. Numerous studies have shown that cAMP also modulates transepithelial ion transport by increasing Na^+/K^+ ATPase trafficking to the membrane in many different cell types (Gonin *et al.*, 2001, Lecuona *et al.*, 2009). Interestingly, it was shown

that this increased trafficking of the pump to the membrane, stimulated by cAMP, is in fact dependent on intracellular free Ca^{2+} levels (Gonin *et al.*, 2001). This indicates that increased concentrations of both cAMP and Ca^{2+} may be required for Na^+/K^+ ATPase activation in our study.

In addition, when ligands bind to GPCRs in the plasma membrane, the result is often activation of phospholipase C (PLC), which cleaves membrane lipids to produce inositol triphosphate (IP_3) and diacylglycerol (DAG) (Toumi *et al.*, 2011). IP_3 then releases Ca^{2+} from various intracellular stores, including the endoplasmic reticulum (ER), while DAG activates different forms of protein kinase C (PKC). The majority of Ca^{2+} release in non-excitable cells, such as epithelial cells, is through IP_3-sensitive Ca^{2+} channels in the ER. In the airways, it is now well-established that cAMP and Ca^{2+} are potent inducers of epithelial secretion via activation of CFTR and CaCC respectively. Since the exact identity of the CaCC channel in the airways has been open to much debate, it is therefore unknown whether Ca^{2+}, alone or complexed with calmodulin, directly activates CaCCs or whether phosphorylation by Ca^{2+} dependent protein kinases, such as classical PKCs, is required. TDCA has previously been shown to increase Cl^- secretion via mobilization of intracellular Ca^{2+} resulting in the activation of CaCC and basolateral K^+ channels in colonic epithelium (Devor *et al.*, 1993). These reports clearly indicate that cAMP and Ca^{2+} are capable of activating CFTR, CaCC and Na^+/K^+ ATPase, which are all also activated by TDCA. This led to the hypothesis that TDCA activation of these ion transport proteins involves mobilization of either or both cAMP and Ca^{2+}.

Signal transduction by cAMP or Ca^{2+} can involve activation of specific protein kinase cascades such as PKA or PKC. PKA is one of the most common cAMP dependent protein kinases, which regulates many different cellular processes. PKC on the other hand belongs to a family of protein kinases activated by Ca^{2+}, DAG or phospholipids that are critical to many cellular processes such as regulation of transcription, immune responses, cell growth and modulation of membrane structure events. Importantly for this study, PKA is known to activate CFTR by phosphorylation of its regulatory subunit, at a

number of different serine residues. Likewise, it has been reported that phosphorylation of CFTR by PKC is also required for enhancement of responses stimulated by acute PKA activation of CFTR (Jia *et al.*, 1997). Furthermore Cl^- secretion in the airways has been shown to be modulated by PKA activation of basolateral K^+ channels (Fung *et al.*, 2011). PKA has also been found to increase the activity of Na^+/K^+ ATPase in the airway smooth muscle (Elmedal *et al.*, 2006). In the heart, an inhibitory complex known as phospholemman (PLM) associates with and inhibits Na^+/K^+ ATPase. Both PKA and PKC are able to increase Na^+/K^+ATPase activity by phosphorylation of different serine residues on PLM, thus relieving PLM induced pump inhibition (Han *et al.*, 2010).

Additionaly, PKA has been reported to increase Na^+K^+ ATPase activity in proximal convoluted tubule cells by increasing cell surface abundance of Na^+/K^+ ATPase (Gonin *et al.*, 2001). In contrast, under conditions where the concentration of CO_2 is elevated, PKA has more recently been shown to reduce pump activity by regulating endocytosis of Na^+/K^+ ATPase in alveolar epithelial cells (Lecuona *et al.*, 2013). Since the results from the previous chapter indicate that TDCA increases the activity of CFTR and Na^+/K^+ ATPase, and appears to increase Na^+/K^+ ATPase trafficking to the membrane, it was hypothesized that TDCA may be activating PKA or PKC in response to elevation of cAMP or Ca^{2+} respectively. Therefore the roles played by PKA and PKC in TDCA stimulation of Cl^- secretion will also be investigated in this chapter.

In summary, the primary aim of this chapter was to identify the signalling molecules involved in TDCA stimulation of Cl^- secretion. Specifically in this chapter the following studies will be reported:

1) TDCA mobilization of intracellular Ca^{2+}
2) TDCA generation of cAMP
3) TDCA activation of PKA
4) The contribution of PKA and PKC to TDCA-induced Ca^{2+} mobilization or stimulation of I_{sc}

5-2 Results

5-2.1 TDCA increases Ca^{2+} mobilization in Calu-3 cells.

In order to investigate whether TDCA can affect mobilization of intracellular Ca^{2+} in Calu-3 cells, Ca^{2+} imaging of cells grown on glass and loaded with Fura-2 for 30 min was performed, as described in detail in chapter 2 (section 2-5). According to the power calculations performed, it was determined that n = 2 would be required to establish whether TDCA significantly increased intracellular Ca^{2+} in Calu-3 cells. As illustrated in fig 5.1 A & C, acute treatment with 25 μM TDCA produced a rapid and transient increase in $A_{340/380}$ ratio of 0.92 ± 0.13 in intracellular Ca^{2+} compared to a change of 0.01 ± 0.01 for untreated controls ($p = 0.0001$, $n = 8$). Store depletion can secondarily activate plasma membrane Ca^{2+} channels facilitating an influx of Ca^{2+} into the cytosol. Once the $A_{340/380}$ ratio had returned to baseline values after TDCA treatment, cells were treated with 2 μM thapsigargin, in order to determine whether TDCA was affecting Ca^{2+} release from thapsigargin sensitive stores. According to the power calculations performed, it was determined that n = 3 would be required to establish whether TDCA significantly increased thapsigargin stimulated Ca^{2+} mobilization in Calu-3 cells. As shown in fig 5.1 B & D, we found that pre-treatment with TDCA significantly increased thapsigargin mobilization of Ca^{2+} to 2.05 ± 0.30 ($A_{340/380}$) compared with an increase of 1.20 ± 0.20 ($A_{340/380}$) for thapsigargin treatment alone ($p = 0.017$, $n = 6$). This suggested that TDCA increased intracellular Ca^{2+} from a source other than the endoplasmic reticulum.

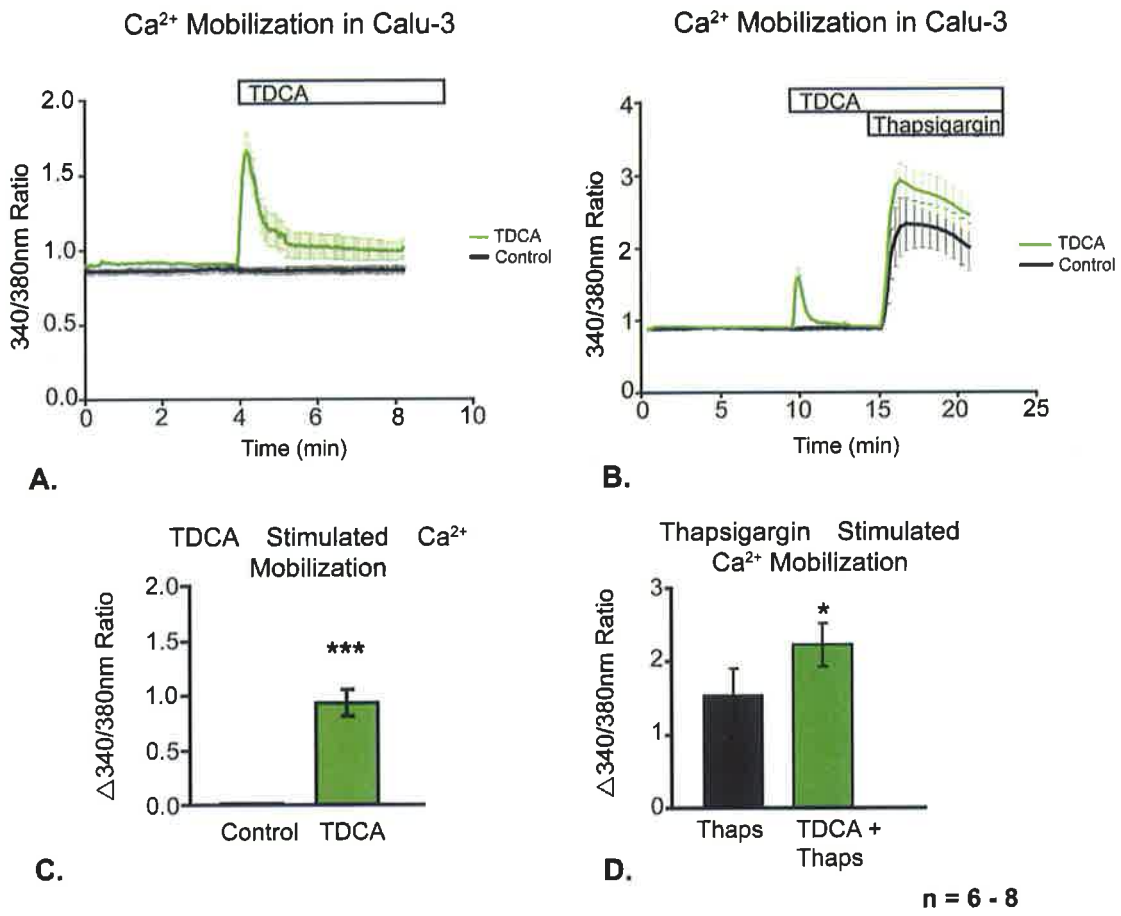

Fig.5.1 TDCA stimulates Ca^{2+} mobilization in Calu-3 cells and increases thapsigargin stimulated Ca^{2+} mobilization. A & B Fura-2 ratio values recorded during experiments. We found that acute treatment with 25μM TDCA produced **C.** an increase of 0.92 ± 0.13 ($A_{340/380}$) in intracellular Ca^{2+} compared with 0.01 ± 0.01 ($A_{340/380}$) for untreated controls (p = 0.0001, n = 8) and **D.** an increase in thapsigargin stimulated Ca^{2+} mobilization to 2.05 ± 0.30 ($A_{340/380}$) after TDCA treatment compared with 1.20 ± 0.20 ($A_{340/380}$) for untreated controls (p = 0.017, n = 6)

5-2.2 TDCA stimulates Ca^{2+} influx from the extracellular environment in Calu-3 cells.

Given that TDCA causes intracellular Ca^{2+} mobilization, the next set of experiments investigated whether TDCA was capable of stimulating Ca^{2+} influx into the cell from the extracellular environment. To test this, the Ca^{2+} imaging experiments in the previous section were repeated using a Ca^{2+} free buffer, containing the Ca^{2+} chelator, EGTA (Table 2.9). Under these

conditions, it was observed that TDCA stimulation of Ca^{2+} mobilization was abolished, fig 5.2. In addition, TDCA did not increase thapsigargin stimulated Ca^{2+} mobilization in the absence of extracellular Ca^{2+}. This suggested that TDCA mobilization of Ca^{2+} was due to increased influx of Ca^{2+} and hence accounted for the increased intracellular level of Ca^{2+} observed upon depletion of the Ca^{2+} stores using thapsigargin.

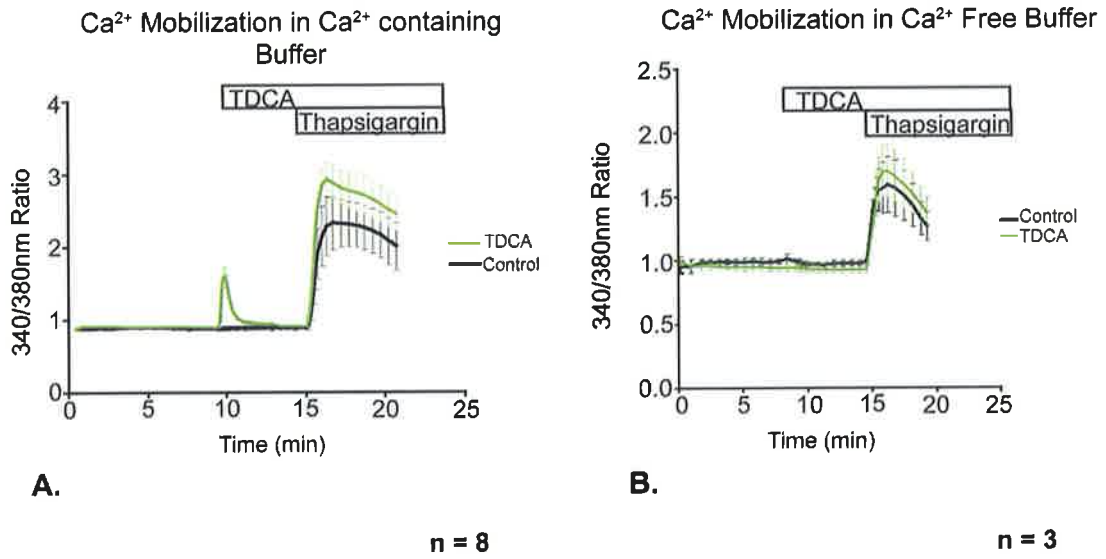

Fig.5.2 TDCA stimulates Ca^{2+} influx from the extracellular space in Calu-3 cells. A & B Fura-2 ratio values recorded during experiments with Calu-3 cells. **B.** Under calcium-free bathing conditions (Ca^{2+}-free EGTA buffer), the normal TDCA stimulation of Ca^{2+} mobilization (seen in **A**) was abolished. TDCA was also unable to significantly increase thapsigargin mobilization of Ca^{2+} in the absence of extracellular Ca^{2+}.

5-2.3 TDCA increases thapsigargin stimulated Ca^{2+} mobilization in NuLi-1 but not CuFi-1 cells.

In order to determine the effect of TDCA on Ca^{2+} mobilization in surface cells of the airway epithelium, Fura-2 experiments were repeated in NuLi-1 and CuFi-1 cells. It was found that TDCA increased basal Ca^{2+} mobilization by 19.6 ± 11.9 % in CuFi-1 cells, and 36.45 ± 25.7 % in NuLi-1 cells, which was not significant as the increase in intracellular Ca^{2+} was abolished with

increasing passage number (n = 7). According to the power calculations performed, it was determined that n = 4 would be required to establish whether TDCA significantly increased thapsigargin stimulated Ca^{2+} mobilization in NuLi-1 cells. It was observed that pre-treatment with TDCA significantly increased thapsigargin mobilization of Ca^{2+} in NuLi-1 cells by 74.8 ± 29.6 % ($p = 0.04$, $n = 6$), but had no effect on thapsigargin responses in CuFi-1 cells. This further confirms that TDCA affects Ca^{2+} mobilization in healthy airway epithelial cells and suggests a role for CFTR in mobilization of intracellular Ca^{2+} levels, possibly through CFTR-dependent ATP, as previously described for UDCA (Fiorotto *et al.*, 2007), or CFTR regulation of Ca^{2+} channels in the plasma membrane (Vachel *et al.*, 2013).

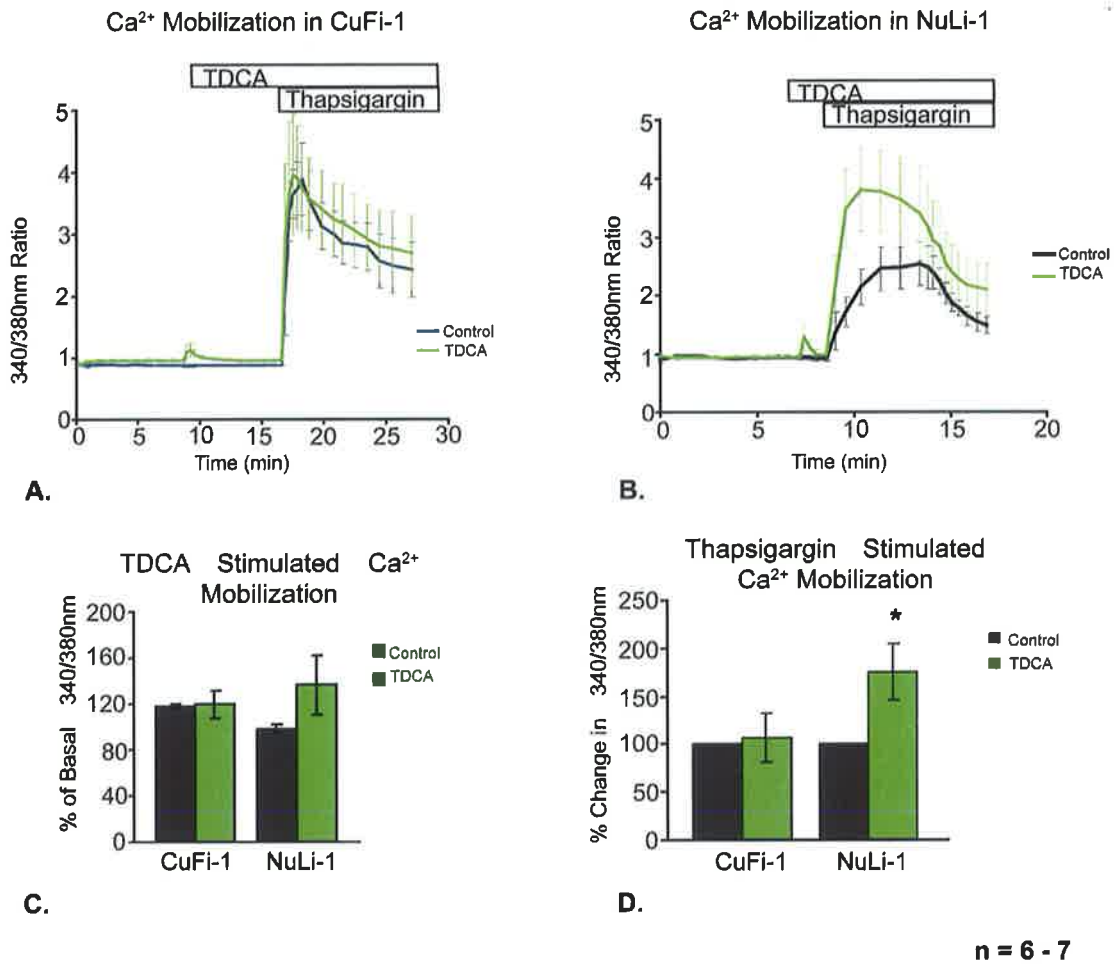

Fig.5.3 TDCA increases thapsigargin stimulated Ca^{2+} mobilization in NuLi-1 but not CuFi-1 cells. A & B, Fura-2 ratio values recorded during experiments with CuFi-1 and NuLi-1. **C**. TDCA increased basal Ca^{2+} mobilization by 19.6 ± 11.9 % in CuFi-1, and 36.45 ± 25.7 % in NuLi-1, which was not significant. **D.** Pre-treatment with TDCA significantly increased thapsigargin mobilization of Ca^{2+} in NuLi-1 by 74.8 ± 29.6 % but had no effect on thapsigargin responses in CuFi-1 ($p = 0.04$, $n = 6$).

5-2.4 TDCA stimulation of I_{sc} in Calu-3 cells is not completely dependent on Ca^{2+} mobilization.

In order to determine the contribution made by intracellular Ca^{2+} to TDCA stimulation of Cl^- secretion, it was investigated whether TDCA could further stimulate Cl^- secretion after depletion of the intracellular stores with thapsigargin. Before performing the Ussing chamber experiment, it first

needed to be established whether TDCA could further stimulate Ca^{2+} mobilization after thapsigargin treatment in Calu-3 cells. It was found that addition of TDCA to cells, after thapsigargin stimulated responses had stabilized, did not further stimulate Ca^{2+} mobilization fig 5.4 B. This result indicated that if TDCA was able to further stimulate Cl^- secretion after thapsigargin treatment in Ussing chambers, then TDCA stimulation of Cl^- secretion would involve another 2nd messenger in addition to Ca^{2+}. As shown in fig 5.4 A & C, acute treatment with TDCA after thapsigargin increased I_{sc} by 3.99 ± 1.36 μAmps/cm^2, compared with a decrease of 11.48 ± 3.23 μAmps/cm^2 in control values recorded over the same period. As TDCA is unable to further increase intracellular Ca^{2+} after thapsigargin treatment, this result indicates that this TDCA stimulation of Cl^- secretion is independent of intracellular Ca^{2+}. In addition, these results indicated that pre-treatment with TDCA prior to thapsigargin treatment appeared to increase thapsigargin stimulated I_{sc} responses to 73.77 ± 18.68 μAmps/cm^2, compared with an increase of 63 ± 15.96 μAmps/cm^2 in untreated controls. As shown in section 5-2.1, pre-treatment with TDCA significantly increases thapsigargin mobilization of Ca^{2+}, therefore this apparent increase in thapsigargin stimulated I_{sc} responses, stimulated by TDCA, is likely dependent on Ca^{2+}. These results indicate that TDCA stimulation of Cl^- secretion in Calu-3 cells involves mobilization of Ca^{2+}, in addition to another intracellular 2nd messenger.

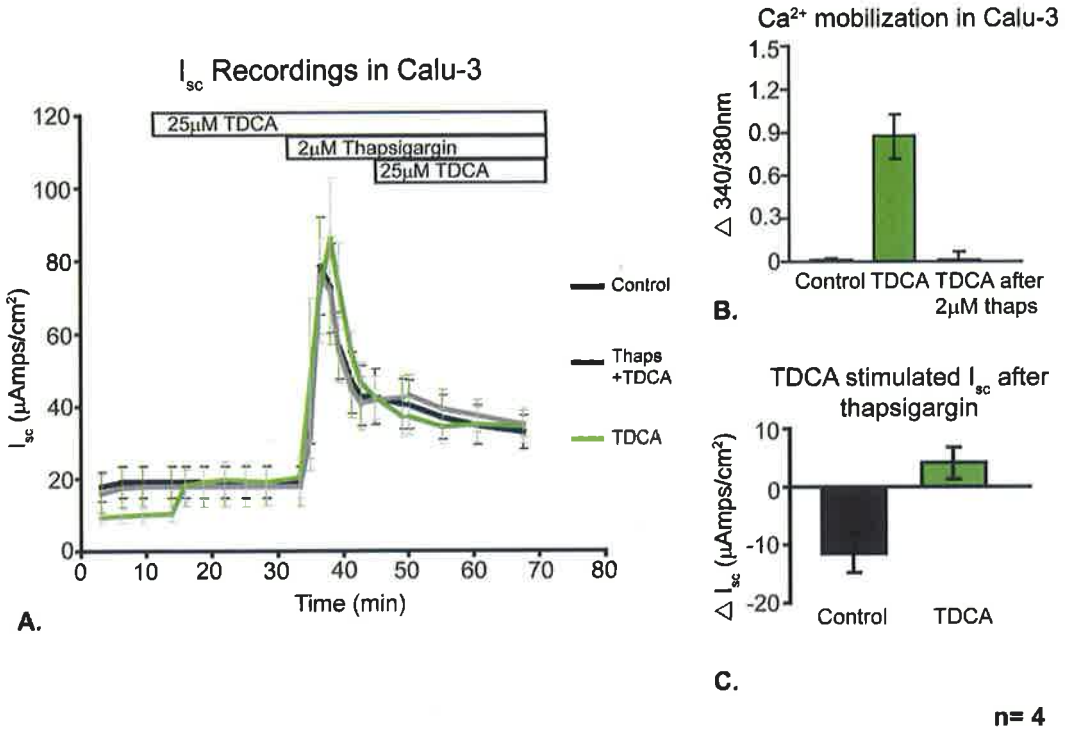

Fig.5.4 TDCA can still stimulate secretion but is unable to mobilize Ca^{2+} in Calu-3 cells after thapsigargin treatment. A. I_{sc} recorded during Ussing chamber experiments showing thapsigargin stimulated responses pre- or post- TDCA treatment in Calu-3. **B.** Changes in Fura-2 ratio after TDCA treatment. TDCA was unable to further stimulate Ca^{2+} mobilization after pre-treatment with thapsigargin in Calu-3. **C.** I_{sc} responses observed after TDCA treatment of Calu-3 in Ussing chambers. Cells were pre-treated with thapsigargin and once the thapsigargin-induced I_{sc} began to stabilize, TDCA was added. TDCA appeared to further increase I_{sc} by 3.99 ± 1.36 μAMPs/cm^2 after thapsigargin treatment, compared with a decrease of 11.48 ± 3.23 μAMPs/cm^2 recorded over the same period in cells treated with thapsigargin alone.

5-2.5 The effect of Bis I on TDCA stimulation of I_{sc} in Calu-3 cells.

PKC involvement in transduction of the Ca^{2+} signal induced by TDCA was investigated using 500 nM bisindolylmaleimide I (Bis I). Bis I is a potent inhibitor of all the known isoforms of PKC and has previously been used to probe for PKC-mediated pathways such as transduction of hormone, cytokine and growth factor signals. As shown in fig 5.5, pre-treatment with Bis I, reduced TDCA stimulation of I_{sc} to 0.75 ± 0.51 μAmps/cm^2 which was similar

to the 0.55 ± 0.65 μAMPs/cm^2 oscillation in I_{sc} recorded in DMSO control cells over the same period, while TDCA, after DMSO pre-treatment, increased basal I_{sc} by 2.65 ± 1.15 μAmps/cm^2, fig 5.5. According to the power calculations performed, it was determined that n = 8 would be required to establish whether pre-treatment with Bis I significantly attenuated TDCA stimulation of I_{sc} in Calu-3 cells. These results suggested that activation of PKC is required for TDCA stimulation of Cl^- secretion in Calu-3 cells.

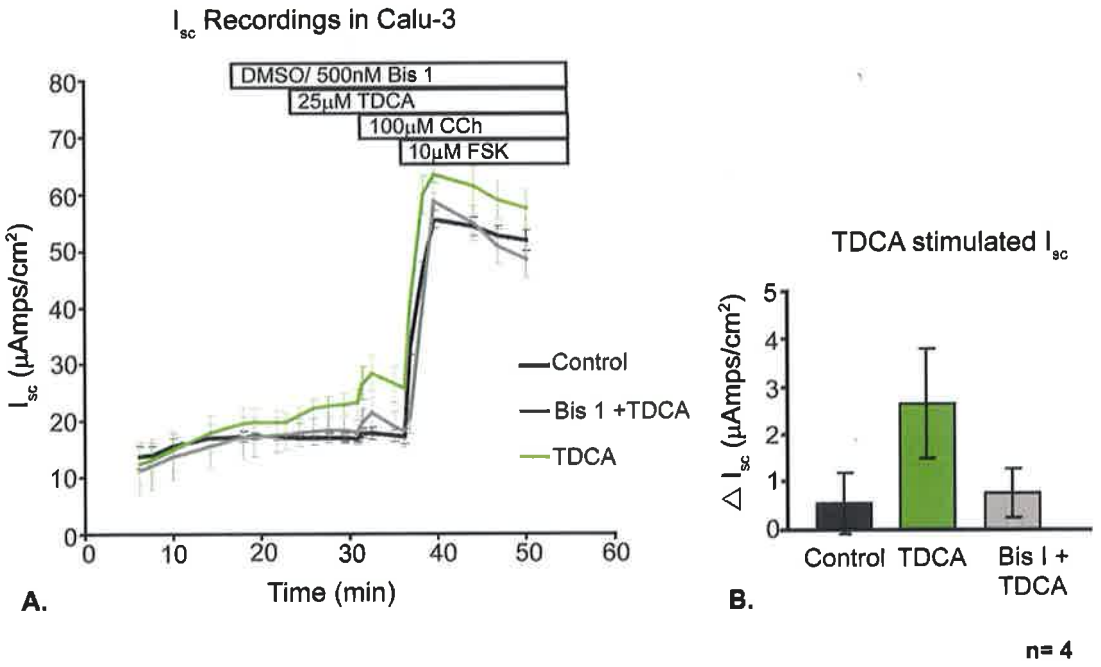

Fig.5.5 The effect of Bis I on TDCA stimulation of I_{sc}. A. I_{sc} recorded during Ussing chamber experiments showing TDCA stimulated responses after pre- treatment with 500 nM Bis I in Calu-3 cells. **B.** I_{sc} responses observed after TDCA treatment. Pre-treatment with Bis I reduced TDCA stimulated I_{sc} responses to 0.75 ± 0.51 μAmps/cm^2 which was similar to DMSO control values of 0.55 ± 0.65 μAMPs/cm^2, while TDCA, after DMSO pre-treatment, increased basal I_{sc} by 2.65 ± 1.15 μAmps/cm^2 (n = 4, p = n.s)

5-2.6 Inhibition of PKC by Bis I does not affect TDCA mobilization of Ca^{2+} in Calu-3 cells.

It has been reported that several PKC isozymes are capable of differentially regulating store-operated Ca^{2+} channels resulting in increased Ca^{2+} influx into cells (Gönczi *et al.*, 2002). Since it was already established that TDCA

stimulates Ca^{2+} influx into Calu-3 cells, and the results obtained in the previous section suggested a role for PKC activity in TDCA signal transduction, PKC involvement in TDCA-induced mobilization of intracellular Ca^{2+} was assessed. Calu-3 cells grown on glass and loaded with Fura-2 were pre-treated with either Bis I or DMSO before acute treatment with 25 μM TDCA. As can be seen in fig 5.6, TDCA produced a 47.86 ± 35.01 % increase in Ca^{2+} mobilization when pre-treated with DMSO only, while TDCA induced a 29.75 ± 28.28 % increase in Ca^{2+} after pre-treatment with Bis I. Due to the large variation in responses it appears that Bis I does not inhibit TDCA influx of Ca^{2+} and hence PKC is not involved in TDCA mobilization of Ca^{2+} in Calu-3 cells.

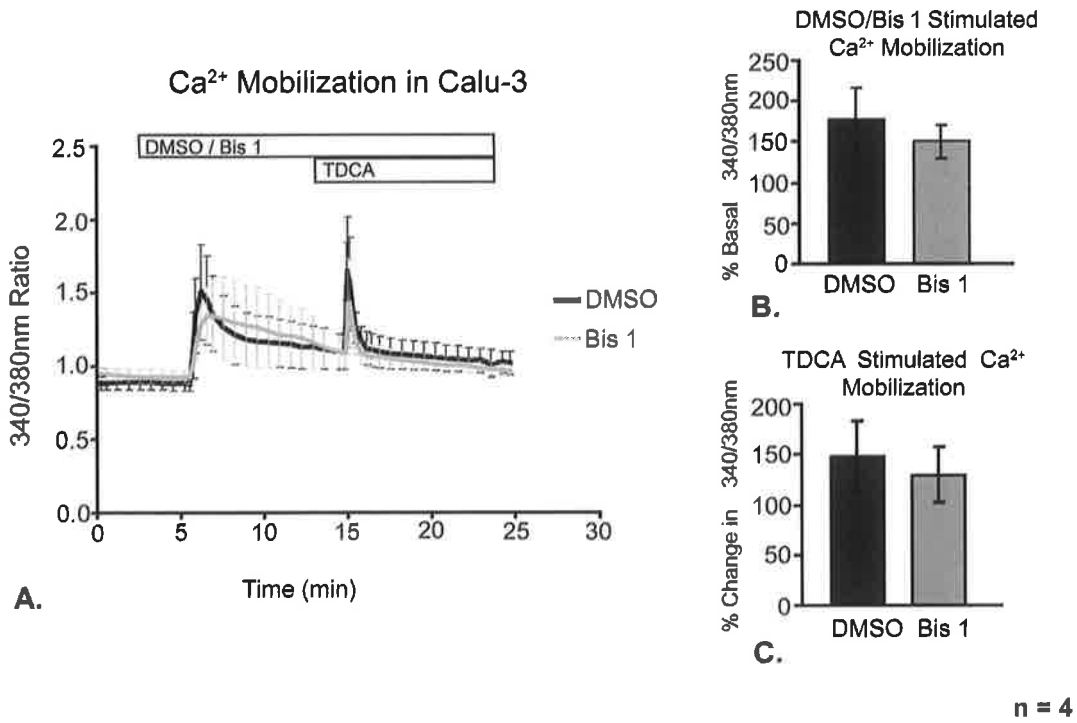

Fig.5.6 Pre-treatment with Bis I does not affect TDCA mobilization of Ca^{2+} in Calu-3 cells. A. Fura-2 ratio values recorded during experiments with Calu-3 cells pre-treated with Bis I or DMSO. **B.** Fura-2 responses observed after treatment with DMSO and Bis I normalized to % of basal 340/360nm ratio. DMSO and Bis I stimulate intracellular Ca^{2+} mobilization to a similar magnitude in Calu-3 suggesting that this increase in intracellular Ca^{2+} is due to the DMSO vector. **C.** Fura-2 responses observed after treatment with TDCA normalized to % of basal 340/360nm ratio TDCA increased Ca^{2+} mobilization by 47.86 ± 35.01 % in DMSO pre-treated cells, and by 29.75 ± 28.28 % in Bis I pre-treated cells

5-2.7 TDCA does not affect phosphorylation of PKCα

UDCA has been shown to stimulate fluid secretion in cholangiocytes by a multistep process requiring activation of both PKCα and PKCε to stimulate Cl^- secretion and hence fluid secretion (Fiorotto *et al.*, 2007). Since PKCα is one of the classical PKC isoforms that is activated by Ca^{2+}, DAG, and direct interaction with the cell membrane, the involvement of PKCα in TDCA signal transduction was investigated. To test this, the effect of TDCA on PKCα phosphorylation, and hence activity of this enzyme, was examined. Calu-3 cells were treated basolaterally with TDCA or CCh for 5 min at 37°C. Cells were immediately placed on ice and proteins were harvested, quantified and a Western blot for phosphorylated PKCα and total PKCα was performed as detailed in chapter 2 (2-3). As can be seen from fig 5.7, acute treatment with TDCA did not affect phosphorylation of PKCα, indicating that PKCα is unlikely to be involved in TDCA stimulation of Cl^- secretion. According to the power calculations performed, it was determined that n = 46 would be required to establish whether pre-treatment with TDCA significantly affected phosphorylation of PKCα in Calu-3 cells.

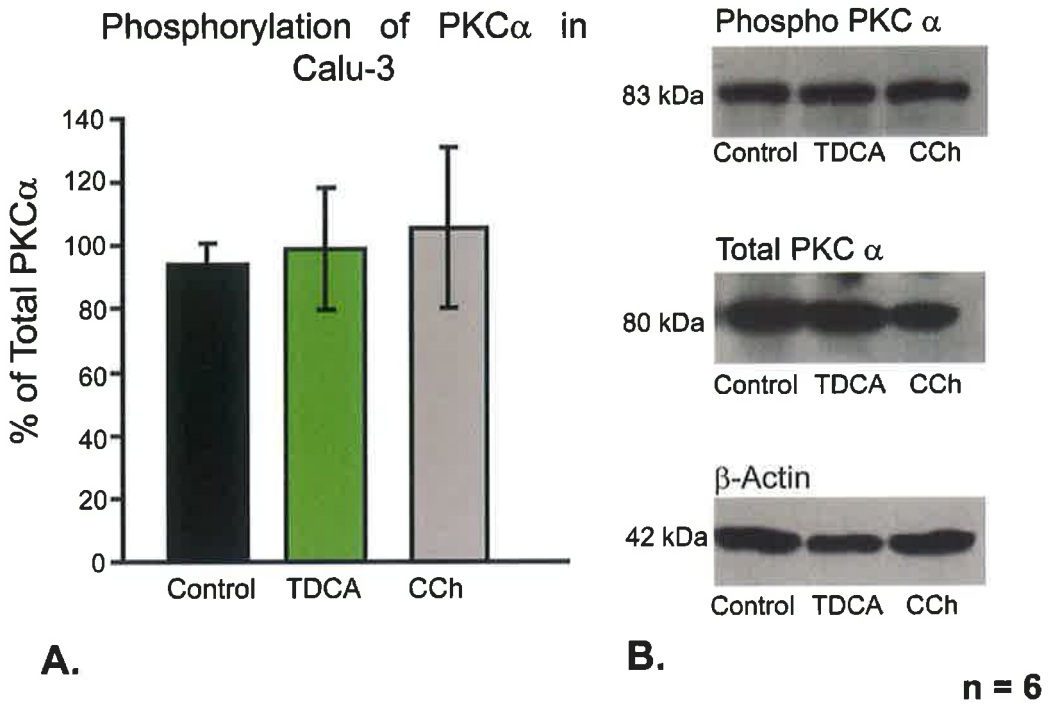

Fig.5.7 TDCA does not affect phosphorylation of PKCα in Calu-3 cells. Calu-3 cells were treated basolaterally with 25 μM TDCA or 100 μM CCh for 5 min prior to protein extraction and separation by SDS-PAGE. **A.** Relative phosphorylation of PKCα normalized to % of total PKCα for each sample. The % of phosphorylated PKCα relative to total values for control, TDCA-treated and CCh-treated were 94.31 ± 6.35 %, 98.89 ± 19.36 %, and 105.51 ± 25.48 % respectively. Therefore TDCA does not appear to affect phosphorylation of PKCα. **B.** Representative Western blots for phospho PKCα, total PKC α and β-actin in each sample.

Other isoforms of PKC, such as PKCβ or PKCδ, should be included in this investigation. PKCβ is another member of the 'classical' PKC isoforms that increases activity in response to intracellular Ca^{2+}. It has been reported in intestinal cells that basolateral protease-activated receptor 2 (PAR-2) - induced Cl^- secretion involves activation of PKCβ and PKCδ (van der Merwe *et al.*, 2009). Furthermore, PKCδ is known to regulate the activity of certain isoforms of adenylyl cyclase, and has been shown to potentiate cAMP production in response to bile acid agonists in the gallbladder (Chignard *et al.*, 2003).

5-2.8 TDCA increases intracellular cAMP in Calu-3 cells

As it had been confirmed in section 5-2.4 that TDCA stimulation of Cl^- secretion is not completely dependent on Ca^{2+}, the next intracellular 2nd messenger that came under investigation was cAMP, which has been reported to activate CFTR and Na^+/K^+ ATPase. Using a commercially available competitive ELISA for cAMP, intracellular concentration of cAMP after TDCA or Fsk treatment was measured. Cells grown on semi-permeable supports under ALI for 9-12 days were treated basolaterally with 25 μM TDCA or 10 μM Fsk for 5 min prior to performing the cAMP assay as described in detail in chapter 2 (section 2-6). Fsk is known to elevate intracellular cAMP levels via activation of adenylyl cyclase and so was included as a positive control in the assay. According to the power calculations performed, it was determined that n = 4 would be required to establish if TDCA significantly increased cAMP levels in Calu-3 cells. As shown in fig 5.8, TDCA significantly increased intracellular cAMP to 13.94 ± 2.89 (pmol/mg) ($p = 0.04$, $n = 8$) compared with untreated control values of 9.68 ± 1.72 (pmol/mg), while Fsk increased intracellular cAMP levels to 511.48 ± 188.35 (pmol/mg) ($p = 0.0075$, $n = 8$).

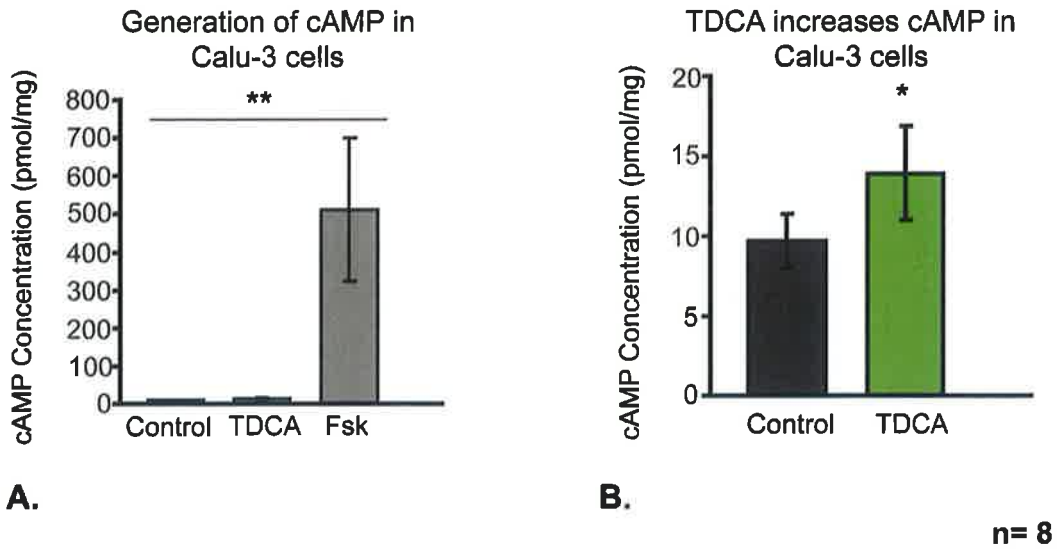

Fig.5.8 TDCA increases basal cAMP levels in Calu-3 cells. Calu-3 cells were treated with 25 μM TDCA or 10 μM Fsk for 5 min before investigation of cAMP levels using an EIA direct cAMP kit from Sigma-Aldrich. **A & B.** cAMP concentration (pmol/mg) measured after treatment of Calu-3 cells with TDCA or Fsk. **A.** Fsk increased intracellular cAMP levels to 511.48 ± 188.35 (pmol/mg) ($p = 0.0075$, $n = 8$). **B**. TDCA significantly increased intracellular cAMP to 13.94 ± 2.89 (pmol/mg) compared to untreated control values of 9.68 ± 1.72 (pmol/mg) ($p = 0.04$, $n = 8$).

5-2.9 The effect of TDCA on PKA activity in Calu-3

After confirmation that TDCA increases intracellular cAMP concentration in Calu-3 cells, it was assessed whether this increase in cAMP also activates PKA in Calu-3 cells. To examine this, a commercially available kit from Promega that contains a fluorescent peptide, which can be phosphorylated by PKA and hence separated according to charge on an agarose gel, was used. This assay works on the basis that the more active PKA there is in the sample, the more negatively charged peptide migrating towards the anode. As per the cAMP assay, cells grown on semi-permeable supports under ALI for 9-12 days were treated basolaterally with 25 μM TDCA or 10 μM Fsk for 5 min prior to protein extraction and performing the PKA assay as described in detail in chapter 2 (section 2-7). After densiometric analysis of the bands was performed using Photoshop software, the relative intensity of each sample

was normalized to % of control. As shown in fig 5.9, TDCA slightly increased PKA activity by 35 ± 19 % while Fsk significantly increased PKA activity by 241 ± 40 % ($p = 0.0053$, $n = 4$). Although TDCA was able to increase PKA activity in all 4 experiments, the magnitude of this increase varied greatly between passages, as can be seen in fig 5.9 B, and so TDCA induced change in PKA activity was not found to be statistically significant. According to the power calculations performed, it was determined that n = 8 would be required to establish whether TDCA significantly increased PKA activity in Calu-3 cells.

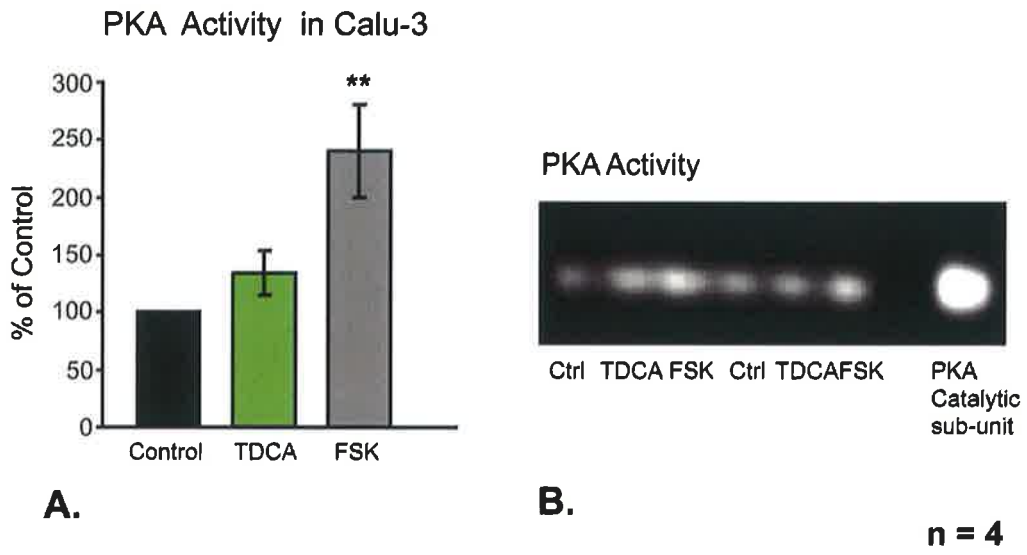

Fig.5.9 The effect of TDCA on PKA activity in Calu-3 cells. Calu-3 cells were treated with 25 μM TDCA or 10 μM Fsk for 5 min before proteins were extracted and assayed for PKA activity. Using a Promega kit, proteins were combined with a fluorescent peptide, that was phosphorylated by PKA and samples were run on an agarose gel. **A, B.** Phosphorylated peptides migrate towards the anode and all samples were normalized to % of control. Increases in phosphorylation of the fluorescent peptide were taken to represent increased PKA activity in Calu-3. Acute treatment with TDCA appeared to produce a 35 ± 19 % increase in PKA activity which was not significant, while Fsk significantly increased PKA activity by 241 ± 40 % ($p = 0.0053$, $n = 4$).

Thirty years ago it was reported that 50% activation of PKA could be achieved when intracellular cAMP concentrations were increased to approximately 9 pmol/10^6 cells (~1 ml) in a murine model of lymphosarcoma cells (Michnoff *et al.*, 1983). Protein yields from the Calu-3 cells used in this study were in the

range of 1.6 - 8.5 mg/ml. Since the basal levels of cAMP in the Calu-3 cells used for this study were ~ 9 pmol/mg protein, this would suggest that Calu-3 cells contain a large quantity of constitutively active PKA, which is likely to be required for the establishment of a pro-secretory serous cell phenotype. TDCA increases cAMP levels by ~4 pmol/mg in Calu-3 cells. Therefore, based on the report by Michnoff *et al*, this increase in cAMP would be expected to increase PKA activity by ~25%, which is similar to the PKA activity values observed in Calu-3 cells after TDCA treatment here. Furthermore, fsk-induced activation of PKA is ~5-fold higher than that of TDCA, while the fsk-induced increase in cAMP is ~37-fold higher than TDCA induced cAMP increases. This observation indicates that PKA is maximally activated after treatment with fsk and demonstrates how changes in PKA activity may be disproportionate to changes in the intracellular concentration of cAMP. Based on these results, it was important to perform further experiments, using an inhibitor of PKA, to determine the contribution made by PKA to TDCA stimulation of Cl^- secretion in the airway epithelium

5-2.10 Pre-treatment with the PKA inhibitor H89 reduces TDCA mobilization of Ca^{2+} in Calu-3 cells.

PKA has previously been shown to play a role in the cross talk between Ca^{2+} and cAMP signals, in particular in the regulation of Ca^{2+} release from intracellular stores (Braiman *et al.*, 1998). In order to test whether PKA is involved in TDCA mobilization of Ca^{2+} in Calu-3 cells, Ca^{2+} imaging experiments in cells loaded with Fura-2 and pre-treated with either DMSO or 10 μM N-[2-(p-Bromocinnamylamino)ethyl]-5-isoquinolinesulfonamide (H89), an inhibitor of PKA, were performed. The change in $A_{340/380}$ recorded after treatment with H89 or DMSO was normalized to % of basal $A_{340/380}$ recorded before treatment. As shown in fig 5.10, both H89 and DMSO stimulated an increase in intracellular Ca^{2+} with DMSO increasing basal Ca^{2+} by 56.76 ± 32.16 %, while H89 increased Ca^{2+} by 157 ± 56.57 %. In addition it was observed that after pre-treatment with h89, TDCA was no longer able to stimulate Ca^{2+} mobilization in Calu-3 cells compared to an increase in Ca^{2+}

mobilization of 66.57 ± 30.96 % induced by TDCA in DMSO-treated control cells.

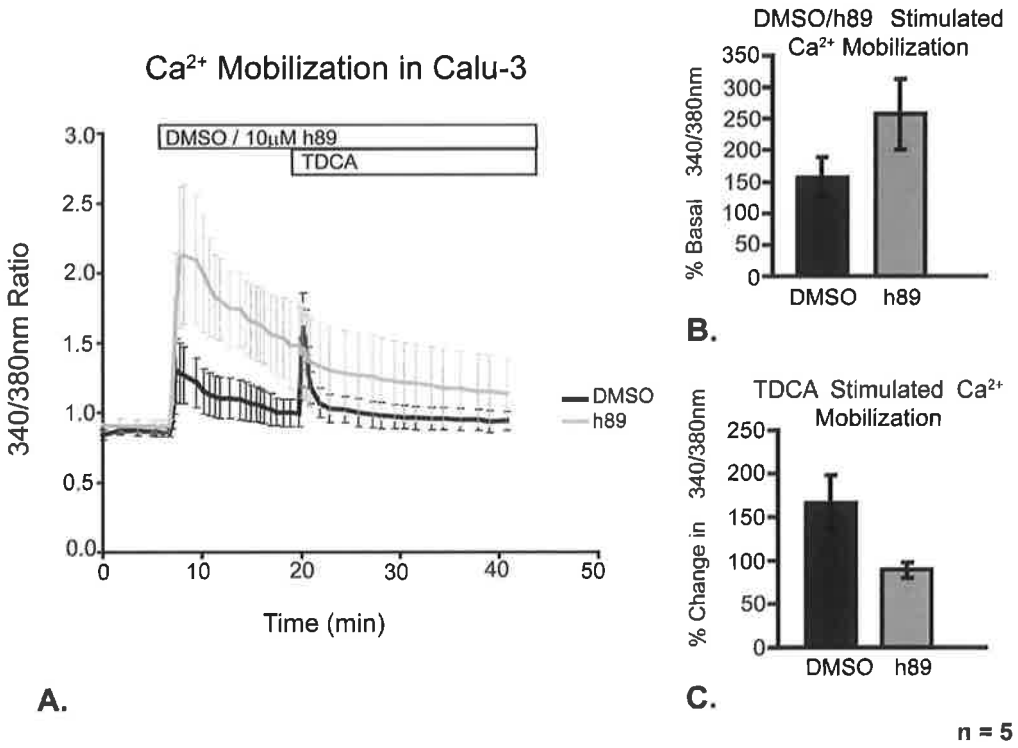

Fig.5.10 Pre-treatment with H89 reduces TDCA mobilization of Ca^{2+} in Calu-3 cells. A. Fura-2 ratio values recorded during experiments with Calu-3 cells pre-treated with H89 or DMSO. **B.** Fura-2 responses observed after treatment with DMSO and h89 normalized to % of basal $A_{340/380}$ ratio. Both DMSO vector and H89 stimulate an increase in intracellular Ca^{2+} in Calu-3. DMSO increased basal Ca^{2+} levels by 56.76 ± 32.16 % while H89 increased Ca^{2+} levels by 157 ± 56.57 %. **C**. Fura-2 responses observed after treatment with TDCA normalized to % of basal $A_{340/380}$ ratio. TDCA was unable to further mobilize Ca^{2+} in H89 pre-treated cells, while TDCA increased intracellular Ca^{2+} by 66.57 ± 30.96 % in DMSO-treated control cells.

5-2.11 Pre-treatment with H89 does not inhibit TDCA stimulation of Cl^- secretion in Calu-3 cells.

Building on the results obtained in the previous two sections, the final investigation performed in this chapter was to assess PKA involvement in

TDCA stimulation of I_{sc}. Ussing chamber experiments in normal Krebs solution were performed and cells were pre-treated bi-laterally with 10 μM h89 or DMSO. The I_{sc} was allowed to stabilize prior to treatment with TDCA, followed by CCh and Fsk. As shown in fig 5.11, pre-treatment with h89 did not inhibit TDCA stimulated I_{sc}, indicating that TDCA stimulation of Cl^- secretion is not dependent on PKA.

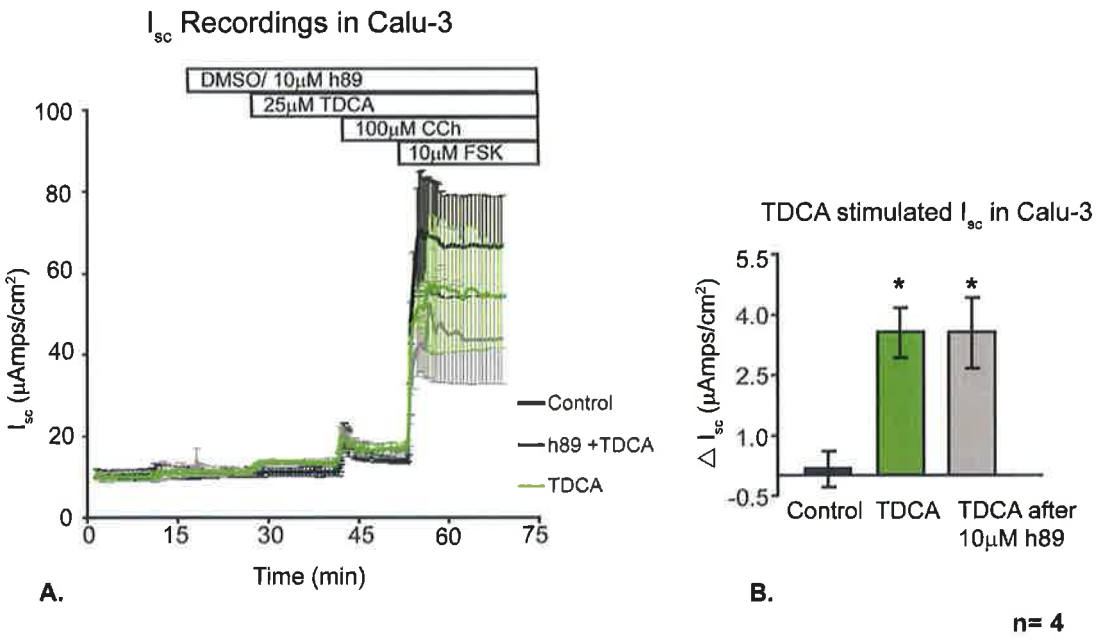

Fig.5.11 Pre-treatment with H89 does not inhibit TDCA stimulation of I_{sc}. A. I_{sc} values recorded during experiments with Calu-3 pre-treated with h89 or DMSO. **B.** I_{sc} responses observed after treatment with TDCA. TDCA increased I_{sc} by 3.57 ± 0.62 (μAmps/cm^2) and 3.55 ± 0.89 (μAmps/cm^2) in the DMSO and H89 pre-treated cells respectively, compared with I_{sc} oscillations of 0.17 ± 0.45 (μAmps/cm^2) observed in DMSO only control cells (n = 4).

5-3 Discussion

In the previous 2 chapters it has been proven that TDCA can acutely stimulate Cl^- secretion in airway epithelial cells, when applied basolaterally, by activating CFTR, CaCC and Na^+/K^+ ATPase pump. The differential regulatory mechanisms of the ion transport proteins activated by TDCA suggested that its prosecretory effects might be mediated by one or more shared intracellular 2^{nd} messengers. Therefore in this chapter the aim was to identify the signalling molecules involved and to elucidate the kinase pathways participating in TDCA-stimulated Cl^- secretion in the airways. As Ca^{2+} and cAMP are well recognised mediators of airway secretory responses, these were the first two signalling molecules to be investigated in this study.

It is also well established that many bile acids, including TDCA, are capable of increasing intracellular Ca^{2+} in a concentration dependent manner by increasing either Ca^{2+} release from internal stores or inducing a cellular influx of Ca^{2+}, or both (Devor *et al.*, 1993, Fiorotto *et al.*, 2007, Dharmsathaphorn *et al.*, 1989, Moschetta *et al.*, 2003). After establishing that TDCA, at the low concentration used in this study, was capable of stimulating Ca^{2+} mobilization within airway epithelial cells, it was then important to ascertain the source of this Ca^{2+}. In this Calu-3 model, TDCA stimulation of Ca^{2+} mobilization was abolished under conditions where free extracellular Ca^{2+} had been removed, indicating that TDCA stimulated a cellular Ca^{2+} influx in Calu-3 cells, in agreement with previously published data from colonic epithelial studies (Moschetta *et al.*, 2003, Dharmsathaphorn *et al.*, 1989).

Interestingly, in contrast with Calu-3 cells, TDCA alone had no effect on Ca^{2+} mobilization but was shown to increase thapsigargin mobilization of Ca^{2+} in NuLi-1 cells. However, TDCA had no effect on Ca^{2+} mobilization in CuFi-1 cells. Thapsigargin is an inhibitor of the sarco / endoplasmic reticulum Ca^{2+} ATPase (SERCA) responsible for the filling of intracellular Ca^{2+} stores. Inhibition of SERCA rapidly increases intracellular Ca^{2+} levels in a sustained manner as the intracellular Ca^{2+} stores become depleted. This suggests that in the non-CF cells, TDCA stimulates an influx of Ca^{2+} into the cells that

appears to be pumped directly into the intracellular stores. However, this TDCA induced influx of Ca^{2+} appears to be absent in CF cells. One possible reason for this is that Ca^{2+} influx is increased under resting conditions in CF cells, as has been recently reported (Kunzelmann and Mehta, 2013, Vachel *et al.*, 2013), which would account for the increased thapsigargin stimulated responses recorded in CuFi-1 control cells, compared with NuLi-1 control cells (section 5-2.3). Under these conditions, it is possible that Ca^{2+} influx might occur through the same airway plasma membrane channels as activated by TDCA, such as the store operated Ca^{2+} entry (SOCE) channels STIM, ORAI or the receptor operated Ca^{2+} entry (ROCE) channel TRPV4 (Lorenzo *et al.*, 2008), and therefore TDCA will not have an additive effect on Ca^{2+} influx. The observation that TDCA increased thapsigargin stimulated Ca^{2+} mobilization in NuLi-1 cells to approximately the same level as controls in CuFi-1 cells would support this explanation.

Alternatively, TDCA may induce Ca^{2+} influx by a process of membrane depolarization, which is absent in CF cells, such as activation of CFTR (Mukherjee *et al.*, 2013, Liu *et al.*, 2009). Since our electrophysiological studies have shown that TDCA stimulated basal I_{sc} in Calu-3 cells, but not NuLi-1 cells, this may suggest that TDCA results in higher levels of membrane depolarization in Calu-3 cells than NuLi-1 cells and hence might account for the differences in Ca^{2+} mobilization between the 2 cell lines. Furthermore, Calu-3 cells display characteristics of a more secretory phenotype than NuLi-1 cells, such as larger responses to CCh and FSK in Ussing chambers. This suggests that Calu-3 cells may be more sensitive to Ca^{2+} mobilizing agonists than NuLi-1 cells and hence might explain the varying Ca^{2+} responses to TDCA in both cell lines as shown in this study. However, the differences might also be accounted for by the culture conditions, since both cell lines were grown on glass, in a non-differentiated state, which may result in differential expression of Ca^{2+} channels or receptors across the cell lines.

The cross-talk that occurs between cAMP and Ca^{2+} signalling pathways is now widely-accepted. Ca^{2+} regulates the activity of adenylyl cyclases and phosphodiesterases that control cAMP levels, while cAMP regulates the

activity of SERCA and IP_3 receptors that carefully monitor intracellular Ca^{2+} concentrations. Furthermore, it has recently been suggested that the link between the 2 may be mediated by CFTR (Kunzelmann and Mehta, 2013) or by PKA and PKC. After determining that TDCA stimulation of Cl^- secretion was affected by, but not completely dependent on Ca^{2+}, the study was then focused on TDCA modulation of intracellular cAMP levels. It has previously been reported that many bile acids, including TDCA, can regulate cAMP production in various different epithelial tissues (Chignard *et al.*, 2003, Keating *et al.*, 2009, Ao *et al.*, 2013). Since TDCA had been shown earlier in this study to activate CFTR and Na^+/K^+ ATPase, it was expected that TDCA would increase intracellular cAMP levels, which was confirmed in section 5-2.8 of this report. These results indicated that our original hypothesis had been correct; TDCA stimulates Cl^- secretion in airway epithelial cells via mobilization of intracellular Ca^{2+} and cAMP. After identification of these two 2^{nd} messengers mediating TDCA secretory responses, it was then important to assess the contribution made to TDCA stimulated Cl^- secretion by proteins known to transduce Ca^{2+} and cAMP-dependent signals. Since it is now well established that PKA can activate CFTR via phosphorylation of its regulatory subunit, and it had already been confirmed in this study that TDCA activates CFTR and increases cAMP, TDCA was therefore also expected to increase PKA activity in Calu-3.

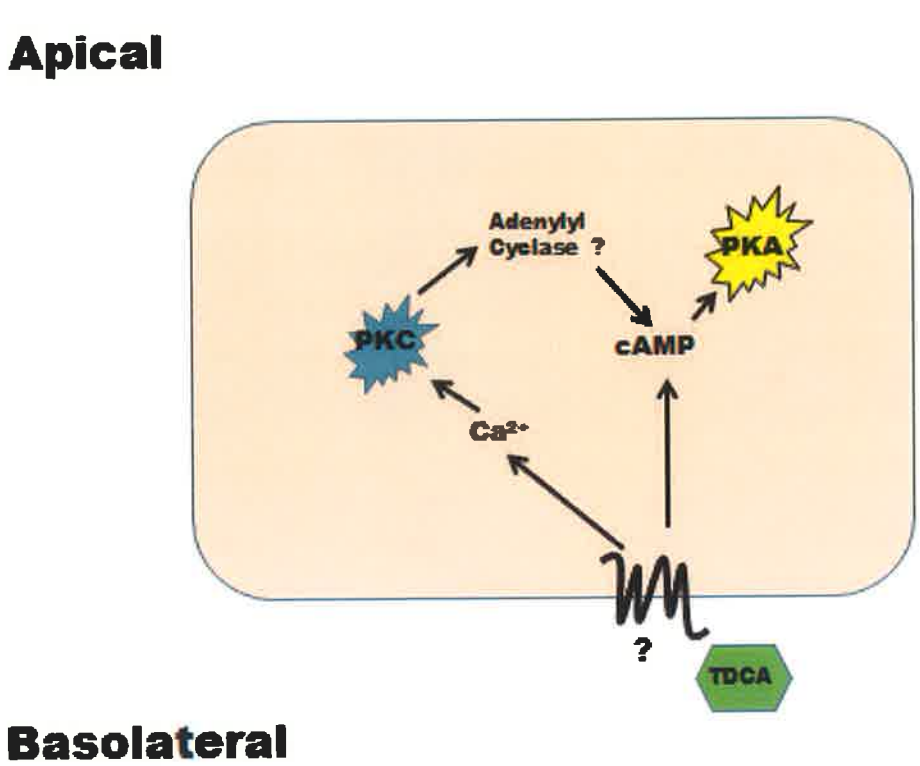

Fig.5.12. Signalling molecules involved in TDCA stimulation of Cl^- secretion in airway epithelial cells. TDCA increases intracellular Ca^{2+} concentration, which stimulates Cl^- secretion through CaCC and can activate certain isoforms of PKC. Our data indicates that TDCA stimulation of secretion is dependent on PKC. PKC has been reported to regulate adenylyl cyclase production of cAMP. TDCA increases intracellular cAMP and PKA activity. PKA is known to activate CFTR and to regulate trafficking of Na^+/K^+ ATPase to the membrane. Further investigation is required to identify the receptor through which TDCA stimulation of secretion is initiated.

The effect of TDCA on the activity of PKA, activated by cAMP, or PKCα, one of the classical PKC isoforms activated by Ca^{2+}, was investigated. The taurine conjugate of UDCA, TUDCA, had previously been reported to induce PKCα translocation to the membrane and accumulation of DAG, which can activate PKCα, at the membrane of hepatocytes (Beuers, 1997). More recently it has been shown co-operation between PKCα and PKA, mediated TUDCA exertion of anti-cholestatic effects in hepatocytes, as bile flow was

reduced when both were inhibited but was unaffected when either PKA or PKCα alone was inhibited (Wimmer *et al.*, 2008). The results presented in this chapter suggest that TDCA may increase PKA activity but not that of PKCα. However, TDCA may be able to activate other PKC isozymes which contribute to regulation of airway homeostasis. It has previously been reported that the PKC signalling pathway participates in modulation of airway inflammatory responses during acute lung injury caused by TDCA induced acute pancreatitis (Zhao *et al.*, 2006). Therefore, in order to determine whether activation of PKA or any of the other isoforms of PKC were required for TDCA-induced Ca^{2+} mobilization or stimulation of I_{sc}, two inhibitors- H89, an inhibitor of PKA, and Bis I, an inhibitor of all isoforms of PKC, were employed. Our results demonstrate that pre-treatment with H89 abolishes TDCA stimulated influx of Ca^{2+}, suggesting that TDCA mobilization of Ca^{2+} appears to be regulated by PKA. However, as shown in fig 5.10, the elevated $A_{340/380}$ ratio in the H89 treated cells was similar to the peak $A_{340/380}$ ratio recorded after treatment with TDCA in the DMSO control. H89 is an ATP-site inhibitor which blocks phosphorylation of PKA regulatory subunits but it has been previously reported that H89 may have non- specific effects on other protein kinases and SERCA (Hussain *et al.*, 1999, Yuan and Bers, 1995, Lee and Linstedt, 2000). Therefore, H89 may interfere with TDCA mobilization of Ca^{2+} by a manner other than inhibition of PKA, and so PKA involvement in TDCA-induced mobilization of Ca^{2+} cannot be conclusively determined from these experiments. In order to confirm that PKA activity is involved in TDCA stimulation of secretion, these experiments would need to be repeated using a more specific inhibitor of PKA or a cAMP antagonist such as Rp-cAMPs, which prevents dissociation of the PKA holoenzyme (Boundy *et al.*, 1998).

Finally, in order to assess whether activation of PKC was required for TDCA stimulation of Cl^- secretion or Ca^{2+} mobilization, cells were pre-treated with Bis I, before TDCA. It has recently been reported that PKC regulates Ca^{2+} oscillations in airway smooth muscle cells (Mukherjee *et al.*, 2013), in addition to previous reports that PKC regulates ion transport via activation of CFTR and Na^+/K^+ ATPase (Han *et al.*, 2010, Jia *et al.*, 1997). In this study, inhibition

of PKC did not appear to affect TDCA stimulated mobilization of Ca^{2+} but results from Ussing chamber experiments indicate that TDCA stimulation of I_{sc} is dependent on PKC activity. In addition to direct phosphorylation of ion transport proteins by PKC, another possible explanation for this inhibition of TDCA simulated I_{sc} could be PKC regulation of TDCA induced cAMP production. It has been reported that TCDCA and TUDCA increase fluid secretion in the gall bladder epithelium via PKC-mediated regulation of adenylyl cyclase isoforms and hence cAMP production (Chignard *et al.*, 2003). Further research into the activation of specific isoforms of PKC by TDCA will be required, in addition to investigation of how PKC may be involved in the cross-talk between intracellular Ca^{2+} and cAMP signalling, that participate in the regulation of airway secretion by bile acids.

In summary, the aim of this chapter was to identify the signalling molecules participating in TDCA stimulation of Cl^- secretion in the airways. The results presented here confirm that TDCA increases intracellular concentrations of both Ca^{2+} and cAMP, two 2^{nd} messengers known to be involved in Cl^- secretion. Transduction of the Ca^{2+} and cAMP signal appears to be via PKC and PKA respectively, with data presented here suggesting a dependence on PKC for TDCA induced secretion. Further investigation of the receptors involved in TDCA stimulation of Cl^- secretion is necessary and will be examined in the following chapter.

Chapter 6

The involvement of bile acid receptors in TDCA stimulation of airway secretion

6-1 Introduction

Results from the previous three chapters build on our understanding into how bile acids can modulate airway epithelial ion transport at low concentrations. So far, this study has shown that TDCA can acutely stimulate Cl^- secretion, when applied basolaterally, through activation of CFTR, CaCC, and Na^+K^+ ATPase. This process involves mobilization of cAMP and Ca^{2+}, in addition to apparent activation of PKA and PKC. Since conjugated bile acids are impermeable to cell membranes, and TDCA has no effect when applied apically, this suggests that a bile acid receptor is present at the basolateral membrane through which TDCA induced secretion can signal. Alternatively a bile acid transporter may be present, which facilitates TDCA entry, leading to activation of intracellular receptors. The aim of this chapter is therefore to determine whether either of the known bile acid receptors FXR or TGR5, which have previously been shown to be expressed in the lung (Zhou *et al.*, 2013), participate in TDCA-induced stimulation of Cl^- secretion in the airway.

As described in more detail in chapter 1 (section 1.6.4-6), there are 2 distinct classes of receptors through which bile acids can signal; nuclear receptors and GPCRs. Although to date, many different types of nuclear receptor have been described as targets for bile acids, the only nuclear receptor focused on in this study is the farnesoid X receptor (FXR). FXR was first identified by Makishima *et al* in 1999, and is known to play an important role in regulating the synthesis and metabolism of bile acids and enterohepatic circulation of bile acids (Makishima *et al.*, 1999, Abu-Hayyeh *et al.*, 2013). It has been well-documented in the literature that GW4064 is a specific agonist for FXR. Activation of FXR by GW4064 results in FXR translocation to the nucleus, which can sometimes be difficult to study in biological systems (Mroz *et al.*, 2013). Instead, one marker that has been shown to be a reliable indicator of FXR activation is increased expression of fibroblast growth factor 19, (FGF19) (Li *et al.*, 2004). FGF19 is thought to participate in negative feedback control of bile acid synthesis, which is regulated by FXR.

It has recently been reported that the 4 different isoforms of FXR endogenously expressed in human hepatocytes, FXR -α1, -α2, -α3 and -α4, each show similar specificities for individual bile acid species, and equal sensitivities to unconjugated or conjugated bile acids (Vaquero *et al.*, 2013). Since FXR is a member of the nuclear receptor family, which are known to be present in the cytosol or nucleus of cells, and conjugated bile acids are impermeable to cell membranes, bile acid transporters are therefore required in order to facilitate entry of conjugated bile acids into the cell, and hence FXR activation. It has also been suggested that trafficking of conjugated bile acids to the nucleus is concentration dependent, and that conjugated bile acids require additional cellular components, not involved in the uptake process, in order to activate FXR (Vaquero *et al.*, 2013, Monte *et al.*, 2008).

This investigation focused on FXR as it has previously been found to modulate epithelial ion transport through regulation of both the activity and expression of different ion transport proteins (Mroz *et al.*, 2013, Keating and Keely, 2009b). FXR has been shown to increase glucose-induced insulin secretion by non-genomic effects in pancreatic β-cells, demonstrating that this receptor does not function solely as a transcription factor (Düfer *et al.*, 2012a). Acute activation of FXR by TCDCA and GW4064 have been reported to increase intracellular Ca^{2+} and inhibit K^+ current through K^+_{ATP} channels in mouse β-cells (Düfer *et al.*, 2012b). In addition, FXR has previously been shown to be expressed in the lung and to participate in tissue repair after acute lung injury (Zhang *et al.*, 2012). These findings support the hypothesis that TDCA may acutely stimulate Cl^- secretion through activation of FXR in the airway.

The second bile acid receptor under investigation in this study is the GPCR, TGR5 (also known as M-BAR or BG37 or GPBAR1), which was identified in 2002 and led to the establishment of non-genomic functions of bile acids (Maruyama *et al.*, 2002, Kawamata *et al.*, 2003). TGR5 is expressed on the plasma membrane and is internalized in response to direct activation by bile acid agonists, increasing intracellular cAMP production and resulting in rapid

signalling responses (Kawamata *et al.*, 2003). Agonists for TGR5 include lithocholic acid (LCA), oleanolic acid (OA) and the synthetic ligand 6α-ethyl-23(*S*)-methyl-3 α,7 α,12 α -trihydroxy-5 β -cholan-24-oic acid (INT777). It has recently been shown that activation of TGR5 in response to its agonists increases intracellular concentrations of both cAMP and Ca^{2+} in pancreatic β-cells (Kumar *et al.*, 2012). One important feature of TGR5 activation is that conjugated bile acids appear to be agonists of TGR5 without the need for a specific transporter, as required with most nuclear receptors. Furthermore, in recent years there have been increasing reports in the literature indicating that TGR5 plays a role in bile acid induction of epithelial secretion (Toumi *et al.*, 2011, Ward *et al.*, 2013). TGR5 has been described as an important regulator of both basal colonic secretion and also secretion in response to cholinergic stimulation in the rat colon (Ward *et al.*, 2013). In addition, TGR5 involvement has been implicated in in CDCA activation of CFTR via cAMP/PKA pathway in T84 cells, while TGR5 activation in the epithelium of the gallbladder also stimulates Cl^- secretion through activation of CFTR (Ao *et al.*, 2013, Keitel *et al.*, 2009). Since TDCA is a conjugated bile acid that has already been shown, in chapter 5, to increase intracellular cAMP and Ca^{2+}, TGR5 therefore seemed to be a likely target for TDCA induction of Cl^- secretion.

These reports, along with the results from the previous chapters, support the hypothesis that initiation of TDCA induced Cl^- secretion is via activation of either TGR5 or FXR. Therefore the primary aim of this chapter was to assess the contribution made by TGR5 or FXR activation to Calu-3 I_{sc}, and to determine whether either receptor is involved in TDCA stimulation of I_{sc}. Specifically we will describe investigations on the:

1) Effects of GW4064 on FGF19 mRNA levels, and FXR protein expression as indicators of FXR activation in Calu-3 cells
2) Effect of GW4064 treatment on I_{sc} responses in Calu-3 cells, in comparison with TDCA
3) TGR5 expression levels in Calu-3 cells after TDCA treatment
4) TDCA stimulation of I_{sc} after siRNA knockdown of TGR5 in Calu-3

6-2 Results

6-2.1 GW4064 increases FGF19 mRNA expression in Calu-3

Prior to investigating the effects of FXR activation on I_{sc}, it first needed to be confirmed that GW4064, the synthetic agonist for FXR, could activate FXR in Calu-3 cells. In order to do this, expression of FGF19 was investigated after 2 hr and 24 hr bi-lateral incubations with 5 μM GW4064. FGF19 expression has previously been shown to increase upon FXR activation and is therefore a reliable indicator of FXR activation (Li *et al.*, 2004). Calu-3 cells, grown under ALI on semi-permeable supports for 9-12 days were treated bi-laterally with 5 μM GW4064, or DMSO for 2 hr or 24 hr, before RNA was harvested, used to generate cDNA, and real time qRT-PCR was performed as described in detail in chapter 2 (section 2-9).

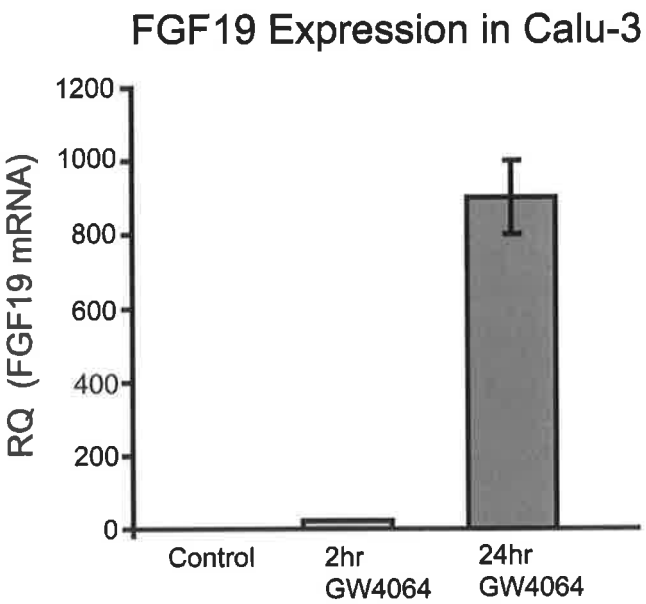

Fig.6.1 GW4064 increases FGF19 expression in Calu-3 cells. Values represent relative quantities (RQ) of FGF19 mRNA in each sample after 2 or 24 hr treatment with 5 μM GW4064. FGF19 mRNA increased to 24.6 ± 0.2 Arbitrary Units (A.U) after 2 hr GW4064 treatment, and 903.2 ± 99.8 A.U after 24 hr GW4064, compared with an RQ value of 1 A.U for the control, (n = 2).

As shown in fig 6.1, FGF19 mRNA levels begin to increase after 2 hr GW4064 treatment and appear to be maximal after 24 hr GW4064 treatment. This result suggests that GW4064 treatment increases FGF19 expression in Calu-3 cells, and hence activates FXR.

6-2.2 GW4064 increases FXR expression in Calu-3

The previous result indicated that GW4064 appeared to activate FXR, with the greatest effect after 24 hr incubation. In order to investigate the effects of GW4064 on FXR expression, Calu-3 cells were again treated with DMSO or 5 μM GW4064 for 24 hr before proteins were harvested, separated via SDS-PAGE and a Western Blot for FXR expression was performed, as described in chapter 2 (section 2-3).

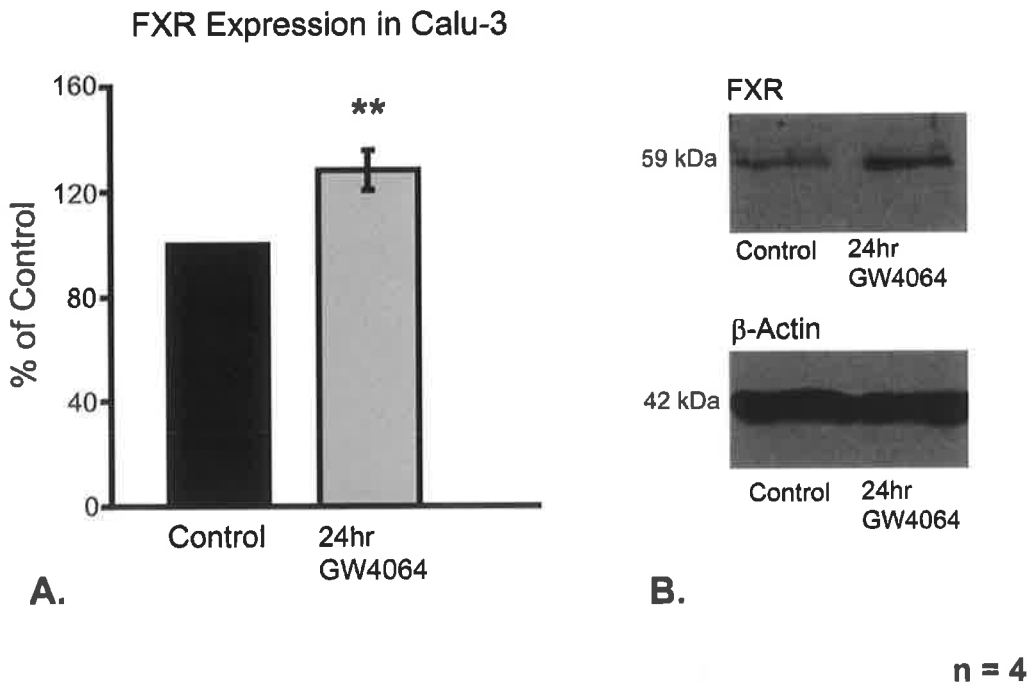

Fig.6.2 24hr GW4064 treatment increases FXR expression in Calu-3 cells. A. Values represent relative quantity of FXR, normalized to % of control. 24 hr treatment with GW4064 significantly increased FXR expression by 28.2 ± 7.6 %, (n = 4, p = 0.003). **B.** Representative Western blot for FXR and β-actin in each sample.

According to the power calculations performed, it was determined that n = 3 would be required to establish whether GW4064 significantly increased FXR expression in Calu-3 cells. As shown in fig 6.2, 24 hr GW4064 treatment significantly increased FXR expression by 28.2 ± 7.6 %, (n = 4, p = 0.003). These results suggest that GW4064 is a specific agonist of FXR that increases both the activity and expression of FXR in Calu-3.

6-2.3 Acute activation of FXR does not affect I_{sc} in Calu-3 cells.

Having established that GW4064 can activate FXR in Calu-3 cells, the effect of acute activation of FXR on Calu-3 I_{sc} was then investigated. Calu-3 cells grown under ALI on Costar snapwells for 9 – 12 days, were mounted in Ussing chambers and the basal I_{sc} was recorded for 15 min prior to treatment with 5 μM GW4064 or DMSO bilaterally. The I_{sc} was recorded for a further 20 min and allowed to stabilize. 100 μM CCh was added basolaterally and the transient CCh-induced Cl^- secretion was measured. Again, I_{sc} was allowed to stabilize for a further 15 min before adding 10 μM Fsk and the sustained Fsk-induced Cl^- secretion was measured. The change in basal I_{sc} recorded after acute GW4064 treatment was 0.06 ± 0.13 ($\mu Amps/cm^2$), which was similar to oscillations in control values of -0.65 ± 0.42 ($\mu Amps/cm^2$), indicating that acute activation of FXR does not affect Calu-3 I_{sc}, fig 6.3 A, (n = 5). Similarly GW4064 pre-treatment did not affect subsequent CCh stimulated I_{sc} responses but appeared to increase Fsk stimulated responses by 48.2 ± 36.7 % after acute GW4064 treatment, which was not statistically significant due to large variation in responses. These data indicate that acute activation of FXR does not affect I_{sc} in Calu-3.

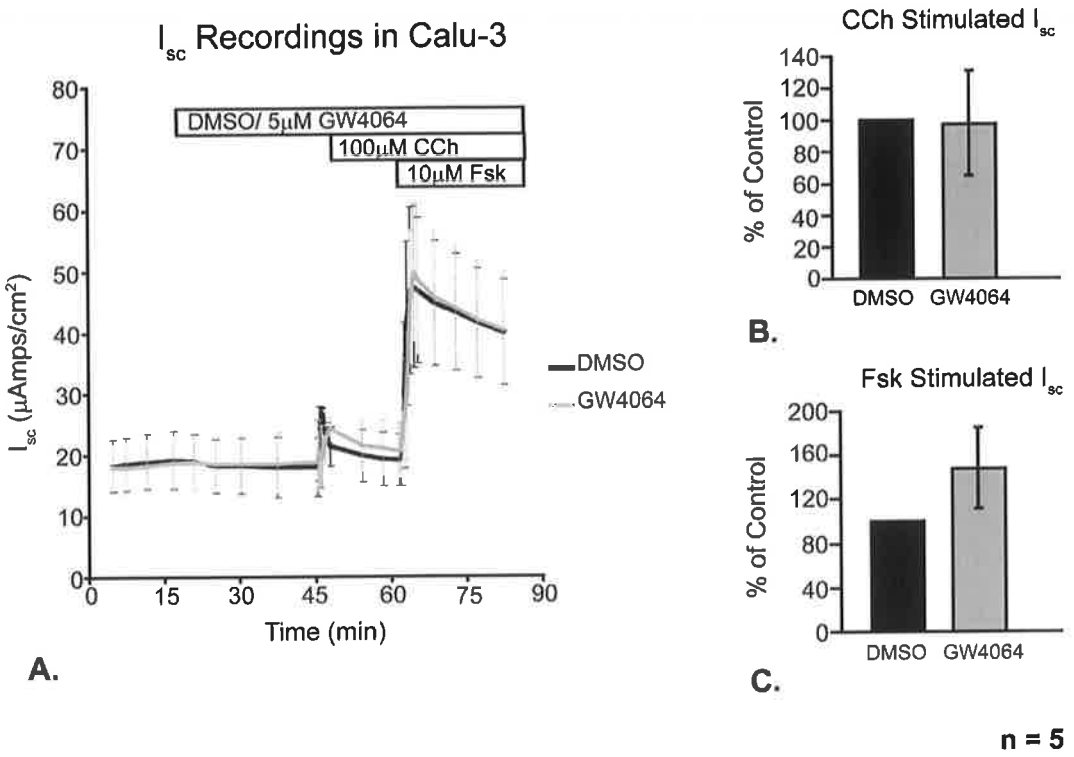

Fig.6.3 Acute activation of FXR does not affect I_{sc} in Calu-3 cells. A. I_{sc} values recorded during experiments with Calu-3 treated with GW4064 or DMSO. **B.** Change in I_{sc} values represented as % of control after CCh treatment. Acute GW4064 treatment does not affect basal I_{sc} or CCh stimulated responses. **C.** Change in I_{sc} values represented as % of control after Fsk treatment. Acute GW4064 appeared to increase Fsk stimulated responses by 48.2 ± 36.7 %, (n = 5).

6-2.4 Chronic activation of FXR does not affect I_{sc} in Calu-3 cells.

Subsequently, the effect of chronic activation of FXR on Calu-3 I_{sc} was investigated. Calu-3 cells were treated bi-laterally with 5 μM GW4064 or DMSO for 24 hr at 37°C. After this period, cells were mounted in Ussing chambers and the basal I_{sc} was recorded for 20 min prior to treatment with 100 μM CCh basolaterally and the transient CCh-induced Cl^- secretion was measured. I_{sc} was allowed to stabilize for a further 15 min before adding 10 μM Fsk and the sustained Fsk-induced Cl^- secretion was measured. As shown in fig 6.4, 24 hr treatment with GW4064 appeared to increase CCh stimulated I_{sc} responses and decrease Fsk stimulated I_{sc} responses, but these effects were not reproducible or statistically significant. Therefore these results suggest that chronic activation of FXR does not affect Calu-3 I_{sc}.

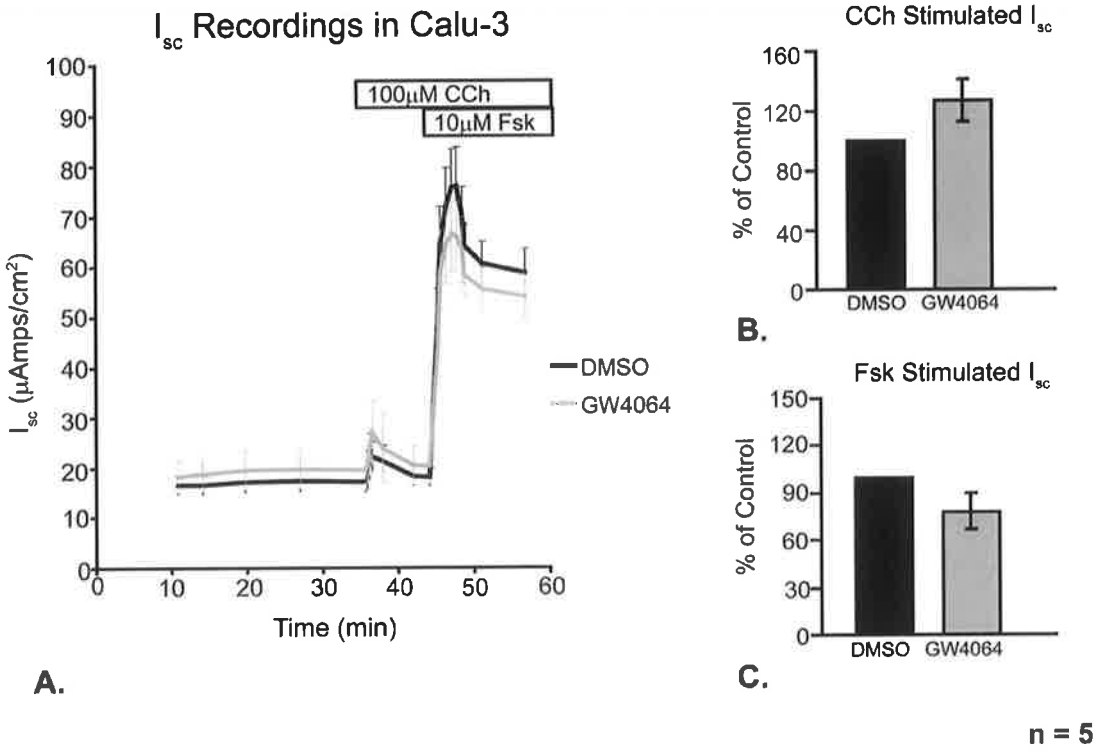

Fig.6.4 Chronic activation of FXR does not affect I_{sc} in Calu-3. A. I_{sc} values recorded during experiments with Calu-3 treated with 24hr GW4064 or DMSO. **B.** Change in I_{sc} values represented as % of control after CCh treatment. 24 hr GW4064 appeared to increase CCh stimulated responses by 26.8 ± 13.81 %, (p = 0.2, n = 5). **C.** Change in I_{sc} values represented as % of control after Fsk treatment. 24 hr GW4064 appeared to decrease Fsk stimulated responses by 21.8 ± 11.92 %, (p = 0.09, n = 5).

6-2.5 TDCA stimulation of I_{sc} is independent of FXR activation in Calu-3 cells.

In order to compare the effects of TDCA and GW4064 on Calu-3 I_{sc}, cells grown in ALI on Costar snapwells for 9 – 12 days, were mounted in Ussing chambers and the basal I_{sc} was recorded for 10 min prior to treatment of control and TDCA inserts with DMSO bilaterally. The I_{sc} was recorded for a further 10 min and allowed to stabilize before treatment with 5 μM GW4064 or 25 μM TDCA. Again, the I_{sc} was recorded and allowed to stabilize between subsequent 100 μM and 10 μM Fsk treatments. As shown in fig 6.5, pre-treatment with DMSO does not affect basal I_{sc} or the ability of TDCA to stimulate secretion, indicating that if TDCA was signalling through FXR,

GW4064 should also be able to induce secretion in Calu.-3. This result suggests that TDCA stimulation of I_{sc} is independent of FXR activation.

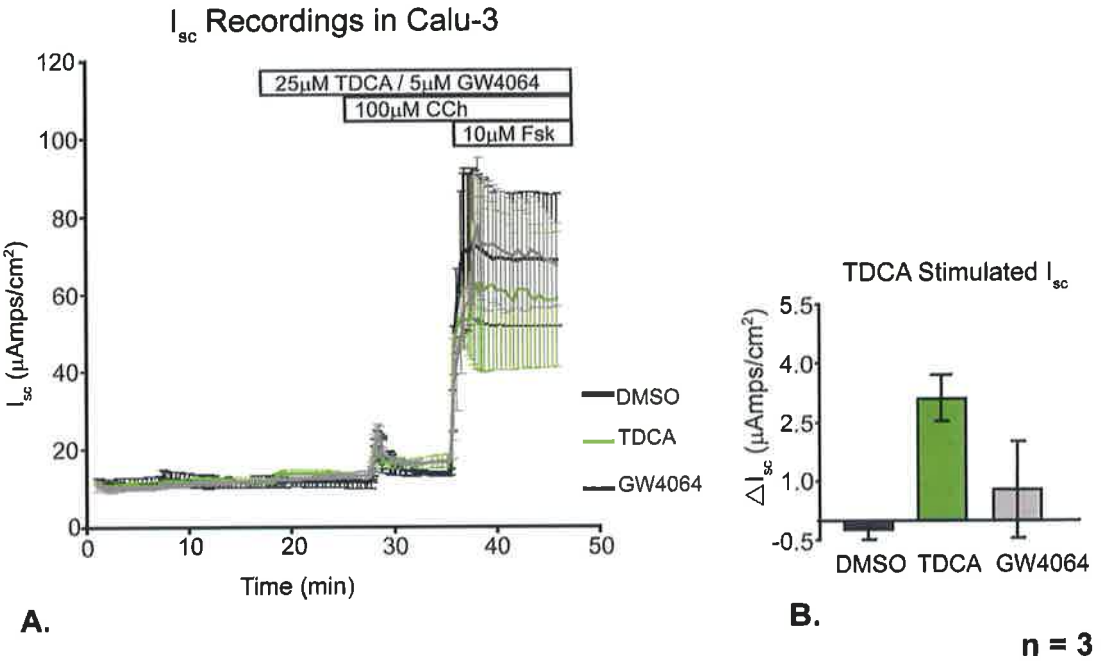

Fig.6.5 TDCA stimulates I_{sc} independently from FXR activation A. Mean ± SEM I_{sc} (μAmps/cm^2) values recorded during experiments with Calu-3 treated with 5 μM GW4064 , DMSO + TDCA or DMSO only. **B.** I_{sc} responses observed after TDCA / GW4064 treatment. The increases in basal I_{sc} by TDCA and GW4064 were 3.1 ± 0.6 (μAmps/cm^2), 0.8 ± 0.2 (μAmps/cm^2) respectively, compared with an oscillation of -0.3 ± 0.2 (μAmps/cm^2) for DMSO control over the course of the experiment (n = 3). TDCA or GW4064 pre-treatment did not affect subsequent CCh or Fsk induced responses.

6-2.6 TDCA does not acutely affect TGR5 expression in Calu-3 cells.

Having determined that acute activation of FXR does not affect secretion in Calu-3 cells, the focus of this research progressed to studying the involvement of TGR5 in TDCA stimulation airway Cl^- secretion. First TGR5 expression in Calu-3 cells needed to be confirmed, and the effect of acute treatment with TDCA on TGR5 abundance at the correct size band on Western blot membranes, was also investigated. Calu-3 cells grown on semi-permeable supports were treated basolaterally with 25 μM TDCA for 5 min before proteins were harvested and Western blot for TGR5 was performed as

described in chapter 2 (section 2-3). As shown in fig.6.6, Calu-3 cells express TGR5 and acute TDCA treatment does not appear to affect abundance of fully formed TGR5 in Calu-3 cells.

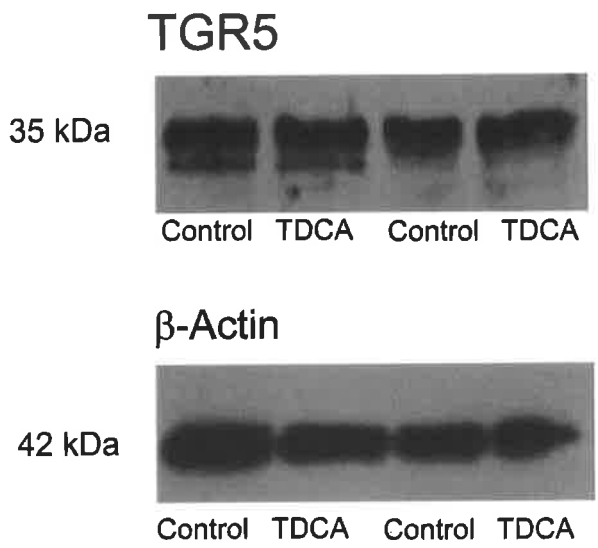

Fig.6.6 TDCA does not acutely affect TGR5 expression. Representative Western blot for TGR5 and β-actin in Calu-3. Acute treatment with TDCA does not affect abundance of fully formed TGR5, suggesting that TDCA does not interfere with TGR5 processing.

6-2.7 TGR5 siRNA knockdown effects on TGR5 expression in Calu-3 cells.

Since it had been established in our earlier studies that TDCA stimulates Cl^- secretion in Calu-3 cells via mobilization of cAMP and Ca^{2+}, we investigated the possible involvement of TGR5, which has been shown to induce signalling through increasing intracellular levels of cAMP and Ca^{2+}. To the best of our knowledge, since the discovery of TGR5 is relatively recent, specific inhibitors of TGR5 have not yet been identified. Although the synthetic ligand, INT777, has been described as a specific agonist for TGR5, it is not yet commercially available. In addition, although oleanolic acid and LCA are also known to be agonists for TGR5, it is unknown whether they exclusively activate TGR5 or whether they can also activate other bile acid receptors. In order to specifically investigate TGR5 involvement in TDCA stimulated Cl^- secretion, siRNA knockdown of TGR5 was performed, as described in detail in chapter 2

(section 2-8). Firstly the efficacy of the siRNA had to be determined. Three different transfection time points were selected- 24 hr, 48 hr and 72 hr, since the effect of siRNA knockdown by exogenous siRNA transfected into cells is transient in nature, usually appearing ~24 hr after transfection and lasting no longer than 72 hr post transfection.

Calu-3 cells were transfected with a mix of 3 different commercially available pre-designed TGR5 siRNAs (360 nM of each) to increase the efficiency of TGR5 knockdown. In addition, control cells were transfected with either negative siRNA or vector in each experiment. The Poly(ethyleneimine)-Poly(ethylene) glycol (PEI-PEG) vector developed by Hibbitts *et al* from RCSI school of Pharmacy was used as a transfection vector for these knockdown experiments, as it has been shown to increase siRNA nanoparticle uptake and luciferase knockdown in Calu-3 cells when compared with commercially available unmodified polyethyleneimine (PEI) (Hibbitts *et al.*, 2011). The concentration of vector used was determined by the ratio of the positively charged amine groups of the polymer (N) to the negatively charged phosphate groups of the nucleic acid (P), termed the N/P ratio. In general, the higher the N/P ratio, the more positively charged and smaller the nanoparticle containing the siRNA formed. N/P 15 was the highest concentration of vector with which Hibbitts *et al* observed efficient transfection of Calu-3 cells, and beyond this level, aggregation of particles and cell toxicity occurred. Therefore, N/P 15 was the first concentration of vector used in this study in order to increase transfection efficiencies of TGR5 siRNA.

After transfection of Calu-3 cells and incubation for 24-72 hr, proteins were harvested from cells and used for Western blot for TGR5 as described in chapter 2 (sections 2- 8 & 3). As shown in fig 6.7. 48 hr transfection decreased TGR5 relative intensity to 2.18 ± 0.07 AU compared with values of 2.72 ± 0.52 AU for negative siRNA or 2.73 ± 0.12 AU for vector only transfected cells (n = 3). This indicated that the combination of siRNAs used was specific for TGR5, and that 48 hr transfection of Calu-3 with TGR5 siRNA decreased TGR5 expression by ~20%. On the other hand, 24 hr or 72 hr transfections with TGR5 siRNA did not appear to affect TGR5 expression

levels. This is likely to be due to the transient nature of exogenous siRNA, which may only begin to interfere with TGR5 expression after 24 hr and regeneration of the TGR5 protein may be restored after 72 hr.

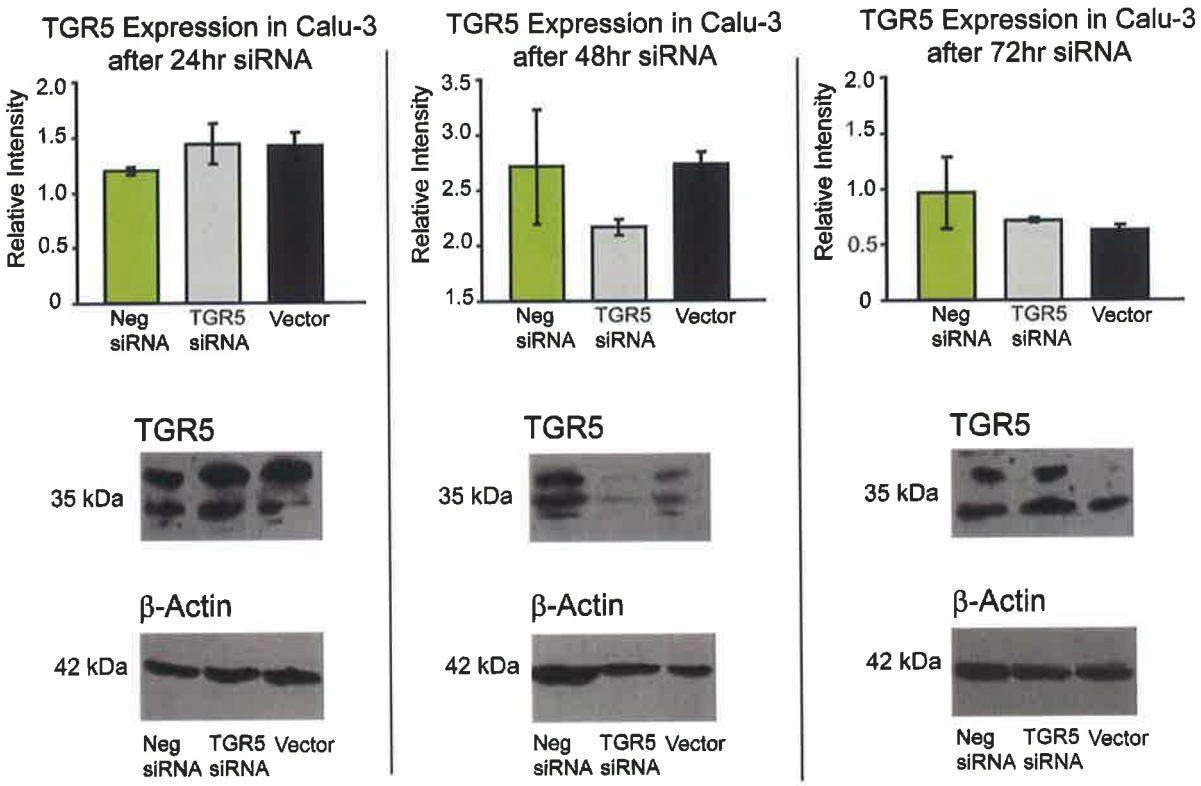

Fig.6.7 TGR5 siRNA knockdown effects on TGR5 expression in Calu-3 cells. Values represent relative quantity of TGR5, normalized to β-actin, after 24/48/72 hr transfection with neg siRNA, TGR5 siRNA or PEI-PEG vector only. Representative blots for each time point are shown underneath each graph. 24 or 72 hr transfections did not appear to affect TGR5 expression levels. However 48 hr transfection decreased TGR5 relative intensity to 2.18 ± 0.07 AU compared with values of 2.72 ± 0.52 AU for negative siRNA or 2.73 ± 0.12 AU for vector only transfected cells (n = 3).

TGR5 expression at the protein level alone was taken to represent knockdown efficiency and hence determine how effective transfection with siRNA had been. However, it would be beneficial to also measure the transfection efficiency by using fluorescently labelled siRNAs, that could then be visualised with microscopy in order to determine the % of cells that had

actually been successfully transfected with siRNA. By doing so, the optimal concentration of transfection vector required could easily be monitored.

6-2.8 High concentrations of PEI-PEG transfection vector is toxic to Calu-3 cells.

After determining that siRNA transfection with N/P 15 PEI-PEG appeared to knockdown TGR5 expression, the effect of TGR5 knockdown on TDCA stimulation of I_{sc} was investigated. Calu-3 cells that were grown on Costar snapwells, and transfected as described in the previous section for 24 or 48 hr using N/P 15 PEI-PEG as a transfection vector, were mounted in Ussing chambers and the basal I_{sc} was recorded. As shown in fig. 6.8 A, 24 hr transfection with N/P 15 PEI-PEG appears to be toxic to cells due to the large oscillations in basal I_{sc} observed during the experiment.

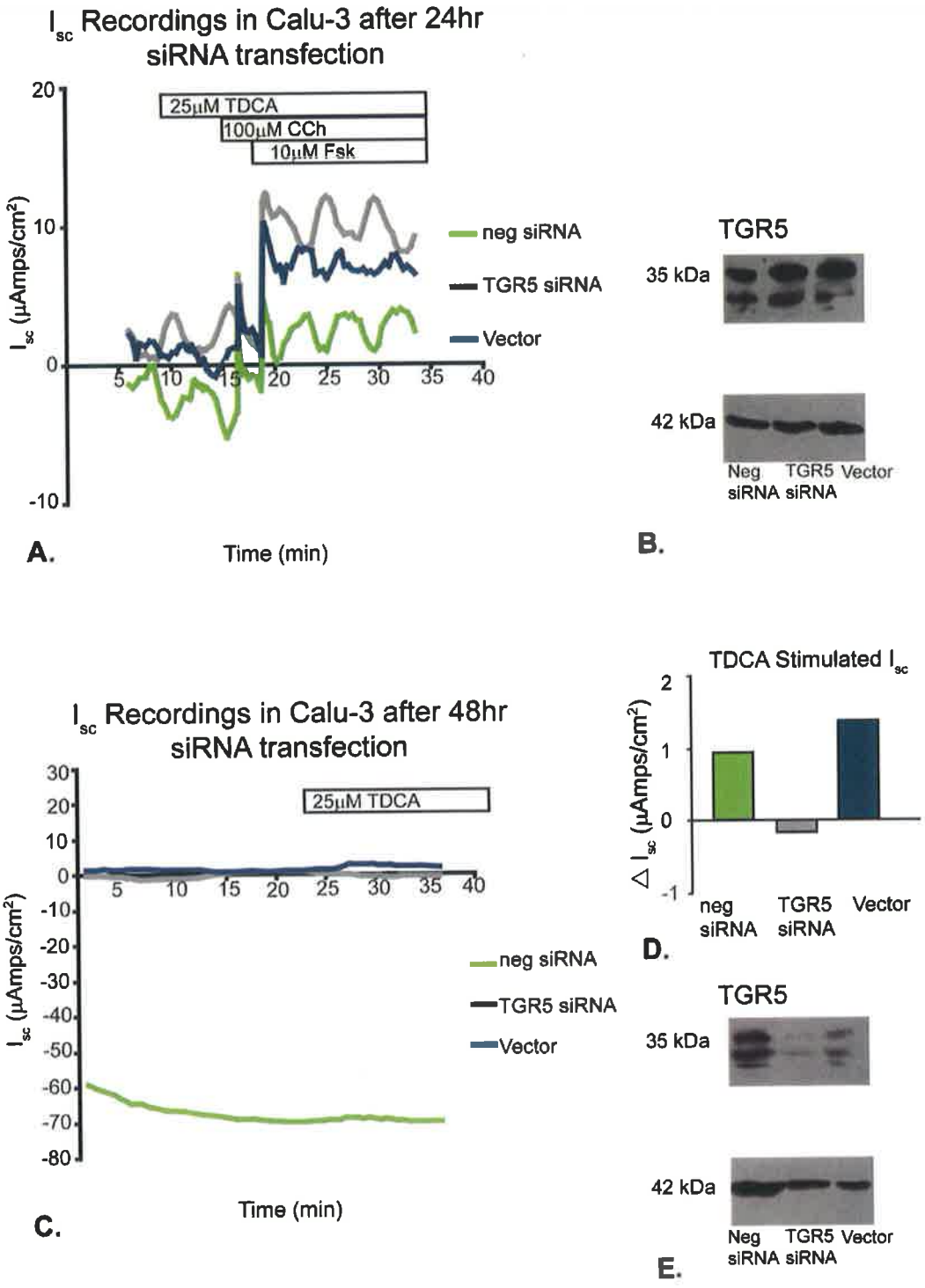

Fig.6.8. A high concentration of PEI-PEG transfection vector is toxic to cells. A, C Representative experiments showing I_{sc} recorded in Calu-3 cells after 24 hr or 48 hr transfection (n = 3). **B, E.** Representative Western blots of TGR5 and β-actin after 24 hr or 48 hr transfection (n = 3). **C.** I_{sc} responses observed after TDCA treatment in cells transfected for 48hrs. 24 hr transfection with N/P 15 PEI-PEG appears to be toxic to cells due to the large oscillations in basal I_{sc} observed during the experiment and failure to clamp the voltage of the epithelium to zero, indicating loss of integrity of the tissue. After 48 hr transfection with N/P 15

PEI-PEG, the basal I_{sc} is almost completely abolished due to loss of epithelial integrity as a result of vector toxicity to the cells. Although basal I_{sc} was almost abolished in these cells, TDCA appeared to increase basal I_{sc} by 0.94 or 1.38 (μAmps/cm^2) in the neg siRNA and vector only transfected cells respectively, while TDCA decreased I_{sc} by 0.16 (μAmps/cm^2) in the TGR5 siRNA transfected cells.

These oscillations occur as a result of failure to clamp the voltage of the epithelium to zero, indicating loss of integrity of the tissue. After 48 hr transfection with N/P 15 PEI-PEG, the basal I_{sc} was almost completely abolished due to loss of epithelial integrity resulting from vector toxicity to the cells, fig. 6.8 C. However, although basal I_{sc} was almost abolished in these cells, both the neg siRNA and vector only transfected cells appeared to respond to TDCA while the TGR5 siRNA transfected cells did not, which suggests that TDCA stimulation of I_{sc} correlated with TGR5 expression, fig 6.8 E. However, it was difficult to determine the contribution made to TDCA stimulation of I_{sc} under these conditions due to toxicity of the vector at this concentration. Therefore the vector concentration was reduced to a level where efficient delivery of siRNA into cells could occur, without inducing toxicity and disruption of the epithelial barrier function.

6-2.9 48hr TGR5 siRNA transfection decreases TGR5 expression and reduces TDCA stimulation of Cl^- secretion in Calu-3 cells.

Building on the results from the previous 2 sections, the siRNA transfections were repeated using a lower concentration of N/P 10 PEI-PEG for 48 hr. Calu-3 cells were transfected with 360 nM TGR5 siRNA mix, 360 nM neg siRNA, or N/P 10 PEI-PEG vector only for 48 hr and an untreated control was also included in these experiments. TEER was measured for each insert before transfection and again 48 hr post-transfection to monitor epithelial integrity and hence determine toxicity of the vector. Cells were then mounted in Ussing chambers and the basal I_{sc} was recorded for 5 min prior to treatment with 25 μM TDCA basolaterally and the I_{sc} was recorded for a further 5 - 10 min. After Ussing chamber experiments, proteins were immediately harvested and used for Western blot analysis of TGR5.

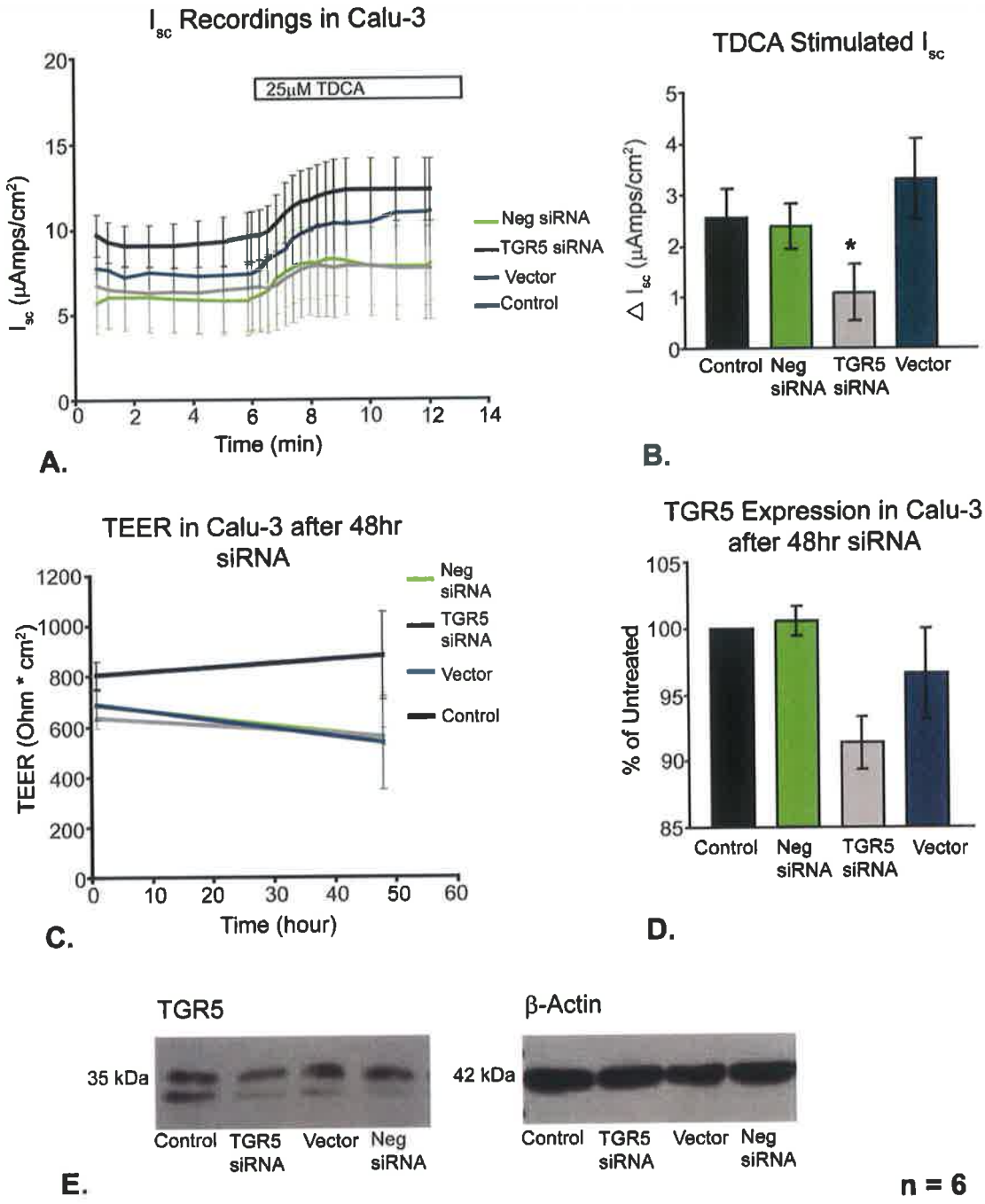

Fig.6.9 48hr TGR5 siRNA transfection using N/P 10 PEI-PEG attenuates TDCA stimulation of basal I_{sc}. **A.** I_{sc} values recorded during experiments with Calu-3 after 48 hr transfection **B.** I_{sc} responses observed in transfected cells after TDCA treatment. TDCA responses in Calu-3 cells treated with 360nM TGR5 siRNA for 48 hr were significantly reduced to 1.09 ± 0.56 (μAmps/cm^2), compared with the untreated control responses of 2.56 ± 0.56 (μAmps/cm^2) to TDCA (n = 6, p = 0.047). TDCA responses were 2.38 ± 0.45 (μAmps/cm^2) and 3.31 ± 0.79 (μAmps/cm^2) for negative siRNA or vector transfected cells respectively, which were similar to control values. **C.** 48 hr siRNA treatment of Calu-3 decreased in TEER by 130.7 ± 58.6, 74.7 ± 60.9, 154.4 ± 56.4 Ohm*cm^2 in neg siRNA, TGR5

siRNA and vector transfected cells respectively, while TEER increased by 75.6 ± 53.7 Ohm*cm^2 over the 48 hr period in the untreated control cells. This small reduction in TEER indicated that toxicity of the concentrations of PEI-PEG and siRNA used was low enough to maintain viability in the cells. **D.** TGR5 expression levels represented as % of untreated control after 48 hr transfection of Calu-3. 48hr treatment with TGR5 siRNA produced a 9 ± 2 % decrease in TGR5 expression indicating low levels of TGR5 knockdown had been induced. **E.** Representative Western blot for TGR5 and β-actin expression after 48hr transfection

As shown in fig 6.9 A & B, Calu-3 cells treated with 360 nM TGR5 siRNA for 48 hr showed significantly attenuated responses to TDCA, which were not seen with transfection of negative siRNA or vector alone, when compared with an untreated control, ($n = 6$, $p = 0.047$). Although TDCA responses after TGR5 siRNA transfection were smaller than those for cells transfected with negative siRNA or vector only, this decrease in I_{sc} was not statistically significant. According to the power calculations performed, it was determined that $n = 8$ would be required to establish whether TDCA stimulated I_{sc} was significantly attenuated in Calu-3 cells transfected with TGR5 siRNA for 48 hr compared with cells transfected with neg siRNA for 48 hr. In addition, the TEER was only slightly reduced in transfected cells after 48 hr, fig 6.9 C, indicating that N/P10 PEI-PEG was a suitably non-toxic concentration to use as a transfection vector. However, as can be seen in fig 6.9 D & E, 48 hr transfection with TGR5 siRNA only produced a 9 ± 2 % decrease in TGR5 expression when compared with control. This implies that although N/P10 PEI-PEG is less toxic than N/P15 PEI-PEG, delivery of siRNA is not as efficient. These results suggest that even a small reduction in TGR5 expression seems to result in attenuation of TDCA stimulated Cl^- secretion, but optimization of the transfection vector is required in order to confirm TGR5 involvement in this process.

6-3 Discussion

The primary aim of this chapter was to determine whether activation of FXR or TGR5 was involved in TDCA stimulation of Cl^- secretion in the airways. Having confirmed in chapter 5 that TDCA mobilizes Ca^{2+} and cAMP in Calu-3 cells, FXR and TGR5 appeared to be likely targets for activation by TDCA as both have previously been reported to increase intracellular Ca^{2+} in response to bile acid agonists (Kumar *et al.*, 2012, Düfer *et al.*, 2012b). In addition, activation of TGR5 is also known to increase intracellular cAMP (Kawamata *et al.*, 2003). Furthermore, both of these receptors have repeatedly been shown to participate in bile acid induced secretion in epithelial tissues (Keating and Keely, 2009b, Mroz *et al.*, 2013, Toumi *et al.*, 2011, Ward *et al.*, 2013, Keitel *et al.*, 2009). Although FXR is a nuclear receptor and therefore more likely to participate in chronic modulation of secretion though regulation of transcription, previous work carried out within our research group has shown that nuclear receptors, such as the estrogen receptor, can regulate epithelial ion transport independently of protein synthesis and gene transcription (Saint-Criq *et al.*, 2012).

In addition, it has been reported that acute activation of FXR by GW4064, the specific agonist for FXR, rapidly increased intracellular Ca^{2+} and regulated K_{ATP} channels in pancreatic β-cells (Düfer *et al.*, 2012b). This demonstrated that FXR activation can exert non-genomic effects, which was important for this investigation since TDCA stimulation of Cl^- secretion is an acute effect. In our study, GW4064 was shown to increase both the activity and the expression of FXR but had no effect on Calu-3 I_{sc} after chronic or acute treatment. Given that, under the same experimental conditions, parallel treatment with TDCA increased basal I_{sc} in Calu-3, while GW4064 treatment did not affect I_{sc}, this suggested that TDCA stimulation of I_{sc} was not through activation of FXR. In order to confirm this, further experiments using pre-treatment with guggulsterone, an antagonist for FXR, prior to TDCA treatment should be performed.

The focus of this investigation next turned to TGR5, which is known to be an important component of the bile acid signalling network. TGR5 expression was first confirmed in Calu-3 cells, and acute treatment with TDCA was shown not to affect abundance of TGR5 at the correct size band as analysed by Western blot, indicating that acute TDCA treatment does not appear to affect post-translational modification of TGR5. In order to determine the specific role for TGR5 in TDCA induced Cl^- secretion, TGR5 knockdown experiments were performed. TGR5 knockdown in gastric and oesophageal adenocarcinoma had previously been shown to significantly decrease TDCA induced cell proliferation, demonstrating that TDCA signals through TGR5 (Cao *et al.*, 2013, Hong *et al.*, 2010). In addition TGR5 knockout in mice has been shown to decrease bile acid induced Cl^- secretion through CFTR in the gall bladder epithelium (Keitel *et al.*, 2009). These studies supported our hypothesis that siRNA knockdown of TGR5 in Calu-3 cells would attenuate TDCA stimulation of Cl^- secretion.

For many years now, the commercially available synthetic PEI polymer has been used as a transfection vector, as PEI is known to complex and encapsulate any nucleic acid with which it interacts, due to its highly cationic nature. The higher the molecular weight of PEI used the more efficient the transfection. However, higher molecular weights of PEI are more cytotoxic. Recently, a new PEI transfection vector has been developed, PEI conjugated with polyethylene glycol (PEI-PEG), and this has been shown to reduce cytotoxicity and improve transfection efficiencies in Calu-3 cells (Hibbitts *et al.*, 2011). The initial attempt to knockdown TGR5 in this study employed both PEI and PEI-PEG as transfection vectors for delivery of siRNA to Calu-3 cells, using concentrations of both in the range N/P 7 – 15 and incubation times of 24 - 72hr. However, PEI-PEG was the only vector that appeared to induce TGR5 knockdown after siRNA transfection and so is the only data shown here. PEI was more toxic to Calu-3 than PEI-PEG, and no change in TGR5 expression was observed at any time-point after PEI transfection.

The results in this chapter indicate that the TGR5 siRNA mix employed in this study was specific for TGR5 and was capable of decreasing TGR5 expression

by ~20% after 48 hr, if delivered into the cells in high enough concentrations using N/P 15 PEI-PEG as a transfection vector. However this concentration of PEI-PEG was highly toxic to the cells and the effect of TGR5 knockdown on TDCA stimulation of I_{sc} could not be measured. Upon reduction of the PEI-PEG concentration to N/P 10, TGR5 expression was only reduced by ~ 9% after 48 hrs, indicating reduced transfection efficiencies. Despite an apparently small knockdown of TGR5 under these conditions, TDCA stimulation of I_{sc} was significantly reduced in TGR5 siRNA transfected cells compared to untreated control values, and also showed smaller responses to TDCA than neg siRNA or vector only transfected cells. This indicated that the reduction in TDCA stimulated I_{sc} was not entirely due to toxicity of the vector suggesting that reduced expression of TGR5 also appeared to reduce TDCA stimulation of I_{sc}.

However, as TGR5 expression appeared to only be reduced by ~ 9% using Western blot analysis, while the decrease in TDCA stimulated I_{sc} observed was almost 50% attenuation of control responses, the TDCA stimulated responses appeared disproportionate to knockdown levels. One possible explanation for this might be that TGR5 expression may begin to increase after 48hr siRNA transfection and appear on Western blot membranes showing total TGR5, but this newly synthesized TGR5 may not be properly processed to the membrane at this stage, and hence unable to interact with TDCA. However, a more detailed investigation into this processing of TGR5 would be required. In order to confirm TGR5 involvement in TDCA stimulation of I_{sc}, further optimization of the transfection vectors will be required, to increase TGR5 knockdown efficiencies. Furthermore, Ussing chamber experiments should be performed in non-transfected cells using parallel treatments with the TGR5 agonists OA and LCA, along with TDCA to determine if they stimulate basal I_{sc} in the same manner, which would suggest that activation of TGR5 is involved in TDCA stimulation of I_{sc}.

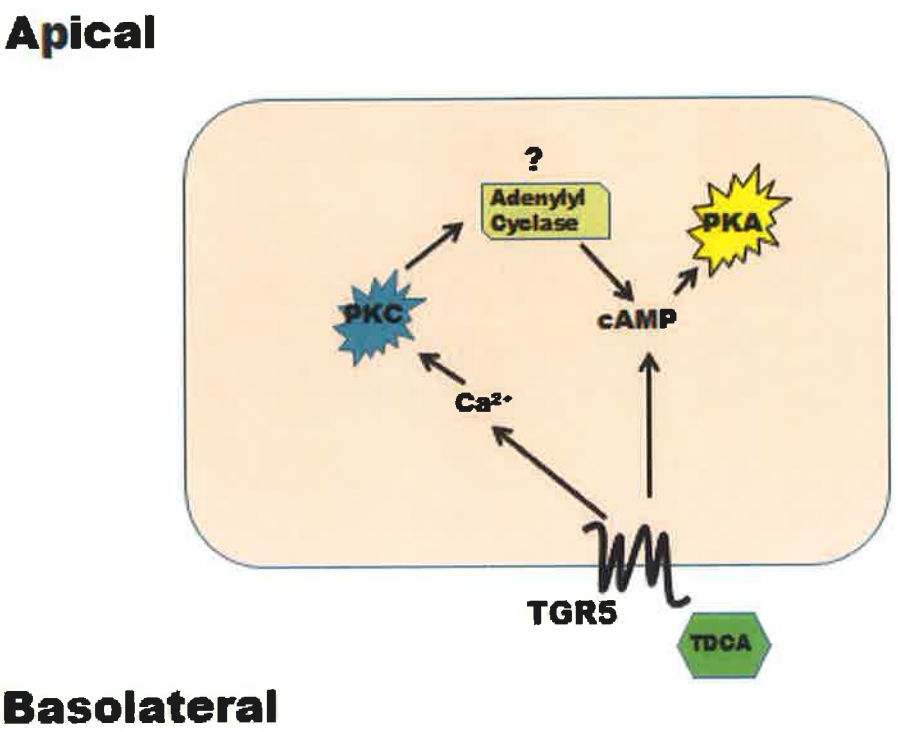

Fig.6.10. Proposed model of signalling by TDCA in airway epithelial cells. TDCA increases intracellular Ca^{2+} concentration, which stimulates Cl^- secretion through CaCC and can activate certain isoforms of PKC. Our data indicates that TDCA stimulation of secretion is dependent on PKC. PKC has been reported to regulate adenylyl cyclase production of cAMP. TDCA increases intracellular cAMP and PKA activity. PKA is known to activate CFTR and to regulate trafficking of Na^+/K^+ ATPase to the membrane. Due to the sidedness displayed by TDCA in stimulation of Cl^- secretion, it would appear that a basolateral membrane receptor is required for induction of TDCA signalling. Reduction of TGR5 expression through siRNA interference appears to attenuate secretory responses to TDCA, suggesting that TGR5 is the receptor involved in this process.

The results in this chapter indicate that activation of FXR is not required for TDCA stimulation of I_{sc} in Calu-3 cells but may implicate TGR5 activation in this process. From the TGR5 knockdown experiments performed here, it seems that even a small reduction in TGR5 expression can decrease TDCA stimulation of Cl^- secretion, suggesting that TGR5 is required for TDCA induced secretion. Given that in the previous chapters TDCA has been shown to increase intracellular Ca^{2+} and cAMP levels in addition to increasing the

activity of CFTR in Calu-3 cells, while TGR5 activation has previously been reported to be involved in these processes in other tissues (Keitel *et al.*, 2009, Kumar *et al.*, 2012), these findings support the TGR5 knockdown results shown here. The results presented in this chapter provide a starting point for further investigation into the role played by TGR5 in TDCA stimulation of airway Cl^- secretion and a more detailed assessment is required to confirm TGR5 involvement in this process.

Chapter 7

General discussion & Perspectives

7-1 General Discussion:

Emerging evidence from the literature over the past twenty years has indicated that bile acids are present in the lungs of patients with many different respiratory disorders. In turn, this has highlighted the need for an in-depth investigation into the role played by bile acids in the modulation of airway homeostasis. In 1997, total bile acids were shown to be elevated in the BAL from the lungs of infants under 12 months at autopsy after sudden infant death syndrome (Hills *et al.*, 1997). Since then bile acids have been associated with worsening prognosis of many conditions such as cystic fibrosis (CF), ventilator associated pneumonia (VAP), bronchiolitis obliterans syndrome (BOS), idiopathic pulmonary fibrosis (IPF) and respiratory distress syndrome (RDS) but no direct correlation between the two has yet been established (Zecca *et al.*, 2004, D'Ovidio *et al.*, 2005, Pauwels *et al.*, 2012, Savarino *et al.*, 2013, Zecca *et al.*, 2008). As discussed in chapter 1, bile acids may be aspirated into the lung during episodes of gastroesophageal reflux, or be taken up from the blood under conditions where circulating bile acids levels are increased. Evidence for both entry pathways has been reported and it has been shown that bile acid aspiration produces severe chemical pneumonitis in a porcine lung model, while injected bile acids have been shown to produce severe pulmonary edema in rabbits (Kaneko *et al.*,1990, Porembka *et al*, 1993, Perez *et al*, 2009)

To date, the majority of investigations of bile acids in the lung have focused on bile acid disruption of epithelial integrity via decay of junctional proteins, in addition to bile acid induced inflammatory responses or signalling pathways, thought to modulate airway fibrosis or BOS (Zhou *et al.*, 2013, Perng *et al.*, 2007, Su *et al.*, 2013). Furthermore, it has been shown that the presence of bile in the airways can lead to biofilm formation, which may be an important factor contributing to airway colonization by opportunistic microorganisms (Reen *et al.*, 2012). Since bile acids have been shown for many years to be potent modulators of epithelial ion transport in numerous different tissues, namely the colon and gallbladder, the primary goal of this thesis was to investigate whether bile acids could also affect secretion in the airways and to

improve our understanding of the mechanisms by which this process occurs (Ao *et al.*, 2013, Devor *et al.*, 1993, Dharmsathaphorn *et al.*, 1989, Fiorotto *et al.*, 2007, Keating and Keely, 2009a, Keely *et al.*, 2007, Kelly *et al.*, 2013).

As previously noted, the major challenge for this investigation was the lack of adequate reports in the literature to indicate the level of bile acids likely to be found in the lung, and also to identify the most abundant species of bile acid present. The bile acids selected for this study were DCA, UDCA and TDCA, while it was decided that the highest concentration of each bile acid used should be lower than 32 μM previously reported in BAL (D'Ovidio *et al.*, 2005), which would suggest physiological relevance of results. Furthermore, serum bile acid levels in fasting individuals have been reported to be in the range of 1-5 μM, but can increase rapidly upon ingestion of food or under certain conditions such as intrahepatic cholestasis of pregnancy (ICP), which occurs during late pregnancy. During ICP, circulating bile acid concentrations can reach 40 - 60 μM in the mother and 60 – 120 μM in the newborn (Zecca *et al.*, 2004, Zecca *et al.*, 2008, Keely *et al.*, 2010). Under these conditions bile acids in the airways are likely to have been taken up by from the blood.

The results presented in this thesis demonstrate that, at a concentration of 25 μM, each of the bile acids DCA, UDCA and TDCA were all able to modulate Calu-3 ion transport, in a structurally – specific and time-dependant manner. However the opposing secretory effect observed with DCA after chronic and acute incubations, or the absence of acute or chronic effects for UDCA and TDCA respectively, suggested that numerous different signalling pathways might have been involved in this process. Furthermore, TDCA was found to stimulate basal I_{sc} but had no effect on secretagogue induced secretion, while DCA and UDCA did not affect basal I_{sc} but did modulate I_{sc} responses to secretagogues in a time dependent manner, suggesting differential secretory mechanisms utilized by conjugated and unconjugated bile acids.

It is possible that one or more of these effects may have been induced through differential activation of a tyrosine receptor kinase such as the EGFR receptor, which is known to acutely inhibit and chronically stimulate colonic

CCh induced Cl^- secretion (Keely and Barrett, 2000, Mroz and Keely, 2012b, Uribe *et al.*, 1996). Furthermore, chronic activation of FXR has been shown to inhibit Cl^- secretion in the colon by decreasing CFTR expression (Mroz *et al.*, 2013). Therefore chronic treatment with UDCA might differentially regulate responses to CCh and Fsk by activation of both EGFR and FXR, while DCA might only act through EGFR. Of course there are many other types of receptor tyrosine kinases and bile acid receptors, such as fibroblast growth factor receptor (FGFR) and PXR, which could potentially also be responsible for transduction of DCA and UDCA signals. However, it not surprising that UDCA may elicit its effects through independent signalling mechanisms to DCA, since UDCA has been used in therapies aimed at reducing the pathological effects of other bile acids such as in treatments for ICP or gallstone disease where it decreases the toxicity of other bile acids (Guarino *et al.*, 2013).

In addition conjugated bile acids are known to be impermeable to cell membranes due to their size and charge and therefore it is likely that TDCA signals through a basolateral receptor, such as TGR5. Signalling through TGR5 usually results in rapid responses, while lower concentrations of taurine conjugated bile acids have been reported to activate TGR5 compared with unconjugated bile acids (Kawamata *et al.*, 2003). This may account for the acute stimulation of I_{sc} observed when TDCA was applied basolaterally, while DCA and UDCA did not appear to have a basolateral effect on secretion, at 25 μM concentration. Since TDCA was the only bile acid able to stimulate basal secretion in Calu-3 cells, the study focused on elucidation of the mechanisms by which TDCA stimulated airway secretion, in order provide a better insight into the physiological role played by bile acids in the modulation of airway epithelial ion transport, rather than the effects of bile acids on secretagogue - induced secretion. In addition, the majority of bile acids in circulation are conjugated bile acids and therefore there is a higher probability of conjugated bile acids, such as TDCA coming into contact with the airway epithelium.

In this thesis it was established that TDCA stimulated Cl^- secretion in Calu-3 cells without affecting TEER, indicating that the concentration of TDCA used in this study was non-toxic to the cells. It was also confirmed that TDCA stimulated Cl^- secretion though the transcellular pathway, rather than increasing paracellular permeability as had previously been reported for bile acids (Chen *et al.*, 2011, Su *et al.*, 2013). Elucidation of the ion transport proteins involved in this process demonstrated that acute TDCA treatment stimulated secretion by increasing the activity of CFTR, CaCC and Na^+/K^+ ATPase in Calu-3 cells. Furthermore TDCA also appeared to potentiate CFTR generated I_{sc} in NuLi-1 cells and appeared to increase basal I_{sc} in non-CF primary bronchial epithelium but more primary samples would be required to confirm this observation. In contrast TDCA did not seem to affect I_{sc} in CuFi-1 or CF primary cells. These investigations were important in order to establish whether the ion transport effects of TDCA were limited to the secretory cells of the airway SMGs or whether TDCA could also induce secretion in the surface epithelial cells. It would appear that TDCA was capable of modulating ion transport in each of the non-CF cells investigated here, and hence indicates that TDCA potentially modulates the secretory capacity of airway epithelial cells in general.

TDCA has previously been reported to stimulate Cl^- secretion via an IP_3 mediated release of intracellular Ca^{2+} and hence activate CaCC and K^+ channels, which seemed to partially explain the process by which TDCA stimulated secretion in Calu-3 cells (Devor *et al.*, 1993). However, due to the nature of regulation by CFTR, CaCC and Na^+/K^+ ATPase, it was apparent that more than one signaling molecule might be involved in this process, but that cross-talk between the different signaling molecules was likely to occur. It is well accepted that CFTR is activated by phosphorylation of its regulatory domain by PKA, which is dependent on intracellular cAMP. Furthermore, it has also been reported that cAMP/PKA regulates Na^+/K^+ ATPase trafficking to the membrane (Gonin *et al.*, 2001, Lecuona *et al.*, 2013). In addition to reports indicating that TDCA increases intracellular Ca^{2+}, it has also been shown that taurine conjugated bile acids potentiate adenylyl cyclase activity, and hence

increase intracellular cAMP, in a PKC dependent manner (Devor *et al.*, 1993, Chignard *et al.*, 2003).

I have demonstrated that TDCA stimulated secretion in Calu-3 cells is dependent on mobilization of intracellular Ca^{2+} and cAMP. A detailed investigation into TDCA mobilization of Ca^{2+} revealed that TDCA stimulated Ca^{2+} influx into the cell, which was in agreement with previously published data from colonic epithelial studies (Moschetta *et al.*, 2003, Dharmsathaphorn *et al.*, 1989). It was observed that TDCA increased PKA activity but inhibition of PKA by h89 did not affect TDCA stimulation of I_{sc}. This seemed to suggest that PKA was not involved in TDCA stimulation of Cl^- secretion. However, further investigation into the role played by PKA in this process will be required as h89 alone was shown to produce a large increase in intracellular Ca^{2+} in Calu-3 cells, which appeared to interfere with TDCA induced Ca^{2+} influx. H89 is an ATP-site inhibitor which blocks phosphorylation of PKA regulatory subunits but it has been previously reported that h89 may have non- specific effects on other protein kinases and SERCA (Hussain *et al.*, 1999, Yuan and Bers, 1995, Lee and Linstedt, 2000). Therefore, in order to confirm that PKA activity is involved in TDCA stimulation of secretion, these experiments would need to be repeated using a more specific inhibitor of PKA or a cAMP antagonist such as Rp-cAMPs, which prevents dissociation of the PKA holoenzyme (Boundy *et al.*, 1998).

In contrast, bisindolylmalemides have been reported to be highly selective inhibitors for the PKC family of enzymes (Wilkinson *et al.*, 1993), and in this thesis, pre-treatment with bis I appeared to attenuate TDCA stimulation of Cl^- secretion, implying that this process required activation of PKC. However, PKC involvement in this process needs to be confirmed, and further investigation of the role played by PKC, along with elucidation of the PKC isoforms activated by TDCA will be required. Nonetheless, data previously reported in the gall bladder that shows bile acid regulation of adenylyl cyclase is dependent on PKC would support these results (Chignard *et al.*, 2003). This suggests that cross-talk between TDCA induced increases in intracellular

Ca^{2+} and cAMP may be regulated by PKC, and hence that PKC activity might play a key role in bile acid induced secretion in the airways.

The findings that TDCA acutely increased intracellular Ca^{2+} and cAMP suggested that activation of TGR5, which has previously been reported to stimulate Cl^- secretion through elevation of Ca^{2+} and cAMP, might be involved in TDCA stimulated Cl^- secretion in this Calu-3 model (Keitel *et al.*, 2009, Kumar *et al.*, 2012, Ward *et al.*, 2013). Alternatively, it has also been reported that acute activation of FXR can modulate secretion by increasing intracellular Ca^{2+} levels (Düfer *et al.*, 2012b). Therefore, the role played by both of these receptors in Calu-3 ion transport was investigated in this thesis. My data indicated that GW4064, the specific agonist for FXR, was able to activate FXR and increase FXR expression in Calu-3 cells. However, neither acute nor chronic activation of FXR with GW4064 had any effect on either basal or secretagogue induced secretion in Calu-3 cells, indicating that FXR did not appear to be involved in TDCA stimulation of Cl^- secretion in this model. Furthermore, TGR5 knockdown experiments of Calu-3 cells demonstrated that 48hr post-transfection, I_{sc} responses to TDCA in cells transfected with TGR5 siRNA were attenuated, when compared with the TDCA stimulated I_{sc} responses in control, neg siRNA or vector transfected cells. These results implied that TGR5 was involved in TDCA stimulation of I_{sc}, however further optimization of these experiments would be required to confirm this finding. Higher levels of TGR5 knockdown, as assessed by Western blot, were achieved using increased concentrations of vector but this was correlated to elevated cell toxicity and as a result Ussing chamber experiments could not be performed. On the other hand, relatively low levels of TGR5 knockdown (~ 9%) were achieved when non-toxic concentrations of vector were used. This demonstrated that the siRNA used here was specific for TGR5 but that the transfection efficiencies needed to be improved, either by increasing the concentration of the vector slightly or by switching to another commercially available vector such as Lipofectamine 2000. In addition, Ussing chamber experiments of non-transfected cells treated in parallel with TDCA and the TGR5 agonists OA and LCA should also be performed to support TGR5 involvement in TDCA stimulation of Cl^- secretion. Nonetheless, even though

the level of TGR5 knockdown in these experiments was relatively low, attenuation of TDCA stimulated responses could still be observed. Therefore these experiments provide a good basis for further investigation of the role played by TGR5 in TDCA stimulation of airway Cl^- secretion.

Taken together the results presented in this thesis demonstrate that both conjugated and unconjugated bile acids modulate airway ion transport in a structure-sidedness and time dependent manner. Bile acids are well established mediators of epithelial ion transport, with much of this work having previously been performed in the colon (Ao *et al.*, 2013, Devor *et al.*, 1993, Keely *et al.*, 2007, Kelly *et al.*, 2013). However, reports have shown that the effects of bile acids vary depending on the concentration used and the nature of the tissue under investigation (Keating *et al.*, 2009, Venglovecz *et al.*, 2008, Chignard *et al.*, 2003). These differences in secretory responses to bile acids would appear to be physiologically relevant in tissues involved in digestion after consumption of a meal. Upon ingestion of food, increased secretion of bile acids and insulin by the gallbladder and pancreas would be required, while the primary role of the intestinal tract would be absorption of nutrients. However, bile acids are not known to play a physiological role in the lungs but rather induce pathophysiological effects. As the airway epithelium is both absorptive and secretory, and the concentration of bile acids in BAL have been reported to be in the range of 1- 32 μM (D'Ovidio *et al.*, 2005, Pauwels *et al.*, 2012), it was important to conduct a thorough investigation of the effects of bile acids on airway epithelial ion transport within this concentration range. Therefore this thesis is timely to bridge the gap between what was already known about bile acid regulation of epithelial ion transport in the literature, and the numerous reports indicating the presence of bile acids in the lung.

In this thesis, a model of the molecular mechanisms underlying TDCA stimulation of Cl^- secretion in airway epithelial cells is proposed for the first time, as shown in fig 7.1. TDCA increases the activity of CFTR, CaCC and Na^+/K^+ ATPase by elevating intracellular Ca^{2+} and cAMP levels in a PKC-dependent manner, which appears to be mediated by activation of TGR5.

This model shares similarities with previously published data from the colon and gallbladder demonstrating that activation of TGR5 by bile acids results in increased cAMP and Ca^{2+} production and hence increase Cl^- secretion through CaCC and CFTR (Ao *et al.*, 2013, Keitel *et al.*, 2009, Toumi *et al.*, 2011, Ward *et al.*, 2013). However, 2 important differences between bile acid-induced secretion in the colon and lung have been identified in this study. Firstly, although TDCA is capable of increasing intracellular Ca^{2+} in airway epithelium, TDCA does not affect the basal activity of basolateral K^+ channels, as had previously been reported in the colon (Devor *et al.*, 1993). This was surprising given that Calu-3 cells have previously been reported to express basolateral Ca^{2+}-activated K^+ channels that respond to apical stimulation of purinergic receptors (Wang *et al.*, 2008). Secondly, although Calu-3 cells express FXR that could be activated by GW4064, neither acute nor chronic activation of FXR had any effect on Calu-3 I_{sc}, which is in contrast to previous reports from colonic epithelium (Keating and Keely, 2009b, Mroz *et al.*, 2013). This suggests that FXR involvement in secretory responses in the airway may have become redundant to other more physiologically relevant mechanisms of ion transport regulation such as activation of purinergic receptors or channel activating receptors. FXR activation in the airway may contribute to innate immune responses or inflammation. Furthermore, these findings demonstrate how responses of intracellular signals such as Ca^{2+} and cAMP to bile acids vary across tissues and suggest that other intermediary factors such as PKA and PKC isoforms may be involved in these processes.

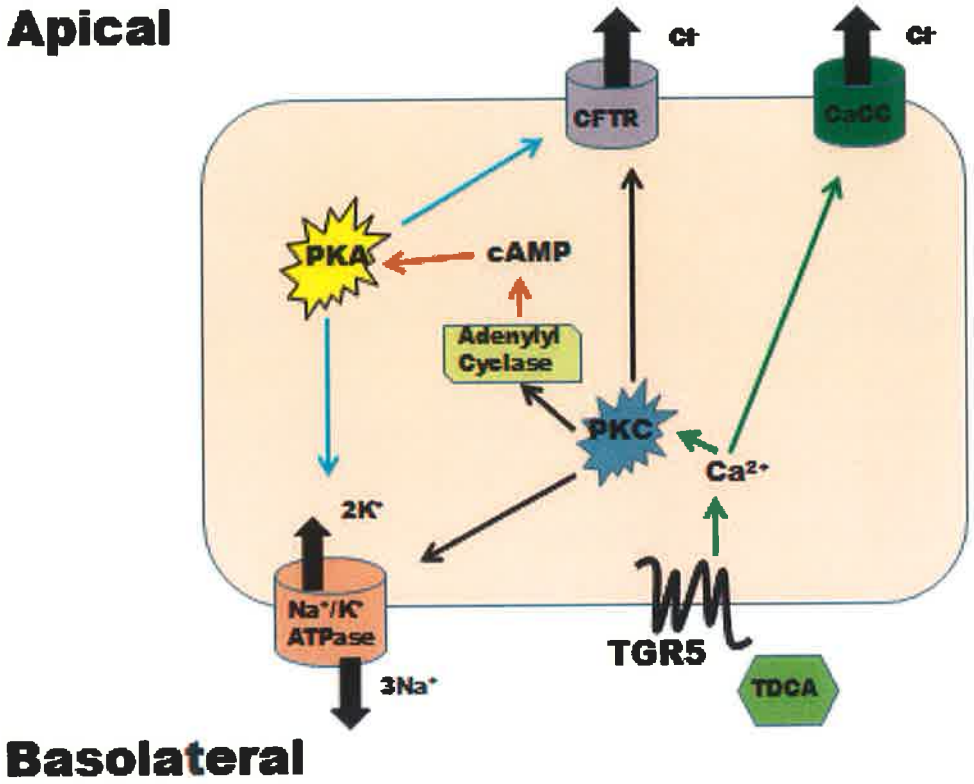

Fig.7.1. Proposed model of the molecular mechanisms underlying TDCA stimulated Cl^- secretion in airway epithelial cells. TDCA stimulates Cl^- secretion in airway epithelium by increasing the activity of CFTR, CaCC and Na^+/K^+ ATPase. TDCA increases intracellular Ca^{2+} concentration, which stimulates Cl^- secretion through CaCC and can activate certain isoforms of PKC. Our data indicate that TDCA stimulation of secretion is dependent on PKC. PKC has been reported to activate CFTR, Na^+/K^+ ATPase and regulate adenylyl cyclase production of cAMP. TDCA increases intracellular cAMP and PKA activity. PKA is known to activate CFTR and to regulate trafficking of Na^+/K^+ ATPase to the membrane. Due to the sidedness displayed by TDCA in stimulation of Cl^- secretion, it would appear that a basolateral membrane receptor is required for induction of TDCA signalling. Reduction of TGR5 expression through siRNA interference attenuates secretory responses to TDCA, suggesting that TGR5 is the receptor involved in this process.

This thesis provides novel insights into the molecular mechanisms of bile acid modulation of airway epithelial ion transport. The studies are important for improving our understanding of how bile acids, found in the lungs, can exacerbate airway pathology. Under physiological conditions in healthy lungs,

airway epithelial ion transport is tightly regulated to maintain an adequate level of ASL bathing the airway surfaces. ASL homeostasis is very important to airway defense by facilitating mucociliary clearance and hence removal of pathogens out of the lung. Bile acid modulation of ion transport may therefore disrupt ASL homeostasis and MCC, thus increasing the risk of airway infection. In the case of CF, where airways lack functional CFTR but Na^+ hyperabsorption through ENaC also occurs, bile acids may be capable of increasing Na^+/K^+ ATPase activity and hence increase the driving force for Na^+ absorption, to further reduce ASL and MCC.

Furthermore, bile acids interfering with the secretory capacity of developing airway epithelium in the foetus of ICP mothers may lead to the development of RDS in the new born infant. Bile acids have already been reported to enhance the activity of the inflammatory mediator, secretory phospholipase A2 (sPLA2), which is known to be a key enzyme in the development of lung injury due to surfactant dysfunction (De Luca *et al.*, 2009). In addition, GCDCA has recently been shown to inhibit surfactant secretion in rat alveolar epithelial type II cells (Zhangxue *et al.*, 2012). Over 20 years ago, it was reported that intra-tracheal injection of TCA could induce fatal pulmonary edema in rabbits and that subsequent injection with exogenous surfactant could prevent damage to the lung caused by bile acid induced edema (Kaneko *et al.*, 1990). These reports, together with the findings in this thesis, suggest that bile acids in the lung might perform a 'double hit' leading to the development of RDS and pulmonary edema. Firstly, bile acids may induce lung injury by inhibiting surfactant secretion, and secondly in the absence of adequate surfactant regulation, bile acids may increase fluid secretion in the lung leading to pulmonary edema.

Likewise, elevated levels of bile acids in the airway of the foetus may increase the secretory capacity of the lung immediately after birth, and possibly result in disruption of fluid clearance, which is critical to proper airway function in the newborn (Zecca *et al.*, 2008). CDCA has previously been reported to increase alveolar epithelial permeability as a result of decay of junctional proteins (Su *et al.*, 2013). Therefore, it is possible that a combination of TDCA and CDCA

in the lungs may lead to flooding of the airways by increasing both transcellular secretion and paracellular fluid transport in the airway epithelium, which might interfere with gas exchange in the alveoli. Furthermore, this may contribute to pancreatitis-associated lung injury, induced by TDCA, which is characterized by significant pulmonary edema and inflammatory infiltration of the alveoli (Xia *et al.*, 2010).

It is well-documented that inflammation causes disease by fluid shifts across cell membranes, which can often lead to changes in muscle function and generation of pain. Furthermore, inflammation and secretion are physiologically linked in their participation in airway defense. It has been proposed that pro-inflammatory cytokines, released in response to inhaled insults, stimulate secretion in order to increase the fluidity of the mucus layer and hence improve clearance of pathogens and particulate from the airway surface (Galietta *et al.*, 2004). Allergic inflammation of the airways was reported to produce a pro-secretory phenotype that was mediated by IL-13 and IL-4, in the bronchial epithelium of mice (Anagnostopoulou *et al.*, 2010). In terms of what is already known about the role played by bile acids contributing to airway pathology, it has been reported that CDCA increases IL-8 production in alveolar epithelial cells leading to development of VAP (Wu *et al.*, 2009), while IL-8 mediated neutrophilic airway inflammation has been implicated as a mechanism of bile acid induced BOS after lung transplantation (Vos *et al.*, 2008). In addition, CDCA, but not GCDCA, was shown to induce airway fibroblast proliferation by increasing p38-MAP kinase mediated TGF-β and CCN2 production (Perng *et al.*, 2007, Perng *et al.*, 2008).

More than 2 decades ago, it was speculated that intracellular accumulation of Ca^{2+} in airway epithelial cells was a contributing factor to airway pneumonitis (Oelberg *et al.*, 1990), and therefore this suggests a link between TDCA mobilization of Ca^{2+} in the airways presented in this thesis, and development of airway inflammation. One possible explanation for how our findings might correlate with previously published data, on bile acid induced inflammatory fibrosis in the lung, might come from a recent study in 2013, where it was

reported that the Ca^{2+} binding protein S100A9 promotes fibroblast proliferation in human embryo lung fibroblasts, via upregulation of IL-8, IL-6 and IL-1β production in an extracellular-regulated kinase (ERK) 1/2, MAP kinase, nuclear transcription factor (NF)-κB dependent process (Xu *et al.*, 2013). However, it has also been shown that TCDCA can help prevent airways fibrosis in mouse lungs by decreasing expression of TNF-α and increasing MMP9 expression (Zhou *et al.*, 2013), and therefore it is difficult to estimate the effect that TDCA would have on airway fibrosis, without further investigation. In addition, increased PLC β-3 induced intracellular Ca^{2+} signalling in CF bronchial cells has been reported to activate PKCα and PKCβ, leading to the activation of NF-κB and IL-8 production, resulting in excessive neutrophillic inflammation (Bezzerri *et al.*, 2011). Cross-talk between the inflammatory and secretory responses to bile acids may also occur through mobilization of cAMP as it has previously been reported that, in the SMG of pig models, TNF-α and IL-1β are capable of stimulating Cl^- secretion through CFTR in a cAMP dependent manner (Baniak *et al.*, 2012b). However, it has recently been shown that activation of CFTR and TMEM16A in CF airway epithelia attenuates IL-8 secretion and hence down regulates inflammation (Veit *et al.*, 2012), which based on the results presented in this thesis would suggest an anti-inflammatory role for TDCA in the airways.

These reports therefore suggest a link between TDCA modulation of Cl^- secretion and regulation of inflammatory molecules in the airways, which might be mediated through intracellular signalling of cAMP and Ca^{2+} but further investigation into the correlation between the two is required. Emerging evidence from the literature suggest that TGR5 is involved in modulation of immune response. It has been shown that activation of TGR5 results in cAMP- dependent attenuation of cytokine generation (Cipriani *et al.*, 2011). Furthermore, TGR5 had been reported to act as a negative regulator of inflammation by inhibiting the phosphorylation of NF-κB in mice (Wang *et al.*, 2011), which suggests that targeting of TGR5 shows promise as a therapeutic tool for inflammatory airway disease.

In conclusion, the data presented in this thesis demonstrate for the first time that low concentrations of bile acids in the airways modulate airway epithelial ion transport. In particular, TDCA stimulates Cl^- secretion by raising intracellular Ca^{2+} and cAMP levels through apparent activation of TGR5, which leads to increasing activity of CFTR, CaCC and Na^+/K^+ ATPase. These findings may be of benefit in instances of acute lung injury resulting in pulmonary edema or RDS in the newborn, where therapeutic inhibition of TGR5 might alleviate pathogenesis by inhibiting bile acid induced airway secretion. Furthermore, if TDCA is can increase ASL volume in CF airways by inducing secretion through CaCC, administration of TDCA or targeting of TGR5 may show some therapeutic promise in restoration of ASL volume in CF airways.

7-2 Perspectives:

In order to fully understand the impact of bile acids present in the lung on airway pathophysiology, a comprehensive investigation of the effects of bile acids on inflammatory mediators that contribute to conditions such as VAP and BOS would need to be performed, so that the relationship between bile acid modulation of ion transport and inflammation can be determined. Most importantly however, before any definitive role for bile acids participating in lung disease can be confirmed, a detailed characterization of the bile acids most commonly found in the airways needs to be performed. In addition, the exact concentration of bile acids present in the lungs also needs to be established, since bile acids often have opposing effects at low and high concentrations. Such studies will underscore the pathophysiological contribution made by bile acids in the airways.

Continuing on from the results presented in this thesis, it would be important to investigate whether the TDCA induced Cl^- secretion translates into increases in ASL height in human primary epithelial cells, and what effect TDCA has on ASL in CF tissues. These experiments would help determine the physiological relevance of bile acid induced secretion in the airways and whether bile acids will interfere with MCC or contribute to airway flooding. Furthermore, it will be interesting to see if TDCA decreases ASL due to activation of Na^+/K^+ ATPase in CF tissues, or if TDCA helps to restore ASL to 'normal' levels through activation of CaCC, which will hence determine whether TDCA exacerbates CF lung disease or may indicate that TDCA antagonism shows promise for therapeutic application.

Additionally, it will be essential to confirm the role played by TGR5 in TDCA signal transduction, as TGR5 may represent a therapeutic target for prevention of bile acid induced lung disease. Likewise, investigation of the role played by EGFR in the modulation of airway epithelial ion transport by DCA and UDCA may be important for improving our understanding of how the secretory responses to these bile acids differ in the airways.

Communications and Awards

Oral Presentations:

The 6th Annual Meeting of the Irish Epithelial Physiology Group, 25/10/13, Kilkenny, Ireland

Hendrick S, Greene CM, Keely SJ, Harvey BJ. Modulation of Cl^- Secretion by Bile Acids in Airway Epithelial Cells.

The Physiological Society Themed Meeting; Epithelia and Smooth Muscle Interactions in Health and Disease, 11/12/13, Dublin, Ireland

Hendrick S, Greene CM, Keely SJ, Harvey BJ. Modulation of Cl^- Secretion by Bile Acids in Airway Epithelial Cells.

Poster Presentations:

European Cystic Fibrosis Society Meeting 2012, 08/06/12, Dublin, Ireland

Hendrick S, Greene CM, Keely SJ, Harvey BJ. Modulation of Ion Secretion by Bile Acids in Calu-3 Airway Epithelial Cells.

Physiology 2012, 03/07/12, Edinburgh, UK

Hendrick S, Greene CM, Keely SJ, Harvey BJ. Modulation of Ion Secretion by Bile Acids in Calu-3 Airway Epithelial Cells.

'Emerging Treatments for Lung Disease' workshop, organised by The Royal Irish Academy Committee for Life Sciences, 07/09/12, Dublin, Ireland

Hendrick S, Greene CM, Keely SJ, Harvey BJ. Modulation of Ion Secretion by Bile Acids in Calu-3 Airway Epithelial Cells.

European Cystic Fibrosis Society Basic Science Meeting 2013, 21/03/13, Malaga, Spain

Hendrick S, Greene CM, Keely SJ, Harvey BJ. Bile Acid Modulation of Cl^- Secretion in Calu-3 Airway Epithelial Cells.

BIOPIC Meeting 2013, 25/03/13, Dublin, Ireland

Hendrick S, Greene CM, Keely SJ, Harvey BJ. Bile Acid Modulation of Cl^- Secretion in Calu-3 Airway Epithelial Cells.

International Union of Physiological Science (IUPS) Meeting 2013, 23/07/13, Birmingham, UK

Hendrick S, Greene CM, Keely SJ, Harvey BJ. Bile Acid Modulation of Cl^- Secretion in Calu-3 Airway Epithelial Cells.

The Physiological Society Themed Meeting; Epithelia and Smooth Muscle Interactions in Health and Disease, 11/12/13, Dublin, Ireland

Hendrick S, Greene CM, Keely SJ, Harvey BJ. Modulation of Cl^- Secretion by Bile Acids in Airway Epithelial Cells.

Publication:

American Journal of Physiology; Lung Cellular and Molecular Physiology

(Submitted 04/12/13)

Hendrick S, Greene CM, Keely SJ, Harvey BJ. Bile acids stimulate chloride secretion through CFTR and calcium-activated Cl^- channels in Calu-3 airway epithelial cells

Awards:

Travel Award from the Physiological Society £379 to attend Physiology 2012 Meeting 3-6 /07/12 in Edinburgh, UK.

Student Helper free registration and accommodation Award from the European Cystic Fibrosis Society to attend ECFS Basic Science 2013 Meeting 20-24/03/13 in Malaga, Spain.

Travel Award from the Physiological Society £500 to attend IUPS 2013 Meeting 21-26 /07/13 in Birmingham, UK

List of figures

List of tables

Bibliography

ABU-HAYYEH, S., PAPACLEOVOULOU, G. & WILLIAMSON, C. 2013. Nuclear receptors, bile acids and cholesterol homeostasis series - bile acids and pregnancy. *Mol Cell Endocrinol,* 368, 120-8.

ANAGNOSTOPOULOU, P., DAI, L., SCHATTERNY, J., HIRTZ, S., DUERR, J. & MALL, M. 2010. Allergic airway inflammation induces a pro-secretory epithelial ion transport phenotype in mice. *Eur Respir J,* 36, 1436-47.

ANDO, M., UTIDA, S. & NAGAHAMA, H. 1975. Active transport of chloride in eel intestine with special reference to sea water adaptation. *Comp Biochem Physiol A Comp Physiol* 51, 27-32.

AO, M., SARATHY, J., DOMINGUE, J., ALREFAI, W. & RAO, M. 2013. Chenodeoxycholic Acid Stimulates Cl- Secretion via cAMP Signaling and Increases Cystic Fibrosis Transmembrane Conductance Regulator Phosphorylation in T84 Cells. *Am J Physiol Cell Physiol,* E-pub ahead of print.

APODACA, G., GALLO, L. I. & BRYANT, D. M. 2012. Role of membrane traffic in the generation of epithelial cell asymmetry. *Nat Cell Biol,* 14, 1235-43.

ASANO, J., NIISATO, N., NAKAJIMA, K., MIYAZAKI, H., YASUDA, M., IWASAKI, Y., HAMA, T., DEJIMA, K., HISA, Y. & MARUNAKA, Y. 2009. Quercetin stimulates Na+/K+/2Cl- cotransport via PTK-dependent mechanisms in human airway epithelium. *Am J Respir Cell Mol Biol,* 41, 688-95.

ASEERI, A., BRODLIE, M., LORDAN, J., CORRIS, P., PEARSON, J., WARD, C. & MANNING, N. 2012. Bile acids are present in the lower airways of people with cystic fibrosis. *Am J Respir Crit Care Med,* 185, 463.

BALLARD, S. & INGLIS, S. 2004. Liquid secretion properties of airway submucosal glands. *J Physiol* 556, 1-10.

BALLARD, S. T., TROUT, L., GARRISON, J. & INGLIS, S. K. 2006. Ionic mechanism of forskolin-induced liquid secretion by porcine bronchi. *Am J Physiol Lung Cell Mol Physiol,* 290, L97-104.

BANIAK, N., LUAN, X., GRUNOW, A., MACHEN, T. & IANOWSKI, J. 2012a. The cytokines interleukin-1β and tumor necrosis factor-α stimulate CFTR-mediated fluid secretion by swine airway submucosal glands. *Am J Physiol Lung Cell Mol Physiol.,* 303, L327-33.

BANIAK, N., LUAN, X., GRUNOW, A., MACHEN, T. & IANOWSKI, J. 2012b. The cytokines interleukin-1β and tumor necrosis factor-α stimulate CFTR-mediated fluid secretion by swine airway submucosal glands. *Am J Physiol Lung Cell Mol Physiol.,* 303, L327-33.

BAUMAN, N., SANDLER, A. & ET, A. 1996. Respiratory manifestations of gastroesophageal reflux disease in pediatric patients. *Ann Otol Rhinol Laryngol,* 105, 23-32.

BEGENISICH, T. & MELVIN, J. 1998. Regulation of chloride channels in secretory epithelia. *J Membr Biol* 163, 77-85.

BEGUIN, P., BEGGAH, A. T., CHIBALIN, A. V., BURGENER-KAIRUZ, P., JAISSER, F., MATHEWS, P. M., ROSSIER, B. C., COTECCHIA, S. & GEERING, K. 1994. Phosphorylation of the Na,K-ATPase alpha-subunit by protein kinase A and C in vitro and in intact cells. Identification of a novel motif for PKC-mediated phosphorylation. *J Biol Chem,* 269, 24437-45.

BERTRAND, C. & FRIZZELL, R. 2003. The role of regulated CFTR trafficking in epithelial secretion. *Am J Physiol Cell Physiol. ,* 285, C1-18.

BEUERS, U. 1997. Effects of bile acids on hepatocellular signaling and secretion. *Yale J Biol Med. ,* 70, 341-6.

BEZZERRI, V., D'ADAMO, P., RIMESSI, A., LANZARA, C., CROVELLA, S., NICOLIS, E., TAMANINI, A., ATHANASAKIS, E., TEBON, M., BISOFFI, G., DRUMM, M., KNOWLES, M., PINTON, P., GASPARINI, P., BERTON, G. & CABRINI, G. 2011. Phospholipase C-β3 is a key modulator of IL-8 expression in cystic fibrosis bronchial epithelial cells. *J Immunol,* 186, 4946-58.

BHALLA, V. & HALLOWS, K. 2008. Mechanisms of ENaC regulation and clinical implications. *J Am Soc Nephrol* 19, 1845-54.

BILLET, A., LUO, Y., BALGHI, H. & HANRAHAN, J. W. 2013. Role of Tyrosine Phosphorylation in the Muscarinic Activation of the Cystic Fibrosis Transmembrane Conductance Regulator (CFTR). *J Biol Chem,* 288, 21815-23.

BILLINGTON, C. K. & HALL, I. P. 2012. Novel cAMP signalling paradigms: therapeutic implications for airway disease. *Br J Pharmacol,* 166, 401-10.

BLONDEAU, K., PAUWELS, A., DUPONT, L., MERTENS, V., PROESMANS, M., OREL, R., BRECELJ, J., LOPEZ-ALONSO, M., MOYA, M., MALFROOT, A., DE WACHTER, E., VANDENPLAS, Y., HAUSER, B. &

SIFRIM, D. 2010. Characteristics of gastroesophageal reflux and potential risk of gastric content aspiration in children with cystic fibrosis. *J Pediatr Gastroenterol Nutr,* 50, 161-6.

BONNY, O., CHRAIBI, A., LOFFING, J., JAEGER, N. F., GRUNDER, S., HORISBERGER, J. D. & ROSSIER, B. C. 1999. Functional expression of a pseudohypoaldosteronism type I mutated epithelial Na+ channel lacking the pore-forming region of its alpha subunit. *J Clin Invest,* 104, 967-74.

BORGSTROM, B., DAHLQVIST, A., LUNDH, G. & SJOVALL, J. 1957. Studies of intestinal digestion and absorption in the human. *J Clin Invest,* 36, 1521-36.

BOUNDY, V., CHEN, J. & NESTLER, E. 1998. Regulation of cAMP-dependent protein kinase subunit expression in CATH.a and SH-SY5Y cells. *J Pharmacol Exp Ther.,* 286, 1058-65.

BRAIMAN, A., ZAGOORY, O. & PRIEL, Z. 1998. PKA induces Ca^{2+} release and enhances ciliary beat frequency in a Ca^{2+}-dependent and -independent manner. *Am J Physiol,* 275, c790-7.

BUSUTTIL, A., MORE, I. A. & MCSEVENEY, D. 1977. A reappraisal of the ultrastructure of the human respiratory nasal mucosa. *J Anat,* 124, 445-58.

BUTTON, B., BOUCHER, R. & GROUP, U. O. N. C. V. L. 2008. Role of mechanical stress in regulating airway surface hydration and mucus clearance rates. *Respir Physiol Neurobiol,* 163, 189-201.

BUTTON, B., CAI, L. H., EHRE, C., KESIMER, M., HILL, D. B., SHEEHAN, J. K., BOUCHER, R. C. & RUBINSTEIN, M. 2012. A periciliary brush promotes the lung health by separating the mucus layer from airway epithelia. *Science,* 337, 937-41.

CAO, W., TIAN, W., HONG, J., LI, D., TAVARES, R., NOBLE, L., MOSS, S. & RESNICK, M. 2013. Expression of bile acid receptor TGR5 in gastric adenocarcinoma. *Am J Physiol Gastrointest Liver Physiol.* , 304, g322-7.

CAPUTO, A., CACI, E., FERRERA, L., PEDEMONTE, N., BARSANTI, C., SONDO, E., PFEFFER, U., RAVAZZOLO, R., ZEGARRA-MORAN, O. & GALIETTA, L. J. 2008. TMEM16A, a membrane protein associated with calcium-dependent chloride channel activity. *Science,* 322, 590-4.

CARSON, M., TRAVIS, S. & WELSH, M. 1995. The two nucleotide-binding domains of cystic fibrosis transmembrane conductance regulator (CFTR) have distinct functions in controlling channel activity. *J Biol Chem* 270, 1711-7.

CHAMBERS, L., ROLLINS, B. & TARRAN, R. 2007. Liquid movement across the surface epithelium of large airways. *Respir Physiol Neurobiol* 159, 256-70.

CHEN, X., OSHIMA, T., TOMITA, T., FUKUI, H., WATARI, J., MATSUMOTO, T. & MIWA, H. 2011. Acidic bile salts modulate the squamous epithelial barrier function by modulating tight junction proteins. *Am J Physiol Gastrointest Liver Physiol,* 301, G203-9.

CHENG, S. H., RICH, D. P., MARSHALL, J., GREGORY, R. J., WELSH, M. J. & SMITH, A. E. 1991. Phosphorylation of the R domain by cAMP-dependent protein kinase regulates the CFTR chloride channel. *Cell,* 66, 1027-36.

CHIGNARD, N., MERGEY, M., VEISSIÈRE, D., POUPON, R., CAPEAU, J., PARC, R., PAUL, A. & HOUSSET, C. 2003. Bile salts potentiate adenylyl cyclase activity and cAMP-regulated secretion in human gallbladder epithelium. *Am J Physiol Gastrointest Liver Physiol.,* 284, G205-12.

CIARDIELLO, F. & TORTORA, G. 1998. Interactions between the epidermal growth factor receptor and type I protein kinase A: biological significance and therapeutic implications. *Clin Cancer Res,* 4, 821-8.

CIPRIANI, S., MENCARELLI, A., CHINI, M. G., DISTRUTTI, E., RENGA, B., BIFULCO, G., BALDELLI, F., DONINI, A. & FIORUCCI, S. 2011. The bile acid receptor GPBAR-1 (TGR5) modulates integrity of intestinal barrier and immune response to experimental colitis. *PLoS One,* 6, e25637.

CLAUDEL, T., STAELS, B. & KUIPERS, F. 2005. The Farnesoid X receptor: a molecular link between bile acid and lipid and glucose metabolism. *Arterioscler Thromb Vasc Biol.,* 25, 2020-30.

COLLINS, F. S. 1992. Cystic fibrosis: molecular biology and therapeutic implications. *Science,* 256, 774-9.

COYNE, C., VANHOOK, M., GAMBLING, T., CARSON, J., BOUCHER, R. & JOHNSON, L. 2002. Regulation of airway tight junctions by proinflammatory cytokines. *Mol Biol Cell,* 13, 3218-34.

CRYSTAL, R. G., RANDELL, S. H., ENGELHARDT, J. F., VOYNOW, J. & SUNDAY, M. E. 2008. Airway epithelial cells: current concepts and challenges. *Proc Am Thorac Soc,* 5, 772-7.

CUTHBERT, A., SUPURAN, C. & MACVINISH, L. 2003. Bicarbonate-dependent chloride secretion in Calu-3 epithelia in response to 7,8-benzoquinoline. *J Physiol,* 551, 79-92.

D'OVIDIO, F., MURA, M. & ET, A. 2005. Bile acid aspiration and the development of bronchiolitis obliterans after lung transplantation. *J Thorac Cardiovasc Surg,* 129, 1144-52.

D'OVIDIO, F., MURA, M., RIDSDALE, R., TAKAHASHI, H., WADDELL, T., HUTCHEON, M., HADJILIADIS, D., SINGER, L., PIERRE, A., CHAPARRO, C., GUTIERREZ, C., MILLER, L., DARLING, G., LIU, M., POST, M. & KESHAVJEE, S. 2006. The effect of reflux and bile acid aspiration on the lung allograft and its surfactant and innate immunity molecules SP-A and SP-D. *Am J Transplant,* 6, 1930-8.

DAVIS, C. & DICKEY, B. 2008. Regulated airway goblet cell mucin secretion. *Annu Rev Physiol,* 70.

DAWSON, A. M. 1967. Bile salts and fat absorption. *Gut,* 8, 1-3.

DE LUCA, D., MINUCCI, A., ZECCA, E., PIASTRA, M., PIETRINI, D., CARNIELLI, V., ZUPPI, C., TRIDENTE, A., CONTI, G. & CAPOLUONGO, E. 2009. Bile acids cause secretory phospholipase A2 activity enhancement, revertible by exogenous surfactant administration. *Intensive Care Med.* , 35, 321-6.

DE POITIERS, W., LORD, P. W., BILES, B. & WHIMSTER, W. F. 1980. Bronchial gland histochemistry in lungs removed for cancer. *Thorax,* 35, 546-51.

DE ROOIJ, J., ZWARTKRUIS, F., VERHEIJEN, M., COOL, R., NIJMAN, S., WITTINGHOFER, A. & BOS, J. 1998. Epac is a Rap1 guanine-nucleotide-exchange factor directly activated by cyclic AMP. *Nature,* 396, 474-7.

DEVOR, D., SEKAR, M., FRIZZELL, R. & DUFFEY, M. 1993. Taurodeoxycholate activates potassium and chloride conductances via an IP3-mediated release of calcium from intracellular stores in a colonic cell line (T84). *J Clin Invest,* 92, 2173-81.

DEVOR, D. C., SINGH, A. K., LAMBERT, L. C., DELUCA, A., FRIZZELL, R. A. & BRIDGES, R. J. 1999. Bicarbonate and chloride secretion in Calu-3 human airway epithelial cells. *J Gen Physiol,* 113, 743-60.

DHARMSATHAPHORN, K., HUOTT, P., VONGKOVIT, P., BEUERLEIN, G., PANDOL, S. & AMMON, H. 1989. Cl^- Secretion Induced by Bile Salts: A Study of the Mechanism of Action Based on a Cultured Colonic Epithelial Cell Line. *J Clin Invest,* 84, 945-953.

DÜFER, M., HÖRTH, K., KRIPPEIT-DREWS, P. & DREWS, G. 2012a. The significance of the nuclear farnesoid X receptor (FXR) in β cell function. *Islets,* 4, 333-8.

DÜFER, M., HÖRTH, K., WAGNER, R., SCHITTENHELM, B., PROWALD, S., WAGNER, T., OBERWINKLER, J., LUKOWSKI, R., GONZALEZ, F., KRIPPEIT-DREWS, P. & DREWS, G. 2012b. Bile acids acutely stimulate insulin secretion of mouse β-cells via farnesoid X receptor activation and K(ATP) channel inhibition. *Diabetes,* 61, 1479-89.

EISENHUT, M. & WALLACE, H. 2011. Ion channels in inflammation. *Pflugers Arch,* 461, 401-21.

ELMEDAL, L., MULVANY, M. & SIMONSEN, U. 2006. Involvement of guanylyl cyclase, protein kinase A and Na+ K+ ATPase in relaxations of bovine isolated bronchioles induced by GEA 3175, an NO donor. *Pulm Pharmacol Ther.,* 19, 179-88.

ENGELHARDT, J. F., YANKASKAS, J. & ET, A. 1992. Submucosal glands are the predominant site of CFTR expression in the human bronchus. *Nat Genet* 2, 240-8.

FACTOR, P. 2001. Role and regulation of lung Na+/K+-ATPase. *Cell Mol Biol,* 47, 347-61.

FARQUHAR, M. & PALADE, G. 1963. Junctional complexes in various epithelia. *J Cell Biol* 17, 375-412.

FINKBEINER, W. E., ZLOCK, L. T., MEHDI, I. & WIDDICOMBE, J. H. 2010. Cultures of human tracheal gland cells of mucous or serous phenotype. *In Vitro Cell Dev Biol Anim,* 46, 450-6.

FIOROTTO, R., SPIRLÌ, C., FABRIS, L., CADAMURO, M., OKOLICSANYI, L. & STRAZZABOSCO, M. 2007. Ursodeoxycholic acid stimulates cholangiocyte fluid secretion in mice via CFTR-dependent ATP secretion. *Gastroenterology,* 133, 1603-13.

FISCHER, A. J., GOSS, K. L., SCHEETZ, T. E., WOHLFORD-LENANE, C. L., SNYDER, J. M. & MCCRAY, P. B., JR. 2009. Differential gene expression in human conducting airway surface epithelia and submucosal glands. *Am J Respir Cell Mol Biol,* 40, 189-99.

FRIZZELL, R. A., RECHKEMMER, G. & SHOEMAKER, R. L. 1986. Altered regulation of airway epithelial cell chloride channels in cystic fibrosis. *Science,* 233, 558-60.

FU, L., RAB, A., TANG, L., ROWE, S., BEBOK, Z. & COLLAWN, J. 2012. Dab2 is a key regulator of endocytosis and post-endocytic trafficking of the cystic fibrosis transmembrane conductance regulator. *Biochem J,* 441, 633-43.

FUNG, J., YUE, G., FUNG, K., MA, X., YAO, X. & KO, W. 2011. Cordyceps militaris extract stimulates Cl(-) secretion across human bronchial epithelia by both Ca(2+)(-) and cAMP-dependent pathways. *J Ethnopharmacol.,* 138, 201-11.

GALIETTA, L., FOLLI, C., CACI, E., PEDEMONTE, N., TADDEI, A., RAVAZZOLO, R. & ZEGARRA-MORAN, O. 2004. Effect of inflammatory stimuli on airway ion transport. *Proc Am Thorac Soc.* , 1, 62-5.

GARCIA-VERDUGO, I., DESCAMPS, D., CHIGNARD, M., TOUQUI, L. & SALLENAVE, J. M. 2010. Lung protease/anti-protease network and modulation of mucus production and surfactant activity. *Biochimie,* 92, 1608-17.

GARNETT, J., HICKMAN, E., TUNKAMNERDTHAI, O., CUTHBERT, A. & GRAY, M. 2013. Protein phosphatase 1 coordinates CFTR-dependent airway epithelial HCO_3^- secretion by reciprocal regulation of apical and basolateral membrane Cl^--HCO_3^- exchangers. *Br J Pharmacol.* , 168, 1946-60.

GEERING, K. 2001. The functional role of beta subunits in oligomeric P-type ATPases. *J Bioenerg Biomembr* 33, 425-38.

GENTZSCH, M., DANG, H., DANG, Y., GARCIA-CABALLERO, A., SUCHINDRAN, H., BOUCHER, R. C. & STUTTS, M. J. 2010. The cystic fibrosis transmembrane conductance regulator impedes proteolytic stimulation of the epithelial Na+ channel. *J Biol Chem,* 285, 32227-32.

GÖNCZI, M., PAPP, H., BÍRÓ, T., KOVÁCS, L. & CSERNOCH, L. 2002. Effect of protein kinase C on transmembrane calcium fluxes in HaCaT keratinocytes. *Exp Dermatol,* 11, 25-33.

GONIN, S., DESCHÊNES, G., ROGER, F., BENS, M., MARTIN, P., CARPENTIER, J., VANDEWALLE, A., DOUCET, A. & FÉRAILLE, E. 2001. Cyclic AMP increases cell surface expression of functional Na,K-

ATPase units in mammalian cortical collecting duct principal cells. *Mol Biol Cell,* 12, 255-64.

GREEN, K. J. & JONES, J. C. R. 1996. Desmosomes and hemidesmosomes: structure and function of molecular components. *FASEB J,* 10, 871-81.

GREENWOOD, I. A., YEUNG, S. Y., HETTIARACHI, S., ANDERSSON, M. & BAINES, D. L. 2009. KCNQ-encoded channels regulate Na+ transport across H441 lung epithelial cells. *Pflugers Arch,* 457, 785-94.

GRUNDER, S., MULLER, A. & ET, A. 2001. Developmental and cellular expression pattern of epithelial sodium channel alpha, beta and gamma subunits in the inner ear of the rat. *Eur J Neurosci* 13, 641-8.

GRYNKIEWICZ, G., POENIE, M. & TSIEN, R. Y. 1985. A new generation of Ca2+ indicators with greatly improved fluorescence properties. *J Biol Chem,* 260, 3440-50.

GUARINO, M., COCCA, S., ALTOMARE, A., EMERENZIANI, S. & CICALA, M. 2013. Ursodeoxycholic acid therapy in gallbladder disease, a story not yet completed. *World J Gastroenterol,* 19, 5029-34.

HAAS, M. 1989. Properties and diversity of (Na-K-Cl) cotransporters. *Annu Rev Physiol* 51, 443-57.

HAAS, M. & FORBUSH, B. 2000. The Na-K-Cl cotransporter of secretory epithelia. *Annu Rev Physiol* 62, 27-32.

HALLOWS, K. R., KOBINGER, G. P., WILSON, J. M., WITTERS, L. A. & FOSKETT, J. K. 2003. Physiological modulation of CFTR activity by AMP-activated protein kinase in polarized T84 cells. *Am J Physiol Cell Physiol,* 284, C1297-308.

HAN, F., BOSSUYT, J., MARTIN, J., DESPA, S. & BERS, D. 2010. Role of phospholemman phosphorylation sites in mediating kinase-dependent regulation of the Na+-K+-ATPase. *Am J Physiol Cell Physiol.,* 229, c1363-9.

HARRIS, M., GARCIA-CABALLERO, A., STUTTS, M. J., FIRSOV, D. & ROSSIER, B. C. 2008. Preferential assembly of epithelial sodium channel (ENaC) subunits in Xenopus oocytes: role of furin-mediated endogenous proteolysis. *J Biol Chem,* 283, 7455-63.

HARVEY, B. J. 1995. Cross-talk between sodium and potassium channels in tight epithelia. *Kidney Int* 48, 1191-9.

HARVEY, B. J. & EHRENFELD, J. 1988. Role of Na+/H+ exchange in the control of intracellular pH and cell membrane conductances in frog skin epithelium. *J Gen Physiol,* 92, 793-810.

HATTRUP, C. & GENDLER, S. 2008. Structure and function of the cell surface (tethered) mucins. *Annu Rev Physiol* 70, 431-57.

HIBBITTS, A., LIEGGI, N., MCCABE, O., THOMAS, W., BARLOW, J., O'BRIEN, F. & CRYAN, S. 2011. Screening of siRNA nanoparticles for delivery to airway epithelial cells using high-content analysis. *Ther Deliv.* , 2, 987-99.

HILLS, B., CHEN, Y., MASTERS, I. & HILLS, Y. 1997. Raised bile acid concentrations in SIDS lungs at necropsy. *Arch Dis Child.* , 77, 120-3.

HOFMANN, A. 1999a. Bile Acids: The Good, the Bad, and the Ugly *News Physiol Sci* 14, 24-29.

HOFMANN, A. 1999b. The Continuing Importance of Bile Acids in Liver and Intestinal Disease. *Arch Intern Med,* 159, 2647-2658.

HOLT, J. A., LUO, G., BILLIN, A. N., BISI, J., MCNEILL, Y. Y., KOZARSKY, K. F., DONAHEE, M., WANG, D. Y., MANSFIELD, T. A., KLIEWER, S. A., GOODWIN, B. & JONES, S. A. 2003. Definition of a novel growth factor-dependent signal cascade for the suppression of bile acid biosynthesis. *Genes Dev,* 17, 1581-91.

HONG, J., BEHAR, J., WANDS, J., RESNICK, M., WANG, L., DELELLIS, R., LAMBETH, D., SOUZA, R., SPECHLER, S. & CAO, W. 2010. Role of a novel bile acid receptor TGR5 in the development of oesophageal adenocarcinoma. *Gut,* 59, 170-80.

HOWE, K., GAULDIE, J. & MCKAY, D. 2002. TGF-beta effects on epithelial ion transport and barrier: reduced Cl^- secretion blocked by a p38 MAPK inhibitor. *Am J Physiol Cell Physiol,* 283, C1667-74.

HUANG, F., ZHANG, H., WU, M., YANG, H., KUDO, M., PETERS, C. J., WOODRUFF, P. G., SOLBERG, O. D., DONNE, M. L., HUANG, X., SHEPPARD, D., FAHY, J. V., WOLTERS, P. J., HOGAN, B. L., FINKBEINER, W. E., LI, M., JAN, Y. N., JAN, L. Y. & ROCK, J. R. 2012a. Calcium-activated chloride channel TMEM16A modulates mucin secretion and airway smooth muscle contraction. *Proc Natl Acad Sci U S A,* 109, 16354-9.

HUANG, J., SHAN, J., KIM, D., LIAO, J., ALPER, S. & HANRAHAN, J. 2012b. Basolateral Cl^- loading by the anion exchanger type 2: role in fluid secretion by the human airway epithelial cell line Calu-3. *J Physiol,* 590, 5299-316.

HUSSAIN, M., DRAGO, G., BHOGAL, M., COLYER, J. & ORCHARD, C. 1999. Effects of the protein kinase A inhibitor H-89 on Ca^{2+} regulation in isolated ferret ventricular myocytes. *Pflugers Arch.,* 437, 529-37.

HYDE, S. C., EMSLEY, P., HARTSHORN, M. J., MIMMACK, M. M., GILEADI, U., PEARCE, S. R., GALLAGHER, M. P., GILL, D. R., HUBBARD, R. E. & HIGGINS, C. F. 1990. Structural model of ATP-binding proteins associated with cystic fibrosis, multidrug resistance and bacterial transport. *Nature,* 346, 362-5.

INOUE, M., KISHIMOTO, A., TAKAI, Y. & NISHIZUKA, Y. 1977. Studies on a cyclic nucleotide-independent protein kinase and its proenzyme in mammalian tissues. II. Proenzyme and its activation by calcium-dependent protease from rat brain. *J Biol Chem,* 252, 7610-6.

ITANI, O. A., CHEN, J. & ET, A. 2011. Human cystic fibrosis airway epithelia have reduced Cl- conductance but not increased Na+ conductance. *Proc Natl Acad Sci USA,* 108, 10260-5.

JAYARAMAN, S., SONG, Y., VETRIVEL, L., SHANKAR, L. & VERKMAN, A. 2001. "Noninvasive in vivo fluorescence measurement of airway-surface liquid depth, salt concentration, and pH.". *J Clin Invest,* 107, 317-324.

JIA, Y., MATHEWS, C. & HANRAHAN, J. 1997. Phosphorylation by protein kinase C is required for acute activation of cystic fibrosis transmembrane conductance regulator by protein kinase A. *J Biol Chem,* 272, 4978-84.

JIN, S. L., RICHARD, F. J., KUO, W. P., D'ERCOLE, A. J. & CONTI, M. 1999. Impaired growth and fertility of cAMP-specific phosphodiesterase PDE4D-deficient mice. *Proc Natl Acad Sci U S A,* 96, 11998-2003.

JORGENSEN, P. & PEDERSEN, P. 2001. Structure-function relationships of Na(+), K(+), ATP, or Mg(2+) binding and energy transduction in Na,K-ATPase. *Biochim Biophys Acta* 1505, 57-74.

KANCHANAPOO, J., AO, M., PRASAD, R., MOORE, C., KAY, C., PIYACHATURAWAT, P. & RAO, M. 2007. Role of protein kinase C-delta in the age-dependent secretagogue action of bile acids in mammalian colon. *Am J Physiol Cell Physiol.,* 293, C1851-61.

KANEKO, T., SATO, T., KATSUYA, H. & MIYAUCHI, Y. 1990. Surfactant therapy for pulmonary edema due to intratracheally injected bile acid. *Crit Care Med.,* 18, 77-83.

KAPLAN, J. & HOLLIS, R. 1980. External Na dependence of ouabain-sensitive ATP:ADP exchange initiated by photolysis of intracellular caged-ATP in human red cell ghosts. *Nature,* 288, 587-9.

KAPLAN, J. H. 2002. Biochemistry of Na,K-ATPase. *Annu Rev Biochem,* 71, 511-35.

KAPPLER, M., ESPACH, C., SCHWEIGER-KABESCH, A., LANG, T., HARTL, D., HECTOR, A., GLASMACHER, C. & GRIESE, M. 2012. Ursodeoxycholic acid therapy in cystic fibrosis liver disease--a retrospective long-term follow-up case-control study. *Aliment Pharmacol Ther.,* 36, 266-73.

KAUER, W., PETERS, J., DEMEESTER, T., FEUSSNER, H., IRELAND, A., STEIN, H. & SIEWERT, R. 1997. Composition and concentration of bile acid reflux into the esophagus of patients with gastroesophageal reflux disease. *Surgery* 122, 874-81.

KAWAMATA, Y., FUJII, R., HOSOYA, M., HARADA, M., YOSHIDA, H., MIWA, M., FUKUSUMI, S., HABATA, Y., ITOH, T., SHINTANI, Y., HINUMA, S., FUJISAWA, Y. & FUJINO, M. 2003. A G protein-coupled receptor responsive to bile acids. *J Biol Chem,* 278, 9435-40.

KEATING, N. & KEELY, S. 2009a. Bile acids in regulation of intestinal physiology. *Curr Gastroenterol Rep* 11, 375-82.

KEATING, N. & KEELY, S. 2009b. W1663 Farnesoid X Receptor Activation Downregulates Chloride Secretion in Colonic Epithelial Cells. *Gastroenterology,* 136, a172-3.

KEATING, N., MROZ, M., SCHARL, M., MARSH, C., FERGUSON, G., HOFMANN, A. & KEELY, S. 2009. Physiological concentrations of bile acids down-regulate agonist induced secretion in colonic epithelial cells. *J Cell Mol Med* 13, 2293-303.

KEELY, S. & BARRETT, K. 2000. Regulation of chloride secretion. Novel pathways and messengers. *Ann N Y Acad Sci.,* 915, 67-78.

KEELY, S. J. 2010. Missing link identified: GpBAR1 is a neuronal bile acid receptor. *Neurogastroenterol Motil* 22, 711-7.

KEELY, S. J., SCHARL, M. M., BERTELSEN, L. S., HAGEY, L. R., BARRETT, K. E. & HOFMANN, A. F. 2007. Bile acid-induced secretion in polarized monolayers of T84 colonic epithelial cells: Structure-activity relationships. *Am J Physiol Gastrointest Liver Physiol,* 292, G290-7.

KEITEL, V., CUPISTI, K., ULLMER, C., KNOEFEL, W., KUBITZ, R. & HÄUSSINGER, D. 2009. The membrane-bound bile acid receptor TGR5 is localized in the epithelium of human gallbladders. *Hepatology,* 50, 861-70.

KELLY, O., MROZ, M., WARD, J., COLLIVA, C., SCHARL, M., PELLICCIARI, R., GILMER, J., FALLON, P., HOFMANN, A., RODA, A., MURRAY, F. & KEELY, S. 2013. Ursodeoxycholic acid attenuates colonic epithelial secretory function. *J Physiol,* 1, 2307-18.

KEREM, E., BISTRITZER, T., HANUKOGLU, A., HOFMANN, T., ZHOU, Z., BENNETT, W., MACLAUGHLIN, E., BARKER, P., NASH, M., QUITTELL, L., BOUCHER, R. & KNOWLES, M. R. 1999. Pulmonary epithelial sodium-channel dysfunction and excess airway liquid in pseudohypoaldosteronism. *N Engl J Med,* 341, 156-62.

KHEIFETS, V. & MOCHLY-ROSEN, D. 2007. Insight into intra- and inter-molecular interactions of PKC: design of specific modulators of kinase function. *Pharmacol Res,* 55, 467-76.

KIM, K. 2012. Role of epithelial mucins during airway infection. *Pulm Pharmacol Ther.*

KIRK, K. & DAWSON, D. 1983. Basolateral potassium channel in turtle colon. Evidence for single-file ion flow. *J Gen Physiol,* 82, 297-329.

KNOWLES, M. & BOUCHER, R. 2002. Mucus clearance as a primary innate defense mechanism for mammalian airways. *J Clin Invest* 109, 571-7.

KNOWLES, M. R., CLARKE, L. L. & BOUCHER, R. C. 1991. Activation by extracellular nucleotides of chloride secretion in the airway epithelia of patients with cystic fibrosis. *N Engl J Med,* 325, 533-8.

KONSTAS, A., KOCH, J. & KORBMACHER, C. 2003. cAMP-dependent activation of CFTR inhibits the epithelial sodium channel (ENaC) without affecting its surface expression. *Pflugers Arch,* 445, 513-21.

KUMAR, D., RAJAGOPAL, S., MAHAVADI, S., MIRSHAHI, F., GRIDER, J., MURTHY, K. & SANYAL, A. 2012. Activation of transmembrane bile acid

receptor TGR5 stimulates insulin secretion in pancreatic β cells. *Biochem Biophys Res Commun.,* 427, 600-5.

KUNZELMANN, K. & MEHTA, A. 2013. CFTR: a hub for kinases and cross-talk of cAMP and Ca^{2+}. *FEBS J,* [Epub ahead of print.

KUNZELMANN, K., TIAN, Y., MARTINS, J., FARIA, D., KONGSUPHOL, P., OUSINGSAWAT, J., WOLF, L. & SCHREIBER, R. 2012. Airway epithelial cells-Functional links between CFTR and anoctamin dependent Cl(-) secretion. *Int J Biochem Cell Biol* 44, 1897-1900.

KUWADA, S., LUND, K., LI, X., CLIFTEN, P., AMSLER, K., OPRESKO, L. & WILEY, H. 1998. Differential signaling and regulation of apical vs. basolateral EGFR in polarized epithelial cells. *Am J Physiol,* 275, c1419-28.

LAMBRECHT, B. & HAMMAD, H. 2012. The airway epithelium in asthma. *Nat Med* 18, 684-92.

LAU, B., COLELLA, M., RUDER, W., RANIERI, M., CURCI, S. & HOFER, A. 2005. Deoxycholic acid activates protein kinase C and phospholipase C via increased Ca2+ entry at plasma membrane. *Gastroenterology,* 128, 695-707.

LECUONA, E., MININ, A., TREJO, H., CHEN, J., COMELLAS, A., SUN, H., GRILLO, D., NEKRASOVA, O., WELCH, L., SZLEIFER, I., GELFAND, V. & SZNAJDER, J. 2009. Myosin-Va restrains the trafficking of Na+/K+-ATPase-containing vesicles in alveolar epithelial cells. *J Cell Sci,* 122, 3915-22.

LECUONA, E., SUN, H., CHEN, J., TREJO, H., BAKER, M. & SZNAJDER, J. 2013. Protein kinase A-Iα regulates Na,K-ATPase endocytosis in alveolar epithelial cells exposed to high CO(2) concentrations. *Am J Respir Cell Mol Biol.* , 48, 626-34.

LEDSON, M., TRAN, J. & ET, A. 1998. Prevalence and mechanisms of gastro-oesophageal reflux in adult cystic fibrosis patients. *J R Soc Med* 91, 7-9.

LEE, M., PENLAND, C., WIDDICOMBE, J. H. & WINE, J. J. 1998. Evidence that Calu-3 human airway cells secrete bicarbonate. *Am J Physiol,* 274, L450-3.

LEE, T. & LINSTEDT, A. 2000. Potential role for protein kinases in regulation of bidirectional endoplasmic reticulum-to-Golgi transport revealed by protein kinase inhibitor H89. *Mol Biol Cell,* 11, 2577-90.

LEW, J., ZHAO, A., YU, J., HUANG, L., DE PEDRO, N., PELÁEZ, F., WRIGHT, S. & CUI, J. 2004. The farnesoid X receptor controls gene expression in a ligand- and promoter-selective fashion. *J Biol Chem,* 279, 8856-61.

LI, J., PIRCHER, P., SCHULMAN, I. & WESTIN, S. 2004. Regulation of Complement C3 Expression by the Bile Acid Receptor FXR. *J Biol Chem,* 280, 7427-34.

LI, W., CHEN, W., MA, Y., TUO, Q., LUO, X., ZHANG, T., SAI, W., LIU, J., SHEN, J., LIU, Z., ZHENG, Y., WANG, Y., JI, G. & LIU, Q. 2012. Methods to measure and analyze ciliary beat activity: Ca^{2+} influx-mediated cilia mechanosensitivity. *Pflugers Arch.,* 464, 671-80.

LIEDTKE, C. M., WANG, X. & SMALLWOOD, N. D. 2005. Role for protein phosphatase 2A in the regulation of Calu-3 epithelial Na+-K+-2Cl-, type 1 co-transport function. *J Biol Chem,* 280, 25491-8.

LIONETTO, M. & SCHETTINO, T. 2006. The Na+-K+-2Cl- cotransporter and the osmotic stress response in a model salt transport epithelium. *Acta Physiol (Oxf,* 187, 115-24.

LIU, Q., ZHENG, Y., KORDE, A., YADAV, V., RATHORE, R., WESS, J. & WANG, Y. 2009. Membrane depolarization causes a direct activation of G protein-coupled receptors leading to local Ca^{2+} release in smooth muscle. *Proc Natl Acad Sci U S A.* , 106, 11418-23.

LIU, X., DRISKELL, R. R. & ENGELHARDT, J. F. 2004. Airway glandular development and stem cells. *Curr Top Dev Biol,* 64, 33-56.

LOMBARDO, L., FOTI, M., RUGGIA, O. & CHIECCHIO, A. 2010. Increased incidence of small intestinal bacterial overgrowth during proton pump inhibitor therapy. *Clin Gastroenterol Hepatol,* 8, 504-8.

LORENZO, I., LIEDTKE, W., SANDERSON, M. & VALVERDE, M. 2008. TRPV4 channel participates in receptor-operated calcium entry and ciliary beat frequency regulation in mouse airway epithelial cells. *Proc Natl Acad Sci U S A.* , 105, 12611-6.

MACVINISH, L., COPE, G., ROPENGA, A. & CUTHBERT, A. 2007. Chloride transporting capability of Calu-3 epithelia following persistent knockdown of the cystic fibrosis transmembrane conductance regulator, CFTR. *Br J Pharmacol.,* 150, 1055-65.

MAKISHIMA, M., OKAMOTO, A. Y., REPA, J. J., TU, H., LEARNED, R. M., LUK, A., HULL, M. V., LUSTIG, K. D., MANGELSDORF, D. J. & SHAN, B. 1999. Identification of a nuclear receptor for bile acids. *Science,* 284, 1362-5.

MALL, M., GRUBB, B. & ET, A. 2004. Increased airway epithelial Na+ absorption produces cystic fibrosis-like lung disease in mice. *Nat Med* 10, 487-93.

MANZANARES, D., GONZALEZ, C. & ET, A. 2011. Functional apical large conductance, Ca2+-activated, and voltage-dependent K+ channels are required for maintenance of airway surface liquid volume. *J Biol Chem,* 286, 19830-9.

MARUYAMA, T., MIYAMOTO, Y., NAKAMURA, T., TAMAI, Y., OKADA, H., SUGIYAMA, E., ITADANI, H. & TANAKA, K. 2002. Identification of membrane-type receptor for bile acids (M-BAR). *Biochem Biophys Res Commun,* 298, 714-9.

MATHIA, N., TIMOSZYK, J., STETSKO, P., MEGILL, J., SMITH, R. & WALL, D. 2002. Permeability characteristics of calu-3 human bronchial epithelial cells: in vitro-in vivo correlation to predict lung absorption in rats. *J Drug Target.* , 10, 31-40.

MATSUI, H., GRUBB, B., TARRAN, R., RANDELL, S., GATZY, J., DAVIS, C. & BOUCHER, R. 1998. Evidence for periciliary liquid layer depletion, not abnormal ion composition, in the pathogenesis of cystic fibrosis airways disease. *Cell,* 95, 1005-15.

MCNAMARA, B., WINTER, D. C., CUFFE, J. E., O'SULLIVAN, G. C. & HARVEY, B. J. 1999. Basolateral K+ channel involvement in forskolin-activated chloride secretion in human colon. *J Physiol,* 519 Pt 1, 251-60.

MEKJIAN, H., PHILLIPS, S. & HOFMANN, A. 1971. Colonic secretion of water and electrolytes induced by bile acids: perfusion studies in man. *J Clin Invest,* 50, 1569-77.

MEYRICK, B., STURGESS, J. M. & REID, L. 1969. A reconstruction of the duct system and secretory tubules of the human bronchial submucosal gland. *Thorax,* 24, 729-36.

MICHNOFF, C., DE LA HOUSSAYE, B. & MASARACCHIA, R. 1983. Kinetics of adenosine 3':5'-monophosphate-dependent protein kinase activation and inhibition of thymidine incorporation into DNA in P1798 lymphosarcoma cells. *Cancer Res,* 43, 3514-20.

MIDTVEDT, T. 1974. Microbial bile acid transformation. *Am J Clin Nutr* 27, 1341-7.

MIKOSHIBA, K. 2007. IP3 receptor/Ca2+ channel: from discovery to new signaling concepts. *J Neurochem,* 102, 1426-46.

MIZUTANI, T., MORISE, M., ITO, Y., HIBINO, Y., MATSUNO, T., ITO, S., HASHIMOTO, N., SATO, M., KONDO, M., IMAIZUMI, K. & HASEGAWA, Y. 2012. Nongenomic effects of fluticasone propionate and budesonide on human airway anion secretion. *Am J Respir Cell Mol Biol.,* 47, 645-51.

MOBASHERI, A., ERRINGTON, R. J., GOLDING, S., HALL, A. C. & URBAN, J. P. 1997. Characterization of the Na+, K(+)-ATPase in isolated bovine articular chondrocytes; molecular evidence for multiple alpha and beta isoforms. *Cell Biol Int,* 21, 201-12.

MONTE, M., MARIN, J., ANTELO, A. & VAZQUEZ-TATO, J. 2009. Bile acids: chemistry, physiology, and pathophysiology. *World J Gastroenterol,* 15, 804-16.

MONTE, M., ROSALES, R., MACIAS, R., IANNOTA, V., MARTINEZ-FERNANDEZ, A., ROMERO, M., HOFMANN, A. & MARIN, J. 2008. Cytosol-nucleus traffic and colocalization with FXR of conjugated bile acids in rat hepatocytes. *Am J Physiol Gastrointest Liver Physiol. ,* 295, g54-g62.

MOSCHETTA, A., PORTINCASA, P., DEBELLIS, L., PETRUZZELLI, M., MONTELLI, R., CALAMITA, G., GUSTAVSSON, P. & PALASCIANO, G. 2003. Basolateral Ca^{2+}-dependent K^{+}-channels play a key role in Cl^{-} secretion induced by taurodeoxycholate from colon mucosa. *Biol Cell,* 95, 155-22.

MROZ, M., KEATING, N., WARD, J., SARKER, R., AMU, S., AVIELLO, G., DONOWITZ, M., FALLON, P. & KEELY, S. 2013. Farnesoid X receptor agonists attenuate colonic epithelial secretory function and prevent experimental diarrhoea in vivo. *Gut,* Epub ahead of print.

MROZ, M. & KEELY, S. 2012a. Epidermal growth factor chronically upregulates Ca(2+)-dependent Cl(-) conductance and TMEM16A expression in intestinal epithelial cells. *J Physiol* 590, 1907-20.

MROZ, M. & KEELY, S. 2012b. Epidermal growth factor chronically upregulates Ca(2+)-dependent Cl(-) conductance and TMEM16A expression in intestinal epithelial cells. *J Physiol.,* 590, 1907-20.

MUKHERJEE, M., PRITCHARD, D. & BOSQUILLON, C. 2012. Evaluation of air-interfaced Calu-3 cell layers for investigation of inhaled drug interactions with organic cation transporters in vitro. *Int J Pharm,* 426**,** 7-14.

MUKHERJEE, S., TRICE, J., SHINDE, P., WILLIS, R., PRESSLEY, T. & PEREZ-ZOGHBI, J. 2013. Ca^{2+} oscillations, Ca^{2+} sensitization, and contraction activated by protein kinase C in small airway smooth muscle. *J Gen Physiol,* 141**,** 165-78.

NAITO, Y. & KANEKO, H. 1972. Reactivated triton-extracted models o paramecium: modification of ciliary movement by calcium ions. *Science,* 174**,** 523-4.

NAMKUNG, W., PHUAN, P. & VERKMAN, A. 2011. TMEM16A inhibitors reveal TMEM16A as a minor component of calcium-activated chloride channel conductance in airway and intestinal epithelial cells. *J Biol Chem* 286**,** 2365-74.

NAMKUNG, W., W. E. FINKBEINER, ET AL 2010. CFTR-adenylyl cyclase I association responsible for UTP activation of CFTR in well-differentiated primary human bronchial cell cultures. *Mol Biol Cell* 21**,** 2639-48.

NAVARRO, J., RAINISIO, M., HARMS, H., HODSON, M., KOCH, C., MASTELLA, G., STRANDVIK, B. & MCKENZIE, S. 2001. Factors associated with poor pulmonary function: cross-sectional analysis of data from the ERCF. European Epidemiologic Registry of Cystic Fibrosis. *Eur Respir J,* 18**,** 298-305.

NEGULESCU, P. & MACHEN, T. 1993. Ca transport by plasma membrane and intracellular stores of gastric cells. *Am J Physiol,* 264**,** C843-51.

NEWTON, A. 1995. Protein Kinase C: Structure, Function and Regulation. *J Biol Chem,* 270**,** 28495-8.

NGUYEN, A. & BOUSCAREL, B. 2008. Bile acids and signal transduction: role in glucose homeostasis. *Cell Signal,* 20**,** 2180-97.

O'MAHONY, F., TOUMI, F., MROZ, M., FERGUSON, G. & KEELY, S. 2008. Induction of $Na^+/K^+/2Cl^-$ cotransporter expression mediates chronic potentiation of intestinal epithelial Cl^- secretion by EGF. *Am J Physiol Cell Physiol,* 294.

OELBERG, D., DOWNEY, S. & FLYNN, M. 1990. Bile salt-induced intracellular Ca^{2+} accumulation in type II pneumocytes. *Lung,* 168**,** 297-308.

OKOLO, C., WONG, T., MOODY, M. & NGUYEN, T. 2002. Effects of bile acids on dog pancreatic duct epithelial cell secretion and monolayer resistance. *Am J Physiol Gastrointest Liver Physiol.,* 283, g1042-50.

PALFREY, H., FEIT, P. & GREENGARD, P. 1980. cAMP-stimulated cation cotransport in avian erythrocytes: inhibition by "loop" diuretics. *Am J Physiol Cell Physiol,* 238, C139-48.

PARIKH, S., BROWNLEE, I., ROBERTSON, A., MANNING, N., JOHNSON, G., BRODLIE, M., CORRIS, P., WARD, C. & PEARSON, J. 2013. Are the enzymatic methods currently being used to measure bronchoalveolar lavage bile salt levels fit for purpose? *J Heart Lung Transplant,* 32, 418-23.

PAUWELS, A., DECRAENE, A., BLONDEAU, K., MERTENS, V., FARRE, R., PROESMANS, M., VAN BLEYENBERGH, P., SIFRIM, D. & DUPONT, L. J. 2012. Bile acids in sputum and increased airway inflammation in patients with cystic fibrosis. *Chest,* 141, 1568-74.

PENNINGTON, C., ROSS, P., MURISON, J. & BOUCHIER, I. 1981. Fluctuations of serum bile acid concentrations during the menstrual cycle. *J Clin Pathol,* 34, 185-6.

PEREZ, M. & BRIZ, O. 2009. Bile-acid-induced cell injury and protection. *World J Gastroenterol,* 15, 1677-89.

PERNG, D., CHANG, K., SU, K., WU, Y., WU, M., HSU, W., TSAI, C. & LEE, Y. 2007. Exposure of airway epithelium to bile acids associated with gastroesophageal reflux symptoms: a relation to transforming growth factor-beta1 production and fibroblast proliferation. *Chest,* 132, 1548-56.

PERNG, D., WU, Y. & ET, A. 2008. Bile acids induce CCN2 production through p38 MAP kinase activation in human bronchial epithelial cells: a factor contributing to airway fibrosis. *Respirology,* 13, 983-9.

PEZZULO, A., STARNER, T., SCHEETZ, T., TRAVER, G., TILLEY, A., HARVEY, B., CRYSTAL, R., MCCRAY, P. J. & ZABNER, J. 2011. The air-liquid interface and use of primary cell cultures are important to recapitulate the transcriptional profile of in vivo airway epithelia. *Am J Physiol Lung Cell Mol Physiol* 300, L25-31.

PEZZULO, A. A., TANG, X. X., HOEGGER, M. J., ALAIWA, M. H., RAMACHANDRAN, S., MONINGER, T. O., KARP, P. H., WOHLFORD-LENANE, C. L., HAAGSMAN, H. P., VAN EIJK, M., BANFI, B.,

HORSWILL, A. R., STOLTZ, D. A., MCCRAY, P. B., JR., WELSH, M. J. & ZABNER, J. 2012. Reduced airway surface pH impairs bacterial killing in the porcine cystic fibrosis lung. *Nature,* 487, 109-13.

POREMBKA, D., KIER, A., SEHLHORST, S., BOYCE, S., ORLOWSKI, J. & DAVIS, K. J. 1993. The pathophysiologic changes following bile aspiration in a porcine lung model. *Chest,* 104, 919-24.

POTTER, G., LESTER, R., BURLINGAME, S., MITCHELL, P. & SCHMIDT, K. 1987. Taurodeoxycholate and the developing rabbit distal colon: absence of secretory effect. *Am J Physiol,* 253, g483-8.

PRINCE, L., WORKMAN, R. J. & MARCHASE, R. 1994. Rapid endocytosis of the cystic fibrosis transmembrane conductance regulator chloride channel. *Proc Natl Acad Sci U S A.* , 91, 5192-6.

PROUD, D. 2008. *The Pulmonary Epithelium in Health and Disease*, John Wiley & Sons Ltd.

PROUD, D. & LEIGH, R. 2011. Epithelial cells and airway diseases. *Immunol Rev* 242, 186-204.

PRULIERE-ESCABASSE, V., CLERICI, C., VUAGNIAUX, G., COSTE, A., ESCUDIER, E. & PLANES, C. 2010. Effect of neutrophil elastase and its inhibitor EPI-hNE4 on transepithelial sodium transport across normal and cystic fibrosis human nasal epithelial cells *Respir Res* 11, 141.

PUCHELLE, E., ZAHM, J. & ET, A. 1987. Rheological properties controlling mucociliary frequency and respiratory mucus transport. *Biorheology* 24, 557-63.

RAIMONDI, F., SANTORO, P., BARONE, M., PAPPACODA, S., BARRETTA, M., NANAYAKKARA, M., APICELLA, C., CAPASSO, L. & PALUDETTO, R. 2008. Bile acids modulate tight junction structure and barrier function of Caco-2 monolayers via EGFR activation. *Am J Physiol Gastrointest Liver Physiol.* , 294, G908-13.

RANDELL, S. & BOUCHER, R. 2006. Effective mucus clearance is essential for respiratory health. *Am J Respir Cell Mol Biol* 35, 20-8.

REEN, F., WOODS, D., MOOIJ, M., ADAMS, C. & O'GARA, F. 2012. Respiratory pathogens adopt a chronic lifestyle in response to bile. *PLoS One,* 7, e45978.

RIORDAN, J. R., ROMMENS, J. M., KEREM, B., ALON, N., ROZMAHEL, R., GRZELCZAK, Z., ZIELENSKI, J., LOK, S., PLAVSIC, N., CHOU, J. L. &

ET AL. 1989. Identification of the cystic fibrosis gene: cloning and characterization of complementary DNA. *Science,* 245, 1066-73.

ROMMENS, J. M., IANNUZZI, M. C., KEREM, B., DRUMM, M. L., MELMER, G., DEAN, M., ROZMAHEL, R., COLE, J. L., KENNEDY, D., HIDAKA, N. & ET AL. 1989. Identification of the cystic fibrosis gene: chromosome walking and jumping. *Science,* 245, 1059-65.

ROWE, S., MILLER, S. & ET, A. 2005. Cystic fibrosis. *N Engl J Med* 352, 1992-2001.

SAINT-CRIQ, V., RAPETTI-MAUSS, R., YUSEF, Y. & HARVEY, B. 2012. Estrogen regulation of epithelial ion transport: Implications in health and disease. *Steroids,* 77, 918-23.

SANDERSON, M. & SLEIGH, M. 1981. Ciliary activity of cultured rabbit tracheal epithelium: beat pattern and metachrony. *J Cell Sci* 47.

SAVARINO, E., CARBONE, R., MARABOTTO, E., FURNARI, M., SCONFIENZA, L., GHIO, M., ZENTILIN, P. & SAVARINO, V. 2013. Gastro-oesophageal reflux and gastric aspiration in idiopathic pulmonary fibrosis patients. *Eur Respir J.*

SCHEURER, S. B., RYBAK, J. N., ROESLI, C., BRUNISHOLZ, R. A., POTTHAST, F., SCHLAPBACH, R., NERI, D. & ELIA, G. 2005. Identification and relative quantification of membrane proteins by surface biotinylation and two-dimensional peptide mapping. *Proteomics,* 5, 2718-28.

SCHROEDER, B., CHENG, T., JAN, Y. & JAN, L. 2008. Expression cloning of TMEM16A as a calcium-activated chloride channel subunit. *Cell,* 134, 1019-29.

SCHULTHEISS, G., SIEFJEDIERS, A. & DIENER, M. 2005. Muscarinic receptor stimulation activates a Ca(2+)-dependent Cl(-) conductance in rat distal colon. *J Membr Biol,* 204, 117-27.

SCHWARTZ, G. J., BARASCH, J. & AL-AWQATI, Q. 1985. Plasticity of functional epithelial polarity. *Nature,* 318, 368-71.

SEAMON, K. B., PADGETT, W. & DALY, J. W. 1981. Forskolin: unique diterpene activator of adenylate cyclase in membranes and in intact cells. *Proc Natl Acad Sci U S A,* 78, 3363-7.

SHAN, J., LIAO, J., HUANG, J., ROBERT, R., PALMER, M., FAHRENKRUG, S., O'GRADY, S. & HANRAHAN, J. 2012. Bicarbonate-dependent chloride

transport drives fluid secretion by the human airway epithelial cell line Calu-3. *J Physiol,* 590, 5273-97.

SINGH, M., KROUSE, M., MOON, S. & WINE, J. 1997. Most basal Isc in Calu-3 human airway cells is bicarbonate-dependent Cl2 secretion. *Am. J. Physiol.,* 272, L690–L698.

SKOU, J. C. 1957. The influence of some cations on an adenosine triphosphatase from peripheral nerves. *Biochem Biophys Acta,* 23, 394-401.

SLEIGH, M., BLAKE, J. & ET, A. 1988. The propulsion of mucus by cilia. *Am Rev Respir Dis,* 137, 726-41.

SLUSARSKI, D. & PELEGRI, F. 2007. Calcium signaling in vertebrate embryonic patterning and morphogenesis. *Developmental Biology,* 307, 1-13.

SMITH, D. J., GAFFNEY, E. A. & BLAKE, J. R. 2008. Modelling mucociliary clearance. *Respir Physiol Neurobiol,* 163, 178-88.

SOLAAS, K., ULVESTAD, A., SÖREIDE, O. & KASE, B. 2000. Subcellular organization of bile acid amidation in human liver: a key issue in regulating the biosynthesis of bile salts. *J Lipid Res,* 41, 1154–1162.

SONG, S., BYRD, J. C., GUHA, S., LIU, K. F., KOUL, D. & BRESALIER, R. S. 2010. Induction of MUC5AC mucin by conjugated bile acids in the esophagus involves the phosphatidylinositol 3-kinase/protein kinase C/activator protein-1 pathway. *Cancer.*

SU, K., WU, Y., CHEN, C., HUNG, M., HSIAO, Y., TSENG, C., CHANG, S., LEE, Y. & PERNG, D. 2013. Bile acids increase alveolar epithelial permeability via mitogen-activated protein kinase, cytosolic phospholipase A2 , cyclooxygenase-2, prostaglandin E2 and junctional proteins. *Respirology,* 18, 848-56.

SUTHERLAND, E. W. & RALL, T. W. 1958. Fractionation and characterization of a cyclic adenine ribonucleotide formed by tissue particles. *J Biol Chem,* 232, 1077-91.

TAKAHASHI, A., CAMACHO, P., LECHLEITER, J. D. & HERMAN, B. 1999. Measurement of intracellular calcium. *Physiol Rev,* 79, 1089-125.

TARRAN, R. 2004. Regulation of airway surface liquid volume and mucus transport by active ion transport. *Proc Am Thorac Soc,* 1, 42-6.

TARRAN, R., BUTTON, B. & BOUCHER, R. C. 2006. Regulation of normal and cystic fibrosis airway surface liquid volume by phasic shear stress. *Annu Rev Physiol,* 68**,** 543-61.

TARRAN, R., GRUBB, B. R., GATZY, J. T., DAVIS, C. W. & BOUCHER, R. C. 2001. The relative roles of passive surface forces and active ion transport in the modulation of airway surface liquid volume and composition. *J Gen Physiol,* 118**,** 223-36.

TASKEN, K. & AANDAHL, E. M. 2004. Localized effects of cAMP mediated by distinct routes of protein kinase A. *Physiol Rev,* 84**,** 137-67.

THEISEN, J., NEHRA, D., CITRON, D., JOHANSSON, J., HAGEN, J. A., CROOKES, P. F., DEMEESTER, S. R., BREMNER, C. G., DEMEESTER, T. R. & PETERS, J. H. 2000. Suppression of gastric acid secretion in patients with gastroesophageal reflux disease results in gastric bacterial overgrowth and deconjugation of bile acids. *J Gastrointest Surg,* 4**,** 50-4.

THERIEN, A. & BLOSTEIN, R. 2000. Mechanisms of sodium pump regulation. *Am J Physiol Cell Physiol* 279**,** C541-66.

TIWARI, A. & MAITI, P. 2009. TGR5: an emerging bile acid G-protein-coupled receptor target for the potential treatment of metabolic disorders. *Drug Discov Today,* 14**,** 523-30.

TOUMI, F., FRANKSON, M., WARD, J. B., KELLY, O. B., MROZ, M. S., BERTELSEN, L. S. & KEELY, S. J. 2011. Chronic regulation of colonic epithelial secretory function by activation of G protein-coupled receptors. *Neurogastroenterol Motil,* 23**,** 178-86, e43.

TRINICK, R., JOHNSTON, N., DALZELL, A. & MCNAMARA, P. 2012. Reflux aspiration in children with neurodisability--a significant problem, but can we measure it. *J Pediatr Surg* 47**,** 291-8.

URBACH, V., VAN KERKHOVE, E., MAGUIRE, D. & HARVEY, B. J. 1996. Rapid activation of KATP channels by aldosterone in principal cells of frog skin. *J Physiol,* 491 (Pt 1)**,** 111-20.

URIBE, J., GELBMANN, C., TRAYNOR-KAPLAN, A. & BARRETT, K. 1996. Epidermal growth factor inhibits Ca(2+)-dependent Cl- transport in T84 human colonic epithelial cells. *Am J Physiol,* 271**,** c914-22.

VACHEL, L., NOREZ, C., BECQ, F. & VANDEBROUCK, C. 2013. Effect of VX-770 (Ivacaftor) and OAG on Ca2+ influx and CFTR activity in G551D and F508del-CFTR expressing cells. *J Cyst Fibros.,* Epub ahead of print.

VAGIN, O., DADA, L., TOKHTAEVA, E. & SACHS, G. 2011. The Na-K-ATPase alpha(1)beta(1) heterodimer as a cell adhesion molecule in epithelia. *Am J Physiol Cell Physiol,* 302, C1271-81.

VAN DER MERWE, J., MOREAU, F. & MACNAUGHTON, W. 2009. Protease-activated receptor-2 stimulates intestinal epithelial chloride transport through activation of PLC and selective PKC isoforms. *Am J Physiol Gastrointest Liver Physio,* 296, G1258-66.

VAQUERO, J., MONTE, M., DOMINGUEZ, M., MUNTANÉ, J. & MARIN, J. 2013. Differential activation of the human farnesoid X receptor depends on the pattern of expressed isoforms and the bile acid pool composition. *Biochem Pharmacol.,* Epub ahead of print.

VEIT, G., BOSSARD, F., GOEPP, J., VERKMAN, A., GALIETTA, L., HANRAHAN, J. & LUKACS, G. 2012. Proinflammatory cytokine secretion is suppressed by TMEM16A or CFTR channel activity in human cystic fibrosis bronchial epithelia. *Mol Biol Cell,* 23, 4188-202.

VENGLOVECZ, V., RAKONCZAY, Z. J., OZSVÁRI, B., TAKÁCS, T., LONOVICS, J., VARRÓ, A., GRAY, M., ARGENT, B. & HEGYI, P. 2008. Effects of bile acids on pancreatic ductal bicarbonate secretion in guinea pig. *Gut,* 57, 1102-12.

VIC, P., TASSIN, E. & ET, A. 1995. Frequency of gastroesophageal reflux in infants and in young children with cystic fibrosis *Arch Pediatr* 2, 742-6.

VOS, R., BLONDEAU, K., VANAUDENAERDE, B., MERTENS, V., VAN RAEMDONCK, D., SIFRIM, D., DUPONT, L. & VERLEDEN, G. 2008. Airway colonization and gastric aspiration after lung transplantation: do birds of a feather flock together? *J Heart Lung Transplant,* 27, 843-9.

WAN, H., WINTON, H. L., SOELLER, C., STEWART, G. A., THOMPSON, P. J., GRUENERT, D. C., CANNELL, M. B., GARROD, D. R. & ROBINSON, C. 2000. Tight junction properties of the immortalized human bronchial epithelial cell lines Calu-3 and 16HBE14o. *Eur Respir J,* 15, 1058-68.

WANG, D., SUN, Y., ZHANG, W. & HUANG, P. 2008. Apical adenosine regulates basolateral Ca^{2+}-activated potassium channels in human airway Calu-3 epithelial cells. *Am J Physiol Cell Physiol,* 294, C1443-53.

WANG, Y., CHEN, W., YU, D., FORMAN, B. M. & HUANG, W. 2011. The G-protein coupled bile acid receptor, Gpbar1 (TGR5), negatively regulates hepatic inflammatory response through antagonizing nuclear factor k light chain enhancer of activated B cells in mice. *Hepatology,* 54, 1421-32.

WANNER, A., SALATHE, M. & O'RIORDAN, T. G. 1996. Mucociliary clearance in the airways. *Am J Respir Crit Care Med,* 154, 1868-902.

WARD, J., MROZ, M. & KEELY, S. 2013. The bile acid receptor, TGR5, regulates basal and cholinergic-induced secretory responses in rat colon. *Neurogastroenterol Motil.,* 25, 708-11.

WAUGH, T., CHING, J., ZHOU, Y. & ME, L. 2013. Influenza A virus (H1N1) increases airway epithelial cell secretion by up-regulation of potassium channel KCNN4. *Biochem Biophys Res Commun,* [Epub ahead of print].

WELSH, M. & MCCANN, J. 1985. Intracellular calcium regulates basolateral potassium channels in a chloride-secreting epithelium. *Proc Natl Acad Sci USA,* 82, 8823-6.

WILKINSON, S., PARKER, P. & NIXON, J. 1993. Isoenzyme specificity of bisindolylmaleimides, selective inhibitors of protein kinase C. *Biochem J,* 294, 335-7.

WIMMER, R., HOHENESTER, S., PUSL, T., DENK, G., RUST, C. & BEUERS, U. 2008. Tauroursodeoxycholic acid exerts anticholestatic effects by a cooperative cPKC alpha-/PKA-dependent mechanism in rat liver. *57,* 10.

WINE, J. & JOO, N. 2004. Submucosal glands and airway defense. *Proc Am Thorac Soc* 1, 47-53.

WONG, S. M., TESFAYE, A., DEBELL, M. C. & CHASE, H. S., JR. 1990. Carbachol increases basolateral K+ conductance in T84 cells. Simultaneous measurements of cell [Ca] and gK explore calcium's role. *J Gen Physiol,* 96, 1271-85.

WONG, W. & SCOTT, J. 2004. AKAP signalling complexes: focal points in space and time. *Nat Rev Mol Cell Biol,* 5, 959-70.

WU, Y., HSU, P., SU, K., LIU, L., TSAI, C., TSAI, S., HSU, W., LEE, Y. & PERNG, D. 2009. Bile acid aspiration in suspected ventilator-associated pneumonia. *Chest,* 136, 118-24.

XIA, X., WANG, F., WANG, Z., WAN, H., XU, W. & LU, H. 2010. Emodin enhances alveolar epithelial barrier function in rats with experimental acute pancreatitis. *World J Gastroenterol.* , 16, 2994-3001.

XU, X., CHEN, H., ZHU, X., MA, Y., LIU, Q., XUE, Y., H, C., WU, W., WANG, J. & ZOU, H. 2013. S100A9 promotes human lung fibroblast cells activation through receptor for advanced glycation end-product-mediated extracellular-regulated kinase 1/2, mitogen-activated protein-kinase and nuclear factor-κB-dependent pathways. *Clin Exp Immunol.* , 173, 523-35.

YANG, Y. D., CHO, H., KOO, J. Y., TAK, M. H., CHO, Y., SHIM, W. S., PARK, S. P., LEE, J., LEE, B., KIM, B. M., RAOUF, R., SHIN, Y. K. & OH, U. 2008. TMEM16A confers receptor-activated calcium-dependent chloride conductance. *Nature,* 455, 1210-5.

YUAN, W. & BERS, D. 1995. Protein kinase inhibitor H-89 reverses forskolin stimulation of cardiac L-type calcium current. *Am J Physiol.* , 268, c651-9.

ZABIN, I. & BARKER, W. 1953. The conversion of cholesterol and acetate to cholic acid. *J Biol Chem* 205, 633-6.

ZABNER, J., KARP, P., SEILER, M., PHILLIPS, S., MITCHELL, C., SAAVEDRA, M., WELSH, M. & KLINGELHUTZ, A. 2003. Development of cystic fibrosis and noncystic fibrosis airway cell lines. *Am J Physiol Lung Cell Mol Physiol* 284, L844-54.

ZAPATA, R., SANDOVAL, L., PALMA, J., HERNÁNDEZ, I., RIBALTA, J., REYES, H., SEDANO, M., TOHÁ, D. & SILVA, J. 2005. Ursodeoxycholic acid in the treatment of intrahepatic cholestasis of pregnancy. A 12-year experience. *Liver Int.* , 25, 548-54.

ZECCA, E., COSTA, S., LAURIOLA, V., VENTO, G., PAPACCI, P. & ROMAGNOLI, C. 2004. Bile acid pneumonia: a "new" form of neonatal respiratory distress syndrome? *Pediatrics,* 114, 269-72.

ZECCA, E., DE LUCA, D., BARONI, S., VENTO, G., TIBERI, E. & ROMAGNOLI, C. 2008. Bile acid-induced lung injury in newborn infants: a bronchoalveolar lavage fluid study. *Pediatrics,* 121, e146-9.

ZHANG, L., LI, T., YU, D., FORMAN, B. M. & HUANG, W. 2012. FXR protects lung from lipopolysaccharide-induced acute injury. *Mol Endocrinol,* 26, 27-36.

ZHANG, L. & SANDERSON, M. 2003. Oscillations in ciliary beat frequency and intracellular calcium concentration in rabbit tracheal epithelial cells induced by ATP. *J Physiol,* 564, 733-49.

ZHANGXUE, H., MIN, G., JINNING, Z., YUAN, S., LI, W., HUAPEI, S., RUI, L. & CHUNYU, Z. 2012. Glycochenodeoxycholate induces rat alveolar epithelial type II cell death and inhibits surfactant secretion in vitro. *Free Radic Biol Med.* , 53, 122-8.

ZHAO, K., XIONG, G., WILBER, M., COHEN, N. & KREINDLER, J. 2012. A role for two-pore K^+ channels in modulating Na^+ absorption and Cl^- secretion in normal human bronchial epithelial cells. *Am J Physiol Lung Cell Mol Physiol,* 302, L4-12.

ZHAO, X., SHI, C., WANG, X. & ANDERSSON, R. 2006. Protein kinase C modulates the pulmonary inflammatory response in acute pancreatitis. *Respir Physiol Neurobiol,* 152, 16-26.

ZHOU, C., SHI, Y., LI, J., ZHANG, W., WANG, Y., LIU, Y. & LIU, J. 2013. The effects of taurochenodeoxycholic acid in preventing pulmonary fibrosis in mice. *Pak J Pharm Sci,* 26, 761-5.

ZHOU, Z., DUERR, J., JOHANNESSON, B., SCHUBERT, S., TREIS, D., HARM, M., GRAEBER, S., DALPKE, A., SCHULTZ, C. & MALL, M. 2011. The ENaC-overexpressing mouse as a model of cystic fibrosis lung disease. *J Cyst Fibros* 10, S172-82.